BOULDER PLACEMENT FOR AQUATIC HABITATS

Maria Heyneke

374945

A research report submitted to the Faculty of Engineering and the Built Environment, University of the Witwatersrand, Johannesburg, in partial fulfilment of the requirements for the degree of Master of Science in Engineering.

Johannesburg, 2019

DECLARATION

I declare that this research report is my own unaided work. It is being submitted to the Degree of Master of Science to the University of the Witwatersrand, Johannesburg. It has not been submitted before for any degree or examination to any other University.

....

(Signature of Candidate)

8th day of August 2019

ABSTRACT

The use of boulders simulates naturally occurring river habitats and has been acknowledged as a tool to reintroduce habitats into channelised river systems. This investigation aimed to provide guidance for increasing and quantifying suitable habitat heterogeneity for aquatic biodiversity. Boulders create hydraulic diversity by altering the velocity and flow depth of water in the immediate surroundings, of which the change in flow depth is small and localised around the boulder edge while changes in velocity can extend from several to hundreds of metres.

Boulders placed in a channel reduce the velocity upstream and downstream of the object and increase the velocity on the sides. The upstream and downstream regions showed much larger areas of disturbed flow when compared to the sides of the boulder. Low percentage variations from uniform flow also occupied the greatest disturbed region areas.

Experimental velocities were compared to the results of a two-dimensional hydrodynamic finite element software, namely Argus ONE and RiverFLO-2D. The software was found to neglect the turbulent wakes downstream of boulders and correction factors were developed to calibrate software output.

The fundamental variables which affect the size of any velocity distribution were identified; these consisted of hydraulic (Froude number) and geometric variables (channel width and boulder diameter). Using these variables empirical relationships were developed to determine the distance from the boulder where a certain velocity percentage variation from uniform velocity was experienced in the upstream, downstream and side directions respectively. The geometric variables were found to be the dominant variables and practical approximations were also developed to determine the velocity changes using only the channel geometry.

The investigation of one boulder revealed that a limiting boulder diameter exists above which blockage of the channel will occur. Following the identification of the blockage ratio limit it was found that below the limit the downstream velocity disturbance is the largest and above the limit the upstream velocity increases to such an extent that flow conditions are changed hundreds of metres upstream.

Two boulders placed on the same axis perpendicular to the direction of flow showed that the disturbed velocity area increased as they were moved closer to each other. A relationship to determine the optimum spacing between boulders was developed. The resultant velocity change caused by two boulders at the optimum spacing was found to be equivalent to one boulder with double the volume. Again, empirical relationships were developed to determine the distance from the boulder where a certain velocity percentage variation from uniform velocity was experienced.

Application of the velocity distribution equations was illustrated by design examples of boulder size selection.

ACKNOWLEDGEMENTS

A very big thank you to Professor Chris James for his guidance and patience and to Steven for all his help in the hydraulics laboratory. Thank you to my parents, Adri, Lisa and Nate for your motivation and support.

TABLE OF CONTENTS

DECLARATION ..... **I**

ABSTRACT ..... **II**

ACKNOWLEDGEMENTS ..... **IV**

LIST OF FIGURES ..... **X**

LIST OF TABLES ..... **XIV**

LIST OF VARIABLES AND ABBREVIATIONS ..... **XVIII**

1 INTRODUCTION **1**

1.1 Layout of Report 2

2 BACKGROUND **4**

2.1 Introduction 4

2.1.1 Current State of Ecosystems 4

2.2 Rehabilitation 5

2.2.1 What is Rehabilitation? 5

2.2.2 Disturbances 7

2.2.3 Techniques 8

2.3 Hydraulic Habitat 8

2.3.1 Tools to Describe Habitat 11

2.4 Boulders 13

2.4.1 Linking Boulders to Habitats 13

2.4.2 Where to Place Boulders 13

2.4.3 How to Place Boulders 14

2.5 Two-Dimensional Modelling 15

2.5.1 Comparing One, Two and Three-dimensional Modelling 16

2.5.2 Learnings from Two-dimensional Modelling 17

2.6 Conclusion 18

3 METHODOLOGY **20**

3.1 Variables of Interest 20
3.2 Key Assumptions 22
3.3 Experimental Models 22
3.3.1 Setup of Experimental Conditions 23
3.3.2 Uniform Flow 24
3.3.3 Velocity Measurement 25
3.4 Argus ONE and RiverFLO-2D 26
3.4.1 Pre-processing in Argus ONE 27
3.4.2 Processing in RiverFLO-2D 30
3.4.3 Post-processing in Argus ONE 32
3.5 Hydraulic Effect of Boulders 33
3.5.1 ZOI 34
3.5.2 Areal Histograms 37
4 SOFTWARE AND EXPERIMENTAL CORRELATION 38
4.1 Experimental Conditions 38
4.1.1 1 Boulder 38
4.1.2 1 Boulder with Larger Blockage Ratios 39
4.1.3 2 Boulders 40
4.2 Experimental Velocity Measurement Points 41
4.3 1 Boulder Results 42
4.3.1 Comparison of Velocities 42
4.3.2 Experimental Versus Software Graphs 44
4.3.3 Downstream Variation 46
4.3.4 Correction Factor 48
4.4 2 Boulders Results 51
4.4.1 Comparison of Velocities 51
4.4.2 Experimental versus Software Graphs 52

4.4.3 Downstream Variation 53
4.4.4 Correction Factor 56
5 INFLUENCE OF 1 BOULDER 57
5.1 Velocity Distribution Investigation 57
5.1.1 ZOI 58
5.1.2 Velocity Histogram 59
5.2 Variable Groupings 60
5.3 Model Conditions 62
5.4 Proving the Relationship 63
5.4.1 Froude Number 63
5.4.2 Blockage Ratio 65
5.4.3 Dimensionless ZOI 66
5.5 Creating the Relationship 68
5.5.1 Setup 69
5.5.2 Results 71
5.5.3 Effectiveness 72
5.6 Practical Approximation 74
5.6.1 Results 74
5.6.2 Effectiveness 75
5.7 Conclusion 77
6 BLOCKAGE RATIO LIMIT 79
6.1 Below and Above the Blockage Limit 80
6.2 Model Conditions 81
6.3 Identifying the Blockage Ratio Limit 82
6.4 Analysis of the Velocity Distribution 85
6.4.1 Upstream 86
6.4.2 Sides 94

6.4.3 Downstream 99
6.5 Conclusion 100
7 INFLUENCE OF 2 TRANSVERSE BOULDERS 103
7.1 Velocity Distribution Investigation 104
7.2 Change in Velocity with Spacing 104
7.3 Spacing Relationship 108
7.3.1 Effectiveness of Spacing at Local Control 108
7.3.2 Blockage Ratio 111
7.3.3 Froude Number 112
7.3.4 Dimensional Analysis 113
7.3.5 Froude Number Ranges 113
7.3.6 Dimensionless Spacing 114
7.3.7 Model Conditions 115
7.3.8 Proving the Relationship 116
7.4 ZOI Relationship at Local Control 117
7.4.1 Setup 117
7.4.2 Results 118
7.4.3 Effectiveness 120
7.5 ZOI Practical Approximation at Local Control 122
7.5.1 Results 122
7.5.2 Effectiveness 124
7.6 Conclusion 126
8 DESIGN EXAMPLES 128
8.1 1 Boulder Below the Blockage Limit 128
8.2 2 Boulders 133
8.3 1 Boulder Above the Blockage Limit 138
9 CONCLUSION AND RECOMMENDATIONS 144

9.1 Software Correlation 144
9.2 1 Boulder Below the Blockage Ratio Limit 144
9.3 1 Boulder Above the Blockage Ratio Limit 145
9.4 2 Boulders 146
9.5 Additional Considerations 146
9.6 Recommendations for Further Research 147
REFERENCES 149
APPENDIX A: SOFTWARE AND EXPERIMENTAL CORRELATION 155
APPENDIX B: 1 BOULDER BELOW THE BLOCKAGE LIMIT MODEL CONDITIONS 175
APPENDIX C: 1 BOULDER BELOW THE BLOCKAGE LIMIT ZOI SOFTWARE AND RELATIONSHIP CORRELATION 177
APPENDIX D: 1 BOULDER ABOVE THE BLOCKAGE LIMIT ZOI SOFTWARE AND RELATIONSHIP CORRELATION 186
APPENDIX E: 2 BOULDERS MODEL CONDITIONS 189
APPENDIX F: 2 BOULDERS ZOI SOFTWARE AND RELATIONSHIP CORRELATION 190

LIST OF FIGURES

Figure 2-1: Flow classes for fish (Cullis et al., 2010:62) 10
Figure 2-2: Extended flow classes for fish (Birkhead, 2010: 203) 10
Figure 2-3: Flow Classes for invertebrates (Birkhead, 2010: 203) 11
Figure 2-4: Zone of influence around a boulder (adapted from Hamuy-Blanco, 2014) 12
Figure 3-1: Hydraulics Laboratory 23
Figure 3-2: Customised computer software system 23
Figure 3-3: Digital flow meter 24
Figure 3-4: V-notch weir 24
Figure 3-5: Water flowing over sluice gate 25
Figure 3-6: Piezometers 25
Figure 3-7: Argus ONE pre-processing model 28
Figure 3-8: RiverFLO-2D control conditions 31
Figure 3-9: Post-processing visual velocity distribution 32
Figure 3-10: Flow depth variations around a boulder 34
Figure 3-11: Velocity variations around a boulder 34
Figure 3-12: Zone of influence around a boulder (adapted from Hamuy-Blanco, 2014) 35
Figure 3-13: ZOI example 36
Figure 3-14: Areal histogram example 37
Figure 4-1: 1 Boulder d=0.110m experiment 39
Figure 4-2: 1.0m width flow disturbances (overhead view) 40
Figure 4-3: 1.0m width flow disturbances (side view) 40
Figure 4-4: 2 Boulders d=0.110m experiment 41
Figure 4-5: 1 Single boulder experimental velocity measurement points 42
Figure 4-6: 2 Double boulder experimental velocity measurement points 42
Figure 4-7: 1 Boulder upstream experimental and software velocities (Test 1, d=0.110m) 43
Figure 4-8: 1 Boulder side experimental and software velocities (Test 1, d=0.110m) 43
Figure 4-9: 1 Boulder downstream experimental and software velocities (Test 1, *d*=0.110m) 44

Figure 4-10: Upstream - Correlation for all 1 boulder experiments........................... 45
Figure 4-11: Sides - Correlation for all 1 boulder experiments 45
Figure 4-12: Downstream - Correlation for all 1 boulder experiments 46
Figure 4-13: 1 Boulder downstream experimental and software velocities (Test 1, *d*=0.1750m) 48
Figure 4-14: 1 Boulder downstream correction factor (Test 1, *d*=0.110m) 49
Figure 4-15: Downstream - Correlation for all 1 boulder experiments with correction factor 50
Figure 4-16: Downstream - Correlation for all 1 boulder experiments with correction factor and no negative velocities 50
Figure 4-17: 2 Boulders upstream experimental and software velocities (Test 2, *d*=0.110m) 51
Figure 4-18: 2 Boulders side experimental and software velocities (Test 2, *d*=0.110m) 51
Figure 4-19: 2 Boulders downstream experimental and software velocities (Test 2, *d*=0.110m) 52
Figure 4-20: Upstream - Correlation for all 2 boulder experiments........................... 52
Figure 4-21: Sides - Correlation for all 2 boulder experiments 53
Figure 4-22: Downstream - Correlation for all 2 boulder experiments 53
Figure 4-13: 1 Boulder downstream experimental and software velocities (Test 1, *d*=0.1750m) 55
Figure 4-23: Downstream - Correlation for all 2 boulder experiments with correction factor 56
Figure 5-1: Model 1 ZOI 58
Figure 5-2: Model 1 velocity histogram showing 10-100% change in velocity.......... 60
Figure 5-3: 1 Boulder Froude number and blockage ratio model conditions 62
Figure 5-4: Upstream ZOI for different Froude numbers and a constant blockage ratio 63
Figure 5-5: Downstream ZOI for different Froude numbers and a constant blockage ratio 64
Figure 5-6: Transverse ZOI for different Froude numbers and a constant blockage ratio 64
Figure 5-7: Downstream ZOI for different Froude numbers and three constant blockage ratios 65

Figure 5-8: ZOI for different blockage ratios 66
Figure 5-9: ZOI normalisation using diameter 67
Figure 5-10: ZOI normalisation using width 68
Figure 5-11: ZOI relationship setup 70
Figure 5-12: Upstream software vs relationship 5-18 73
Figure 5-13: Downstream software vs relationship 5-19 73
Figure 5-14: Sides software vs relationship 5-20 74
Figure 5-15: Upstream software vs relationship 5-22 76
Figure 5-16: Downstream software vs relationship 5-23 77
Figure 5-17: Sides software vs relationship 5-24 77
Figure 6-1: Below blockage limit (Model 1) disturbed flow 81
Figure 6-2: Above blockage limit (Model 27) disturbed flow 81
Figure 6-3: Channel contraction modelling 82
Figure 6-4: Model 27 Froude number 85
Figure 6-5: Upstream approach conditions model 86
Figure 6-6: Model 27 upstream velocity distribution 88
Figure 6-7: Non-linear blockage ratio with choking 89
Figure 6-8: Linear blockage ratio when only including percentage variations higher than the new approach velocity 90
Figure 6-9: Upstream software vs relationship 5-18 for higher blockage ratios 91
Figure 6-10: Increased upstream flow depth 93
Figure 6-11: Froude number greater than or equal to 1 for Model 27 95
Figure 6-12: Side velocity distribution of Model 27 96
Figure 6-13: Velocity increase at the bank of the channel 97
Figure 6-14: Extension of i_b on the bed 98
Figure 6-15: Extension of the velocity increase on the bed 99
Figure 6-16: Downstream software vs relationship 5-19 for higher blockage ratios 100
Figure 7-1: 2 Boulders geometrical setup 103
Figure 7-2: Model 6 *Sp*=1.5m 105
Figure 7-3: Model 6 *Sp*=1.0m 105
Figure 7-4: Model 6 *Sp*=0.8m 105
Figure 7-5: Model 6 *Sp*=0.7m 105
Figure 7-6: Areal velocity change with reduction in spacing (Model 6) 107
Figure 7-7: Linear areal velocity changes up to local control (Model 6) 107

Figure 7-8: Areal histogram with reduction in spacing (Model 6)............................ 108
Figure 7-9: Areal velocity change for 1 boulder and 2 boulders (Model 1 and 2) ... 110
Figure 7-10: Areal velocity change for 1 boulder and 2 boulders (Model 3, 4, 5 and 6) 110
Figure 7-11: Blockage ratio vs areal velocity change 112
Figure 7-12: Froude number vs local control spacing 112
Figure 7-13: Spacing versus blockage ratio (Froude number 0.60-0.70) 114
Figure 7-14: Dimensionless spacing versus blockage ratio (Froude number 0.60-0.70).. 115
Figure 7-15: Model conditions for spacing relationship 116
Figure 7-16 below shows the relationships for the three Froude ranges which were investigated. Each range has a strong linear trend which can be used to easily determine the local control spacing. The channel width was used on each side of the equation and can be cancelled out, resulting in a simple spacing relationship which is only dependant on the boulder diameter. Figure 7-16: Spacing relationships for Froude ranges.. 116
Figure 7-17: 2 boulder ZOI relationship model conditions...................................... 118
Figure 7-18: Upstream software vs relationship 7-5Figure 7-19: Downstream software vs relationship 7-6... 121
Figure 7-20: Sides software vs relationship 7-7 122
Figure 7-21: Upstream software vs relationship 7-9.. 125
Figure 7-22: Downstream software vs relationship 7-10 125
Figure 7-23: Sides software vs relationship 7-11 126
Figure 8-1: 1 boulder below blockage limit design example.................................. 128
Figure 8-2: 2 boulders design example 133
Figure 8-3: 1 boulder above blockage limit design example.................................. 138
Figure 8-4: Upstream approach conditions 141

LIST OF TABLES

Table 2-1: Options for rehabilitation (adapted from Day et al., 2016b) 8
Table 3-1: Pre-processing variables 28
Table 3-2: Hydraulic effect example model 33
Table 4-1: 1 Boulder experimental conditions 39
Table 4-2: 2 Boulder experimental conditions 40
Table 4-3: Downstream correction factors for 1 boulder 49
Table 4-4: Downstream correction factors for 2 boulders 56
Table 5-1: Model 1 Conditions 58
Table 5-2: Model 1 ZOI dimensions 59
Table 5-3: Downstream correction factors for 1 boulder 70
Table 5-4: Upstream ZOI coefficients 71
Table 5-5: Downstream ZOI coefficients 71
Table 5-6: Side ZOI coefficients 72
Table 5-7: % Error and R^2 values 72
Table 5-8: Upstream practical ZOI coefficient 75
Table 5-9: Downstream practical ZOI coefficient 75
Table 5-10: Sides practical ZOI coefficient 75
Table 5-11: % Error and R^2 values practical approximation 76
Table 6-1: Model conditions below and above the blockage limit 80
Table 6-2: High blockage ratio models 81
Table 6-3: Effective width and minimum width 84
Table 6-4: Theoretical and experimental new approach conditions 88
Table 6-5: Upstream disturbance length 92
Table 6-6: Upstream flow depth increase 93
Table 7-1: Model 6 Conditions 104
Table 7-2: Model 1-6 conditions 108
Table 7-3: Areal velocity change 2 boulders vs 1 boulder 111
Table 7-4: Froude number ranges 113
Table 7-5: Froude range 0.60-0.70 spacing variation 114
Table 7-6: Froude number ranges spacing recommendations 117
Table 7-7: Downstream correction factors for 2 boulders 118
Table 7-8: Upstream ZOI coefficients 119

Table 7-9: Downstream ZOI coefficients 119
Table 7-10: Side ZOI coefficients 119
Table 7-11: % Error and R^2 values 120
Table 7-12: Upstream practical ZOI coefficient 123
Table 7-13: Downstream practical ZOI coefficient 123
Table 7-14: Sides practical ZOI coefficient 123
Table 7-15: % Error and R^2 values practical approximation 124
Table 8-1: 1 boulder below blockage limit: ZOI dimensions 132
Table 8-2: 1 boulder below blockage limit: habitats created with relevant ZOI dimensions 132
Table 8-3: 2 boulders: ZOI dimensions 137
Table 8-4: 1 boulder below blockage limit: habitats created with relevant ZOI dimensions 137
Table 8-5: 1 boulder above blockage limit: upstream and downstream ZOI dimensions 143
Table 8-6: 1 boulder above blockage limit: habitats created with relevant ZOI dimensions 143

Table_A- 1: 1 Boulder Test 1 d=0.11m experimental and software results 155
Table_A- 2: 1 Boulder Test 1 d=0.175m experimental and software results 156
Table_A- 3: 1 Boulder Test 1 d=0.235m experimental and software results 157
Table_A- 4: 1 Boulder Test 2 d=0.11m experimental and software results 158
Table_A- 5: 1 Boulder Test 2 d=0.175m experimental and software results 159
Table_A- 6: 1 Boulder Test 2 d=0.235m experimental and software results 160
Table_A- 7: 1 Boulder Test 3 d=0.11m experimental and software results 161
Table_A- 8: 1 Boulder Test 3 d=0.175m experimental and software results 162
Table_A- 9: 2 Boulders Test 1 d=0.076m experimental and software results 163
Table_A- 10: 2 Boulders Test 1 d=0.11m experimental and software results 165
Table_A- 11: 2 Boulders Test 2 d=0.076m experimental and software results 166
Table_A- 12: 2 Boulders Test 2 d=0.11m experimental and software results 167
Table_A- 13: 2 Boulders Test 2 d=0.275m experimental and software results 168
Table_A- 14: 2 Boulders Test 2 d=0.076m experimental and software results 169
Table_A- 15: 2 Boulders Test 3 d=0.11m experimental and software results 170

Table_A- 16: 2 Boulders Test 3 d=0.275m experimental and software results 172
Table_A- 17: 2 Boulders Test 2 d=0.11m experimental and software results 173

Table_B- 1: 1 Boulder below blockage limit model conditions............................... 175

Table_C- 1: Software and relationship ZOI lengths for 1 boulder upstream (10%-30% from uniform velocity) 177
Table_C- 2: Software and relationship ZOI lengths for 1 boulder upstream (40%-60% from uniform velocity) 178
Table_C- 3: Software and relationship ZOI lengths for 1 boulder upstream (70% from uniform velocity) 180
Table_C- 4: Software and relationship ZOI lengths for 1 boulder downstream (20%-40% from uniform velocity) 181
Table_C- 5: Software and relationship ZOI lengths for 1 boulder downstream (50%-70% from uniform velocity) 183
Table_C- 6: Software and relationship ZOI lengths for 1 boulder sides (10%-20% from uniform velocity) 184

Table_D- 1: Software and relationship ZOI lengths for 1 boulder upstream (10%-30% from uniform velocity) 186
Table_D- 2: Software and relationship ZOI lengths for 1 boulder upstream (40%-60% from uniform velocity) 186
Table_D- 3: Software and relationship ZOI lengths for 1 boulder upstream (70% from uniform velocity) 187
Table_D- 4: Software and relationship ZOI lengths for 1 boulder downstream (20%-40% from uniform velocity) 187
Table_D- 5: Software and relationship ZOI lengths for 1 boulder downstream (50%-70% from uniform velocity) 187

Table_E- 1: 2 Boulders model conditions.. 189

Table_F- 1: Software and relationship ZOI lengths for 2 boulders upstream (10%-30% from uniform velocity) ... 190
Table_F- 2: Software and relationship ZOI lengths for 1 boulder upstream (40%-60% from uniform velocity) ... 191
Table_F- 3: Software and relationship ZOI lengths for 1 boulder upstream (70%-90% from uniform velocity) ... 191
Table_F- 4: Software and relationship ZOI lengths for 1 boulder downstream (20%-40% from uniform velocity) ... 192
Table_F- 5: Software and relationship ZOI lengths for 1 boulder downstream (50%-70% from uniform velocity) ... 193
Table_F- 6: Software and relationship ZOI lengths for 1 boulder downstream (80%-90% from uniform velocity) ... 193
Table_F- 7: Software and relationship ZOI lengths for 1 boulder sides (10%-30% from uniform velocity) ... 194
Table_F- 8: Software and relationship ZOI lengths for 1 boulder sides (40%-60% from uniform velocity) ... 195
Table_F- 9: Software and relationship ZOI lengths for 1 boulder sides (70%-90% from uniform velocity) ... 196

LIST OF VARIABLES AND ABBREVIATIONS

Variables

Symbol	**Description**
m, n, o, p and *r* t	The empirical coefficients
P	Density of water
Cv	Velocity correction factor
Cyd	Distance correction factor
D	Representative bed particle size
e	Selective lumping parameter
p	Density of the water
b	Channel width
beff	Effective channel width
bmin	Minimum channel width for choking not to occur
d	Boulder diameter
d/b	Blockage ratio
E	Uniform specific energy
Ec	Critical specific energy
f	Function
Fr	Froude number
g	Gravitational constant
ΔH	Change in flow depth
Hc	Critical depth
H	Flow depth
i	Percentage variation from uniform velocity
i_b	Percentage velocity change at the banks
L	Length of upstream gradually varied profile
LC	Local Control
n	Manning's roughness coefficient
η	Water surface elevation
Q	Discharge
q	Discharge per unit width

Symbol	Description
R	Hydraulic radius
R^2	Coefficient of determination
S	Channel slope
Sp	Spacing between boulders
S_S	Specific gravity
Δt	Time step
t	Time
τ_*	Shield parameter
T_b	Boundary shear stress
τ_o	Uniform shear stress
τ_{oc}	Critical shear stress
U	Vertically averaged velocities in the X direction
v	Uniform velocity
V	Vertically averaged velocities in the Y direction
Δx	Triangle element size
x	Transverse ZOI distance
X	Transverse direction
x_e	Distance from the edge of the boulder to i_b
yd	Downstream ZOI distance
yu	Upstream ZOI distance
Y	Longitudinal direction
Z	Depth direction

Abbreviations

Acronym	Description
BB	Large Boulders
CS	Course Sediment
F	Fast
FD	Fast Deep
FI	Fast Intermediate

Acronym	**Description**
FS	Fast Shallow
FS	Fine sediment
FVS	Fast Very Shallow
GIS	Graphical Information Systems
HSC	Habitat Suitability Criteria
IFIM	Instream Flow Incremental Methodology
MVEG	Marginal Vegetation
PHABSIM	Physical Habitat Simulation Method
S	Slow
SD	Slow Deep
SS	Slow Shallow
SVS	Slow Very Shallow
VF	Very Fast
VS	Very Slow
WUA	Weighted Useable Area
ZOI	Zone of influence

1 INTRODUCTION

Lotic systems have historically provided vital resources for human survival. Freshwater ecosystems serve us by not only providing potable water and food but also supply the agricultural, industrial and recreational sectors. Given the reliance on freshwater it is noteworthy that only 0.006% of the world's freshwater is found in rivers and streams (Malmqvist and Rundle, 2002). Rivers are exploited by the use of their resources but are also subject to flow alterations which ultimately lead to physical habitat and chemistry alterations, direct removal or addition of species and ecosystem destruction (Malmqvist and Rundle, 2002). It is clear that balancing the needs of people as well as the needs of freshwater ecosystems is a critical environmental issue.

Channel disturbances within aquatic habitats have been linked to a decreased abundance and diversity of species (Swales, 1993). Changes in habitat conditions result in homogenous channel forms with near uniform flow regimes; leading to the conclusion that a loss of biodiversity in aquatic ecosystems is due to habitat homogeneity (King et al., 2010; King et al., 2003; Palmer et al., 2010; Harrison et al., 2003). The habitat heterogeneity hypothesis proposes that if a variation of hydraulic conditions is found then a variation of species will be also be found.

Different species require different habitats, but each species also requires a variety of habitats. Rutherfurd et al., (2000a) explains that species need different hydraulic conditions on a day to day basis, for activities such as feeding, resting, reproducing or for refuge from floods. These species will furthermore change habitats requirements in a life cycle as well.

It is therefore necessary to quantify which hydraulic conditions are preferred by certain species throughout their life cycle, in order to create the most suitable heterogeneous habitat conditions. Thereby the focus of this study was to follow a paradigm which aimed to increase suitable habitat heterogeneity for the purpose of aquatic biodiversity.

Bio-engineering which aims to assimilate both biological and engineering principles can be used as a rehabilitation technique (King et al., 2010). Boulders placed in the channel function as bio-engineering instream rehabilitation structures, which aim to increase the habitat diversity. Habitat diversity is achieved by inducing diversity into the hydraulic and substratum conditions (King et al., 2010). The use of boulders is likely to be most effective if the degradation of the physical habitat was due to homogenous instream habitats, which are prone to occur in channelised rivers (King et al., 2010).

1.1 Layout of Report

Section 2 (Background) outlines the literary background. The current degraded state of aquatic ecosystems was highlighted. The principles of rehabilitation were discussed as well as the techniques used for rehabilitation. The placement of boulders is a localised instream measure which can be used to recreate diverse aquatic habitats. The hydraulic habitat of riverine species was investigated to gain a better understanding of why species live where they do. Different ways in which the hydraulic variables, influenced by the placement of a boulder, could be quantified were considered. Lastly the use of two-dimensional hydrodynamic software was investigated.

Section 3 (Methodology) presents the methodology used in the research project. The fundamental variables which affect the velocity and flow depth around a boulder in a channel were identified in order to investigate the impact of boulders in various flow and geometric conditions. The laboratory experiments were undertaken in a flume and the velocity was measured using a three-dimensional water velocity sensor. Following the laboratory experiments, a two-dimensional hydrodynamic finite element software was used, namely Argus ONE and RiverFLO-2D.

In **Section 4 (Software and Experimental Correlation)** the correlation between the software and the experimental results is analysed. Experimental runs were carried out in order to test the accuracy of the Argus ONE and RiverFLO-2D. The correlation between the results was firstly discussed for the case of 1 boulder and then for the case of 2 boulders.

In **Section 5 (Influence of 1 Boulder)** the change in velocities caused by a single boulder placed in the middle of a channel is investigated. This section looked at scenarios where the ratio of the boulder diameter to channel width (blockage ratio) was small enough that boulders only created a local and not a global effect. The variables influencing the size of the resultant velocity distributions were analysed to determine an empirical dimensionless relationship to describe the changes in velocity.

In **Section 6 (Blockage Ratio Limit),** single boulders are investigated for larger blockage ratios. The disturbed area around boulders was clearly different when the blockage ratios became larger. The difference in the velocity distribution was analysed and relationships developed to describe the different behaviour. The empirical dimensionless relationship developed in Section 5 was again applied.

In **Section 7 (Influence of 2 Transverse Boulders)** the case of one boulder is expanded by investigating the velocity disturbance around two boulders to assess the flow interaction. Two boulders were placed on the same transverse axis and the spacing between them varied. Recommendations were made on a favourable spacing and a relationship provided which predicts the velocity change at the favourable spacing.

In **Section 8 (Design Examples)** the findings from Section 5-7 are summarised by means of design examples. These examples aim to provide guidance for rehabilitation practitioners by showing the process of selecting boulder size and calculating the resultant habitat created.

Section 9 (Conclusion and Recommendations) concludes the research report by summarising all findings. Additional considerations were provided, and further research proposed to expand on the use of boulders for aquatic rehabilitation.

2 BACKGROUND

2.1 Introduction

2.1.1 Current State of Ecosystems

The sustainable use of water for economic, social and environmental benefit has been central to water management in South Africa since the advent of democracy. The National Water Act (NWA, No. 36 of 1998) aims at achieving sustainable water use by ascribing equal status to the human needs of water and the ecological needs of water. The White Paper on a National Water Policy for South Africa expands on the protection of water resources in one of its founding principles:

> The quantity, quality and reliability of water required to maintain the ecological functions on which humans depend shall be reserved so that the human use of water does not individually or cumulatively compromise the long-term sustainability of aquatic and associated ecosystems (DWAF, 1997:64)

Given that there are the necessary legislative requirements to protect aquatic ecosystems, the state of these ecosystems show that the underlying principles of water legislation in South Africa have not been effectively implemented. The Department of Environmental Affairs and Tourism (DEAT, 2007) state that aquatic ecosystems are the most threatened out of all ecosystems in South Africa, as they are in the worst present conditions and are also experiencing accelerated loss of functioning. The State of the Environment South Africa (2007:42) brings sobering awareness by way of an integrity assessment which found that “48% of rivers are moderately modified, 26% are critically modified and only 26% of rivers are intact”. The above-mentioned status of water resources calls firstly for South African rivers to be restored and for these measures to be central in future water use projects.

Although the National Water Act protects the water available for ecological functioning, the flow in rivers are no longer the same as their pre-developmental or pre-settlement state. Water in rivers now also meets human needs for sanitation, agriculture, industry and recreation. Water quality has been compromised in many rivers due to a wide array of pollutants and flow changes. An alteration of flow from an original state affects the fish, invertebrates, vegetation and morphology of the river. Flows can be changed in magnitude and flow can also be changed by the duration and frequency of low or high flows (Day et al., 2016c). Rivers have also been structurally altered for water storage and increased conveyance. Water storage changes the upstream release rate while also commonly impedes connectivity, which is needed by aquatic species. Surface roughness is decreased by lining channels with concrete, beds are lowered, banks widened, and vegetation removed to accommodate increasing storm water runoff caused by urbanisation. The decrease in water quality and the changes to the flow regimes and channel geometry have resulted in a decline of aquatic species diversity (*Day* et al., 2016a).

2.2 Rehabilitation

2.2.1 What is Rehabilitation?

An intuitive river management principle would be to protect rivers to prevent degradation and avoid resorting to expensive rehabilitation projects. Although this principle should be the basis of future considerations, the pressing reality is that there are many degraded ecosystems which need interventions. When improving the degraded lotic systems, it is important to differentiate between restoration, rehabilitation and remediation. These three terms differ in the degree in which they aim to return the degraded system to its pre-disturbance state (Lovett and Edgar, 2002).

Fogg and Wells (1998, as cited in King et al., 2003) define river restoration as reinstating an ecosystem to the state prior to disturbance. Although the principle of restoration is an admirable one it is highly unlikely, as the pre-disturbance condition is not always defined, and it would also require the inputs and outputs of the ecosystem to be that of the original system. King et al. (2003) highlight river rehabilitation as an attainable process where the end condition will only resemble its ‘pre-European’ condition but still be in an improved state compared to the degraded system. Lastly it is also necessary to note that if irreversible changes have been made to a river, a remediation principle could be used instead. Lovett and Edgar (2002) explain that river remediation aims to improve the ecosystem, but the end point will not resemble the pre-disturbance condition.

The Water Research Commission has recently published the first comprehensive river rehabilitation manual for South Africa. Day et al. (2016b) built on the definitions above, while also acknowledging that aquatic ecosystems are both dynamic and complex, to produce five key principles for river rehabilitation, namely:

1. Return the ecosystem to a more natural state.
2. Rehabilitation is an interdisciplinary activity.
3. Treat the problem and not the symptoms.
4. Rivers are dynamic systems.
5. Monitoring of rehabilitation projects is essential.

The first principle re-emphasises the definition of rehabilitation, in that any rehabilitation project should strive to return the ecosystem to a more natural state. Secondly river rehabilitation should be recognised as an interdisciplinary activity. The interactions of ecological, hydrological and geomorphological factors determine the state of a riverine ecosystem. The diverse system determinates should similarly be modelled in a rehabilitation project by accounting for each of the factors independently whilst also considering their interaction (Day et al., 2016b). Not only do the factors affecting the state of an ecosystem need to be considered but they also need to be balanced to the needs of the surrounding community. Rutherfurd et al., (2000a) concisely summarise the interdisciplinary principle by noting that river rehabilitation is a subdivision of catchment management.

River rehabilitation should thirdly aim to address the underlying problem rather than treating the symptoms. The underlying problem will exhibit small scale symptoms within the river reach (Day et al., 2016b), such as bank erosion or excessive sediment deposition. The identification of the problem again emphasises the need to consider all the interacting elements within the catchment.

It is fourthly imperative that the determination of the natural state should consider the river's fundamental dynamic nature; rivers are neither spatially or temporally homogenous. As a result, a rehabilitation project should proceed with the knowledge that rivers have various natural states due to seasonal flow variations but are also constantly adapting (Day et al., 2016b).

Lastly monitoring should be undertaken following the implementation of a rehabilitation project. Monitoring allows the effectiveness of the project to be evaluated. The effectiveness of any engineering project needs to be monitored but this becomes even more pertinent when considering the complex interactions of catchments. Monitoring also allows for an adaptive management process (Rutherfurd et al., 2000a, Day et al., 2016b) which is necessary for a sustainable rehabilitation project.

2.2.2 Disturbances

King et al. (2003) explain that degradation of aquatic ecosystems can be caused by three main changes; namely physical, hydrological and chemical. The physical and hydrological changes change the flow regime and morphology of the river. A river can be physically altered by changing catchment land-uses or direct changes of the channel geometry. Erosion is increased and flow paths altered by land-use changes such as the replacement of indigenous vegetation with agricultural land or smooth impermeable surfaces, such as concrete. River channels are commonly altered to suit human needs; for example, channels can be deepened and widened to increase capacity. Hydrological changes to rivers directly affect the flow regime. King et al. (2003) explain that the flow regime is changed by the construction of dams, abstraction of water, inter-basin water transfer and effluent discharge. Water quality is degraded by chemical changes from agriculture, industrialisation and urbanisation (King et al., 2003). All three sources of change cause degradation of the aquatic ecosystem by reducing magnitude and diversity of species (King et al., 2003, Day et al., 2016b). A successful rehabilitation project cannot focus on one aspect of degradation but needs to holistically consider the quantity and quality of water within a specific channel.

2.2.3 Techniques

Given the broad range of disturbances, a similarly broad range of options for river rehabilitation exist. Day et al. (2016b) concisely grouped river rehabilitation options into 12 themes, as shown in Table 2-1 below. It should be noted that these rehabilitation themes are not mutually exclusive and will need to be used in conjunction with each other in such a way that rehabilitation interventions complement each other to address the various causes of degradation. This research project focused on expanding interventions under option 10; ‘Improving habitats and biodiversity’.

This investigation focuses on channel disturbance and the effect of channelisation. King et al. (2003) define channelisation as the alteration of channels through narrowing or widening, raising or lowering, straightening, changing substrate or vegetation conditions and constructing embankments. Channelisation not only enables flood relief but also changes the natural conditions of the aquatic habitat.

Table 2-1: Options for rehabilitation (adapted from Day et al., 2016b)

Options for rehabilitation	
1. Managing invasive species	7. Removal of weirs
2. Vegetation establishment	8. Water quality improvements
3. Managing flood risks	9. Rehabilitation and flow regimes
4. Managing river bank erosion	10. Improving habitats and biodiversity ❖ Improving habitat biodiversity in channelised rivers ❖ Improving habitat biodiversity in canals ❖ Improving habitat biodiversity in floodplains
5. Managing channel down cutting	11. Managing rivers for indigenous fish
6. Managing sediment	12. River rehabilitation and society

2.3 Hydraulic Habitat

To understand why riverine species live where they do it is essential to assess their hydraulic habitat. Once their optimal hydraulic habitat is known it is possible to assess how a change in this condition would affect the species, or on the other hand which conditions need to be created when undergoing a rehabilitation initiative. Emphasis will be made on defining and changing local hydraulic conditions for ecological functioning, this is defined as ecohydraulic modelling (Cullis et al., 2010). In South Africa three dominant methods exist which describe the hydraulic habitats of fish and invertebrates, namely Habitat Suitability Criteria (HSC), Hydraulic Biotopes and Flow Classes (Cullis et al., 2010).

The HSC focuses on determining the common hydraulic conditions for a list of species. This is done by collecting velocity, depth and substratum particle sizes where the species under investigation are found. Species are then grouped based on the habitats that they share. A principal challenge to this method is the transferability of data from a particular location to make predictions about a different location; this results in a method which requires enormous amounts of data and time. Given that the HSC uses hydraulic parameters, the HSC can be compared to results from hydraulic modelling (Cullis et al., 2010).

In contrast to linking a hydraulic habitat to a particular species, a hydraulic biotope describes a group of species. A hydraulic biotope can be compiled by visually identified flow types and substratum types. This method is advantageous as it does not require large amounts of data when compared to HSC. A large downfall, especially in regard to this investigation, is that visually identified data are yet to be linked to hydraulic parameters and thus cannot be used in hydraulic modelling.

Flow Classes, whilst being similar to HSC are instead broad predefined categories which are semi-quantitative. The distinction between the classes is made using velocity and flow depth. Kleynhans (1999) (as cited in Cullis et al., 2010) produced four Flow Classes for fish as seen in Figure 2-1 below; where SS = Slow Shallow, FS = Fast Shallow, SD = Slow Deep and FD = Fast Deep.

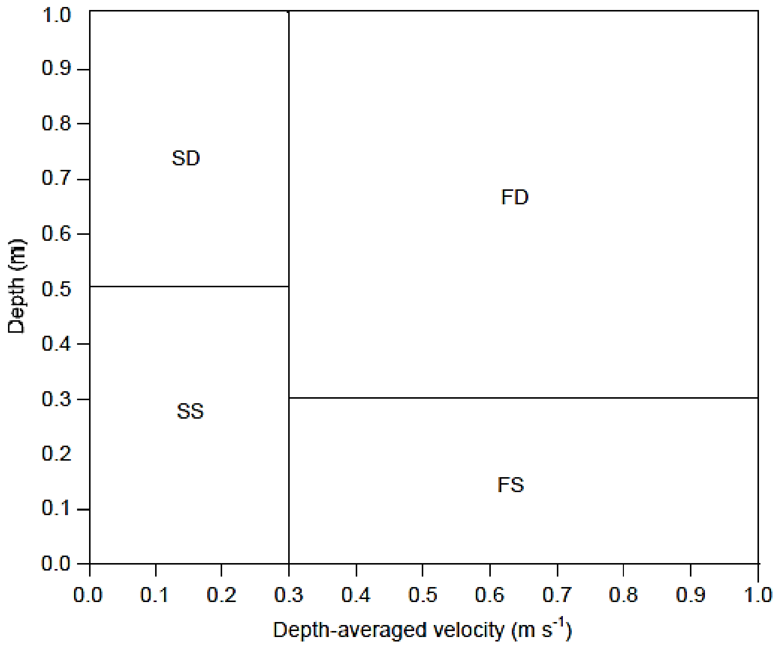

Figure 2-1: Flow classes for fish (Cullis et al., 2010:62)

Using the idea of Flow Classes, it becomes possible to create micro-hydraulic habitats, so that a more diverse species group is found. Figure 2-1 shows Flow Classes which have been divided into smaller ranges by Jordanova et al. (2004) (as cited in Birkhead, 2010); where SVS = Slow Very Shallow, FVS = Fast Very Shallow and FI = Fast Intermediate.

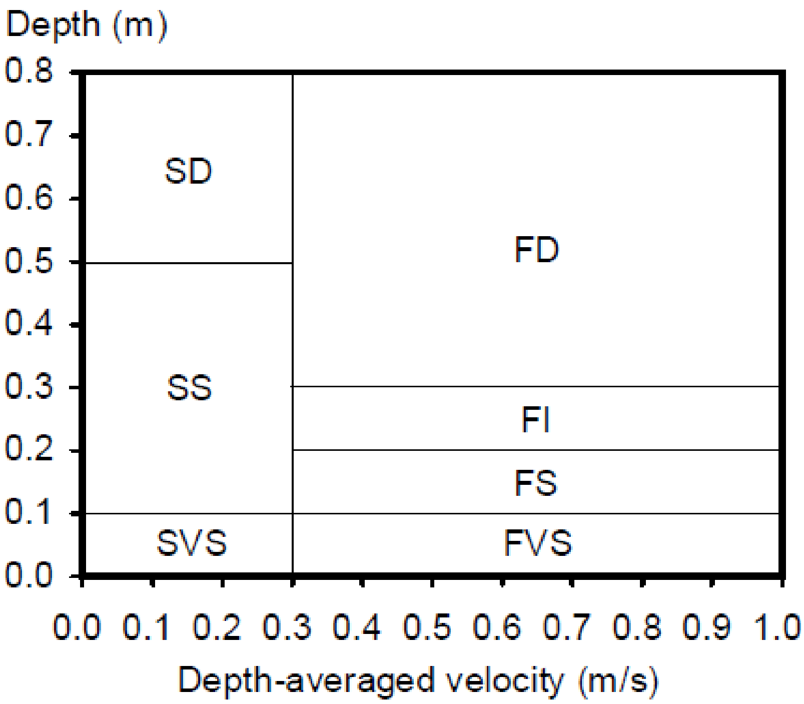

Figure 2-2: Extended flow classes for fish (Birkhead, 2010: 203)

Flow Classes have also been developed for invertebrates. Hirschowitz et al. (2007) (as cited in Birkhead, 2010) separated the Flow Classes using velocity and substrate as shown in

Figure 2-3. The velocity is described by VS = Very Slow, S = Slow, F = Fast and VF = Very Fast. The substrate conditions are described as FS = Fine sediment, CS = Course Sediment, BB = Large Boulders and MVEG = Marginal Vegetation. The Flow Classes are described using the velocity and substrate type; for example, VSFS represents Very Slow velocity and Fine Sediment substrate.

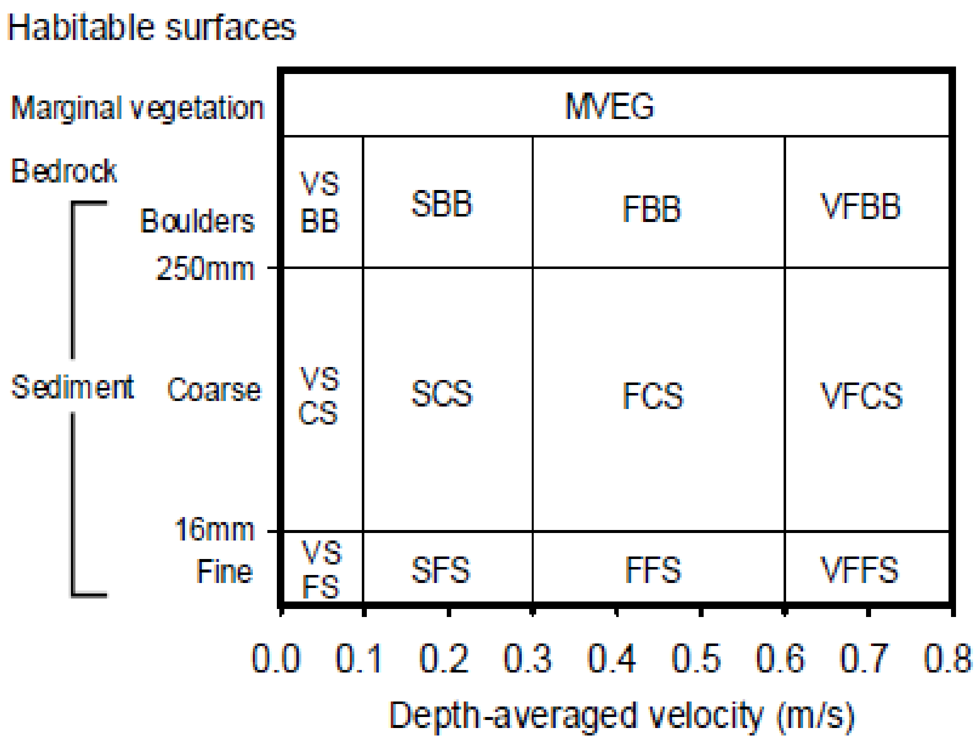

Figure 2-3: Flow Classes for invertebrates (Birkhead, 2010: 203)

2.3.1 Tools to Describe Habitat

The description of hydraulic habitat is however species specific and it would be valuable to describe the velocity variations in terms of magnitude change to undisturbed conditions. Measuring hydraulic change with distance and area are tools which are used to describe hydraulic habitat.

Hamuy-Blanco (2013) quantifies the area whereby the boulder disturbs the flow (changing velocity from uniform conditions) around it by using a Zone of

Influence (ZOI). Figure 2-4 shows how the extent of a ZOI can be defined by its upstream *(yu_i)*, downstream *(yd_i)* and transverse *(x_i)* distances. In these distances *i* represents the percentage variation from the undisturbed velocity. The co-ordinates for all four directions could be connected to indicate an area around the boulder. The final ZOI dimension for a certain percentage range indicates the area around the boulder where one would find either a percentage decrease or increase from uniform velocity. The flow around the sides of a boulder have an increased velocity while the upstream and downstream flow have a decreased velocity. This is discussed in more detail in Section 3.

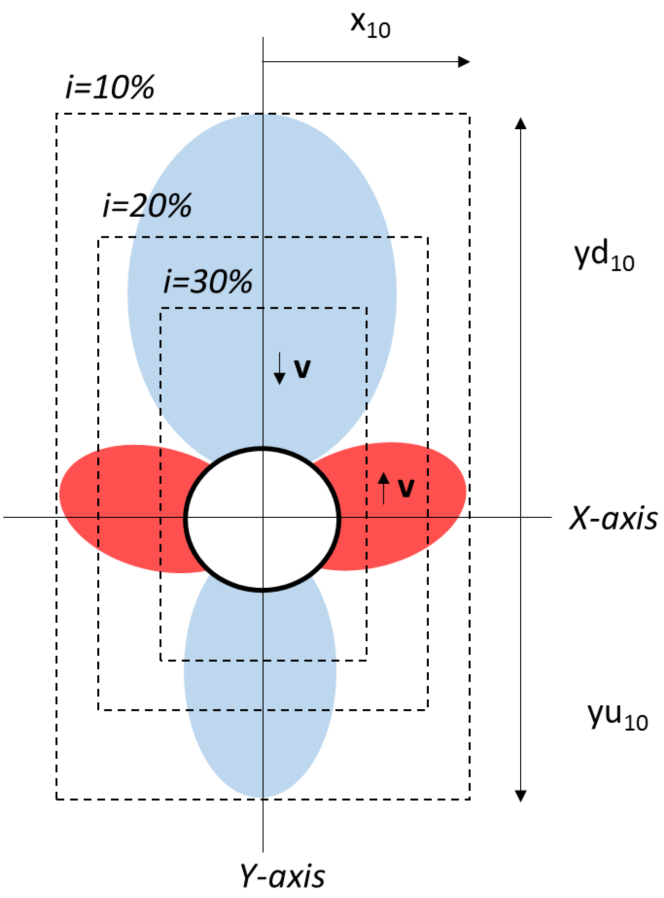

Figure 2-4: Zone of influence around a boulder (adapted from Hamuy-Blanco, 2014)

The Instream Flow Incremental Methodology (IFIM) uses computer models to calculate the relationship between hydraulic conditions and aquatic habitats (Geller, 2010). The output of the IFIM produces a Weighted Useable Area (WUA) which is the amount of physical habitat which is available for a certain flow rate (Jeong et al., 2010). Velocity frequency histograms, which are similar to the WUA approach, will be used in this investigation as similarly used by Hamuy-Blanco (2013) and Riddet (2012). The velocity frequency histogram is constructed by

> considering a grid covering an area of the channel and calculating the velocities at the centre of each grid section. All sections that have a velocity that fall in the same range have their corresponding areas added up and divided by the total area in order to give a proportion and get a frequency histogram (Hamuy-Blanco, 2013:29).

2.4 Boulders

2.4.1 Linking Boulders to Habitats

Boulders create hydraulic diversity by altering the velocity and flow depth of water in the immediate surroundings. Boulders cause the flow velocity to increase along the sides and decrease both upstream and downstream of the boulder (Hamuy-Blanco 2013). The decreased velocity coupled with turbulence creates scour pools downstream of the boulders.

Saldi-Caromile et al. (2004) highlight the benefit of having a velocity gradient around boulders. The low velocity region is surrounded by high velocity flows, which creates a velocity gradient. The high velocity flows commonly contain food, and as a result provide an ideal way for many species to feed while in the low velocity zone. This feeding method requires less energy and boulders have as a result been proven to be effective in rehabilitating habitats for fish such as salmonids (Saldi-Caromile et al., 2004). The downstream scour pool also creates a micro-habitat for aquatic organisms such as invertebrates (Saldi-Caromile et al., 2004). These organisms use this space for protection from predators and to reproduce (Rutherfurd et al., 2000a).

2.4.2 Where to Place Boulders

Saldi-Caromile et al. (2004) suggest that the use of boulders would not be beneficial in channels which have high sediment loads or in areas of deposition. Deposition will occur around the boulder and there is a possibility of the scour pools being filled with sediment or submersion of the boulder by sediment.

Saldi-Caromile et al. (2004) also advise against using boulders on steep channels (gradient steeper than 4%) as these gradients most probably have a step-pool morphology already including boulders or are unstable with erosion which would limit the life span of the boulder. Similarly, further consideration will be required if boulders are to be placed in incised channels as boulder stability could be compromised and bank erosion could be increased.

Day et al. (2016c) similarly do not advocate the use of boulders in rivers with high sediment loads and/or with dynamic bed movement. When considering the river from source to end, a river starts within the mountains, travels down along foothills and ends along large floodplains (Day et al., 2016c). Boulders should be placed in the headwaters or upper parts of foothills where the sediment load is lower and boulders would likely to be present in the systems natural state.

2.4.3 How to Place Boulders

Although there are some recommendations on the placement of boulders there is a need for greater investigation. One principle that has arisen logically is that the boulder should maximise the flow disturbance.

Orientation and position in channel

Rutherfurd et al. (2000b) suggest that the longest dimension of the boulder should be perpendicular to the flow and boulders should be placed near the centre of the channel or in the area with the fastest flows. Furthermore, a boulder should also be placed in the centre so as to avoid bank erosion. Hamuy-Blanco (2013) also found that angular boulders with their most bluff side facing upstream created more disturbance when compared to other shapes. Saldi-Caromile et al. (2004) suggest that the longest dimension of the boulder should be parallel to the flow to reduce excessive scouring and boulder instability, this will however reduce the change in flow.

Patterns

Saldi-Caromile et al. (2004) suggest that boulders should be placed in patterns which replicate natural streams or should be placed in clusters of three to seven. Scheuler and Brown (2004) and Brown and Johnson (1999) suggest that triangular boulders should be used, and they should be placed in groups of three to five. Hamuy-Blanco (2013) on the other hand advised that linear lines of boulders transverse to the direction of flow be used as opposed to non-linear arrangements; this method however does have a lower aesthetic appeal.

Relation to channel width and high flow considerations

Hamuy-Blanco & James (2014) investigated the effects of multiple boulders transverse to the direction of flow. Interestingly, once more boulders were added it was found that the effect extended across the whole width of the channel and a considerable distance upstream. The instance where this occurred was found to be where the boulder to channel width ratio was greater than 0.075.

Guidelines have also implied a similar threshold width but with warning. Scheuler and Brown (2004) suggest that boulders should comprise of less than 10% of the cross-sectional area. Brown and Johnson (1999) advise that boulder diameters should be no more than a 1/8 of the width of the channel and if they are greater, bank stabilisation measures should be considered. Saldi-Caromile et al. (2004) suggest that boulders should be limited to 20-30% of the cross-sectional area to avoid excessive bank scour, debris accumulation and flooding.

Boulders will often retain large pieces of wood, which will create additional habitat (Saldi-Caromile et al., 2004). In high flown, it is recommended that boulders are submerged so that wood can flow over the boulder for additional flooding upstream to be avoided.

2.5 Two-Dimensional Modelling

The use of Flow Classes highlights flow depth and velocity as the central hydraulic variables. These key hydraulic variables need to be assessed by their variation over a localised area surrounding a boulder. Laboratory and field measurements are time consuming and can have physical constraints with regards to channel size and discharge variations. Numerical models reduce the time-consuming nature of manual measurements but also allow for hydraulic habitats to be predicted for a range of options in the design process.

2.5.1 Comparing One, Two and Three-dimensional Modelling

Numerical models have been used since the 1980s with the Physical Habitat Simulation Method (PHABSIM) one-dimensional model being one of the popular tools (Diplas & Shen, 2007). In one-dimensional modelling, flow is only considered in the streamwise/longitudinal area and velocity and flow depth are constant over any transverse section (Birkhead et al., 2007). The approximation of flow variables to be constant over transverse sections is an adequate assumption in large-scale river models, but boulders cause complex and localised flow variations.

The use of two-dimensional modelling to evaluate aquatic habitats has gained momentum over the last few decades. Two-dimensional modelling outputs streamwise and transverse velocity distributions as well as flow depths over any cross-section (Blackburn and Steffler, 2002). These models however still use depth-averaged results. The ability of two-dimensional models to consider transverse flow and velocity gradients over a fine scale allow the effect of boulders to be quantified.

Three-dimensional modelling has also been used in habitat restoration projects albeit to a lesser degree than two-dimensional modelling. Diplas and Shen (2007) investigated the ability of two-dimensional and three-dimensional modelling to predict the velocity profile downstream of a boulder. The three-dimensional model predicted two vortices forming on the downstream edge of the boulder which rotated in opposite directions causing a zone of negative flow behind the boulder, which was closely aligned to measured velocities. The two-dimensional model could not account for the complex turbulence zone and only predicted reduced velocities behind the boulder. Diplas and Shen (2007) noted that velocities further downstream of the boulder were accurately depicted with two-dimensional software and three-dimensional software tended to overpredict the velocities. Diplas and Shen (2007) recommend that the use of two-dimensional modelling to accurately predict the complex flow pattern downstream of boulders requires further investigation.

Pasternack et al. (2005) agree that three-dimensional models have the ability to more accurately simulate wakes and vortices but mentions two key constraints for the use of such models. Firstly, the measurement of three-dimensional velocities and depths for calibration and validation of models to study sites becomes very labour intensive. Secondly, most ecological and hydraulic methods used in rehabilitation have been determined using depth-averaged principles which is in line with two-dimensional modelling (Pasternack et al., 2005).

2.5.2 Learnings from Two-dimensional Modelling

Waddle (2010) compared the results of field measurement to a two-dimensional model at irregular locations around two boulders in a river in Colorado, USA. The velocities and depths that were a considerable distance upstream of the boulders showed smaller errors than those measured close to the boulders. Errors in the depth and velocity prediction from the software were described to be due to errors in the model and errors in measurement. Model errors include discretisation in the mesh, depth averaging and errors within the development of the model. Measuring errors include discretisation of the bathymetric data, instrument calibration and the operation of instruments. Waddle (2010) suggests that the reasoning for the errors within two-dimensional models should be noted and reduced where possible. If care is taken to reduce errors, Waddle (2010) suggests that two-dimensional models are generally accurate in describing habitats.

Crowder and Diplas (2000) analysed the effect of boulders placed in a river for habitat creation using two-dimensional software. The boulders did not change the average velocity for the modelled reach but showed localised changes in velocities. It was noted that although the impact of boulders is localised, boulders were still found to provide habitat, with the observation of trout in the vicinity the boulders. The flow showed large velocity reductions of up to 96% downstream of the boulders. The results also predicted velocity changes 6-8 boulder diameters downstream.

Crowder and Diplas (2000) explain that the bathymetric survey used for two dimensional models is of great importance in the analysis of the velocity profile around obstructions like boulders. In a long reach, the survey data is unlikely to be detailed enough to define obstructions and these features can be, and have been historically, incorporated by changing the roughness of the bed instead. The use of roughness to describe obstacles will result in the calibration of average flow conditions for the reach but the localised velocity changes around the obstacle will be ignored. Defining habitat suitability using a change in roughness will only consider the resultant flow depth and velocity at that point and the valuable habitat created around the obstacle will not be considered, resulting in an underestimation in habitat suitability (Crowder & Diplas, 2005).

Crowder and Diplas (2000) also emphasise the importance of mesh definition in analysing localised velocity changes. It is recommended that mesh density be increased in areas of concern such as near the boulder or at banks which could be susceptible to erosion. The predicted results were found to converge at a certain mesh size, and this would be the optimum density as a denser mesh would only increase the computational costs. Crowder and Diplas (2000) conclude that there is no mesh density that would be suited to all models and that the optimum density should be considered on a case to case basis.

2.6 Conclusion

Human effects on flow regime, water quality and channel alterations have caused a degradation in aquatic health worldwide. There has been a drastic shift of thought over the past few decades to recognise the value of ecosystems and to protect them for future generations. River rehabilitation/remediation projects vary greatly depending on the underlying cause of degradation, rehabilitation goal and locality of the site. These projects are multi-disciplinary involving the understanding of the interactions of ecological, hydrological and geomorphological factors.

This investigation aims to contribute to the knowledge base of improving habitats and biodiversity within rivers by introducing and quantifying hydraulic heterogeneity. Methods used for defining hydraulic habitat consist of species-specific hydraulic conditions, visual analyses and grouping of hydraulic conditions for a range of species. Tools such as the ZOI or areal velocity change are then used to quantify habitat.

The use of boulders for rehabilitation simulates naturally occurring river habitats and has been acknowledged as a widely used tool to reintroduce habitats into degraded systems. The use of boulders is attractive as they are low risk rehabilitation structures. Boulders cover only a small portion of the channel and are therefore unlikely to cause great hydraulic changes within the overall channel reach, whilst still creating valuable local habitats.

The use of boulders is commonly analysed on a case to case basis and there is a lack of placement guidelines that can be used. Although the rehabilitation site should still be analysed, it would be helpful for designers to have a list of placement options available for their consideration.

The analysis of habitat creation is largely undertaken using two-dimensional numerical models. Three-dimensional modelling has also been used in habitat restoration projects albeit to a lesser degree as depth-averaged hydraulic principles are widespread. Two-dimensional modelling has difficulty predicting the turbulent wakes around boulders but has shown to correlate to field measurements at all other locations. The calibration of two-dimensional models is dependent on inputs and it has been found that the bathymetric survey and mesh refinement are important.

3 METHODOLOGY

There were four core methodological components to the research process. Firstly, the fundamental variables which affect the size of any velocity distribution were identified; these consisted of hydraulic variables (flow rate, velocity and flow depth) as well as geometric variables (slope, roughness, channel width and boulder diameter). The models which were investigated varied these fundamental variables in order to analyse velocity distributions.

Experimental runs were then performed to validate the accuracy of the software. The experimental runs were conducted in a customised flume. The velocity distribution in the channel was measured using a Vectrino 3D water velocity sensor. Following the laboratory experiments, a two-dimensional hydrodynamic finite element software was used, namely Argus ONE and RiverFLO-2D. The two programmes are integrated; Argus ONE is a pre- and post- processor while RiverFLO-2D is a processor. Once adequate calibrations were performed the software was used to describe the velocity distributions in a computationally effective manner.

The velocity profile was analysed using velocity measured in the laboratory and software computations. The upstream and downstream directions exhibited decreased velocities while the transverse directions saw an increase in velocities. The velocity changes at any point were calculated as an absolute percentage variation from the uniform value. The area of flow which was disturbed by the placement of a boulder was quantified by using a Zone of influence (ZOI). The ZOI measured the distance from the boulder where a certain percentage variation of velocity was experienced.

3.1 Variables of Interest

The fundamental variables which affect the velocity and flow depth around a boulder in a channel were identified. These variables were used in order to investigate the effect of boulders in various flow and geometric conditions. Subsequent sections used combinations of these fundamental variables in order to describe the velocity distribution or ZOI.

A channel's velocity profile will be affected by the placement of a boulder depending on the uniform velocity. From this it would follow that the variables that determine the size of a ZOI would also be the variables that determine the uniform velocity of a channel. The uniform velocity *(v)* calculated from the Manning formula, requires the input of channel characteristics discharge *(Q),* channel width *(b),* slope *(S)*, Manning's roughness coefficient *(n)* and the flow depth *(H)*.

These variables were varied one at a time to prove that they do indeed change the size of the ZOI. It was found that *Q* and *S* were directly proportional to the ZOI, while *n* and *b* were indirectly proportional. The above variables were used to analyse the effect of boulders for various flow conditions which could be found in a channel. The flow conditions varied within the subcritical flow regime and within the Flow Classes defined by Jordanova et al. (2004) and Hirschowitz et al. (2007).

A channel with the same uniform velocity would have different ZOIs depending on the size of the boulder *(d)* placed within it. Logically, a larger boulder would cause a larger zone of altered flow. It was practically important to allow the relationship to be valid for any size of boulder. The same was necessary for any width, *b,* of the channel. A relationship between *b* and *d* was defined, namely the blockage ratio. The blockage ratio is the sum of the boulder widths divided by the channel width. The use of the blockage ratio eliminates the importance of exactly what *b* and *d* were used, but rather focuses on the relationship between them.

As all relationships that were developed were empirical, it was necessary to arrange the variables in a way that allowed conditions to be analysed which were not used in the formulation. The use of non-dimensional relationships allowed for practical extrapolation. A dimensionless relationship is independent of scale and as a result generalises the problem, allowing predictions to be made for a situation which was not used in the forming of the relationship. This creates additional practical value for the relationship proposed and also reduces the computational effort in determining the relationship. The use of normalised variables has been central in relationship development.

The velocity distribution around a boulder was found to depend on the following variables for the upstream, downstream and transverse directions:

$$Q, \quad v, \quad H, \quad S, \quad n, \quad \frac{d}{b}$$

3.2 Key Assumptions

The following points explain the key assumptions or constants which were used in this research project:

- All boulders were circular and emergent.
- All channels were rectangular.
- Uniform flow was subcritical, defined as having a Froude number below 1.
- A constant Manning's roughness coefficient was used.
- The left and right results were combined to create a set of results for one side. The finite element grid as well as the underlying numerical methods of the modelling software resulted in the sides having small differences in their results. To amalgamate the left and right sides an average of their results was taken.

3.3 Experimental Models

The experiments were conducted in the hydraulics laboratory in the Civil and Environmental Engineering building at the University of the Witwatersrand. The experiments were carried out in a 10m long and 2m wide flume (Figure 3-1), which is controlled by a customised computer software system (Figure 3-2).

The resultant velocity distributions of boulders placed in the channel were measured. Different experimental conditions were analysed by changing the size of boulders, slope of the flume and flow rate. Once an experiment was set up, adjustments and checks were carried out to obtain uniform flow conditions. A velocity sensor was used to measure the velocity around the boulder in order to quantify the flow variations from uniform flow. The hydraulic effect of a boulder was then compared to the effect predicted by computer simulations using RiverFLO-2D and Argus ONE.

Figure 3-1: Hydraulics Laboratory

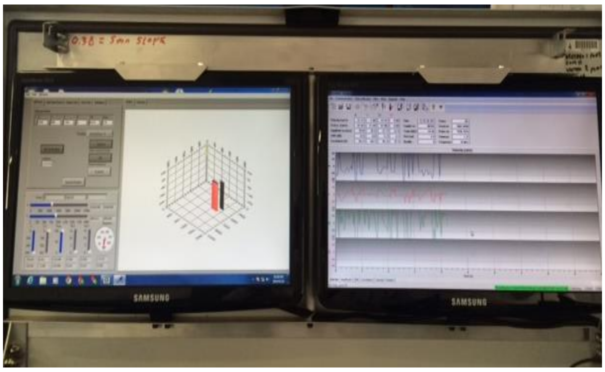

Figure 3-2: Customised computer software system

3.3.1 Setup of Experimental Conditions

The setup of any experimental run firstly required the placing of a boulder and the setting of the required slope and flow rate. Boulders were simulated in the flume by placing emergent cylinders onto the bed. The diameters of the boulders were varied but the breadth of the flume kept constant due to practical constraints (discussed further in Section 4.1.2). Different hydraulic conditions were set by adjusting the slope and flow rate of the flume. The slope and the flow rate were both inputted into the computer system, which makes the necessary adjustments. The roughness was kept constant for all experiments, from previous experimental runs *n* was found to be 0.010.

The computer system controls the slope of the flume by using two hydraulic jacks on the downstream end of the flume. A calibration was developed by comparing the computer input value to the slope measured by surveying equipment.

The water used by the flume is stored in a sump and is pumped into a header tank, it then flows into the flume and is recirculated by the header tank. The flow rate was specified in the computer system, the computer system proceeds to open the flow valve to the required quantity. The flow rate was also checked using a digital flow meter which has been installed in the feeder pipes (Figure 3-3). Lastly a v-notch weir was used as a last check (Figure 3-4); the flow rate was calculated using a calibrated stage discharge relationship.

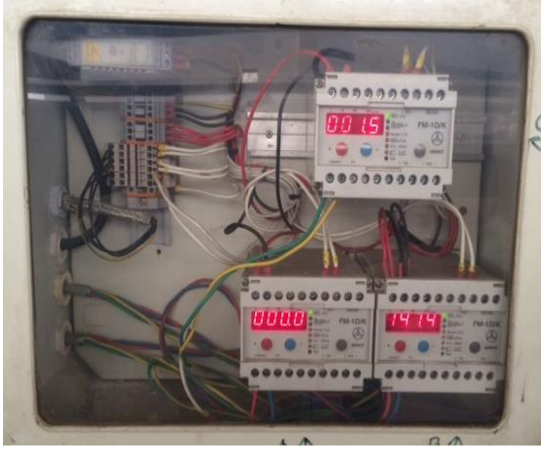

Figure 3-3: Digital flow meter

Figure 3-4: V-notch weir

3.3.2 Uniform Flow

All experiments required uniform flow to be present. Uniform flow was firstly obtained in an empty channel and then the same conditions were set, and a boulder placed in the channel. This allowed the effect of the boulder to be quantified by relating the velocity changes to the uniform flow velocity.

Once the slope and flow rate had been set, a sluice gate at the end of the flume (Figure 3-5) was adjusted to obtain the needed uniform flow. Uniform flow was achieved when the velocity and flow depths in the channel were constant throughout. A rough estimation of flow depths was made by measuring tapes which were placed at 10 positions along the flume. Once these flow depths were equal, precision flow depth measurements were made using a set of piezometers shown in Figure 3-6. The piezometers were attached to the flume bed at the same 10 positions.

The last check for uniform flow was the measurement of velocity using a Vectrino probe. The flow was uniform once the measured velocity was equal to the calculated value from the Manning equation and the measured velocity was constant throughout the flume. The velocity was measured at various points along the length of the flume.

Figure 3-5: Water flowing over sluice gate

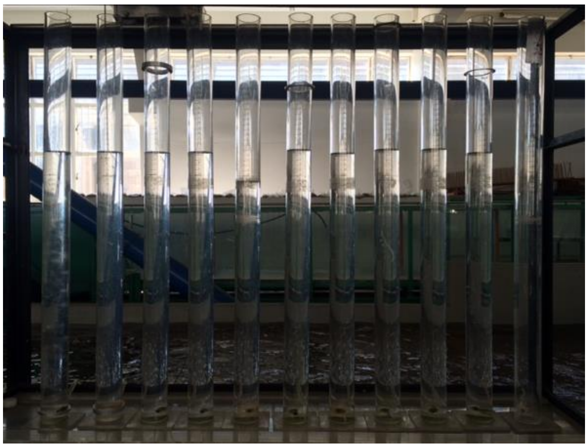

Figure 3-6: Piezometers

3.3.3 Velocity Measurement

The velocity was measured using the Nortek Vectrino 1 side looking probe, which is a three-dimensional water velocity sensor. The probe is mounted onto a supportive carriage way, which allows the probe to be moved in the transverse, longitudinal and depth directions. Once the carriageway was moved to the desired location by the computer system the Vectrino firmware installed on the same system was used to take readings.

The Vectrino uses the Doppler Effect to measure the velocity of the water. Nortek AS (2004) explain that the bistatic sonar probe emits sound pulses through its main beam, the pulses bounce off suspended particles in the water which are moving at the same speed of the water. The pulses are returned and received by the four side beams. The difference of frequencies of the emitted and received sound pulses allowed the calculation of the velocity of flow.

The data points were measured using the Vectrino side probe. All data points were measured for 40 seconds; this was to ensure that an adequate average velocity could be found. The velocity readings of the Vectrino fluctuated slightly in the order of magnitude of 0.010m/s. Boundary layer interactions cause the velocity to vary within the flow depth. The readings were as a result taken at 0.50 of the total flow depth, which have been prescribed as best practice by Pierce et al. (1941) and the United Stated Department Bureau of Reclamation (2001) as cited in Hamuy-Blanco (2013).

3.4 Argus ONE and RiverFLO-2D

Argus ONE has different operating forms; this project specifically used the software as an integrated application. RiverFLO-2D has been integrated with Argus ONE by means of a Plug-in-Extension. Argus ONE is a finite element pre- and post-processor which uniquely combines GIS with numerical modelling. RiverFLO-2D (FLO-2D Software, 2009) is the processor in this software suite; it is a hydrodynamic finite element model which simulates flow through a channel. The model represents the flow field in two dimensions allowing the effect of boulders to be more closely investigated.

Argus ONE was used to define the geometric setup of the problem. Argus ONE was then used to create a triangular finite element mesh over the model area. The automatic mesh generation tool within the programme was used. The mesh is generated using Delaunay triangulation algorithms (Riddet, 2012) and complies with three discretisation rules:

- Minimise the number of elements to effectively use computational power;
- Increase the number of nodes around boundaries or objects of interest; and
- Ensure that all elements are not acute or obtuse (Argus Holdings, 1997).

The model created in Argus ONE was exported to RiverFLO-2D which then used a finite element method to solve the model. RiverFLO-2D has three underlying assumptions. Firstly RiverFLO-2D uses the shallow water equations which are the resultant of the vertical integration of the Navier-Stokes equations for free surface water flow. Secondly the bed shear stresses are assumed to follow the depth-averaged velocity distributions. Lastly RiverFLO-2D does not account for dispersion or turbulence but rather incorporates the energy losses through Manning's *n* and the momentum equations (Hydronia, 2015). The shallow water differential equations are solved using the Galerkin weighted residual method where the discretised units are the triangular nodes. The sediment continuity equations are described as follows:

$$\frac{\partial \eta}{\partial t} + \frac{\partial UH}{\partial X} + \frac{\partial VH}{\partial Y} = 0 \qquad \text{3-1}$$

$$\frac{\partial U}{\partial t} + U\frac{\partial U}{\partial X} + V\frac{\partial U}{\partial Y} + g\frac{\partial \eta}{\partial X} + \frac{\tau_{bX}}{\rho H} = 0 \qquad 3\text{-}2$$

$$\frac{\partial V}{\partial t} + U\frac{\partial V}{\partial X} + V\frac{\partial V}{\partial Y} + g\frac{\partial \eta}{\partial Y} + \frac{\tau_{bY}}{\rho H} = 0 \qquad 3\text{-}3$$

where;

η is the water surface elevation, *t* is the time, *X* is the transverse direction, *Y* is the longitudinal direction, *U* and *V* are the vertically averaged velocities in the *X* any *Y* directions respectively, *g* is the gravitational constant and *p* is the density of the water. T_{bX} and T_{bY} are the boundary shear stress variables and are defined as follows:

$$\tau_{bX} = \frac{gn^2U\sqrt{U^2+V^2}}{H^{4/3}} \qquad 3\text{-}4$$

$$\tau_{bY} = \frac{gn^2V\sqrt{U^2+V^2}}{H^{4/3}} \qquad 3\text{-}5$$

The following discussion will highlight the procedures used to create, run and analyse the various models used in this research project. The discussion will follow the use of the programmes in their various capacities, starting with Argus ONE as the pre-processor, RiverFLO-2D as the computational engine and then Argus ONE as the post-processor.

3.4.1 Pre-processing in Argus ONE

Argus ONE was used to define the setup of the model by specifying the problem domain, bed elevations, roughness coefficient and the boundary conditions. The model was then completed by creating a triangular finite element mesh over the model. Figure 3-7 below shows an example of a completed pre-processing model. The discussion that follows will elaborate on each aspect of the model.

The GIS modules are represented by different information layers which are used to build a model. Argus ONE categorises layers into information, maps or data layers. In this study the bed elevations and the results were stored on the data layer. The information layer held the boundary conditions and roughness condition. Lastly the maps layer contained the visual plot results.

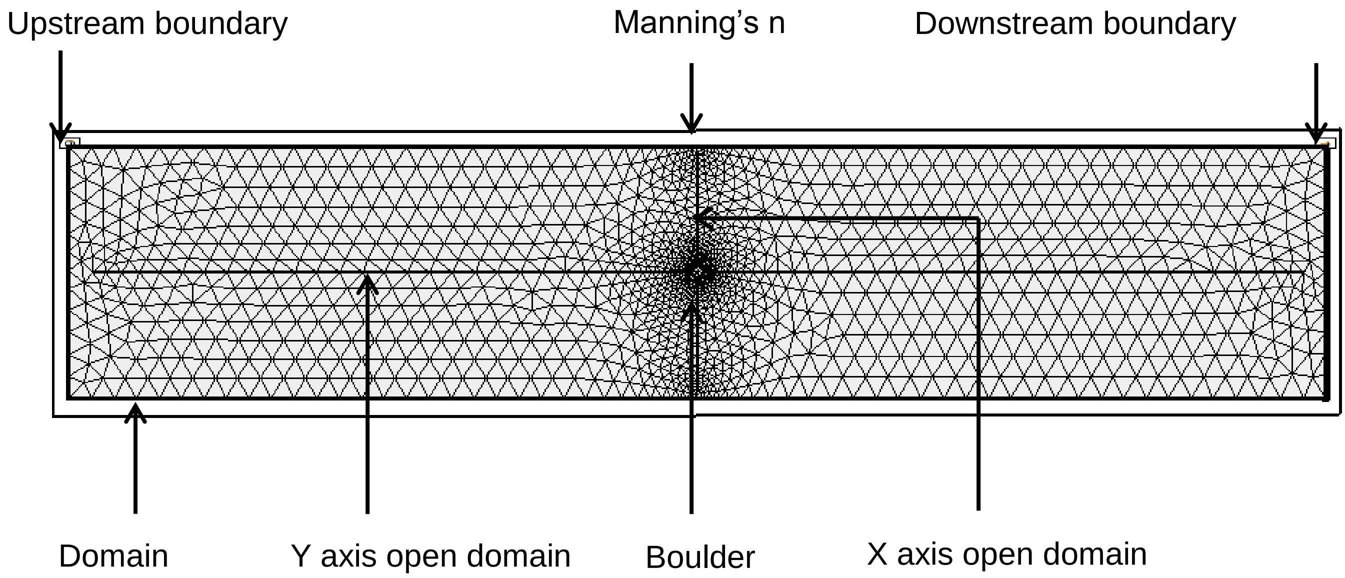

Figure 3-7: Argus ONE pre-processing model

The variables shown in Table 3-1 below were kept constant for all model runs. Their significance will be discussed in the following section.

Table 3-1: Pre-processing variables

Variable	**Value**
Domain outline density	0.180
Open contour density	0.0
Boulder density	0.0180
Manning’s *n*	0.010
Number of smoothing iterations	3.0
Element growth rate	Medium

Bed Elevations

The bed elevations described the geometry of the channel with data points, in the transverse (*X*), longitudinal (Y) and elevation (Z) directions. The data points between the two ends were described by interpolating the slope of the channel. Both the transverse and longitudinal directions had data points every 0.20m. At each point the bed elevation would be calculated by considering the distance from the upstream end and the slope. The *X* and *Y* values contextualised the scale and outline of the channel and the bed elevations were the actual data points onto which a surface was created.

Domain Outline

Once the bed points were stored it was possible to define the domain outline. The domain outline creates a fence around the problem area by drawing a polygon. Within the domain outline the bed surface is held along with the boulders and boundary conditions. The domain outline requires the input of a density which is then translated into the density of the finite element mesh.

Boundary Conditions

The boundary conditions were also polygons which were applied to the inflow and outflow boundaries. A boundary condition required the input of a number representing the type of boundary and a corresponding data file; all models used in this study had the same type of boundary conditions on the upstream and downstream ends. The upstream boundary was assigned a Type 6 boundary conditions and a data file containing a hydrograph. The downstream model was assigned a Type 1 boundary condition which corresponded to a data file containing the water surface elevation, calculated from the uniform flow depth. Both boundary conditions were set to be constant over the time period used.

Manning's *n*

The last information layer required was the Manning's *n* layer. The value was assigned over the entire surface by drawing a polygon around the domain outline, where a value was then entered.

Boulders

The placement of the boulders was the final addition to the model. The boulders were manually drawn into their respective positions and were then modelled as closed domain outlines. The extents of the channel were also closed domain outlines. As with the extent domain a density was specified for the automatic mesh generation.

Open Domains

It was necessary to compare the resultant velocities from the boulder for the experimental and software models. Argus ONE used an automated grid meshing to produce the various elements; the elements however did not correspond to the position of the velocities measured in the laboratory.

The creation of open domain contours ensured that the elemental nodes and measuring points coincided. The open contours were allocated along the *X* and *Y* axes of the boulder. Open contours are internal boundaries within the model, unlike the closed contours which were used to demarcate the river channel and boulder. When using the automated meshing function the nodes of the elements were set along the open contours, allowing one to then calculate the velocity distribution along the axes.

Triangular Mesh

Argus Holdings (1997) explain that in order to create a mesh for a particular project three things need to be done. Firstly, the domain which was meshed had to be defined; this was done in the model setup stage. Following this, mesh densities were entered and lastly the automatic mesh generation commenced.

The density assigned for each domain determines the size of the elements, which allows a modeller to decide on computational expenditure. The density of the domain outline used the default density. The density around the boulders was increased by a factor of 10.0 as this area was the core interest of the study.

3.4.2 Processing in RiverFLO-2D

As mentioned RiverFLO-2D was designed as a Plug-in-Extension for Argus ONE; which makes data easily transferable between the two programmes. The model created in pre-processing was exported from Argus ONE into RiverFLO-2D. RiverFLO-2D required the specification of the conditions under which the model was solved. These specifications were entered into the control tab, an example is shown in Figure 3-8 below. Figure 3-8 shows the values of the parameters used for all model runs. The following discussion will focus on the parameters which were vital for stability.

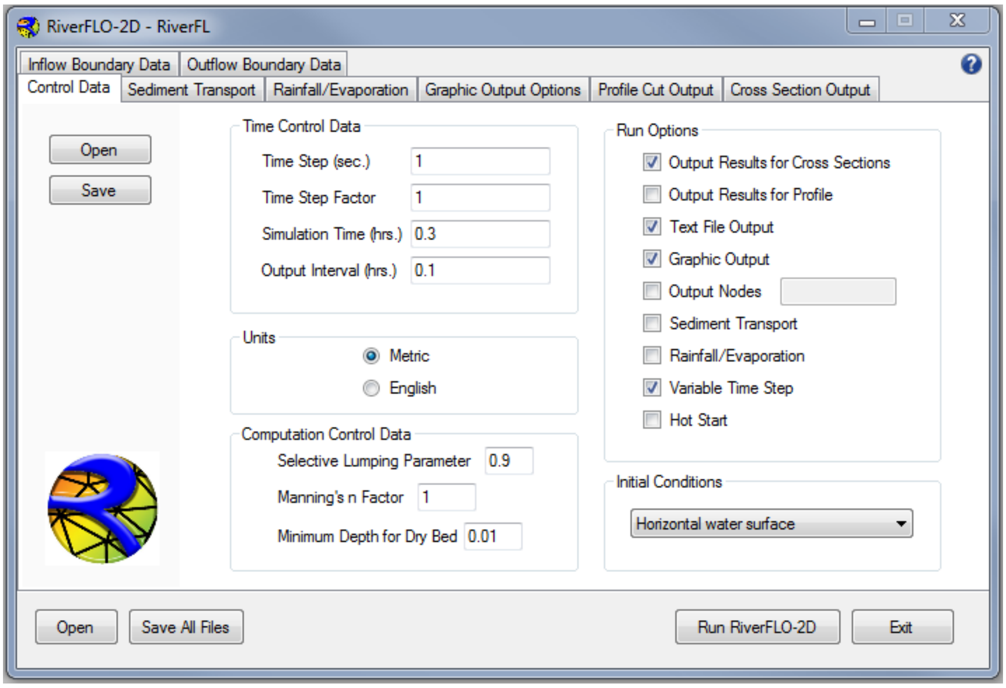

Figure 3-8: RiverFLO-2D control conditions

Time Control Data

The time step was critical to stability of the model, a maximum time step is calculated and the model could become unstable if this is exceeded in the calculation procedure. The maximum time step is defined by using the Courant-Frederick-Lewy condition (Argus Holdings, 1997).

$$\frac{\Delta t}{\Delta x} \leq \frac{4}{3}\left(\frac{3}{gh}\right)^{\frac{1}{2}}(1-e)^{\frac{1}{2}} \qquad \text{3-6}$$

Where Δt is the time step, Δx is the triangle element size and *e* is the selective lumping parameter.

During the simulations the flow depth varies which presents the opportunity for the time step to reach the maximum value. In order to ensure time step stability in test models the variable time step method was utilised. The variable time step allows for any necessary adjustments of the time step during simulation.

The simulation time directly influences the computational time of the model. The simulation time was incrementally decreased from 3 hours to 0.3 hours. At 0.3 hours the computational time was drastically reduced while also ensuring that the flow field results were the same as the longer simulation times.

Initial Conditions

The initial conditions allowed the simulation to start with either a wet or a dry bed. The horizontal water surface (wet bed) option was used in all models; this option starts the simulation at the uniform flow depth as specified by the boundary conditions. The wet bed choice reduced instabilities, confirming the same hypothesis as outlined by Hamuy-Blanco (2013).

3.4.3 Post-processing in Argus ONE

The resultant hydraulic variables were imported into Argus ONE once the computations were executed in RiverFLO-2D. The post-processing of the results took place in map layers, which allowed the results to be visually illustrated after importation. Figure 3-9 below shows an example of a visual representation of the velocity field around a boulder. The different colours indicate different velocity values; red indicates faster flow and blue slower flow.

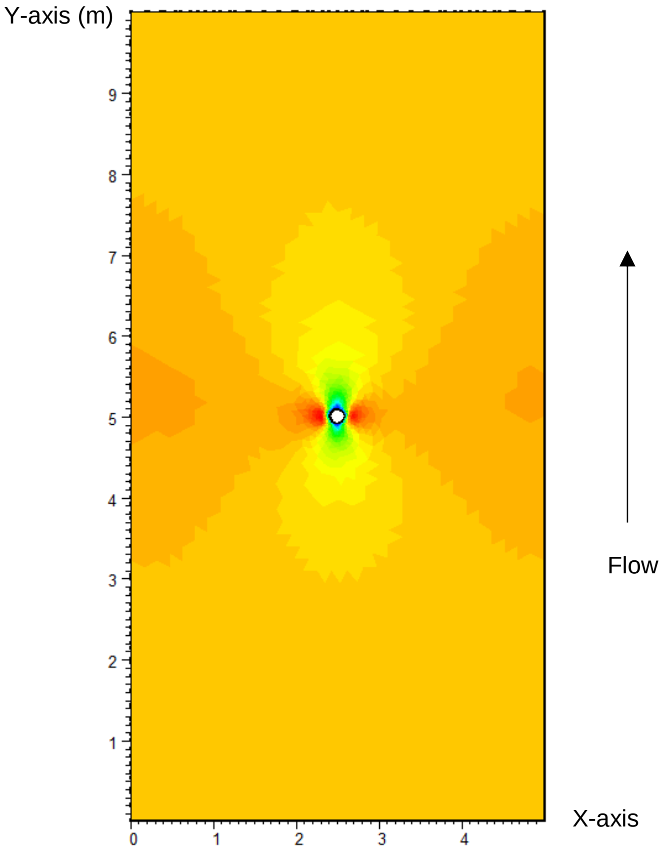

Figure 3-9: Post-processing visual velocity distribution

3.5 Hydraulic Effect of Boulders

The effect that a boulder had on the surrounding flow was quantified in terms of the flow depth and the velocity variations. In quantifying the hydraulic variables two methods were extensively used in the research process; namely the ZOI and areal histograms.

As mentioned, boulders placed in a channel reduce the velocity upstream and downstream of the object and increase the velocity on the sides. The velocity changes at any point were calculated as an absolute percentage variation from the uniform velocity. The same principles applied to the flow depth variations around a boulder.

The effects of boulders were investigated for different Flow Classes, as defined by Jordanova et al. (2004). The Flow Classes are dependent on both flow depth and velocity. It was found that the addition of a boulder in a channel influenced the velocity more than the flow depth. As seen in Figure 3-10 the changes in flow depth were observed at small localised areas around the edge of the boulders. Figure 3-11 shows that the velocity changes on the other hand were in the order of magnitude of several metres. The investigation of the blockage ratio limit did however show substantial flow depth changes. These flow depths were as a result incorporated into the analysis of the boulder (Section 6).

In order to visualise the localised flow depths around a boulder a model was analysed with the software. The model had the following conditions:

Table 3-2: Hydraulic effect example model

Q **(m^3/s)**	***S***	***n***	***b*** **(m)**	***d*** **(m)**	***H*** **(m)**	***v*** **(m/s)**
1.250	0.00080	0.010	5.0	0.20	0.242	1.033

Figure 3-10 and Figure 3-11 below show the variation of flow depth and velocity around a boulder respectively. Here the localised flow depth variation can be seen; as well as the significant velocity variation around the boulder. The hydraulic effect of a boulder was analysed in terms of only velocity when the flow depth changes were localised. When the flow depth changes were significant the hydraulic effect of a boulder was analysed in terms of velocity and flow depth.

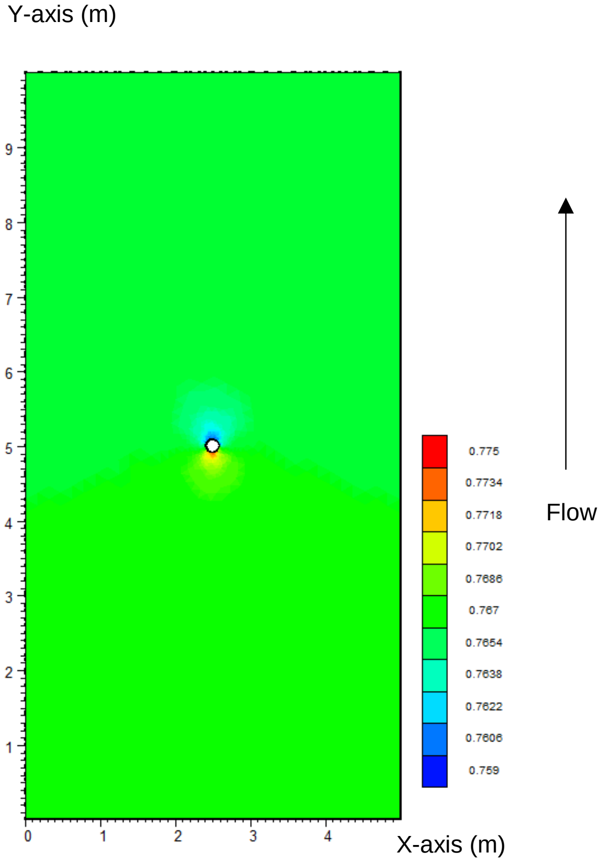

Figure 3-10: Flow depth variations around a boulder

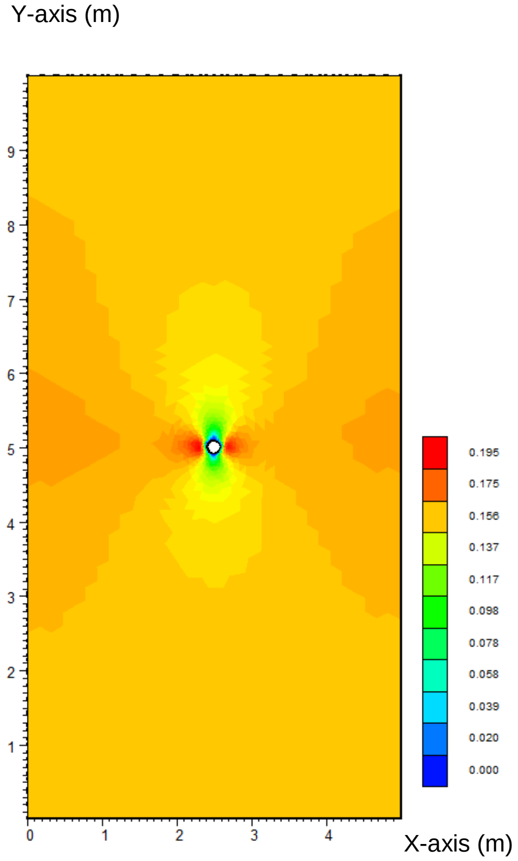

Figure 3-11: Velocity variations around a boulder

3.5.1 ZOI

The area of flow which was disturbed by the placement of a boulder was quantified by using a ZOI. The ZOI measured the distance from the boulder where a certain percentage variation of velocity was experienced.

Figure 3-12 illustrates a typical velocity distribution caused by a boulder as well as how the ZOI quantifies the distribution. The blue and red regions show the changes in velocity around the boulder. The shape and scale of these coloured regions should be noted. The disturbed velocity region is larger in the downstream than upstream direction. The increased velocities seen on the transverse axis exhibit the smallest velocity disturbance area. Figure 3-13 shows how the extent of a ZOI can be defined by its upstream (yu_i), downstream (yd_i) and transverse (x_i) distances. In these distances *i* represents the percentage variation from the undisturbed uniform velocity.

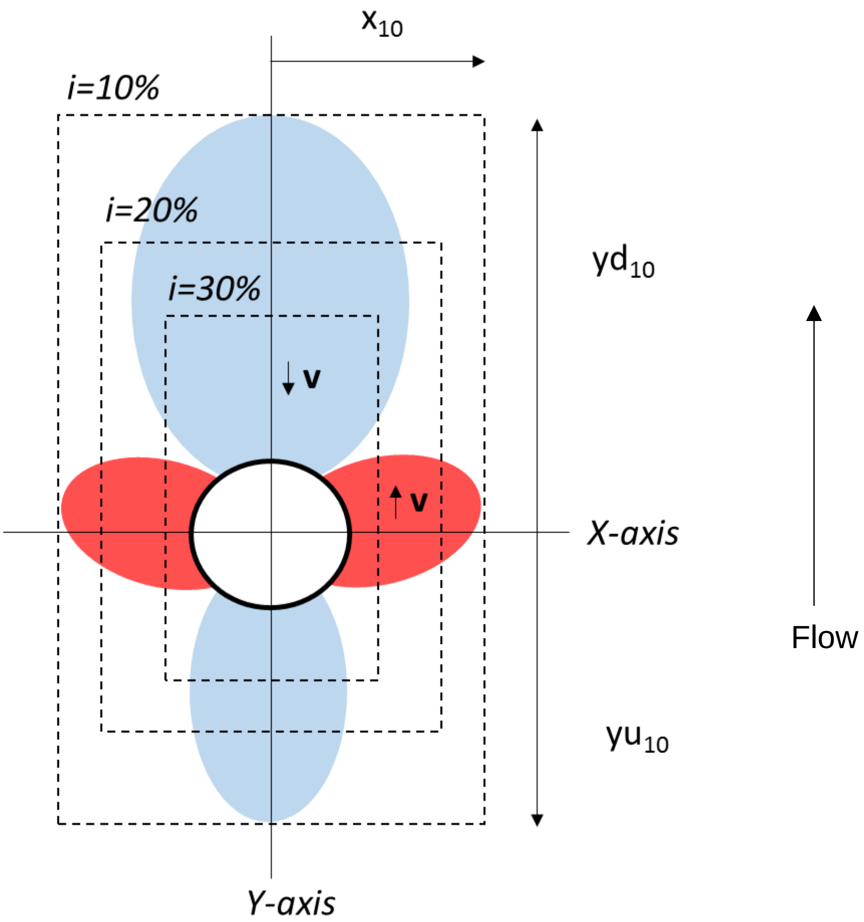

Figure 3-12: Zone of influence around a boulder (adapted from Hamuy-Blanco, 2014)

The centre of the boulder marked the origin of a Cartesian co-ordinate system, the *Y*-axis measured distances upstream and downstream and the *X*-axis distances from the left and right of the boulder. These distances correspond to the location in the channel where the velocity of interest could be found.

The size of the ZOI was calculated for changes in velocity from 0% to 100%. The size of the ZOI decreases when considering higher percentage variations, as these would only occur close to the boulder. The point at which a 10% velocity variation is found on any axis delineates the velocity variation above and below that point into two ranges. The velocity variations beyond the point will range between 0% and 10%. The velocity variations between the boulder and the point will range between 10% and 100%.

The same model used to show the velocity and flow depth variations around a boulder was used as an example to illustrate the ZOI (Table 3-2). Figure 3-14 below shows the ZOI dimensions around a single boulder for a 10% velocity variation. The velocity variation is of a considerable magnitude and can be compared to the boulder diameter (*d*=0.20m). The upstream ZOI is 3.5 times the boulder diameter, downstream approximately 5 times and the sides approximately 4.5 times the boulder diameter.

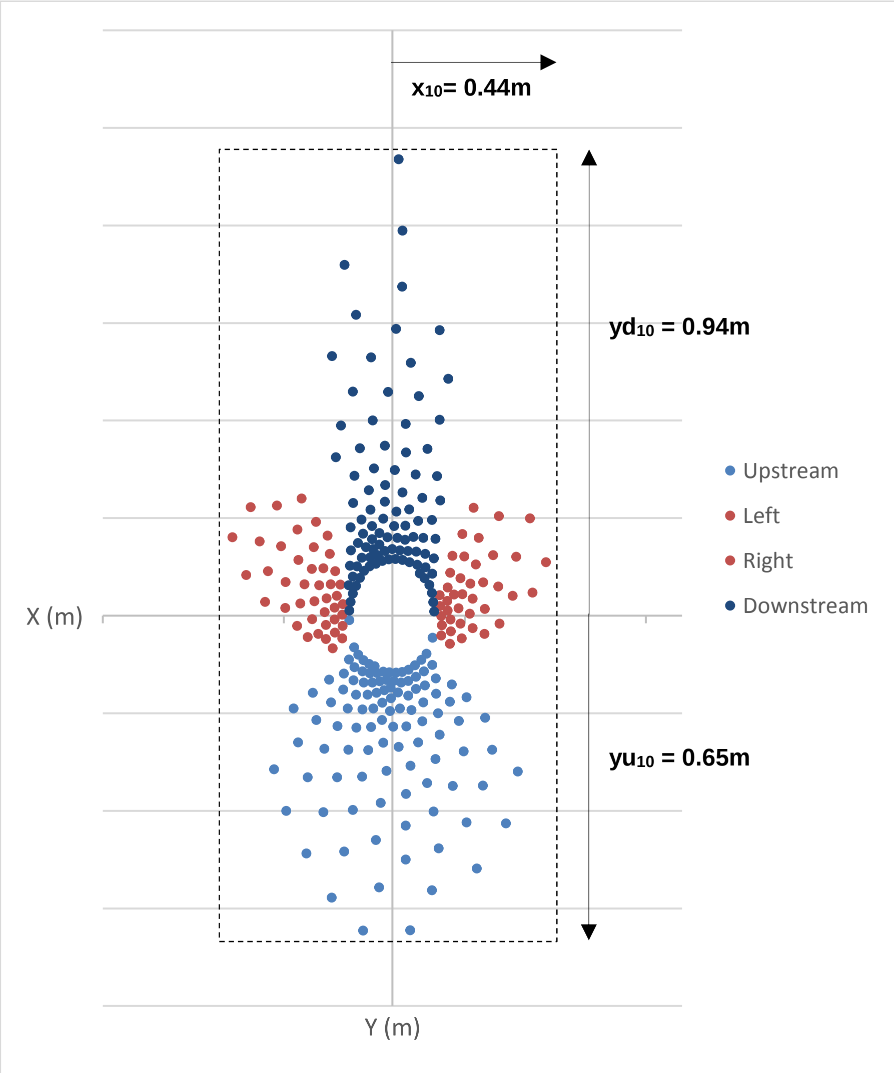

Figure 3-13: ZOI example

3.5.2 Areal Histograms

Areal histograms were another method used to describe the hydraulic effect of boulders. Histograms quantify hydraulic variables with an additional dimension when compared to the ZOI. For any direction the ZOI considered the length along that axis only. A histogram quantified a change in flow using the disturbed area.

The finite element mesh in Argus ONE consists of elements of a certain area with data holding nodes. The velocities at all nodes were considered as the percentage change from the uniform velocity. The areal velocity distribution was calculated by taking the effective area of each node. The effective area consisted of the proportionate areas of all triangular elements surrounding the node. The areas of the velocities which met some given criterion were summed and divided by the total area.

Figure 3-14 below shows an example of an areal histogram for the model conditions shown in Table 3-2. All data points with a percentage variation of 10% or higher where included in the areal analysis. Figure 3-14 shows that the smaller percentage variations constituted a larger area; it also shows that the decreased velocities constituted a larger area when compared to increased velocities.

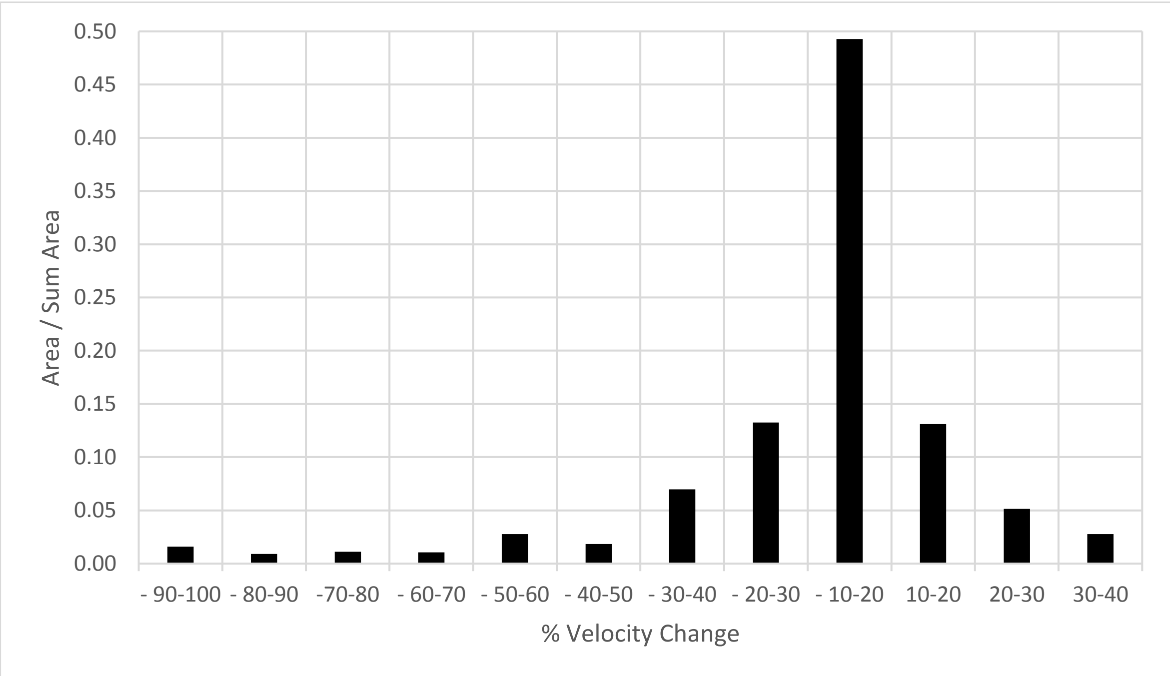

Figure 3-14: Areal histogram example

4 SOFTWARE AND EXPERIMENTAL CORRELATION

Experimental runs were carried out to analyse the calibration/accuracy of Argus ONE and RiverFLO-2D. It was infeasible to complete the research by only using experimental data due to the time-consuming nature of running experiments and due to geometric constraints within the flume. The velocity distribution correlations were analysed for 1 boulder and for 2 boulders placed along the same transverse axis.

The velocity profiles were compared for the upstream, side and downstream directions. The comparison showed that the software adequately predicted velocities in the upstream and side directions for both 1 boulder and 2 boulders.

A poor correlation was found between the software and experimental results due to the software negating the turbulent wakes downstream of the boulder. The software predicted velocities were firstly too high and secondly the predicted velocities were found at smaller *yd* distances. A normalised software velocity distribution was generated by the application of two correction factors; the first factor was applied to velocities and the second factor applied to distances. The correction factors resulted in a much higher coefficient of regression and it was assumed that adequate downstream correlation was reached.

4.1 Experimental Conditions

4.1.1 1 Boulder

The calibration of the software to experimental results was firstly investigated for the simplest case of 1 boulder (Figure 4-1). The experimental conditions were designed to range within the subcritical flow regime and then to cover a range of blockage ratios. Table 4-1 below shows the 3 different tests, which differed in Froude number. Within each test, another 3 tests were carried out where each sub-test consisted of different boulder diameters. Test 3 did not use boulders with a diameter of 0.2350m as the blockage ratio resulted in conditions where the reduction in effective width would just cause a hydraulic jump or choking of the flow.

Table 4-1: 1 Boulder experimental conditions

Test	***Q*** **(m^3/s)**	**S**	***b*** **(m)**	***d*** **(m)**		
1	0.04059	0.00080	2.0	0.110	0.1750	0.2350
2	0.04394	0.00030	2.0	0.110	0.1750	0.2350
3	0.04216	0.000081	2.0	0.110	0.1750	-

Figure 4-1: 1 Boulder d=0.110m experiment

4.1.2 1 Boulder with Larger Blockage Ratios

The experimental results were not conducted for 1 boulder above the blockage ratio which causes choking of the flow (approximately *d/b*>0.10) due to geometrical constraints of the flume. At gentle slopes the maximum flow rate occurred just above the blockage ratio. At steeper slopes the maximum flow in the flume, at a 2.0m width, did not create a flow depth large enough for Vectrino measurements which would not be altered by surface or boundary forces. The flume width was then reduced to 1.0m, by placing a steel partition along the centre line which was held in place with silicone and bricks. Unfortunately, the small joints on the steel portioning created flow disturbances. Additionally, the partition could not be placed flush with the upstream and downstream boundaries causing additional flow disturbances (Figure 4-2).

As discussed in Section 6, it was found that when choking occurs the upstream velocity distribution is altered for large distances, rendering the downstream velocity distribution inconsequential. It has been shown by the experimental runs that the upstream and side velocities are adequately predicted by the software. Given the experimental results for other boulder scenarios and the practical constraints, it was decided that no experimental runs would be conducted for 1 boulder under choking conditions.

Figure 4-2: 1.0m width flow disturbances (overhead view)

Figure 4-3: 1.0m width flow disturbances (side view)

4.1.3 2 Boulders

Experimental runs were lastly conducted for 2 boulders placed transversely to the flow (Figure 4-4). Each boulder was placed 1 boulder diameter away from the centre line resulting in an overall spacing of 2 boulder diameters apart. The experimental conditions were designed to range within the subcritical flow regime and then to cover a range of blockage ratios. Table 4-2 below shows the 3 different tests.

Table 4-2: 2 Boulder experimental conditions

Test	*Q* (m^3/s)	S	*b* (m)	*d* (m)		
1	0.0397	0.00080	2.0	0.0760	0.110	-
2	0.0397	0.00030	2.0	0.0760	0.110	0.2750
3	0.0281	0.0000194	2.0	0.0760	0.110	0.2750

Figure 4-4: 2 Boulders d=0.110m experiment

4.2 Experimental Velocity Measurement Points

The experimental data points were measured on the longitudinal and transverse axes, as the ZOI was defined along these axes. The points, where the velocity was measured, were closer together around the boulder to obtain a more detailed velocity profile. The distance between points varied between 0.50m to intervals of 0.10m within 1.0m of the boulder. A more detailed velocity profile was required around the boulder and a spacing of 0.10m was chosen as it corresponded to the average mesh size around the boulder.

Error! Reference source not found. below shows the location of the measuring points for any given 1 boulder experiment; the boulder was placed in the centre of the flume (1.0m, 5.0m). Figure 4-6 shows the location of the measuring points for 2 boulder experiments where the boulders were placed 2 boulder diameters apart from the centre of the flume (1.0m, 6.50m).

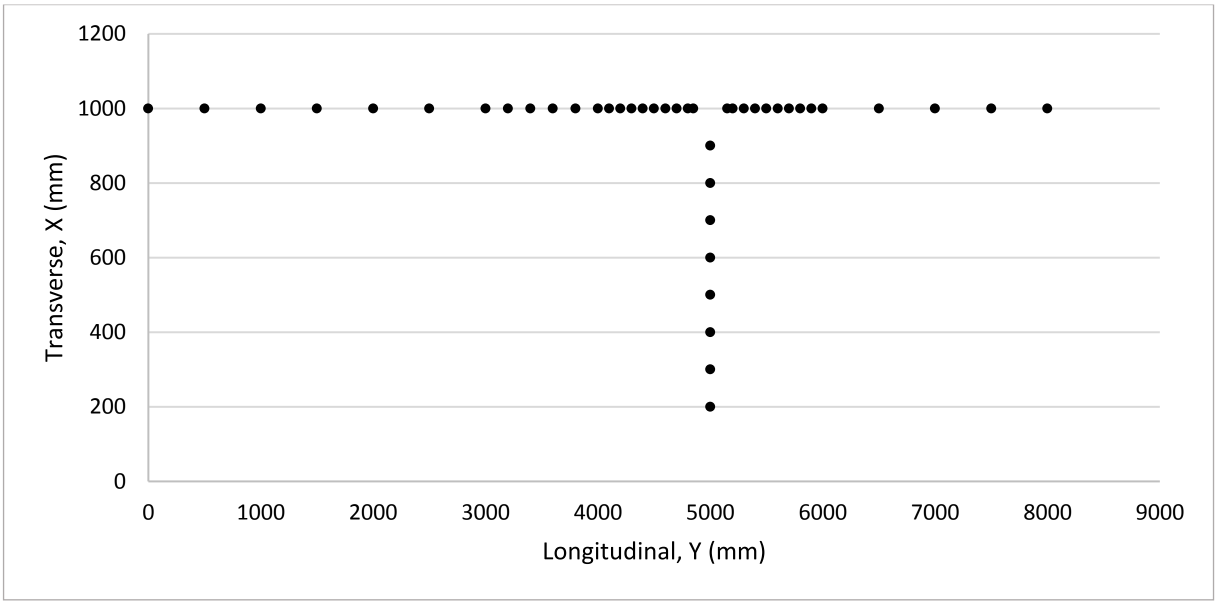

Figure 4-5: 1 Single boulder experimental velocity measurement points

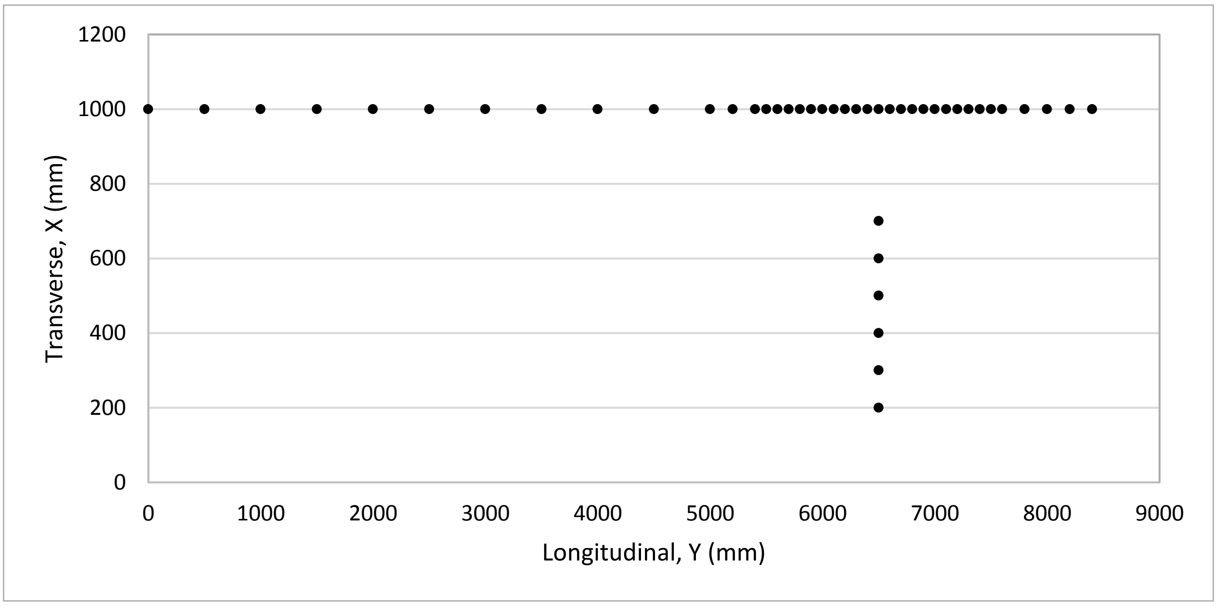

Figure 4-6: 2 Double boulder experimental velocity measurement points

4.3 1 Boulder Results

4.3.1 Comparison of Velocities

Figure 4-7, Figure 4-8 and Figure 4-9 show the velocities in the upstream, side and downstream directions respectively. The figures compare the velocity distributions of the experimental and software runs for Test 1, *d*=0.110m. The correlation between the experimental and software velocities were similar in each direction for all tests therefore the figures below will be used as a representation set to explain all correlations.

The upstream and side directions showed a strong correlation between the software and experimental results. There was a strong correlation between the velocity magnitudes as well as the location of velocities. The software adequately predicted the velocity distributions around 1 boulder for the upstream and side directions.

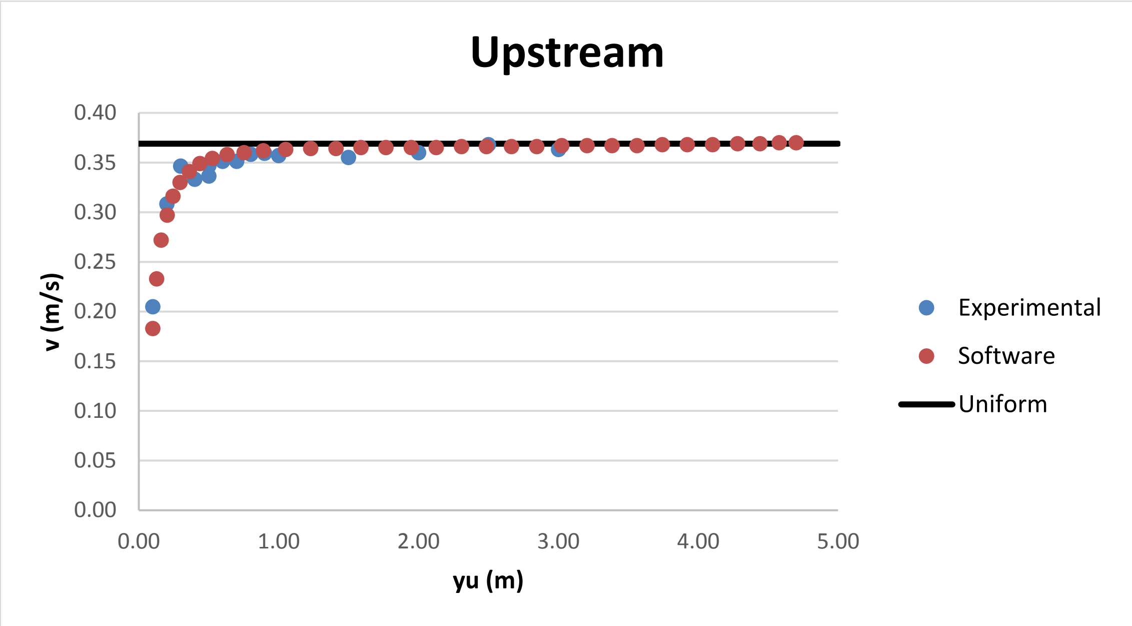

Figure 4-7: 1 Boulder upstream experimental and software velocities (Test 1, d=0.110m)

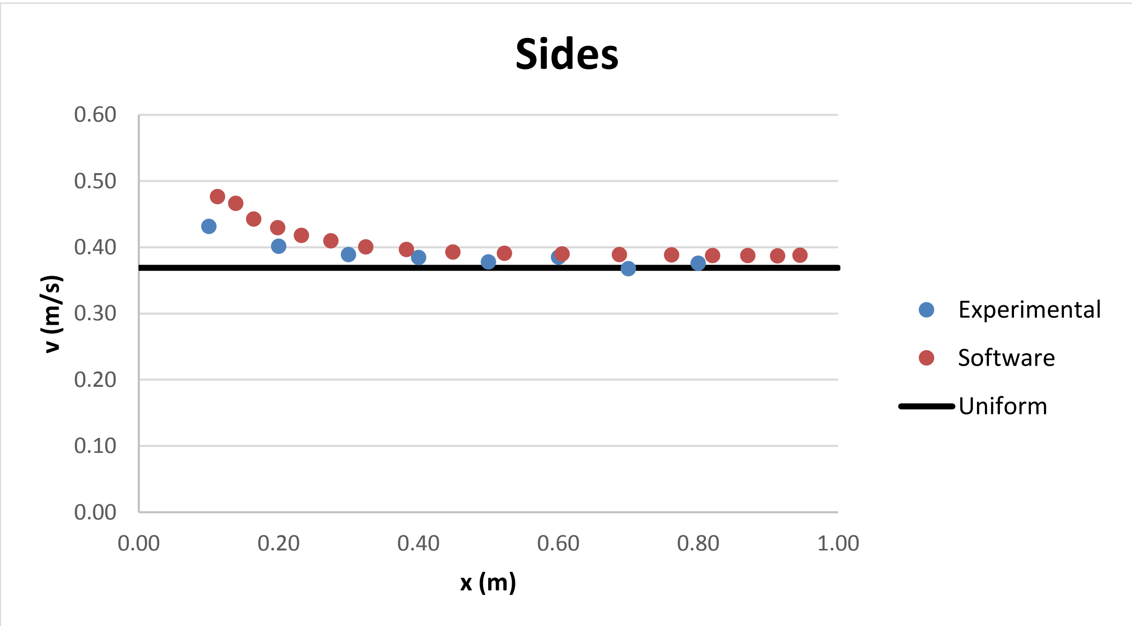

Figure 4-8: 1 Boulder side experimental and software velocities (Test 1, d=0.110m)

Figure 4-9 shows that the software and experimental velocity distributions did not correspond in the downstream direction. The software predicted that the ZOI was smaller than what it was, with the velocity returning to uniform at approximately 1m, but in reality the velocity was altered beyond the geometrical extent of the flume.

Figure 4-9 also shows that the software did not account for the turbulence experienced on the downstream edge of the boulder, shown by the negative velocity readings. As a result of the software neglecting the turbulence the velocity profile was also prematurely predicted.

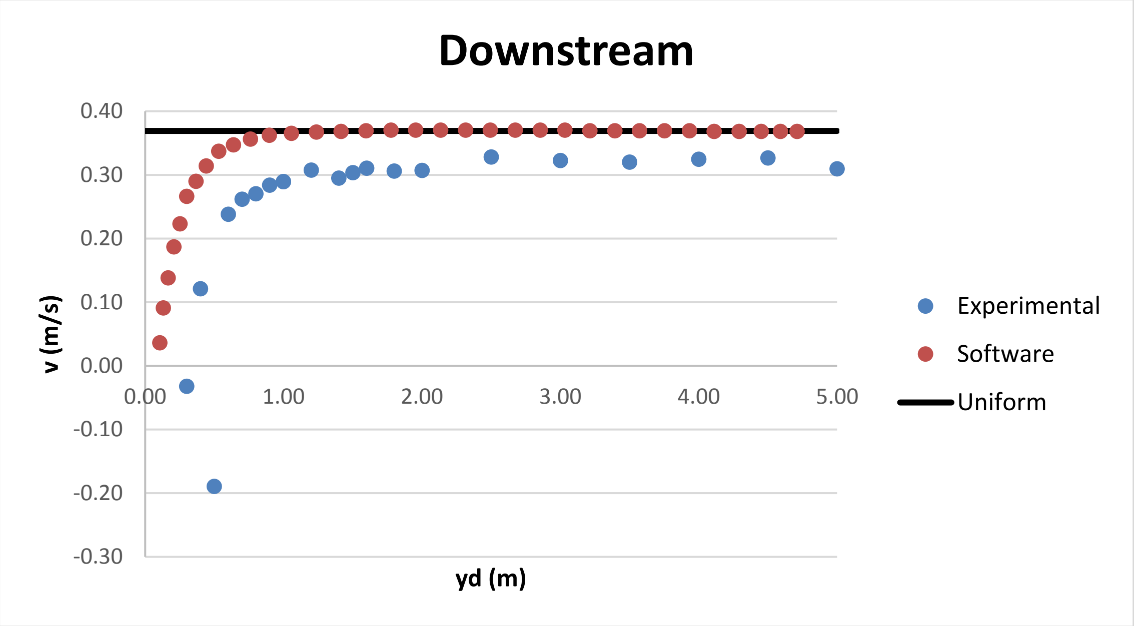

Figure 4-9: 1 Boulder downstream experimental and software velocities (Test 1, *d*=0.110m)

4.3.2 Experimental Versus Software Graphs

The following discussion quantifies the correlation between the software and experimental models. All experimental conditions were considered to obtain an overall view of the correlation. The locations of velocity measurements for the experimental runs were constant. The location of velocity measurements in the software were however different to the experimental locations. The automatic mesh generation used in Argus ONE was utilised in such a way that the triangular nodes were on the axes of interest but the location of the nodes could not be set. Multiple regressions were performed on the software velocity distributions to compare the experimental and software velocities at the same locations.

Figure 4-10, Figure 4-11 and Figure 4-12 below compare the velocity calibrations at the same locations for the experimental and software velocities.. A perfect calibration would be indicated by a straight line with a gradient of 1.0. The upstream and side directions showed a strong correlation as anticipated, with gradients being very close to 1.0. A coefficient of regression (R^2) of 0.85 and 0.95 for the upstream and side directions respectively indicated that there was minimal scatter. The multiple regressions performed on the software results would have caused some additional errors. As a result, the upstream and side directions were regarded as being calibrated satisfactorily.

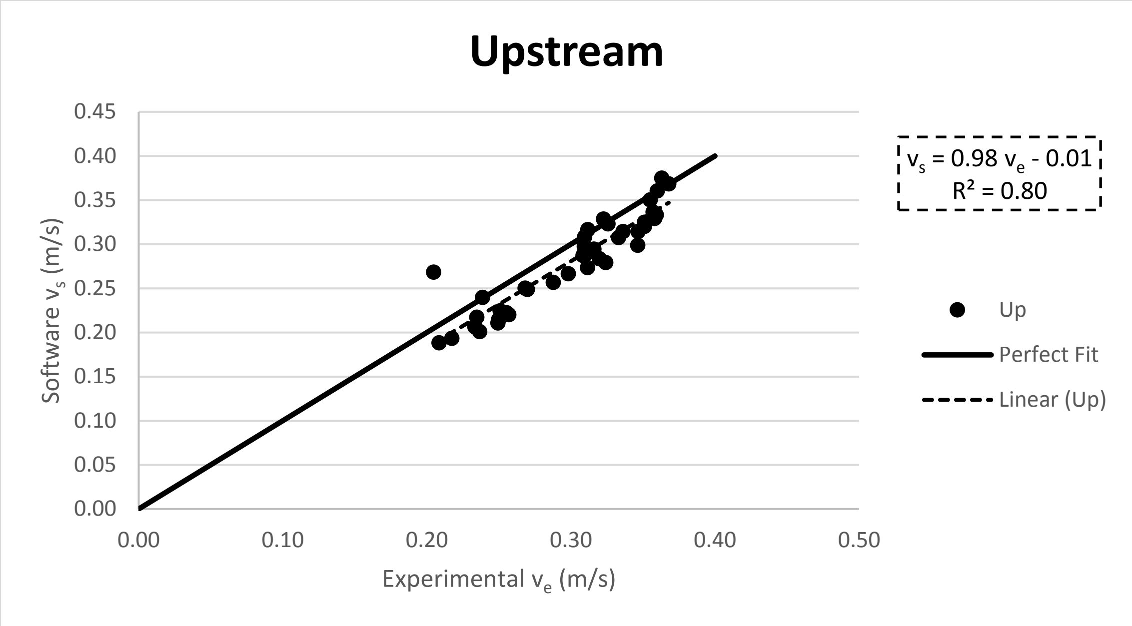

Figure 4-10: Upstream - Correlation for all 1 boulder experiments

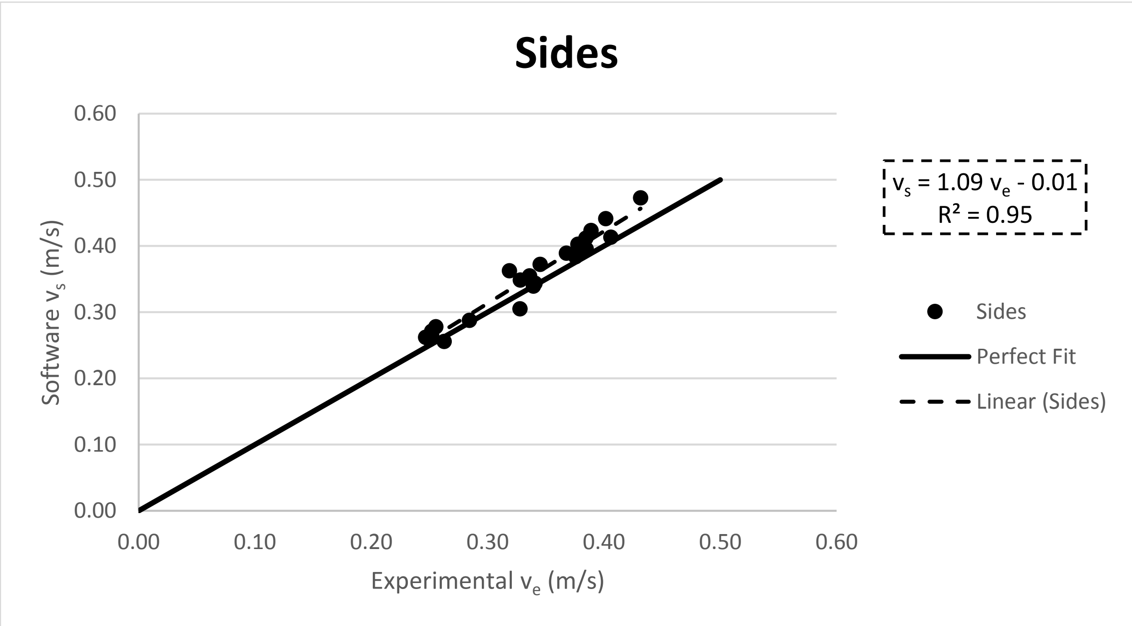

Figure 4-11: Sides - Correlation for all 1 boulder experiments

The downstream direction again showed the discrepancy between the software and experimental results. The largest discrepancy was seen with the smallest and negative velocities which are just downstream of the boulder, where turbulence occurs. The correlation between the velocities strengthened with larger velocities which are found a further distance from the boulder.

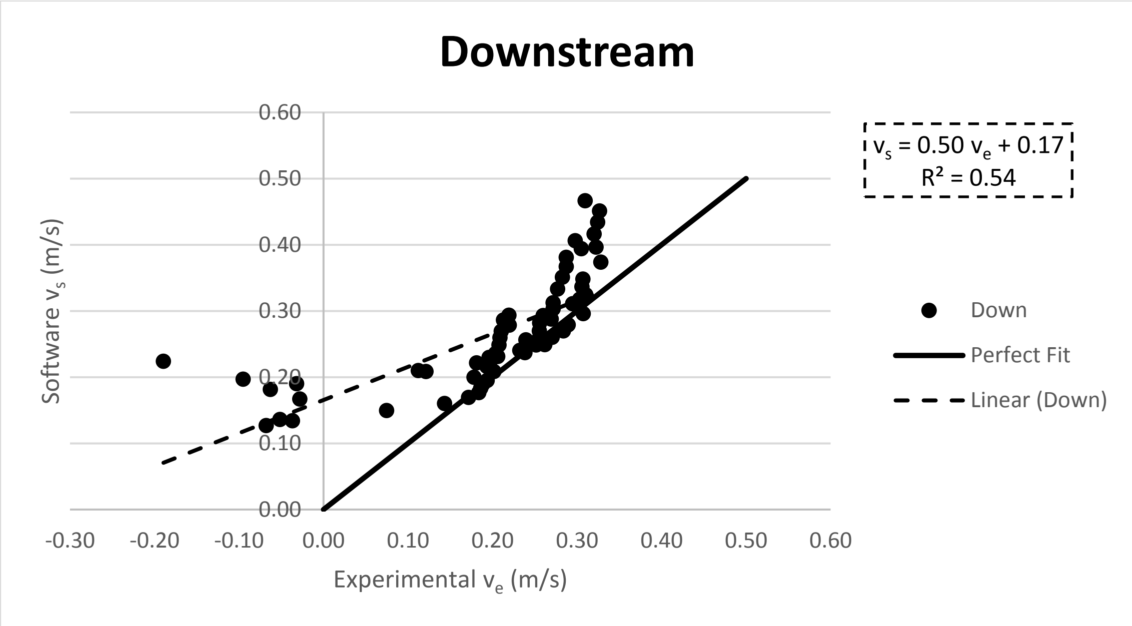

Figure 4-12: Downstream - Correlation for all 1 boulder experiments

4.3.3 Downstream Variation

The experimental and software results show that the model adequately depicted the velocity of the water as it reached the boulder and moved along the sides. The software however failed to simulate the flow field correctly once the water passed the boulder. The flow field at the downstream side of the boulder was analysed in order to understand departure from experimental results.

The discrepancy between the experimental and software velocities was unexpected. Riddet (2012) and Hamuy-Blanco (2013) both used the same experimental equipment and software and found that the experimental and software flow conditions agreed. The finding of the experimental-software discrepancy in this research could be due to the fact that the correlation of each direction was analysed separately.

The downstream velocity profile shows characteristics of the turbulence wake described by Shamloo (1997). The first region is the recirculation region found closest to the downstream boulder edge. Shamloo (1997) explains that the recirculation region is the primary wake where vortex formation causes negative velocities. The Vectrino measured negative velocities at locations which were downstream of the boulder. The negative velocities indicate that the water was moving in the opposite direction when compared to the main flow direction. The negative velocities are indicative of the rearticulating flow wakes.

The remainder of the turbulent wake is defined by Shamloo (1997) as the secondary wake. The secondary wake is comprised of a less defined region where the vortices are shed. Shamloo (1997) explains that the secondary wake extends a large distance downstream. Figure 4-13 shows the experimental and software velocities for Test 1 (d=0.1750m), approximately 0.5m downstream of the boulder the recirculating flow ceases to exist. The velocity profile slowly returns to uniform as the turbulent wake dissipates.

It has been shown that the turbulent wakes around the boulders were measurable. As mentioned previously, RiverFLO-2D does not account for dispersion or turbulence but rather incorporates the energy losses through Manning's n and the momentum equations (Hydronia LLC, 2015). The fact that the hydrodynamic model did not account for turbulence explains why the software and experimental velocities did not correspond in the downstream direction. The sequential nature of the numerical model used by the software explains why the downstream velocities further downstream did not correspond to experimental values. The model used incorrect data at the downstream edge of the boulder, meaning that all velocity points thereafter were also incorrect.

Figure 4-13 also shows that the experimental velocities did not return to uniform in the geometrical extents of the flume. All experimental flow conditions were in the subcritical flow regime, which is controlled from downstream. In the absence of turbulence or energy losses the downstream uniform flow conditions would extend to the downstream edge of the boulder. The experimental velocity results showed that the turbulent wake was unexpectedly large. All experimental results showed that the velocities at the downstream geometrical extent (5m away from the boulder) still had decreased velocities of approximately 15%.

Figure 4-13 below shows a slow return of the downstream velocity to uniform conditions. A trend line showed that uniform conditions would be expected approximately 7.5m away from the boulder.

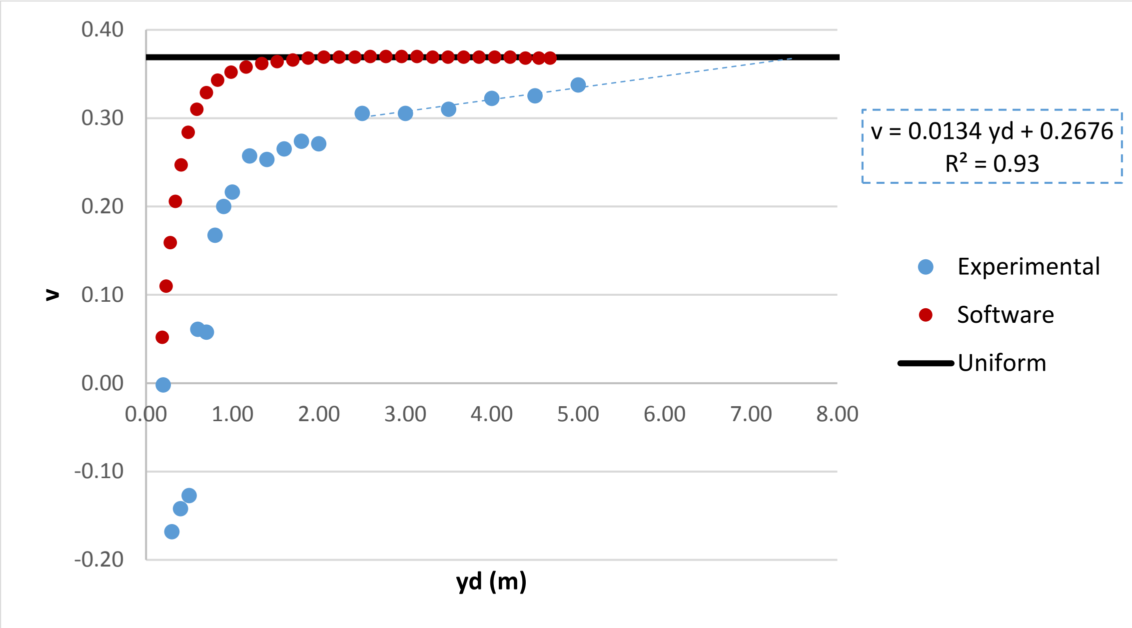

Figure 4-13: 1 Boulder downstream experimental and software velocities (Test 1, *d*=0.1750m)

To create relationships for the downstream direction a correction factor was used. The correction factor ensured calibration of the downstream software velocities to the experimental velocities. As a result of the large downstream disturbed area all percentage variations below 20% were not analysed for the downstream direction. It would be advised that future research projects investigate the downstream velocity disturbance in greater detail.

The downstream software inadequacies lead to a vital conclusion for the use of two-dimensional modelling for boulder rehabilitation projects. It would be advised that rehabilitation practitioners should not use two-dimensional software for the design of boulders. This does however bring additional importance to the empirical results of this research project.

4.3.4 Correction Factor

Although there was a lack of correlation between the software and experimental velocities, the respective distributions did show similarity. Figure 4-14 shows the shape of the velocity distributions were consistent with the exception being the turbulent zone close to the boulder. The software predicted velocities were firstly too high and secondly, the predicted velocities were found at smaller *yd* distances. This observation led to the idea of utilising a correction factor that could normalise the software velocity distributions to the experimental velocity distributions by applying one factor for distance correction and one factor for velocity correction.

The normalised software velocity distribution was generated by the application of two correction factors. The first correction factor (*Cv*) was applied to the velocities, where *Cv* reduced the software velocities. The second correction factor (*Cyd*) was applied to the distances, where *Cyd* increased the software distances. Percentage differences between the experimental and software results were calculated for all tests. *Cv* and *Cyd* were varied and the percentage differences analysed. Both *Cv* and *Cyd* were found to be the same constants respectively for all experimental models. The values for the correction factors were as follows:

Table 4-3: Downstream correction factors for 1 boulder

Velocity Correction Factor, *Cv*	**Distance Correction Factor, *Cyd***
0.850	1.70

Figure 4-14 shows the resultant velocity distribution of the software once the correction factors were applied, the experimental and software velocity distributions showed a strong correlation with the application of correction factors.

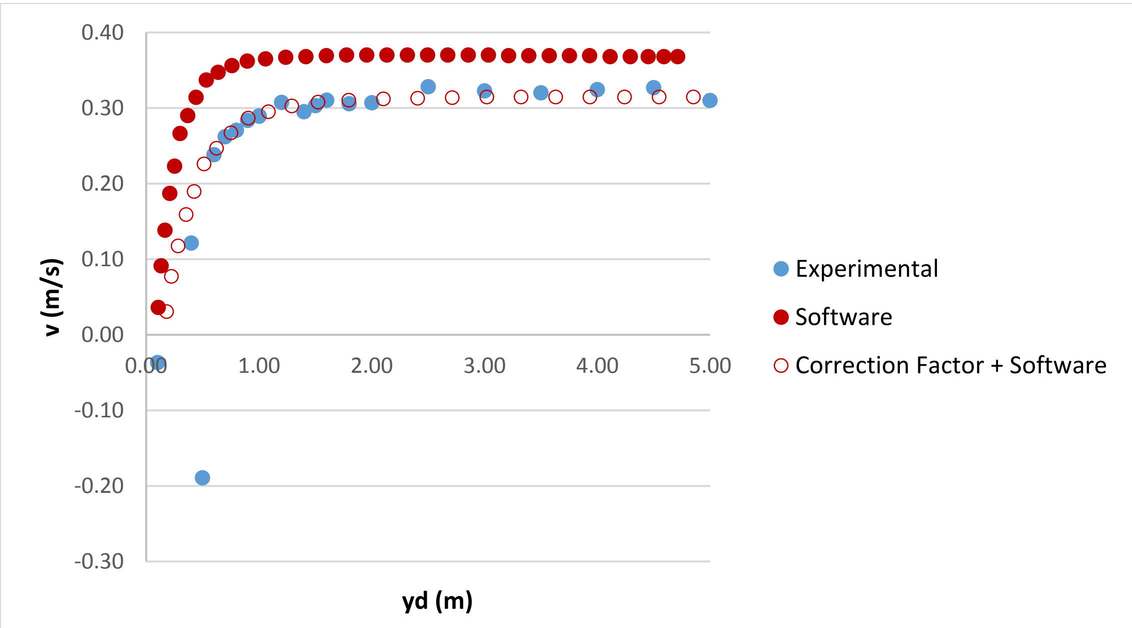

Figure 4-14: 1 Boulder downstream correction factor (Test 1, *d*=0.110m)

Figure 4-15 below illustrates the correlation between experimental and software velocities once the correction factors were applied to all tests. It should be noted that multiple regressions were once again performed to obtain software results at the same locations as the experimental velocities. Figure 4-16 shows the resultant correlation with the removal of negative experimental velocities. The correction factor resulted in a much higher coefficient of regression and it was assumed that adequate downstream correlation was reached.

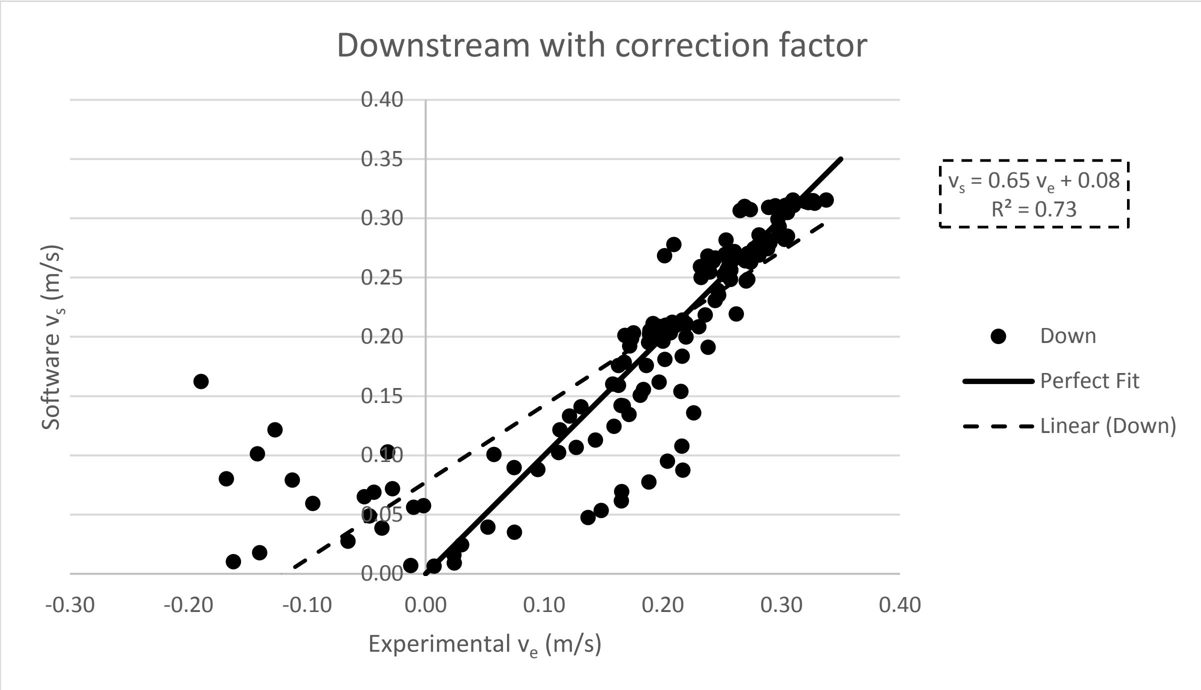

Figure 4-15: Downstream - Correlation for all 1 boulder experiments with correction factor

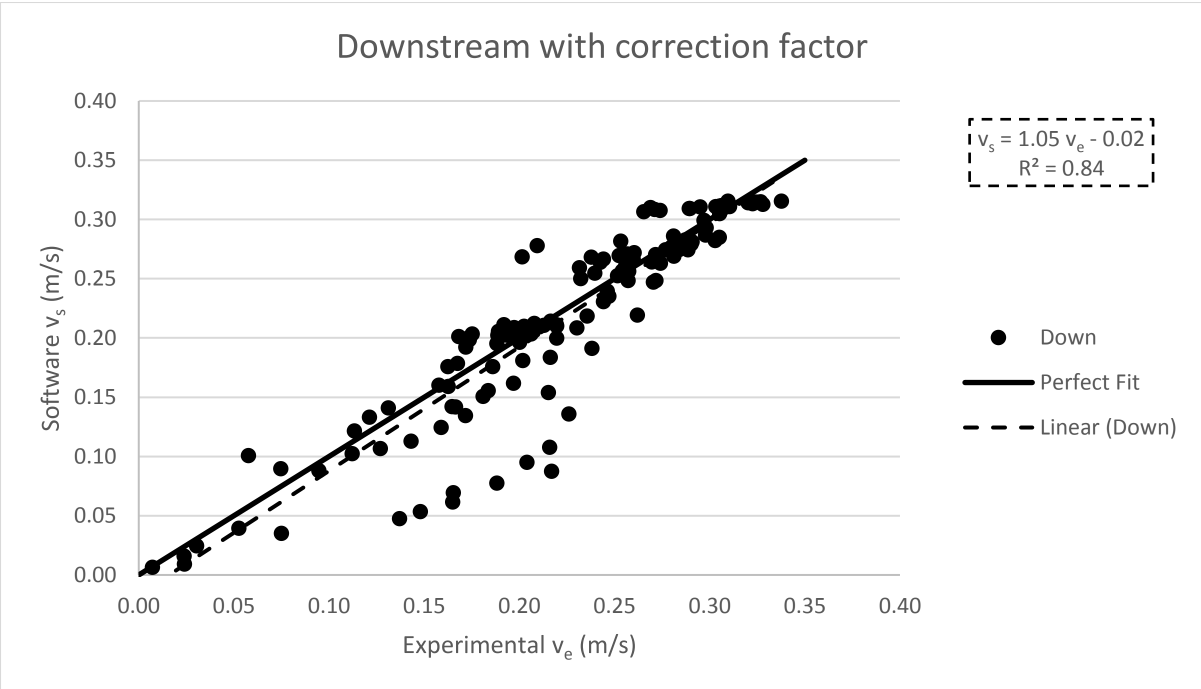

Figure 4-16: Downstream - Correlation for all 1 boulder experiments with correction factor and no negative velocities

4.4 2 Boulders Results

4.4.1 Comparison of Velocities

Figure 4-17, Figure 4-18 and Figure 4-19 show the experimental and software velocities for the upstream, side and downstream directions respectively for an example model (Test 2, *d*=0.110 m). As with 1 boulder, the upstream and side directions showed a strong correlation between the velocity magnitudes as well as the location of velocities. The downstream direction again showed that the software predicts the return to uniform prematurely.

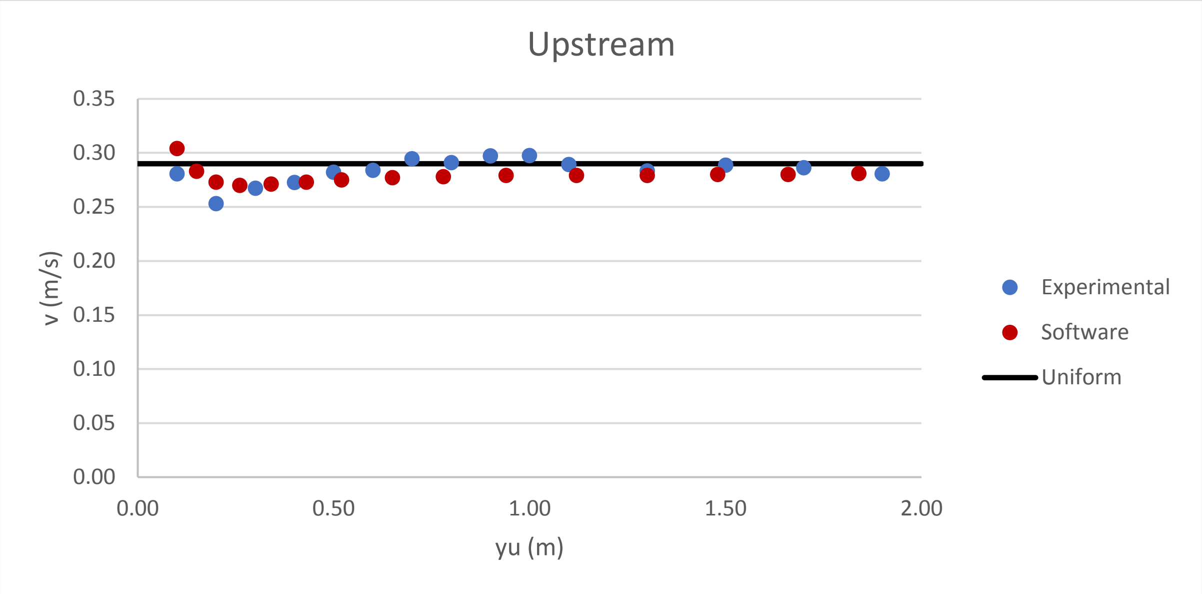

Figure 4-17: 2 Boulders upstream experimental and software velocities (Test 2, *d*=0.110m)

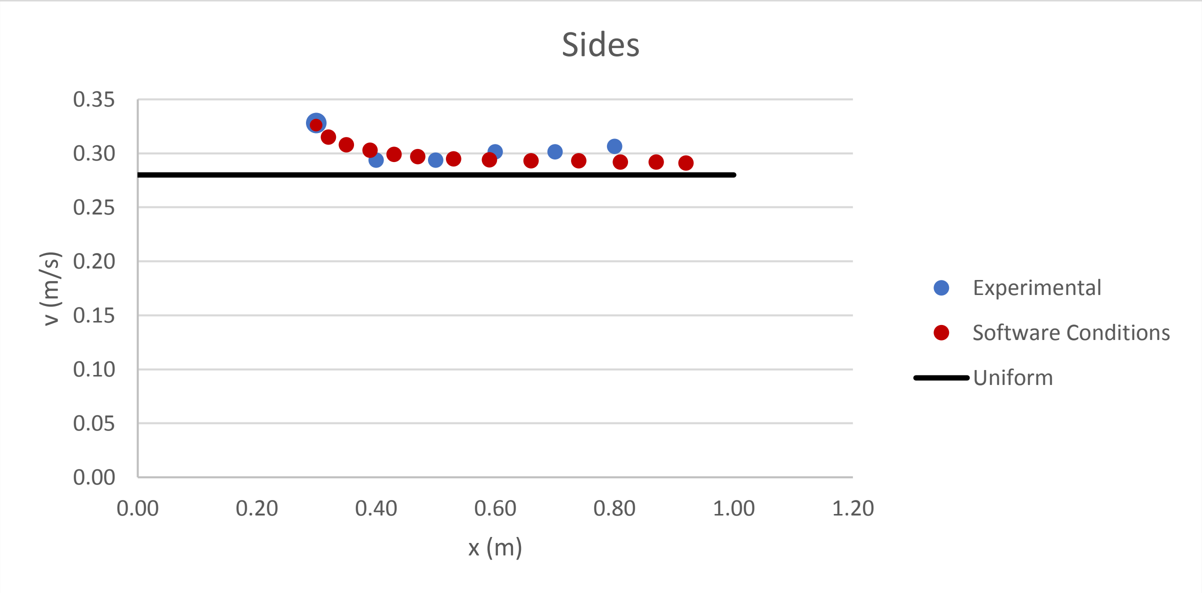

Figure 4-18: 2 Boulders side experimental and software velocities (Test 2, *d*=0.110m)

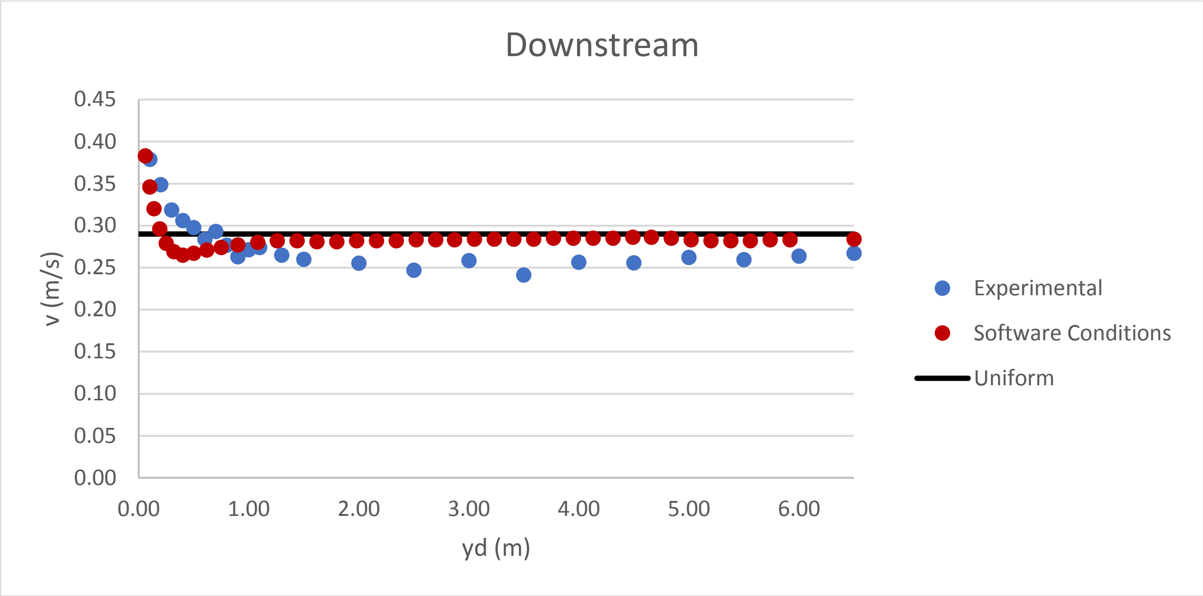

Figure 4-19: 2 Boulders downstream experimental and software velocities (Test 2, *d*=0.110m)

4.4.2 Experimental versus Software Graphs

As with the 1 boulder analysis, multiple regressions were performed on the software velocity distributions to compare the experimental and software velocities at the same locations. Figure 4-20, Figure 4-21 and Figure 4-22 below assess the velocity calibrations by comparing the experimental and software velocities. The upstream and side directions show a strong correlation as anticipated, with gradients being very close to 1. A coefficient of regression (R^2) of 0.93 and 0.95 for the upstream and side directions respectively indicated that there was minimal scatter. The upstream and side directions were regarded as being calibrated satisfactorily.

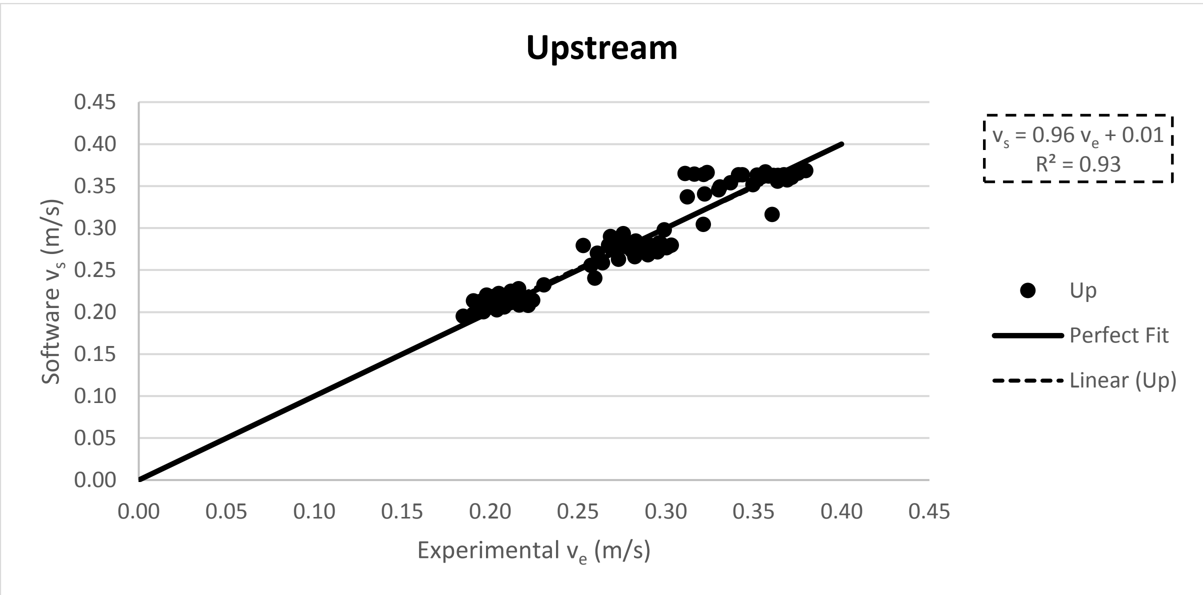

Figure 4-20: Upstream - Correlation for all 2 boulder experiments

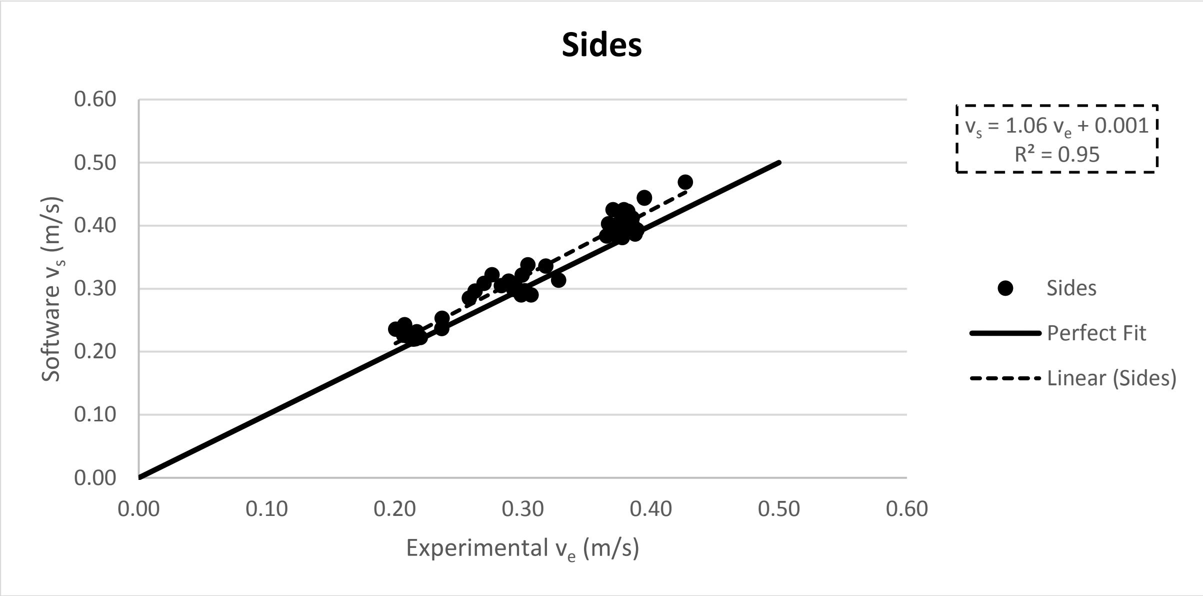

Figure 4-21: Sides - Correlation for all 2 boulder experiments

The initial correlation between the experimental and software results for the downstream direction shows a stronger relationship than that of 1 boulder. It should be noted that no negative velocity readings were recorded experimentally as the experimental readings were taken in between the boulders and not directly downstream as with the 1 boulder experiments. A correction factor was again applied as the coefficient of regression was still about 20% lower than the upstream and side directions.

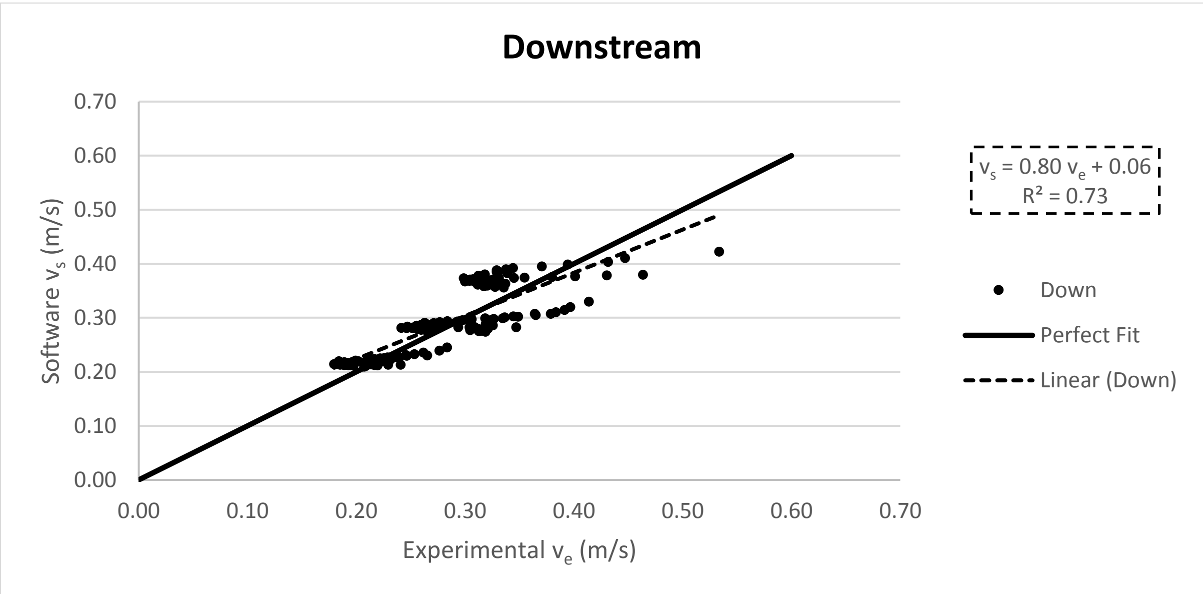

Figure 4-22: Downstream - Correlation for all 2 boulder experiments

4.4.3 Downstream Variation

The experimental and software results show that the model adequately depicted the velocity of the water as it reached the boulder and moved along the sides. The software however failed to simulate the flow field correctly once the water passed the boulder. The flow field at the downstream side of the boulder was analysed in order to understand departure from experimental results.

The discrepancy between the experimental and software velocities was unexpected. Riddet (2012) and Hamuy-Blanco (2013) both used the same experimental equipment and software and found that the experimental and software flow conditions agreed. The finding of the experimental-software discrepancy in this research could be due to the fact that the correlation of each direction was analysed separately.

The downstream velocity profile shows characteristics of the turbulence wake described by Shamloo (1997). The first region is the recirculation region found closest to the downstream boulder edge. Shamloo (1997) explains that the recirculation region is the primary wake where vortex formation causes negative velocities. The Vectrino measured negative velocities at locations which were downstream of the boulder. The negative velocities indicate that the water was moving in the opposite direction when compared to the main flow direction. The negative velocities are indicative of the rearticulating flow wakes.

The remainder of the turbulent wake is defined by Shamloo (1997) as the secondary wake. The secondary wake is comprised of a less defined region where the vortices are shed. Shamloo (1997) explains that the secondary wake extends a large distance downstream. Figure 4-13 shows the experimental and software velocities for Test 1 (d=0.1750m), approximately 0.5m downstream of the boulder the recirculating flow ceases to exist. The velocity profile slowly returns to uniform as the turbulent wake dissipates.

It has been shown that the turbulent wakes around the boulders were measurable. As mentioned previously, RiverFLO-2D does not account for dispersion or turbulence but rather incorporates the energy losses through Manning's n and the momentum equations (Hydronia LLC, 2015). The fact that the hydrodynamic model did not account for turbulence explains why the software and experimental velocities did not correspond in the downstream direction. The sequential nature of the numerical model used by the software explains why the downstream velocities further downstream did not correspond to experimental values. The model used incorrect data at the downstream edge of the boulder, meaning that all velocity points thereafter were also incorrect.

Figure 4-13 also shows that the experimental velocities did not return to uniform in the geometrical extents of the flume. All experimental flow conditions were in the subcritical flow regime, which is controlled from downstream. In the absence of turbulence or energy losses the downstream uniform flow conditions would extend to the downstream edge of the boulder. The experimental velocity results showed that the turbulent wake was unexpectedly large. All experimental results showed that the velocities at the downstream geometrical extent (5m away from the boulder) still had decreased velocities of approximately 15%.

Figure 4-13 below shows a slow return of the downstream velocity to uniform conditions. A trend line showed that uniform conditions would be expected approximately 7.5m away from the boulder.

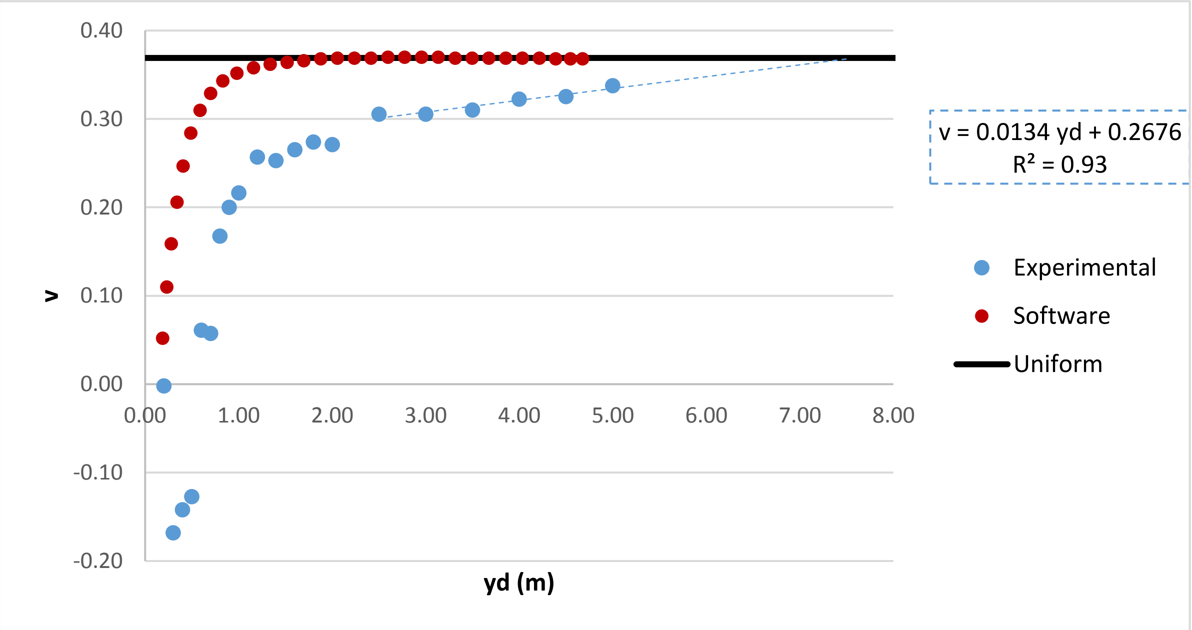

Figure 4-23: 1 Boulder downstream experimental and software velocities (Test 1, *d*=0.1750m)

To create relationships for the downstream direction a correction factor was used. The correction factor ensured calibration of the downstream software velocities to the experimental velocities. As a result of the large downstream disturbed area all percentage variations below 20% were not analysed for the downstream direction. It would be advised that future research projects investigate the downstream velocity disturbance in greater detail.

The downstream software inadequacies lead to a vital conclusion for the use of two-dimensional modelling for boulder rehabilitation projects. It would be advised that rehabilitation practitioners should not use two-dimensional software for the design of boulders. This does however bring additional importance to the empirical results of this research project.

4.4.4 Correction Factor

Cv and *Cyd* were varied and the percentage differences analysed. Both *Cv* and *Cyd* were found to be the same constants respectively for all experimental models. The values for the correction factors were as follows and are shown in Table 4-4. Interesting to note is that *Cv* was almost equal to the 1 boulder factor (0.850) and *Cyd* was double the 1 boulder factor (1.70).

Table 4-4: Downstream correction factors for 2 boulders

Velocity Correction Factor, *Cv*	**Distance Correction Factor, *Cyd***
0.90	3.40

Figure 4-24 below illustrates the experimental and software velocities once the correction factors were applied. It should be noted that multiple regressions were once again performed to obtain software results at the same locations as the experimental velocities. The correction factors resulted in a much higher coefficient of regression and it was assumed that adequate downstream correlation was reached.

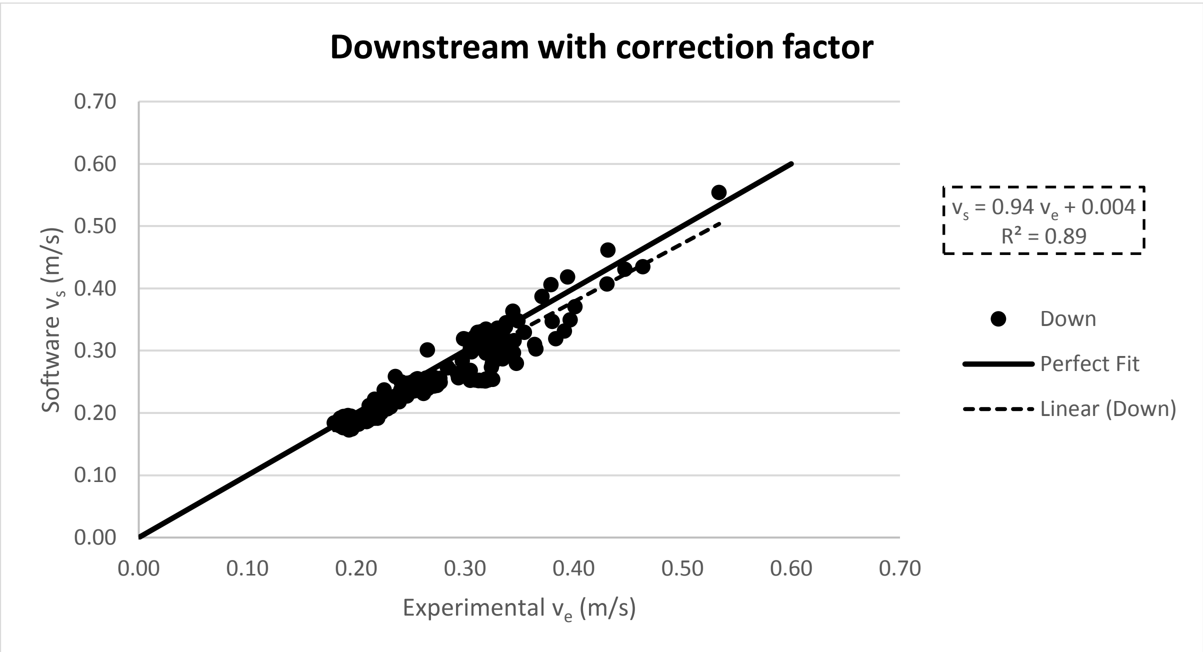

Figure 4-24: Downstream - Correlation for all 2 boulder experiments with correction factor

5 INFLUENCE OF 1 BOULDER

This chapter focuses on the determination of the ZOI dimensions of a single boulder placed in the middle of the channel width.

The velocity distribution around a single boulder for a particular case was analysed with the calculation of the ZOI and an areal velocity histogram. This example helped describe the size of the altered flow as well as the altered flow conditions in each direction.

The area of flow which was disturbed by the placement of a boulder was quantified by using a ZOI. The fundamental variables on which a ZOI depends were grouped whilst taking into consideration dimensional homogeneity for practical convenience. The use of dimensionless variable groupings was utilised in this chapter in order for the proposed ZOI relationship to be applicable to a wider set of hydraulic conditions. The discussion that follows shows the relevance of the chosen variable groupings, which will then be considered as a whole to determine the dependencies between them; yielding an equation that predicts the size of a ZOI.

A relationship which estimates the length of the ZOI has been developed for the upstream, downstream and transverse directions. Initially the limits of the relationship which Hamuy-Blanco (2013) proposed to represent the size of a ZOI were to be determined but the analysis of a larger variation of flow classes allowed for new relationships to be developed.

5.1 Velocity Distribution Investigation

The following discussion investigates the velocity distribution around 1 boulder for a particular case. The velocity distribution was analysed in terms of the ZOI and an areal velocity histogram. This example provided a feel for the size of the disturbed flow area as well as which velocities occurred within the disturbed region. The following discussion used Model 1; which has the following conditions:

Table 5-1: Model 1 Conditions

***Q* (m³/s)**	***S***	***n***	***b* (m)**	***d* (m)**	***H* (m)**	***v* (m/s)**
1.250	0.00080	0.010	5.0	0.20	0.242	1.033

5.1.1 ZOI

Figure 5-1 below shows the ZOI around the boulder under consideration for 10%, 20% and 30% change in velocity. It was noted that the downstream direction had the largest disturbed area and the sides the smallest. It should also be noted that the lower percentage variations have considerably larger lengths when compared to the higher percentage variations which are found close to the boulder. For an effective design it would be advised that the boulder diameter be chosen such that a 10% or 20% change in velocity would cause a change in flow class.

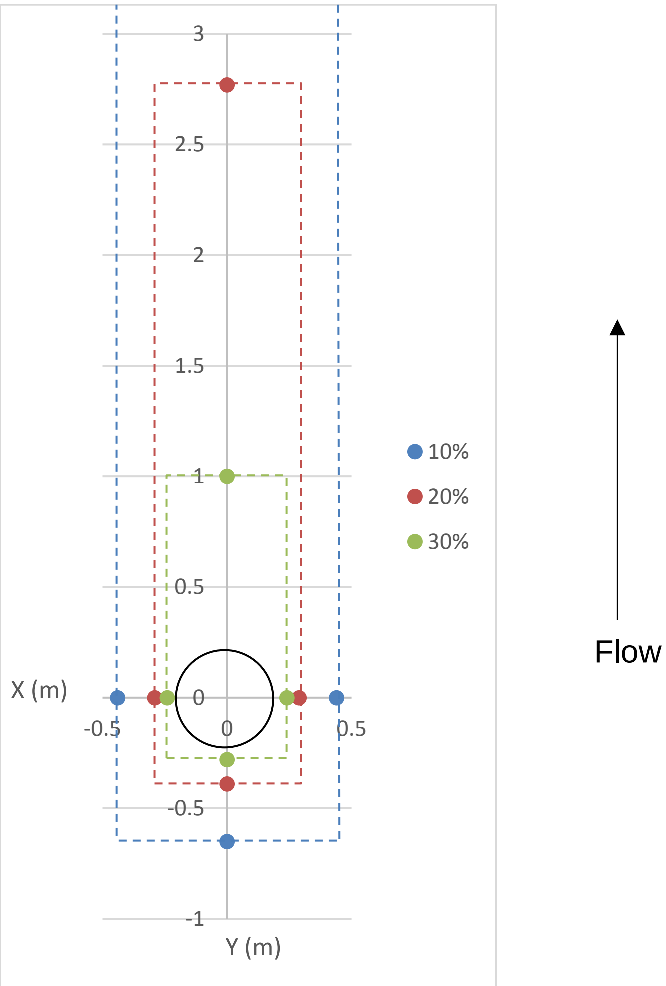

Figure 5-1: Model 1 ZOI

Table 5-2 below shows the magnitude of the ZOI for each direction and for various percentage variations. Also shown is the magnitude of the ZOI in terms of the boulder diameter. Table 5-2 shows that the low percentage variations extend furthest away from the boulder and increasing percentage variations are found closer to the boulder. It was interesting to note that the lower percentage variations had a considerable distance between them; for example the downstream direction showed a 20% disturbance approximately 13.85 boulder diameters downstream and a 30% disturbance 5.0 boulder diameters downstream. Higher percentage variations showed smaller differences in the ZOI length; a 60% disturbance was measured 2.60 boulder diameters downstream while a 70% disturbance was measured 2.55 boulder diameters away. This phenomenon again emphasises the design principle of utilising the smaller percentage variations to obtain the largest area of disturbed flow.

Table 5-2: Model 1 ZOI dimensions

i	***yu* (m)**	***yu/d***	***yd* (m)**	***yd/d***	***x* (m)**	***x/d***
10	0.65	3.25	-	-	0.44	2.20
20	0.39	1.95	2.77	13.85	0.29	1.45
30	0.28	1.40	1.00	5.00	0.24	1.20
40	0.23	1.15	0.78	3.90	-	-
50	0.20	1.00	0.60	3.00	-	-
60	0.17	0.85	0.52	2.60	-	-
70	0.15	0.75	0.51	2.55	-	-

5.1.2 Velocity Histogram

A velocity areal histogram was created in order to describe the velocity distribution. The histogram considered all velocities which had a velocity change greater than 10%. As mentioned, 10% was assumed to be the lowest velocity variation to have a considerable effect on flow classes. The software was used in the generation of a histogram. As a result, an uncalibrated downstream direction has been used. The use of uncalibrated downstream data for the histogram was considered acceptable as the same decreased velocity histogram would exist, the exception being a larger area occupied by the 10-20% velocity range. The resulting histogram was conservative for the decreased 10-20% velocity change range.

Figure 5-2 below shows an areal velocity histogram of Model 1, where the total area was all triangular elements with a velocity change greater than 10%. Again, shown in this method of velocity analysis is the larger area of decreased velocities when compared to the increased velocities. Furthermore, the small percentage variations for both increased and decreased velocities have larger areal coverages.

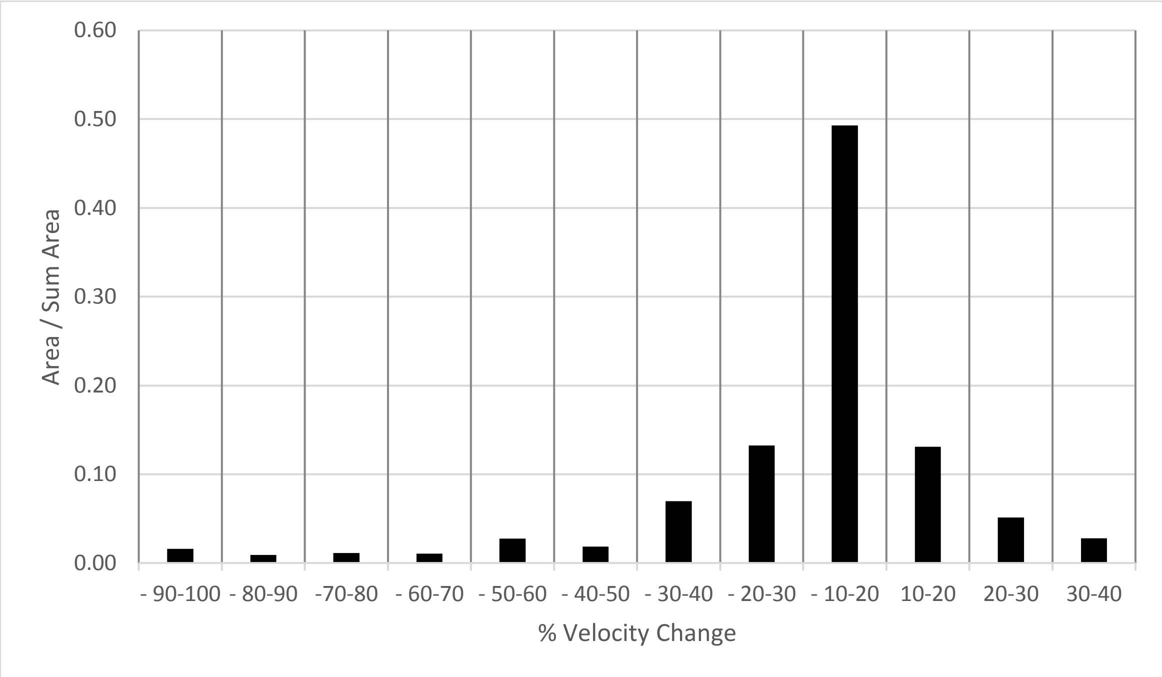

Figure 5-2: Model 1 velocity histogram showing 10-100% change in velocity

5.2 Variable Groupings

As discussed, the fundamental variables describing the ZOI were *Q, v, H, S, n, b* and *d*. A combination of these variables was considered with the aim of practical extrapolation being central. This was achieved by using dimensionless groupings of variables. A dimensionless relationship is independent of scale and as a result generalises the problem, allowing predictions to be made for a situation which was not used in the forming of the relationship. The Froude number, blockage ratio and a ZOI ratio were used.

The Froude number contains all the variables which determine the uniform velocity of a channel but is also a dimensionless number. Substituting Manning's equation (5-2) into the Froude number (5-1) shows how the Froude number contains all channel characteristics.

$$Fr = \frac{v}{\sqrt{gH}} \qquad \text{5-1}$$

$$v = \frac{1}{n} R^{\frac{2}{3}} S^{\frac{1}{2}} \qquad \text{5-2}$$

$$v = \frac{1}{n} \left(\frac{bH}{2b + H}\right)^{\frac{2}{3}} S^{\frac{1}{2}} \qquad \text{5-3}$$

$$Fr = \frac{1}{n} \left(\frac{bH}{2b + H}\right)^{\frac{2}{3}} S^{\frac{1}{2}} \cdot \frac{1}{\sqrt{gH}} \qquad \text{5-4}$$

The length of the ZOI was defined by its upstream *(*yu_i*)*, downstream *(*yd_i*)* and transverse *(*x_i*)* distances. In these distances *i* represents the percentage variation from the undisturbed velocity. For the initial relationship development, the length of the ZOI in any direction was defined by *y*. The equation manipulation above hypothesises that the ZOI will be a function of the Froude number.

$$y = f\ (Fr) \qquad \text{5-5}$$

It was of practical importance to allow the relationship to be valid for any size, *d*, of boulder. The same was necessary for any width, *b,* of the channel. Hamuy-Blanco (2013) also effectively used this relationship.

$$y = f\ \left(\frac{d}{b}\right) \qquad \text{5-6}$$

The ZOI was assumed to be a function of two dimensionless variables, the Froude number and the blockage ratio, and as a result had to have a third variable of dependency to ensure that the equation was dimensionally homogeneous.

A dimensional analysis would suggest that the third variable would have to have length as its unit of measurement. The preliminary investigation of the dependent channel characteristics showed that *b* and *d* caused the largest change in the size of the ZOI. These variables were already taken into consideration by the Froude number and the blockage ratio, which suggests that the ZOI had to have a stronger dependence on one of them than initially assumed. It was decided to express the length of the ZOI in terms of *d* or *b*, in order to have a relationship which was dimensionless throughout.

$$\frac{y}{d\ or\ b} = f\left(\frac{d}{b}, Fr\right) \qquad 5\text{-}7$$

The hypothesised relation of variables served as the base of the relationship development. The ZOI dimensions were analysed by varying these variables. Once it was proved that the size of the ZOI was dependent on these variables the relationship between them was quantified.

5.3 Model Conditions

RiverFLO-2D was used to quantify the velocity variations caused by the placement of a boulder. Numerous models were run which incrementally varied the Froude number and blockage ratio between practical extremities. Figure 5-3 below shows the model conditions used for the formulation of the ZOI relationship.

The models used to develop the relationship varied the Froude number between 0.0 and 1.0 and blockage ratio between 0.0 and 0.1. The Froude number was varied within the subcritical regime while the blockage ratio was varied up to a blockage ratio of 0.1. Chapter 6 discusses blockage ratios larger than approximately 0.1 which cause a local control. The Froude number was varied by using different values of *Q*, *b* and *S*, while the blockage ratio used different values of *b* and *d*. The channel geometry, uniform flow conditions and boulder size used for the 51 models can be found in Appendix B.

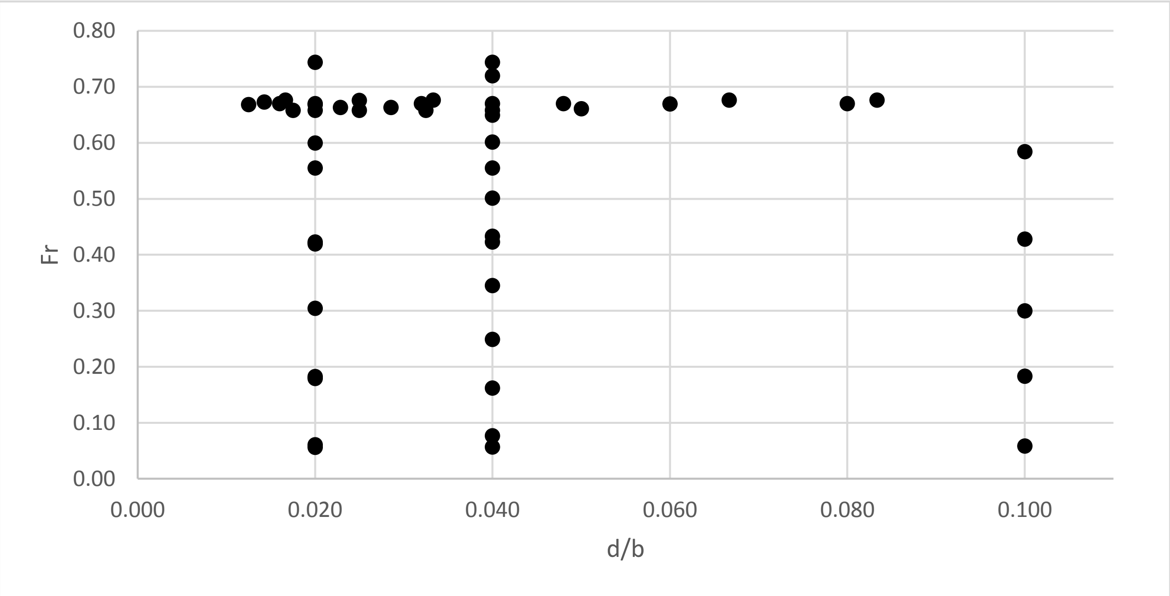

Figure 5-3: 1 Boulder Froude number and blockage ratio model conditions

5.4 Proving the Relationship

It should be noted that this section uses a 20% change in velocity from uniform velocity as a representation for all velocity variations. The other percentage variations followed the same trends and were incorporated into the relationship which was developed.

5.4.1 Froude Number

The dimensional analysis hypothesised that the Froude number could be used to account for the uniform velocity variables (Q*, b, s* and *n*). To determine whether the use of the Froude number was justified the Froude number was varied while the blockage ratio was kept constant. This was done for three different blockage ratios; namely 0.020, 0.040 and 0.100. The instance of having the same Froude number and blockage ratio but using a different *b* and *d* value to obtain the blockage ratio was also analysed.

Models 1-7, 11-15, 30-31 were used as a starting point of the investigation. These models varied the Froude number while keeping the blockage ratio constant, *(d/b* = 0.040*),* but also used the same *d* (0.20m) and *b* (5.0m). As shown in Figure 5-4, Figure 5-5 and Figure 5-6; the size of the ZOI increases with an increase in the Froude number.

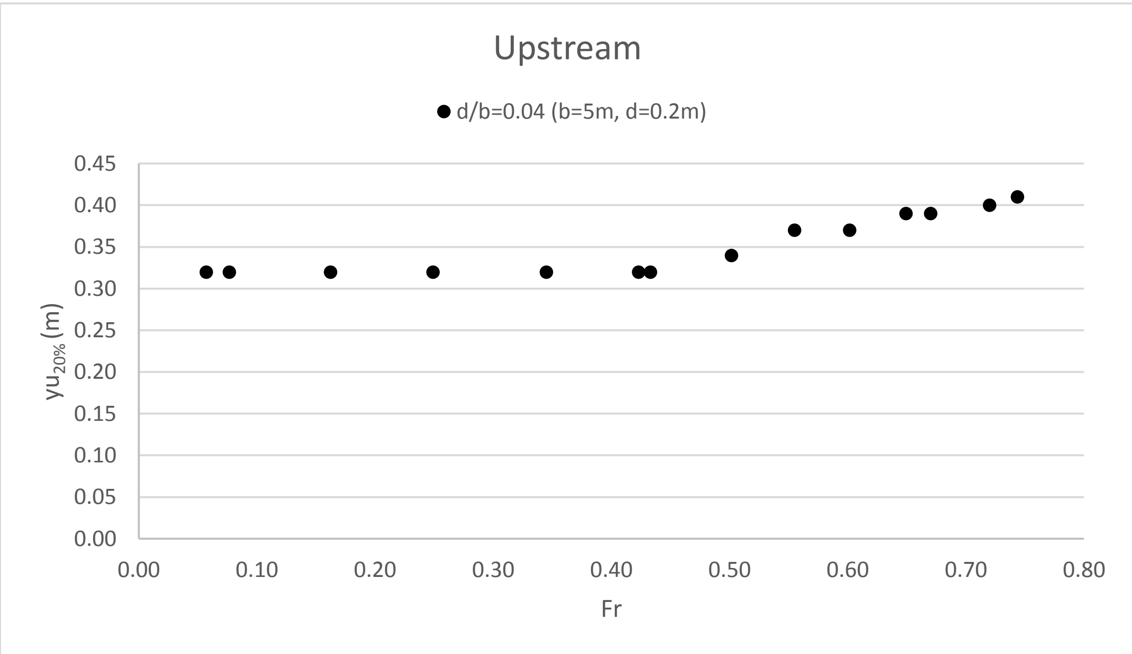

Figure 5-4: Upstream ZOI for different Froude numbers and a constant blockage ratio

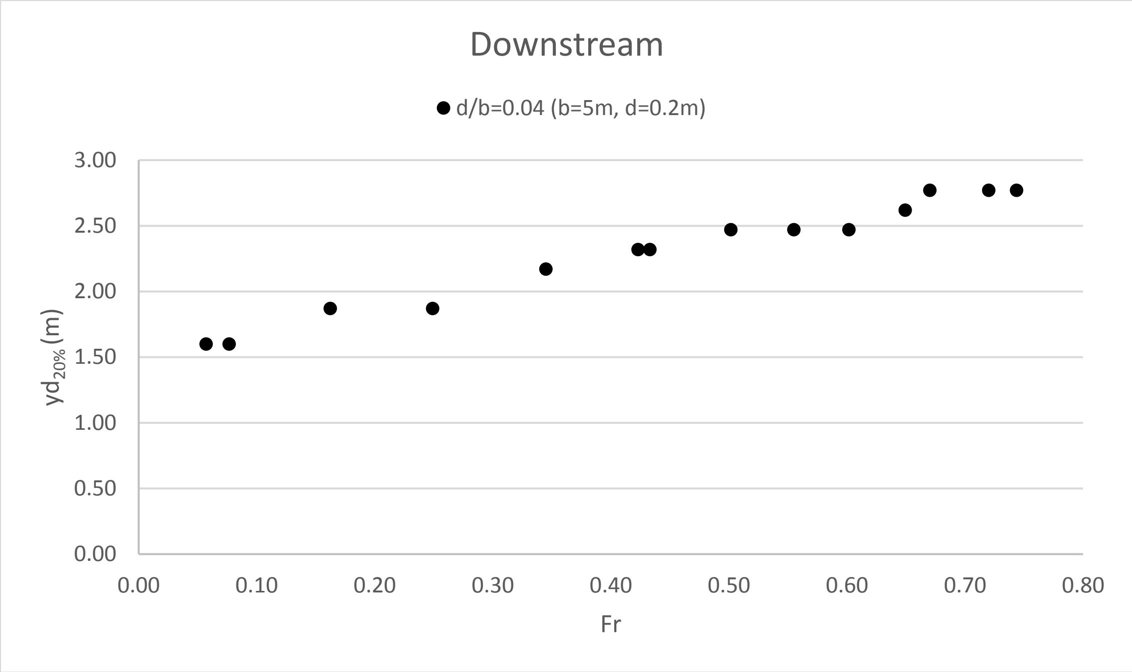

Figure 5-5: Downstream ZOI for different Froude numbers and a constant blockage ratio

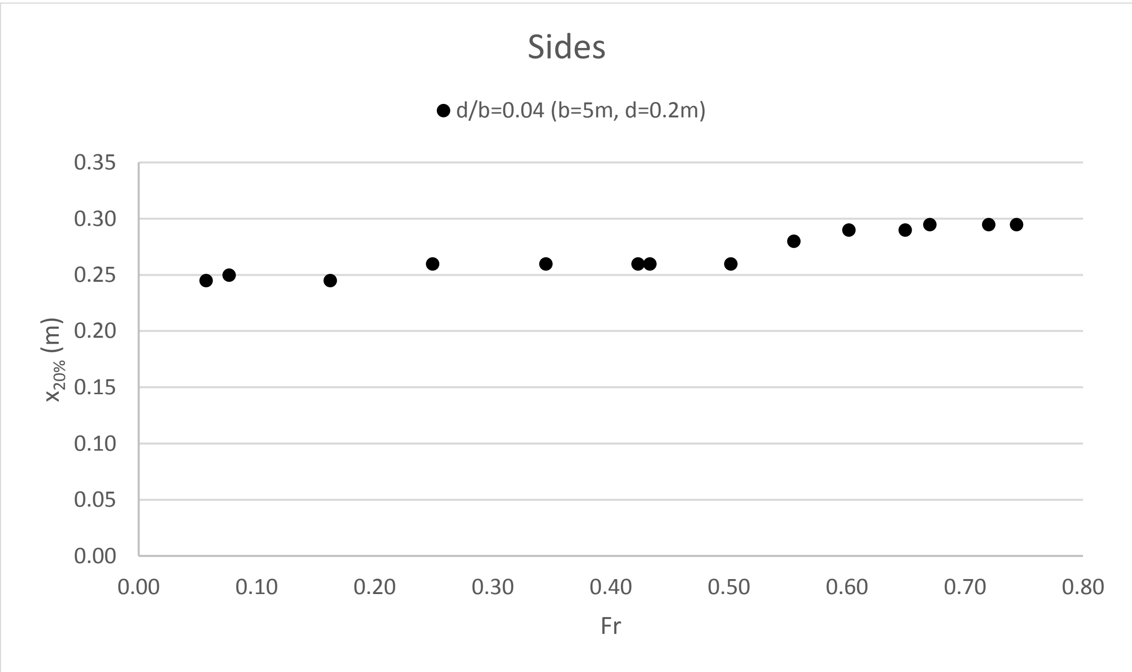

Figure 5-6: Transverse ZOI for different Froude numbers and a constant blockage ratio

Models 16 and 32-38 changed the blockage ratio to 0.020 and used *d*=0.10m and *b*=5.0m. Figure 5-7 below shows the results for the downstream direction. As noted by Hamuy-Blanco (2013) a decrease in the blockage ratio shows a decreased ZOI, this was evident here as well as these models were on a lower curve.

The next step in the analysis again used a blockage ratio of 0.02 but used different values of *b* and *d* to obtain this ratio, namely *d*=0.16m and *b*=8.0m (Models 23, 39-40 and 47-78). Interestingly this curve did not align with the other points which also used a blockage ratio of 0.020. Instead the resulting curve from these models was higher than the ones produced when using *d*=0.10m and *b*=5.0m. This phenomenon was of interest as the same Froude number and blockage ratio yields a different ZOI size.

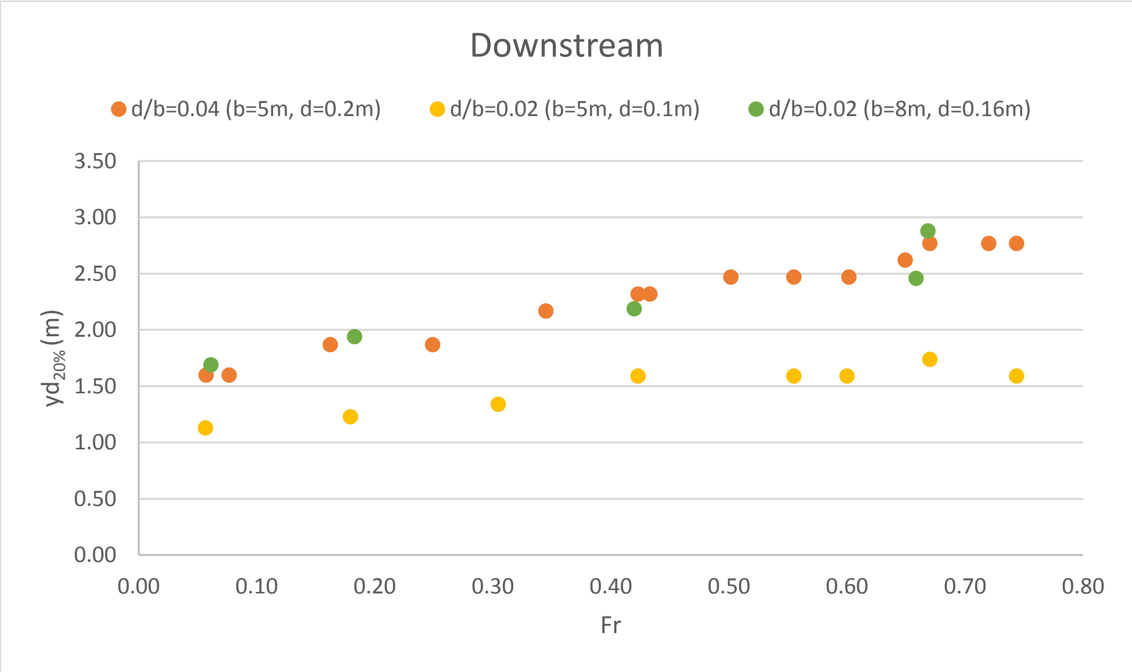

Figure 5-7: Downstream ZOI for different Froude numbers and three constant blockage ratios

An analysis of the variation of Froude numbers, whilst keeping the blockage ratio constant, demonstrated that an increase in the Froude number would also result in an increase of the size of the ZOI. Another important observation was that the size of the ZOI was different when using different *b* and *d* values to obtain the same Froude number and blockage ratio. The ZOI either had a stronger dependence on *b* or *d* than initially assumed.

5.4.2 Blockage Ratio

The aim for the blockage ratio variable was to see how the ZOI changed with a variation of the blockage ratio and to determine at what point the backing up effect occurs. It was found that backing up occurs when the blockage ratio was greater than 0.10; an in-depth discussion of this limit can be found in Section 6.

To explore the impact of the blockage ratio on the ZOI dimension, the blockage ratio was varied between 0.0125 and 0.10. These values were deemed to cover an acceptable range for practical use. When varying the blockage ratio, the Froude number was kept approximately the same, around 0.66-0.68. In order to keep the Froude number the same, the slope and discharge were varied for a particular blockage ratio.

Figure 5-8 shows the resultant ZOI dimensions for the downstream, upstream and transverse directions respectively. The curves showed that the ZOI had a clear dependence on the blockage ratio with variations of a few metres in the size of the respective ZOIs.

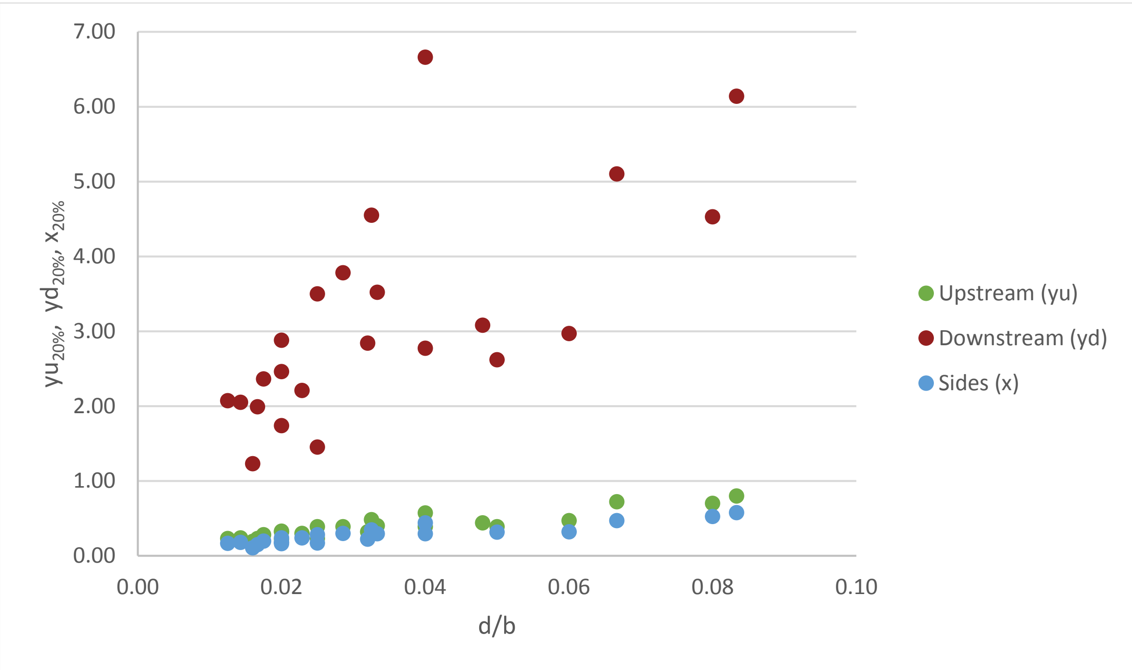

Figure 5-8: ZOI for different blockage ratios

5.4.3 Dimensionless ZOI

To ensure a dimensionally uniform relationship a length variable had to be considered along with the Froude number and blockage ratio. The length variables which were considered to be relevant were the channel width and boulder diameter. As discussed, once the variable had been identified it would be used to convert the

ZOI length into a dimensionless ratio allowing for extrapolation when designing a rehabilitation project.

When choosing between the width of the channel or the boulder diameter it was important to realise that both had already been accounted for in the blockage ratio and Froude number. It was of interest to see which variable the ZOI would have a stronger dependency on than initially assumed.

$$\frac{y}{d \text{ or } b} = f\left(\frac{d}{b}, Fr\right) \quad (5\text{-}8)$$

Using the models which had the same Froude number and different blockage ratios the normalised ZOI length was calculated.

Figure 5-9 shows the resultant plot when dividing the ZOI length by the boulder diameter for all three directions. Following this;

Figure 5-10 shows the effect of dividing the ZOI length by the channel width.

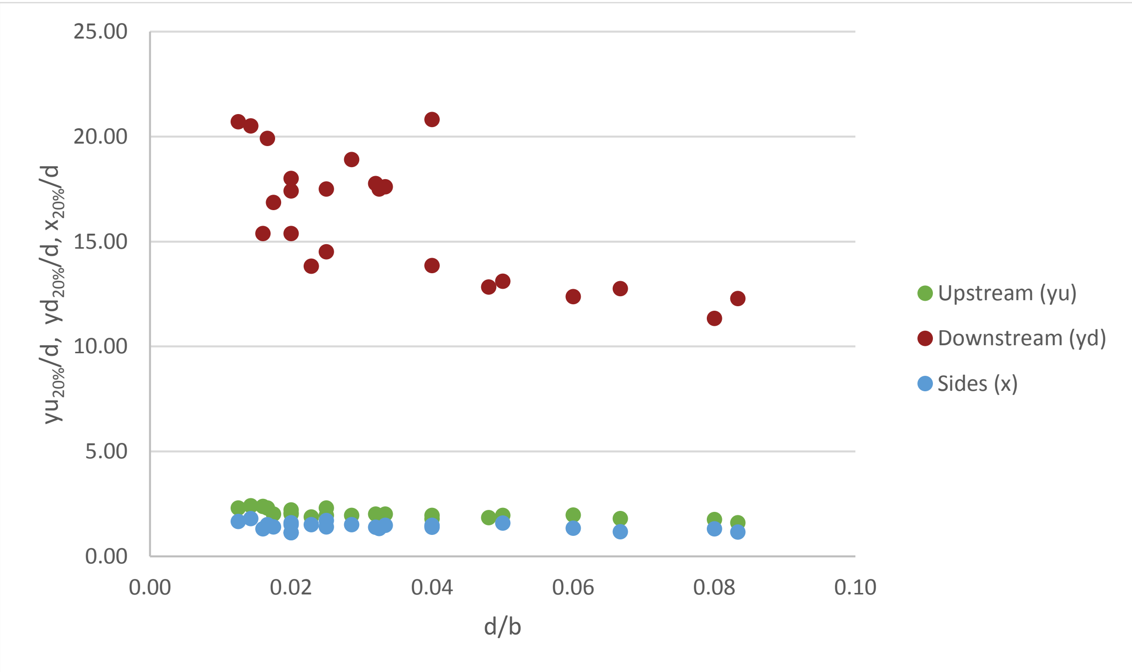

Figure 5-9: ZOI normalisation using diameter

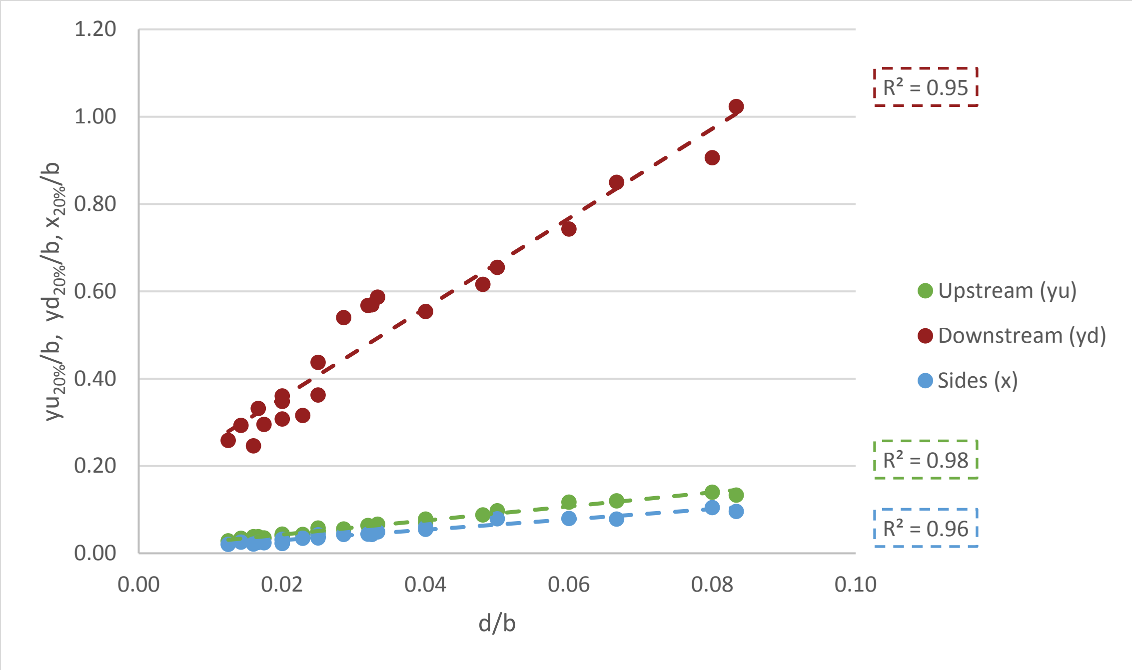

Figure 5-10: ZOI normalisation using width

From comparing the two plots it was clear that the ZOI holds an additional dependence on *b* instead of *d*. The resultant ZOI ratio closely resembled the curve comparing the effect of the blockage ratio to the ZOI length (Figure 5-8). The normalised trend became clearer as the outlying points were normalised into one trend. The concern of the models which had the same Froude number and blockage ratio was rectified as their ZOI ratios were equal.

The use of the channel width was deemed effective to describe the ZOI and create a dimensionless ZOI ratio that will allow for practical extrapolation. The relationship to describe the ZOI in the upstream, downstream and transverse directions was confirmed to be dependent on the Froude number, blockage ratio and channel width, i.e.

$$\frac{y}{b} = f\left(\frac{d}{b}, Fr\right) \qquad 5\text{-}9$$

5.5 Creating the Relationship

The relationship proposed had to be evaluated as a whole to determine the exact way in which all the variables were related. The variables were assigned coefficients to quantify dependencies. The relationship

$$\frac{y}{b} = f\left(\frac{d}{b}, Fr\right) \qquad 5\text{-}10$$

was assumed to have the form

$$\frac{y}{b} = m \times \left(\frac{d}{b}\right)^{o} \times Fr^{\,p} \qquad 5\text{-}11$$

where *m, o* and *p* were the constants to be determined.

In order to determine the values of the coefficients a multiple regression was used. Natural logarithms were applied to transform the equation into the form needed for a multiple regression.

$$\ln\left(\frac{y}{b}\right) = m + \ln\left(\frac{d}{b}\right)^{o} + \ln(Fr)^{p} \qquad 5\text{-}12$$

$$\ln\left(\frac{y}{b}\right) = m + o \times \ln\left(\frac{d}{b}\right) + p \times \ln(Fr) \qquad 5\text{-}13$$

The output of the regression provided values for the *m, o* and *p* constants as well as providing regression statistics which analyse the relationship. The formula was then converted back to its original form as shown below.

$$\ln\left(\frac{y}{b}\right) = m \times \ln\left(\frac{d}{b}\right)^{o} \times \ln(Fr)^{p} \qquad 5\text{-}14$$

$$e^{\ln\left(\frac{y}{b}\right)} = e^{m} \times e^{\ln\left(\frac{d}{b}\right)^{o}} \times e^{\ln(Fr)^{p}} \qquad 5\text{-}15$$

$$\frac{y}{b} = n \times \left(\frac{d}{b}\right)^{o} \times Fr^{\,p} \qquad 5\text{-}16$$

5.5.1 Setup

The following should be noted with regards to the relationship setup:

- The downstream results were calibrated by using the correction factors determined from the experimental results. The experimental runs found that reduced velocities, up to 20% from uniform velocity, extended beyond the boundary of the flume. Only velocities greater than 20% were used to create a relationship for the downstream direction.

Table 5-3: Downstream correction factors for 1 boulder

Velocity Correction Factor, *Cv*	**Distance Correction Factor, *Cyd***
0.850	1.70

- The relationships were developed for percentage variations up to 70% for the upstream and downstream directions and up to 20% for the side direction. Higher percentage variations were not analysed as several models did not have percentage variations higher than these limits and those that did, had small ZOI dimensions.
- The relationship was developed using blockage ratios varying from 0.0125 to 0.10 and Froude numbers in the subcritical flow regime.

As shown in

- Figure 5-10, when the Froude number was constant a linear relationship existed between the blockage ratio and ZOI dimension. Figure 5-11 below has additional points which varied the Froude number for specific blockage ratios. Each Froude number had a linear trend with an increasing blockage ratio each with a different gradient. A total of 51 models were used in the formulation.

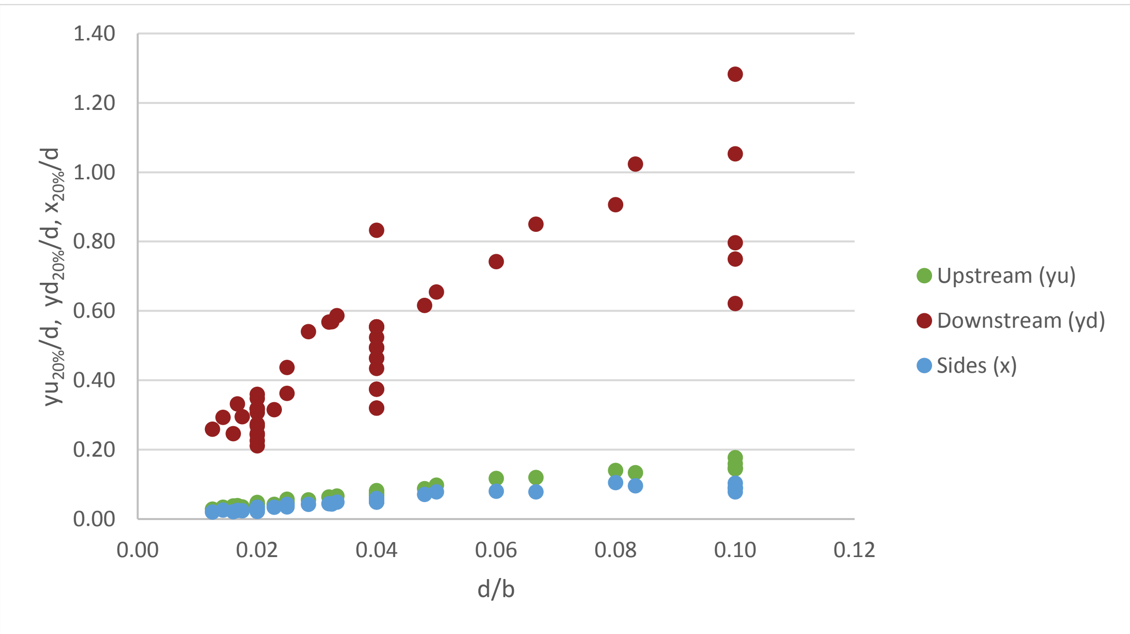

Figure 5-11: ZOI relationship setup

5.5.2 Results

As mentioned, the relationship for each direction had the same form but different constants. Similarly, for each direction the constants varied for different percentage variations. The base relationship was described as follows:

$$\frac{yu_i, yd_i, x_i}{b} = n_i \times \left(\frac{d}{b}\right)^{o_i} \times Fr^{\,p_i} \qquad \text{5-17}$$

The final relationship for each direction is as follows;

Upstream

$$\frac{yu_i}{b} = n_i \times \left(\frac{d}{b}\right)^{o_i} \times Fr^{\,p_i} \qquad \text{5-18}$$

Table 5-4: Upstream ZOI coefficients

Constant	Percentage variation, *i* %						
	10	**20**	**30**	**40**	**50**	**60**	**70**
n_i	1.86	1.12	0.93	0.89	0.70	0.65	0.58
o_i	0.84	0.83	0.87	0.93	0.90	0.92	0.93
p_i	0.07	0.05	0.03	0.03	-0.01	0.01	-0.02

Downstream

$$\frac{yd_i}{b} = n_i \times \left(\frac{d}{b}\right)^{o_i} \times Fr^{\,p_i} \qquad \text{5-19}$$

Table 5-5: Downstream ZOI coefficients

Constant	Percentage variation, *i* %					
	20	**30**	**40**	**50**	**60**	**70**
n_i	6.15	2.24	1.61	1.40	1.25	1.33
o_i	0.72	0.73	0.73	0.74	0.76	0.83
p_i	0.23	0.13	0.15	0.16	0.17	0.16

Sides

$$\frac{x_i}{b} = n_i \times \left(\frac{d}{b}\right)^{o_i} \times Fr^{\,p_i} \qquad 5\text{-}20$$

Table 5-6: Side ZOI coefficients

Constant	Percentage variation, *i* %	
	10	**20**
n_i	1.92	0.78
o_i	0.98	0.82
p_i	-0.02	0.10

5.5.3 Effectiveness

The effectiveness of the created relationship was reviewed by considering two statistical factors. The first step was to predict the ZOI ratio from the relationship formed and then compare this to the computer model result in the form of a percentage variation. The average absolute percentage variation was then found from all the models in any relationship. Secondly the coefficient of determination *(R^2)* was used to analyse how well the model results compared to the developed relationship. Shown in Table 5-7 below is a summary of the average absolute percentage error of the predicted values from the relationship compared to the software output. The majority of these errors are below 10%, showing that the relationship is effective. The effectiveness of the relationship is further proved by the high R^2 values. A more detailed comparison can be found in Appendix C.

Table 5-7: % Error and R^2 values

i (%)	Upstream		Downstream		Sides	
	% Error	**R^2**	**% Error**	**R^2**	**% Error**	**R^2**
10	9.26	0.94	-	-	13.91	0.86
20	7.08	0.97	8.86	0.92	7.99	0.95
30	5.19	0.98	7.52	0.95	-	-
40	8.13	0.95	7.31	0.95	-	-
50	5.01	0.99	7.54	0.95	-	-
60	3.08	0.99	7.16	0.96	-	-
70	3.41	0.99	8.84	0.95	-	-

The effectiveness of the created relationship was also quantified using the dimensional ZOI length. The ZOI length predicted by the software was compared to the ZOI length predicted by the proposed relationship. Figure 5-12, Figure 5-13 and Figure 5-14 show the comparison of lengths for all percentage variations in the upstream, downstream and side directions respectively. An equation with a unit gradient would represent a perfect correlation between the software and proposed relationship; all directions exhibited gradients closely equal to 1. The high R^2 values for each direction furthermore indicated that there was minimal scatter.

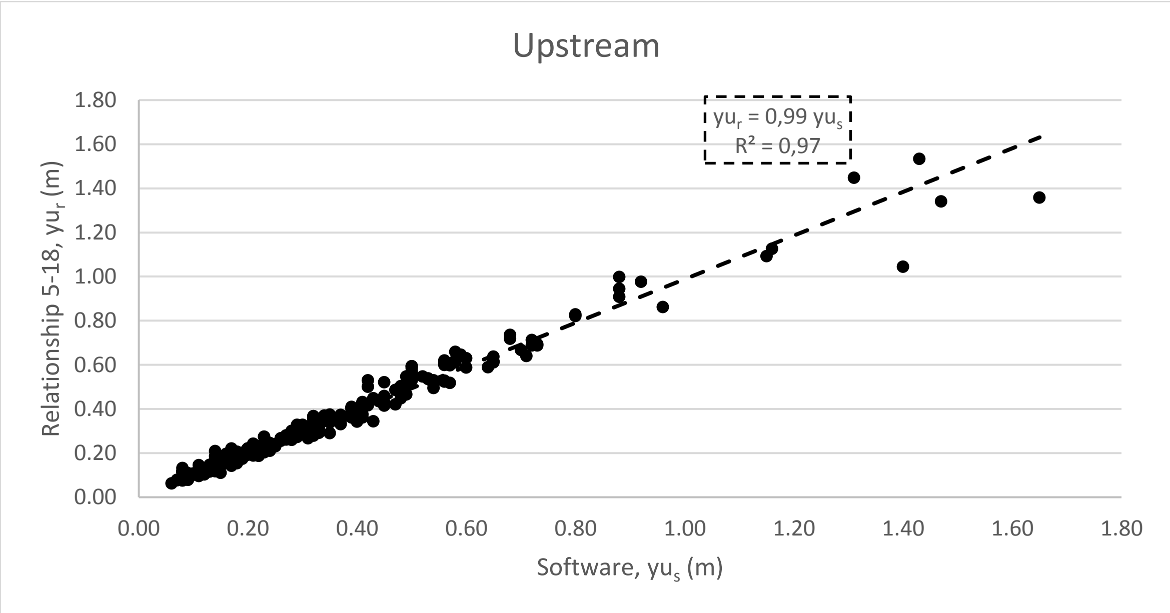

Figure 5-12: Upstream software vs relationship 5-18

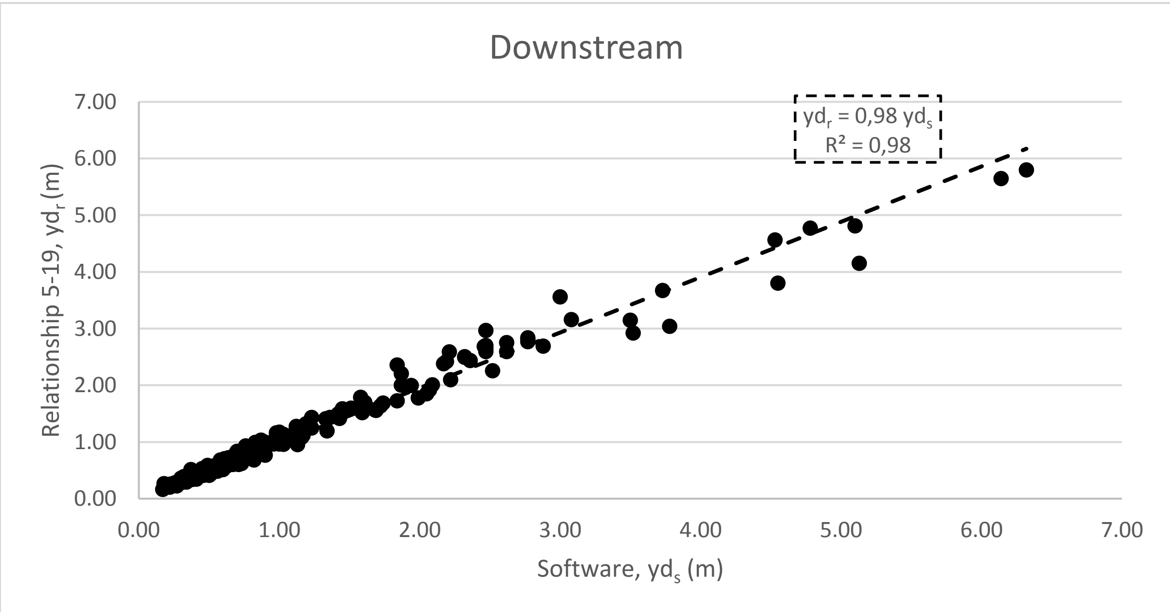

Figure 5-13: Downstream software vs relationship 5-19

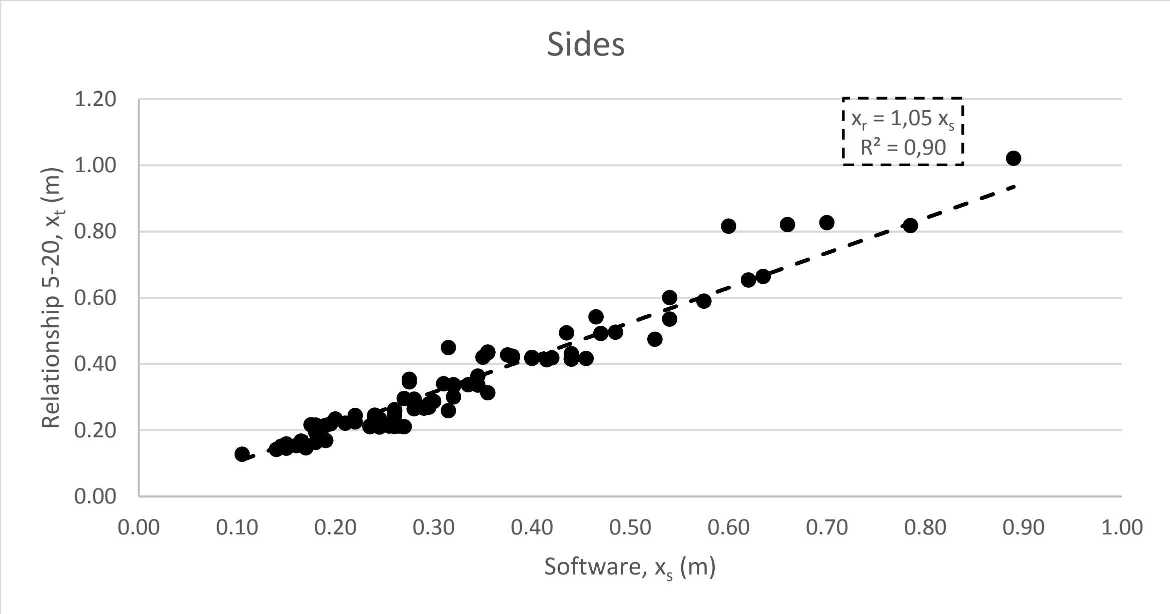

Figure 5-14: Sides software vs relationship 5-20

5.6 Practical Approximation

Table 5-4, Table 5-5 and Table 5-6 show the Froude number coefficient (p_i) was close to zero and less than the other coefficients. The fact that the Froude number coefficient is less than any of the other coefficients and close to zero showed that it was not the primary variable. The primary variable on the other hand was the blockage ratio.

Another ZOI relationship was created which eliminated the Froude number and predicted the ZOI using the blockage ratio only. Having a relationship to describe the ZOI without a Froude number yields a relationship which is independent of hydraulic variables. This held practical convenience as an approximate ZOI size could be calculated irrespective of the design discharge.

5.6.1 Results

A relationship was created to predict the dimensionless ZOI ratio using the blockage ratio. Regressions were undertaken to determine the *r* and *t* coefficients in the relationship below:

$$\frac{yu_i, yd_i, x_i}{b} = r_i \times \left(\frac{d}{b}\right)^{t_i} \qquad \text{5-21}$$

The final relationship for each direction is as follows;

Upstream

$$\frac{yu_i}{b} = r_i \times \left(\frac{d}{b}\right)^{t_i} \qquad 5\text{-}22$$

Table 5-8: Upstream practical ZOI coefficient

Constant	Percentage variation, *i* %						
	10	20	30	40	50	60	70
r_i	1.70	1.05	0.89	0.86	0.71	0.64	0.60
t_i	0.83	0.83	0.86	0.92	0.90	0.92	0.94

Downstream

$$\frac{yd_i}{b} = r_i \times \left(\frac{d}{b}\right)^{t_i} \qquad 5\text{-}23$$

Table 5-9: Downstream practical ZOI coefficient

Constant	Percentage variation, *i* %					
	20	30	40	50	60	70
r_i	4.52	1.87	1.32	1.13	1.00	1.07
t_i	0.69	0.71	0.71	0.72	0.73	0.81

Sides

$$\frac{x_i}{b} = r_i \times \left(\frac{d}{b}\right)^{t_i} \qquad 5\text{-}24$$

Table 5-10: Sides practical ZOI coefficient

Constant	Percentage variation, *i*, %	
	10	20
r_i	1.97	0.66
t_i	0.98	0.79

5.6.2 Effectiveness

The effectiveness of the created relationship was once again quantified by comparing the ZOI predicted by the software to the ZOI ratio predicted by the relationship. Shown in Table 5-11 below is a summary of the average absolute percentage error of the predicted values from the relationship compared to the software output. The errors were larger than when compared to the relationship including the Froude number but were still low enough to be regarded as adequate in an initial design stage.

Table 5-11: % Error and R^2 values practical approximation

***i* (%)**	**Upstream**		**Downstream**		**Sides**	
	% Error	***R*²**	**% Error**	***R*²**	**% Error**	***R*²**
10	9.72	0.93	-	-	13.48	0.86
20	7.63	0.96	16.96	0.77	9.54	0.93
30	5.46	0.98	11.69	0.89	-	-
40	8.67	0.95	11.68	0.89	-	-
50	5.01	0.99	12.81	0.87	-	-
60	3.21	0.99	12.45	0.88	-	-
70	3.35	0.99	13.77	0.88	-	-

Figure 5-15, Figure 5-16 and Figure 5-17 show the comparisons for all percentage variations in the upstream, downstream and side directions respectively. The high R^2 values for each direction furthermore indicated that there was minimal scatter.

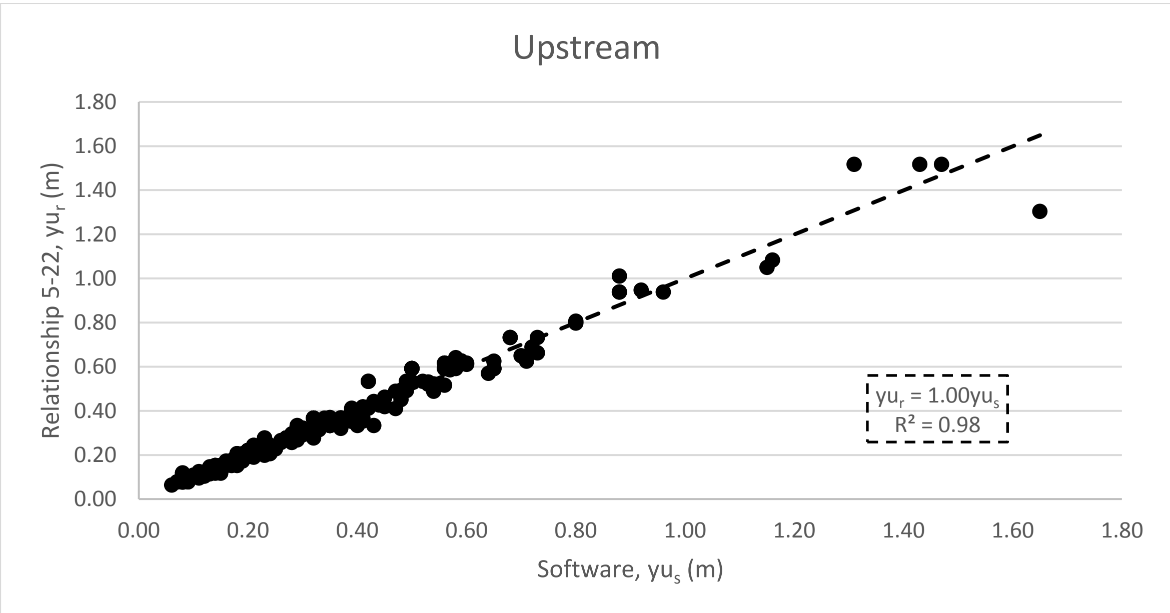

Figure 5-15: Upstream software vs relationship 5-22

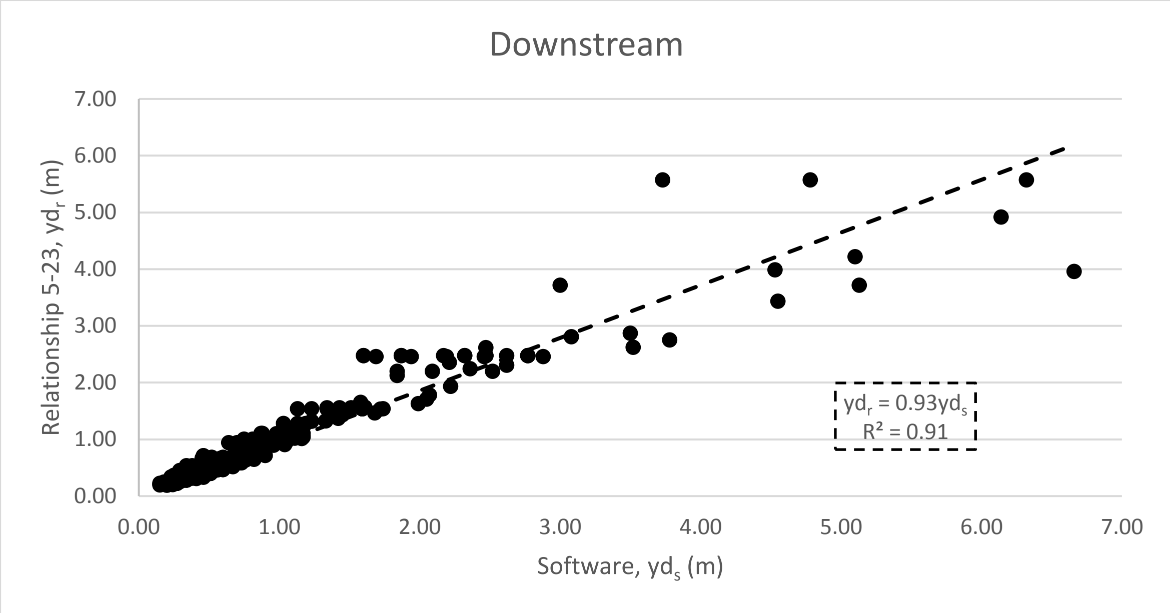

Figure 5-16: Downstream software vs relationship 5-23

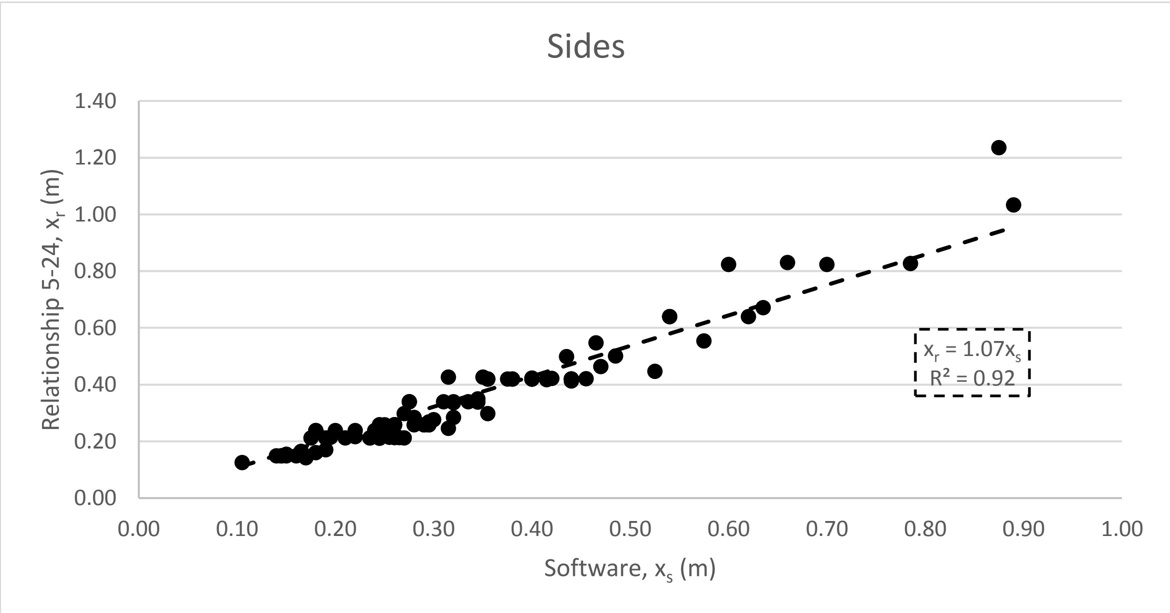

Figure 5-17: Sides software vs relationship 5-24

5.7 Conclusion

The velocity distribution around a single boulder for a particular case was analysed with the calculation of the ZOI and an areal velocity histogram. The ZOI allowed the disturbed region length to be quantified and to be compared to the size of the boulder. The velocity histogram showed the area which different percentage velocity variations occupy. It was observed that the downstream direction showed the largest region of disturbed flow. Furthermore, low percentage variations from uniform velocity occupied the greatest area of disturbed flow. From these findings it is recommended that the chosen boulder diameter should create a change in Flow Class for the 10% or 20% velocity variations in order for a substantial area to be available for targeted species.

The analysis of a larger variation of flow classes allowed for a new relationship to be developed, shown in equation 5-17. Another relationship was developed for the purpose of practical approximation which predicts the ZOI by using the channel width and boulder diameter only, shown in equation 5-21. Neglecting the Froude number results in a relationship which is independent of flow conditions within the channel. This holds practical value as initial boulder designs can be independent of the design discharge.

It was found that the ZOI for the upstream, transverse and downstream directions can be predicted by:

$$\frac{yu_i, yd_i, x_i}{b} = n_i \times \left(\frac{d}{b}\right)^{o_i} \times Fr^{\,p_i} \qquad 5\text{-}17$$

or

$$\frac{yu_i, yd_i, x_i}{b} = r_i \times \left(\frac{d}{b}\right)^{t_i} \qquad 5\text{-}21$$

6 BLOCKAGE RATIO LIMIT

Hamuy-Blanco & James (2014) investigated the effects of multiple boulders transverse to the direction of flow. Interestingly, once more boulders were added it was found that the ZOI extended across the whole width of the channel and a considerable distance upstream. The instance where this occurred was found to be where the blockage ratio was greater than 0.075.

Guidelines have also implied a similar threshold width. Scheuler and Brown (2004) suggest that boulders should comprise less than 10% of the cross-sectional area. Brown and Johnson (1999) advise that boulder diameters should be no more than a 1/8 of the width of the channel. Saldi-Caromile et al. (2004) suggest that boulders should be limited to 20-30% of the cross-sectional area in order to avoid excessive bank scour, debris accumulation and flooding.

The blockage limit was firstly approximated as a blockage ratio of 0.10. The limit was then identified using theoretical energy principles and comparing the boulder to a contraction in the channel width.

The velocity distribution was analysed following the identification of the blockage ratio limit. The velocity distribution differed significantly compared to the velocity distribution below the blockage limit.

Above the blockage limit the upstream velocity changes extended across the entire width of the channel and for large distances upstream of the boulder. Energy principles were used to determine the velocity just upstream of the boulder which extend across the whole channel width and how far upstream the velocity would return to uniform. It was noted that all percentage variations larger than the new approach velocity variation could be estimated using the relationship developed for 1 boulder not in choking conditions (Section 5). Lastly, a relationship was developed to determine the maximum increase in flow depth upstream of the boulder to access flooding risks.

Above the blockage limit the sides of the boulder had larger velocities which extended to the bank of the channel. The increase of the velocity disturbance was of interest due to potential channel erosion and bank stability problems. The scour pools created by increased velocity have been identified as micro-habitats for aquatic organisms such as invertebrates. The increase of velocity on the sides differ from scour pools as it covers a much larger area. Two relationships were developed which can predict the highest percentage velocity increase at the bank of the channel as well as how far this extends on the bed of the channel.

The impact of the boulder on the velocities in downstream direction was found to be the same above and below the blockage limit.

6.1 Below and Above the Blockage Limit

Figure 6-1 and Figure 6-2 below compare the disturbed velocity zones around a boulder below and above the blockage limit for the following model conditions.

Table 6-1: Model conditions below and above the blockage limit

Model	***Q (m^3/s)***	***S***	***n***	***v (m/s)***	***b (m)***	***d (m)***	***d/b***
1	1.250	0.00080	0.010	1.033	5.0	0.20	0.04
27	1.250	0.00080	0.010	1.033	5.0	1.00	0.2

The disturbed velocity zone below the blockage limit had the largest disturbance in the downstream direction and the smallest disturbance on the sides. As the boulder diameter increased the disturbance zone increased in size until the blockage limit. Interestingly once the blockage ratio limit was exceeded the upstream direction had disturbed velocities which extended across the width of the channel and to the upstream extent of the channel. The sides of the boulder showed increased velocities extending to the banks of the channel.

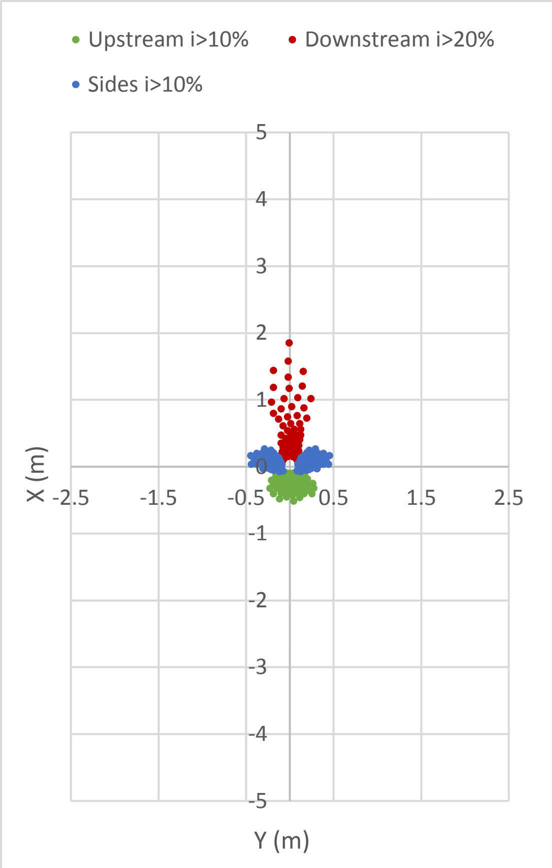

Figure 6-1: Below blockage limit (Model 1) disturbed flow

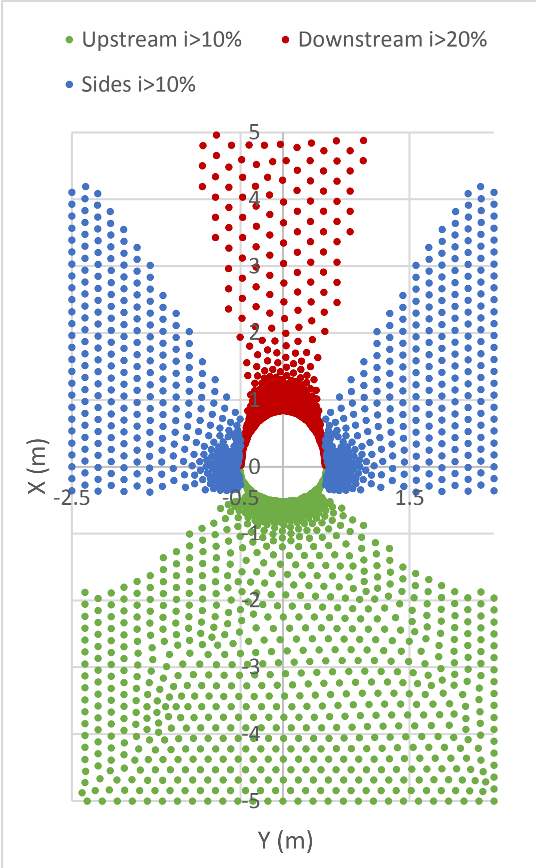

Figure 6-2: Above blockage limit (Model 27) disturbed flow

6.2 Model Conditions

The following models were included which were identified as having high blockage ratios:

Table 6-2: High blockage ratio models

Model	*b* (m)	*d* (m)	*Q* (m^3/s)	*S*	*Fr*	*d/b*
25	5.0	0.6	1.250	0.00080	0.670	0.120
27	5.0	1.0	1.250	0.00080	0.670	0.200
49	6.0	1.0	1.500	0.00080	0.676	0.167
50	6.0	0.6	1.500	0.00080	0.676	0.100
54	4.0	1.0	1.250	0.00080	0.670	0.250

6.3 Identifying the Blockage Ratio Limit

The findings from the resultant ZOI dimensions showed that there was a sudden enlargement with large blockage ratios, which is in line with results obtained from Hamuy-Blanco & James (2014). The large blockage ratios correspond to a small width or large boulder. A control and a subsequent change in flow regime are relevant if one were to consider the hydraulic conditions associated with a small width. The control would cause a change in the ZOI as the flow approaching the boulder is no longer at uniform conditions.

Figure 6-3 below shows a model with a boulder placed in the centre; the placement of the boulder could be seen as a contraction equal to the boulder diameter.

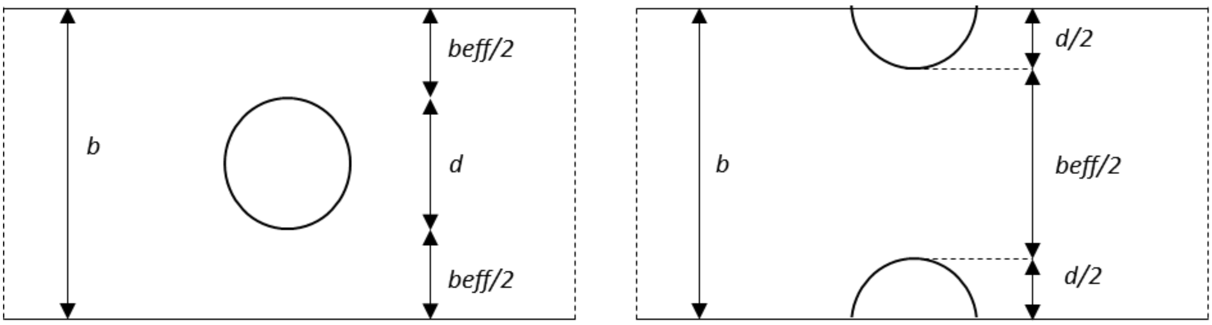

Figure 6-3: Channel contraction modelling

Using this as a modelling tool it was possible to determine the 'width' of the channel that would cause choking. If choking were to occur, then the location of the boulder would become a location for the control of the flow. The flow upstream of the boulder would have to gain energy and become deeper so as to pass the boulder, after the boulder the flow would not return to subcritical but rather a transition to supercritical flow would occur. The supercritical flow will return to uniform conditions by means of a hydraulic jump just downstream of the boulder. The width that would cause choking of the flow was calculated using energy principles.

The first step in determining the possibility of choking would be to calculate the uniform specific energy *(E)* of the channel by

$$E = H + \frac{v^2}{2g} \tag{6-1}$$

The smallest width that can be accommodated without choking would be when the critical specific energy of the contracted *(Ec)* portion is equal to the specific energy of the channel,

$$E = \ Ec \tag{6-2}$$

From this the critical depth *(Hc)* can be determined

$$Hc = \frac{2}{3}\ Ec \tag{6-3}$$

This allows for the corresponding discharge per unit width *(q)* to be determined by

$$Hc = \left(\frac{q^2}{g}\right)^{\frac{1}{3}} \tag{6-4}$$

q can be related back to the width of the channel by considering its definition

$$q = \frac{Q}{bmin} \tag{6-5}$$

The resulting *bmin* calculated represents the minimum channel width for choking not to occur; any value below this width will induce choking. It is important to note the addition of the boulder was modelled as a change in width, so the effective width of the channel can be calculated using

$$beff = b - d \tag{6-6}$$

The above formulation of the choking condition can be summarised into one equation. A boulder will cause choking if the *beff* is less than *bmin.* It can be concluded that a boulder will cause choking of the flow if the following conditions is met:

$$d > b - \frac{Q}{\left(\left(\frac{2}{3}E\right)^3 x\, g\right)^{0.5}} \qquad 6\text{-}7$$

The ZOI dimensions of the models which were identified as choking were analysed, as the ZOI would not necessarily be the same due to the change in control of the flow to the location of the boulder. The choking calculation was initially performed to see if this phenomenon could be the underlying cause of the sudden increase of the ZOI. The models identified as choking (Table 6-2) all had a blockage ratio above 0.010 which was the first approximation of the blockage limit. The models also all had an effective width less than the minimum width for choking not to occur; demonstrating that the use of theoretical energy principles to determine the blockage limit was justified.

Table 6-3: Effective width and minimum width

Model	***d/b***	***bmin* (m)**	***beff* (m)**
25	0.120	4.54	4.40
27	0.200	4.54	4.00
49	0.167	5.47	5.00
50	0.100	5.47	5.40
54	0.250	3.63	3.00

Equating boulder placement to channel contraction is however a modelling assumption so it was checked if any of the points within these models had Froude numbers greater than 1.0, which would indicate supercritical flow. All the models checked for choking showed that Froude numbers greater than one were present on the sides of the boulder, furthermore the water surface elevation plots showed a gradually varied flow profile upstream of the boulder with increasing depth. This indicated that the models were indeed choking.

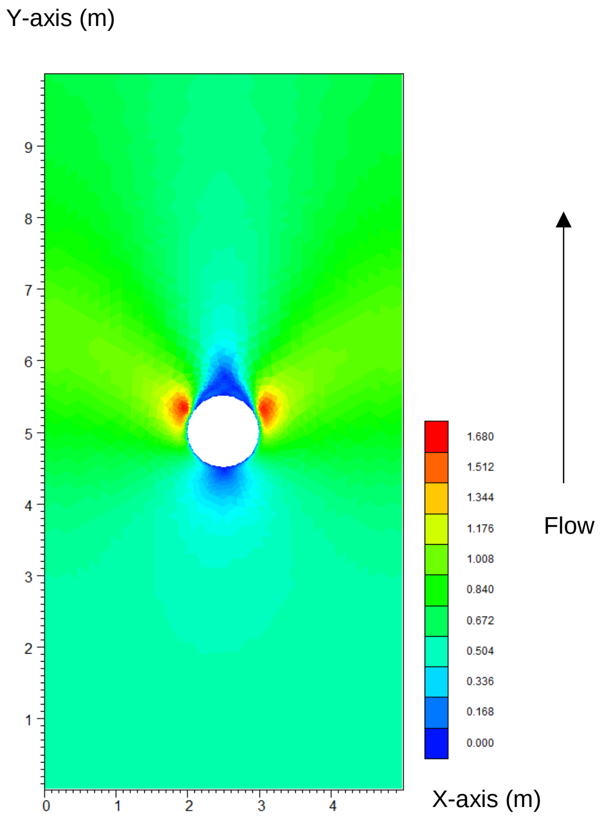

Figure 6-4: Model 27 Froude number

6.4 Analysis of the Velocity Distribution

Once a method was found which could predict the blockage ratio at which choking occurs, the velocity distribution was analysed. It was found that the upstream velocity disturbance was very large. The gradually varied flow profile upstream of the boulder extended hundreds of metres. As a result the upstream direction should be utilised in creating aquatic habitats when using a boulder large enough to exceed the blockage limit. The scenario of using a boulder below the blockage limit differs in that the downstream direction has the largest disturbed velocity area.

In order to utilise the large upstream disturbance, relationships were developed which predict the upstream velocity distribution. The upstream velocity changes were effectively described using the theoretical energy principles already discussed as well as gradually varied flow computations.

The analysis of the velocity distribution also considered potential risks associated with the large upstream disturbance; namely flooding and erosion. The gradually varied flow profile upstream of the boulder created increased flow depths which were no longer localised around the boulder but extended across the width of the channel and some distance upstream. The sides of the boulder had larger velocities which extended to the bank of the channel. Two relationships were developed which can predict the highest percentage velocity increase at the bank of the channel as well as how far this extends on the bed of the channel. The likelihood of the increased velocity causing erosion should be considered when utilising a high blockage ratio design.

The impact of the boulder on the velocities in downstream direction was found to be the same above and below the blockage limit. As a result the relationship developed in Section 5 could be used to describe the downstream ZOI when the blockage ratio is high.

6.4.1 Upstream

All models which were identified as choking were analysed in the upstream direction. These velocity distributions were clearly different to models not choking; the exact differences were noted as well as quantified with energy principles.

6.4.1.1 New approach conditions

The same energy principles used to determine whether a boulder would cause choking were used to determine what effect the boulder had on the upstream flow velocity. The control causes new approach conditions upstream of the boulder, which extend across the whole width of the channel. Figure 6-5 below shows a boulder which has choked the flow.

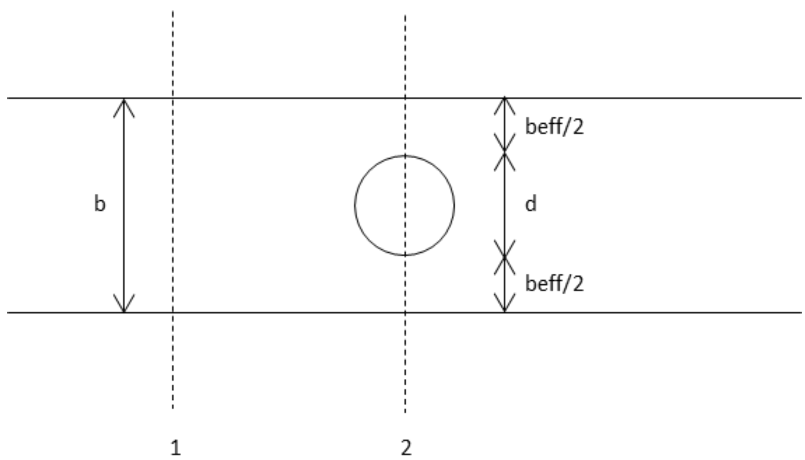

Figure 6-5: Upstream approach conditions model

The flow conditions at 2 will be of the critical condition, determined by the discharge and effective width.

$$Hc = H2 = \sqrt[3]{\frac{\left(\frac{Q}{beff}\right)^2}{g}} \qquad 6\text{-}8$$

The specific energy at 2 will be equal to the specific energy at 1

$$Ec = E2 = \frac{3}{2}\,Hc = E1 \qquad 6\text{-}9$$

The specific energy at 1 differs to that of 2 because of the different channel widths. Solving for the subcritical flow depth at 1 using the specific energy resulted in a flow depth expected upstream of a boulder. The specific energy at 1 can be defined as follows

$$E1 = H1 + \frac{\left(\frac{Q}{b}\right)^2}{2g\,H1^{\,2}} \qquad 6\text{-}10$$

The flow depth allowed for the calculation of the velocity at 1

$$v1 = \frac{\frac{Q}{b}}{H1} \qquad 6\text{-}11$$

The flow depth and velocity upstream of the boulder were the new approach conditions. These conditions would be present upstream of the boulder, moving further upstream of the boulder; a gradually varied M1 profile was present. This profile represented the water returning to uniform conditions some distance upstream.

Model 27 was used as an example. The theoretical analysis predicted that the approach velocity would be in the 10-20% variation range when compared to uniform flow. Figure 6-6 below shows an example of the new approach flow conditions. The velocity changes were characterised by percentage difference ranges for computational and visual simplicity. The software output confirmed this prediction; the 10-20% velocity variations approaching the boulder were seen throughout the width and extended to the geometrical upstream boundary.

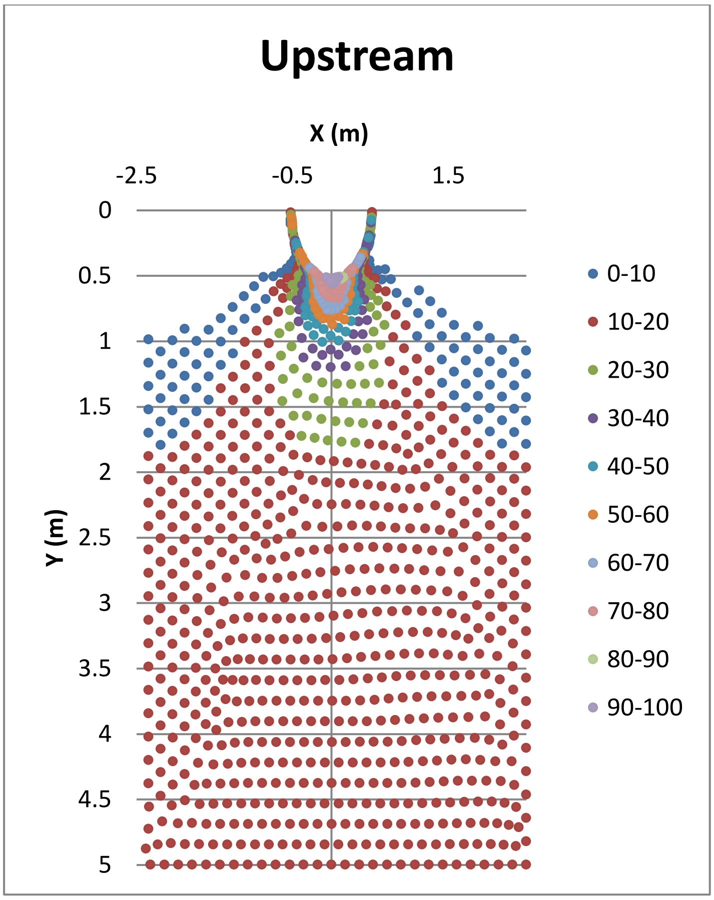

Figure 6-6: Model 27 upstream velocity distribution

All choking models showed new approach velocities in the range predicted by the theoretical analysis. Table 6-4 below shows the theoretical approach velocities which were expected and their difference when compared to the uniform velocity. Also shown in Table 6-4 are the velocity ranges determined by the software. The software ranges were determined by considering which range extended across the full width and to the upstream extent of the channel domain, as shown for Model 27 in Figure 6-6.

Table 6-4: Theoretical and experimental new approach conditions

Model	***v* (m/s)**	***v*1 (m/s)**	**% Difference**	**% Range**	**% Range Software**
25	1.03	0.99	3.78	0-10	0-10
27	1.03	0.88	14.76	10-20	10-20
49	1.04	0.92	11.16	10-20	10-20
50	1.04	1.02	2.31	0-10	0-10
54	1.11	0.89	19.71	10-20	10-20

6.4.1.2 Higher percentage variations

Figure 6-7 below shows the linear trend of small blockage ratios but also has the addition of models identified as chocking choking; all of the models shown have the same Froude number. The choking models present points which are clear outliers to the linear trend for the 10% change in velocity from uniform conditions.

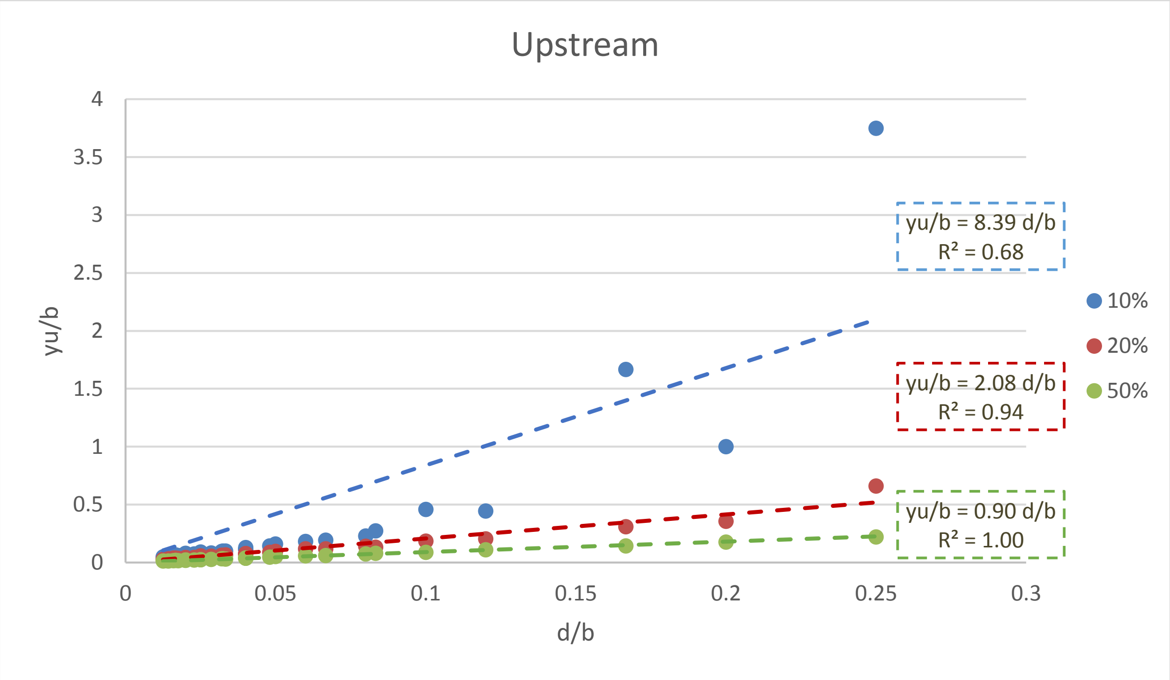

Figure 6-7: Non-linear blockage ratio with choking

For each model identified as choking, all points which were equal to or smaller than the new approach velocity percentage variation were removed as shown in Figure 6-8 below. The resultant plot shows that the removal of the models eliminates the outliers and the linear relationship between the dimensionless ZOI and the blockage ratio returned.

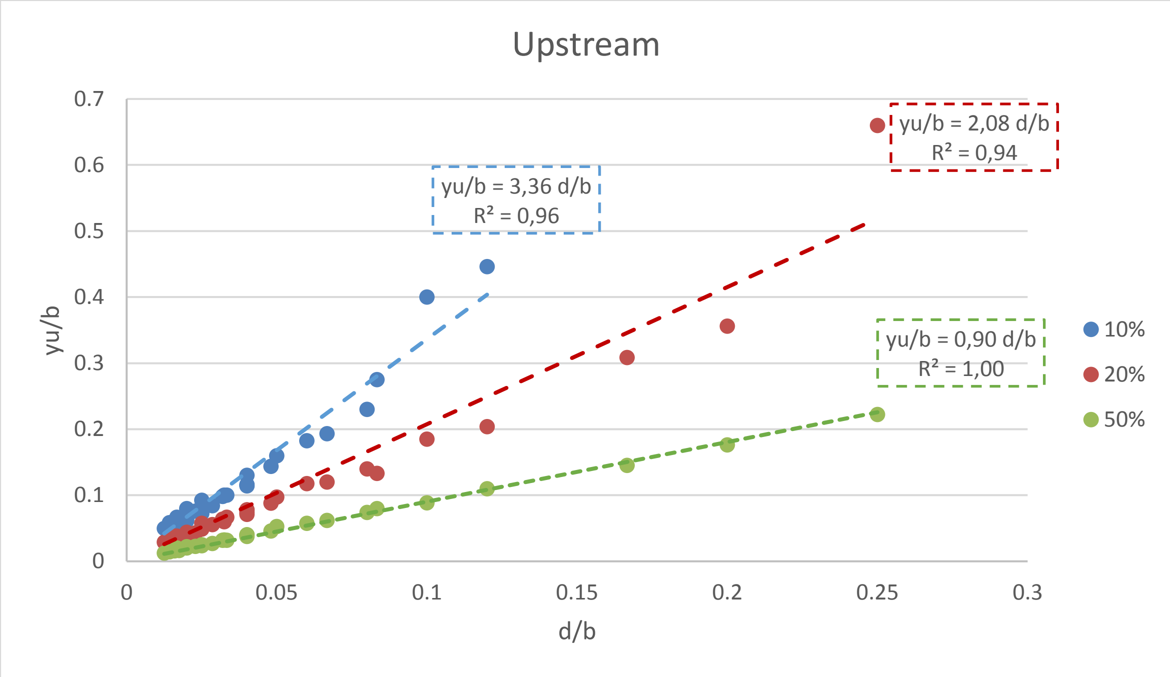

Figure 6-8: Linear blockage ratio when only including percentage variations higher than the new approach velocity

It was assumed that all percentage variations larger than the new approach velocity variation could be estimated using the relationship developed for 1 boulder not in choking conditions (Section 5, equation 5-18).

Figure 6-9 below compares the ZOI length predicted by the software compared to the ZOI length predicted by the proposed relationship for the upstream direction. The comparison between the software and relationship shows that equation 5-18 adequately predicts the ZOI length for decreased velocities which are less than the new approach velocity. A detailed comparison between the software and relationship ZOI length can be found in Appendix D.

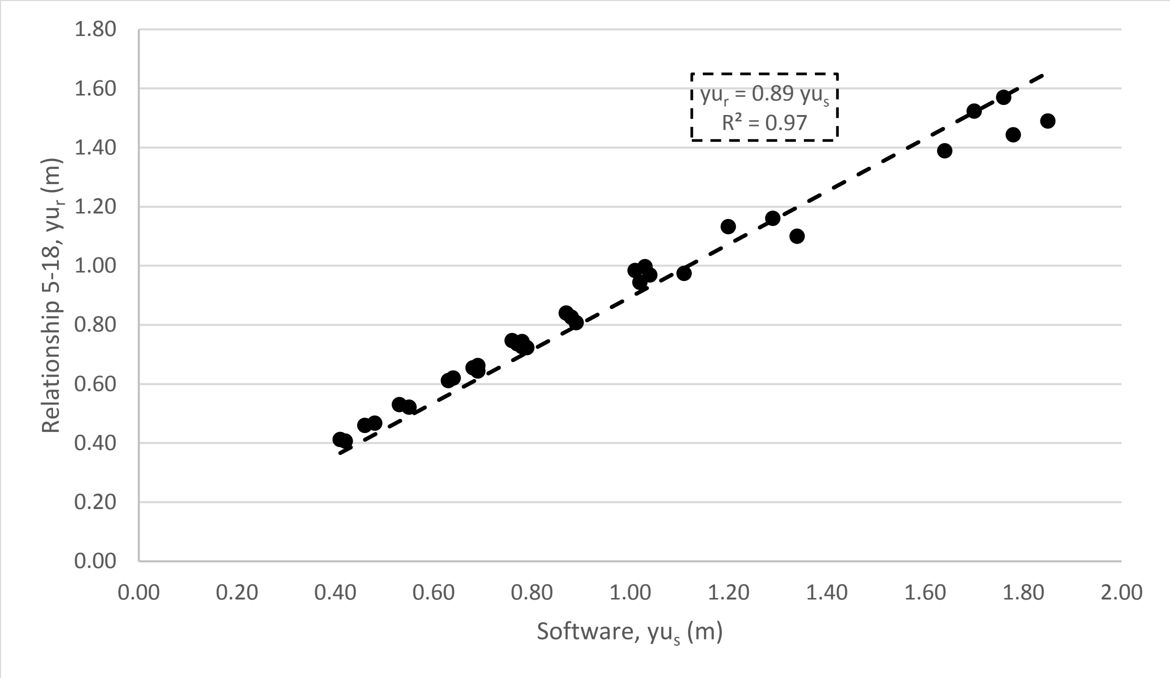

Figure 6-9: Upstream software vs relationship 5-18 for higher blockage ratios

6.4.1.3 GV Flow profile

The approach flow conditions were no longer localised changes caused by the boulder but varied from uniform throughout the whole width of the channel. This allowed for gradually varied flow computations to be used to calculate the distance upstream where uniform flow conditions would be present. The new approach conditions tend to the uniform flow depth in the upstream condition by means of a M1 flow profile.

The energy principles have correctly determined the conditions of choking and the approach velocity. This recommendation assumed that the energy principles will also be effective in determining the gradually varied profile. The gradually varied profile was not verified in the laboratory due to geometrical constraints or by the software due to computational constraints.

The gradually varied flow profile started with the calculated approach velocity and approached uniform flow some distance upstream. Gradually flow computations were used to determine how far a certain velocity percentage was from a boulder.

Samuels (1989) produced a simple estimate for calculating the upstream length (*L*) of a gradually varied profile:

$$L = \frac{0.7\ H1}{S} \quad (6\text{-}12)$$

Firstly, the gradually varied flow computations were used to calculate the upstream length; these were then compared to the length calculated using the method proposed by Samuels (1989). The lengths from the two computational methods converged when the gradually flow computations used small intermediate values. As a result, the relationship proposed by Samuels (1989) was seen as an effective method to estimate the upstream length in a computationally effective manner.

Table 6-5 below shows how far upstream the flow returned to uniform conditions. The distances were considerable in magnitude and would have considerable advantages for the creation of aquatic habitats. The disturbed area caused by the choking increased the velocity variations from a few metres to hundreds of metres.

Table 6-5: Upstream disturbance length

Model	**25**	**27**	**49**	**50**	**54**
***v1* %**	4	15	11	2	20
***H1* (m)**	0.25	0.28	0.27	0.25	0.35
***L* (m)**	220.10	248.45	236.94	215.47	306.30

6.4.1.4 Flooding

Flooding was shown to not be a concern when the boulder does not cause choking; the boulder increased the flow depth minimally at small localised areas. The consideration of flooding could be pertinent when the entire channel width was affected by the boulder. The increased flow depth, seen for hundreds of metres upstream further emphasised the need to consider flooding. Table 6-6 below shows the increase in flow depth caused by boulders placed in a choking position. The maximum flow depth is simply the flow depth calculated from the energy principles. The boulders still did not cause the flow depth to increase substantially; 6.9cm was the largest increase in flow depth as seen in Model 54.

Table 6-6: Upstream flow depth increase

Model	*H* uniform (m)	*H* maximum (m)	*ΔH* (m)
25	0.242	0.252	0.010
27	0.242	0.284	0.042
49	0.241	0.271	0.030
50	0.241	0.246	0.005
54	0.281	0.350	0.069

A relationship was developed which allows the maximum upstream flow depth to be calculated directly from the blockage ratio. Figure 6-10 shows that a linear relationship exists between the increase in flow depth and the blockage ratio, namely:

$$\frac{H\ maximum}{H\ uniform} = 1.53\ \frac{d}{b} + 0.87 \qquad \text{6-13}$$

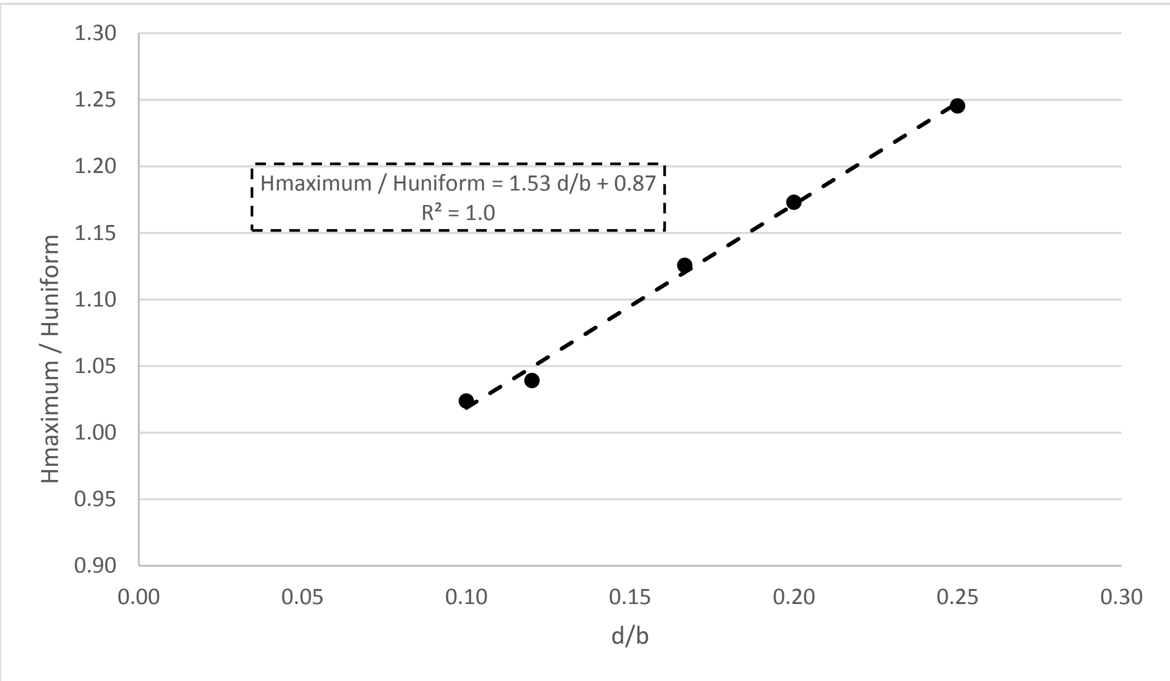

Figure 6-10: Increased upstream flow depth

6.4.2 Sides

Models which were identified as choking showed larger side disturbances. The disturbances were of such a magnitude that the sides of the channel experienced increased velocities; below the blockage ratio limit the bank flow was always uniform. The increase of the velocity disturbance was of interest due to potential channel erosion and bank stability problems. In order to quantify the potential erosive force the velocity increases of the channel was investigated. The scour pools created by increased velocity have been identified as micro-habitats for aquatic organisms such as invertebrates, this velocity differs from scour pools as it covers a much larger area.

The energy analysis has been shown to be effective in predicting the blockage ratio above which choking will occur as well as the new approach conditions upstream of the boulder. The side velocity disturbances were considered to be in the critical flow conditions in the theoretical energy analysis. The theoretical analysis however did not prove to be effective in predicting the velocity distribution on the sides of the boulder.

The first indication of a lack of theoretical correlation was seen in the Froude number on the sides of the boulder. The theoretical analysis predicted that the Froude number would be equal to 1 as the flow conditions were critical. Just downstream of the boulder the Froude number would be greater than 1 due to the supercritical flow regime. The resulting Froude distribution showed that the critical and supercritical flow regimes did not extend across the whole width of the channel but were localised to the side of the boulder.

A complex velocity distribution on the side of the boulder was however expected. The boulder did not simply act as a contraction as the flow variables were not constant throughout the width. The boulder did reduce the flow area but importantly the boulder also acted as an obstacle in the flow. The resulting velocity disturbance on the sides of the boulder was an amalgamation of the theoretical energy principles but also the disturbances caused by the object.

Figure 6-11 below shows an example of the Froude number distribution to the side of a boulder for Model 27. The data points shown had a Froude number greater than or equal to 1. It was noted that the Froude number range under consideration only extended to approximately 1.73m away from the centre; the bank of the channel on the other hand was 2.50m away from the centre.

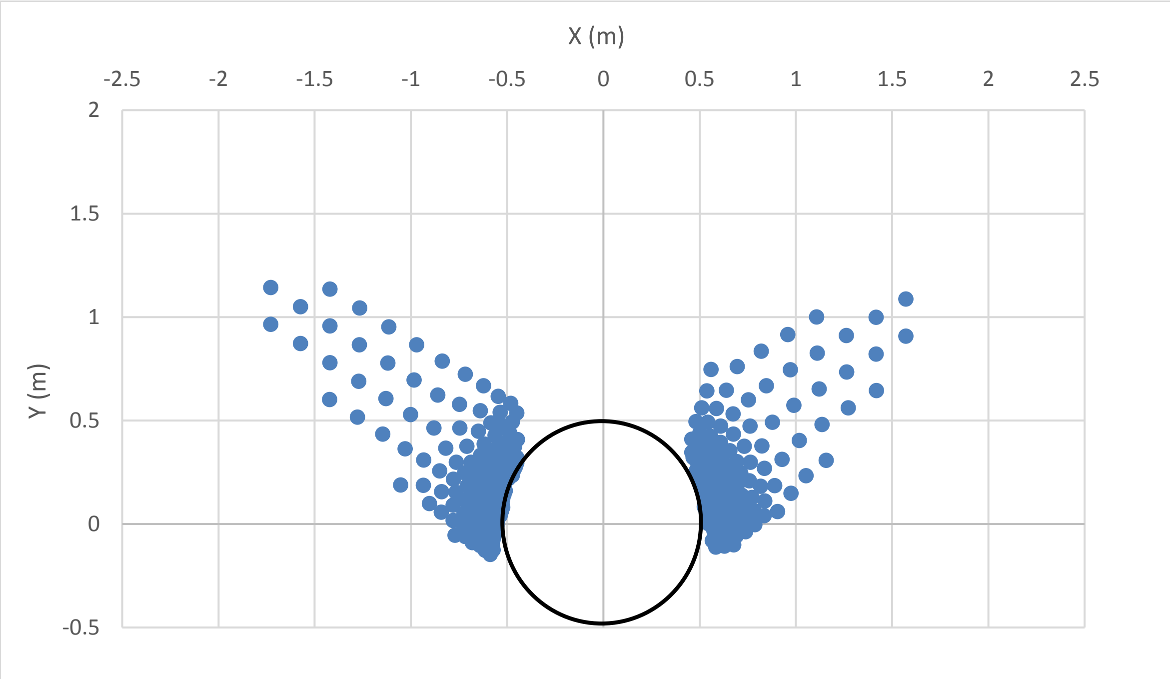

Figure 6-11: Froude number greater than or equal to 1 for Model 27

Figure 6-12 below shows the velocity distribution in percentage ranges from uniform flow for Model 27. The vast increase in the velocity distribution is evident. The velocity changes caused by the boulder extend to the banks of the channel and also extend several metres downstream.

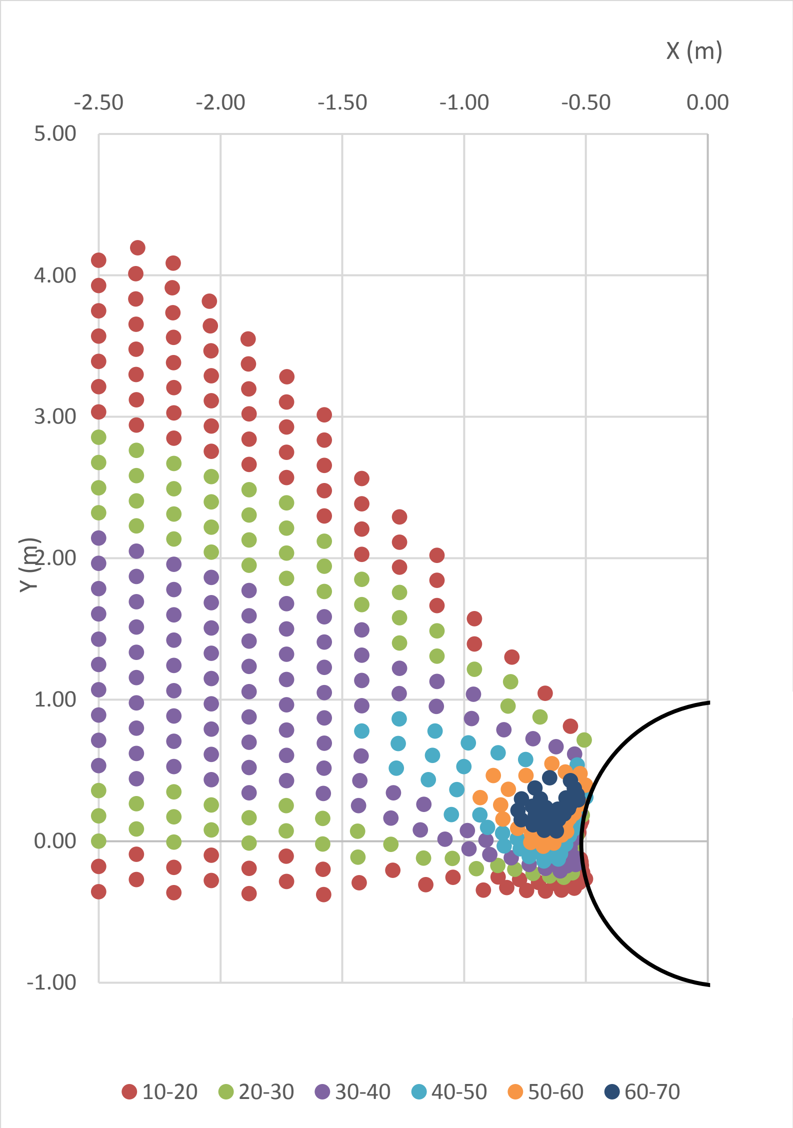

Figure 6-12: Side velocity distribution of Model 27

Figure 6-12 shows that the banks of the channel experienced velocity increases up to 40%. This large velocity increase could cause erosion depending on the material characteristics. The research process allowed for the velocity increase at the banks to be predicted. It should be noted that all percentage variations lower than the highest recorded value would also extend to the banks of the channel.

The side velocity distribution of all models which were choking were analysed. In particular the largest percentage variation experienced on the channel banks were recorded. Bank stability should be ensured using the worst-case scenario being the largest percentage variation.

A trend was found when comparing the highest percentage velocity increase at the banks of the channel to the blockage ratio as shown in Figure 6-13. The velocity increase becomes larger with larger blockage ratios. It is proposed that the blockage ratio should not exceed 0.25 as velocity increases at the bank of the channel are expected to be greater than 50%.

The linear trend line provides a relationship to estimate the largest percentage velocity increase at the banks of the channel:

$$i_b = 220.34 \frac{d}{b} - 10.97 \tag{6-14}$$

where i_b is the velocity increase at the bank of the channel.

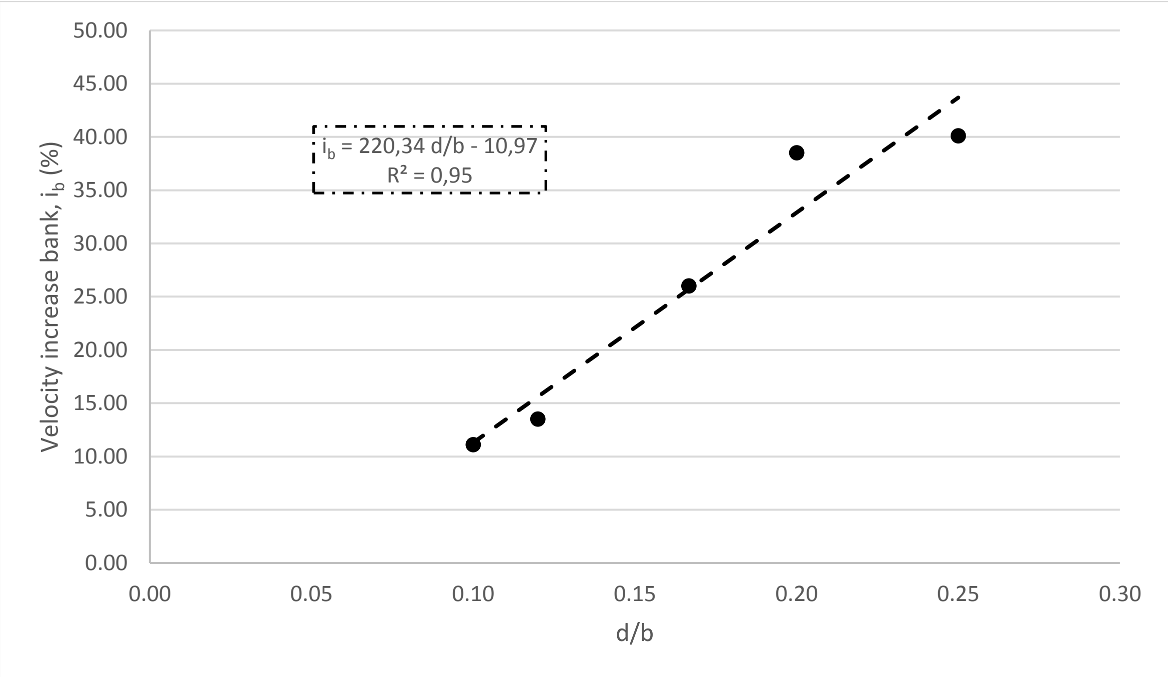

Figure 6-13: Velocity increase at the bank of the channel

Figure 6-14 shows that Model 27 experienced an increased velocity of up to 40% 1m away from the edge of the boulder to the edge of the channel. Figure 6-14 shows that 40% velocity increase is also experienced within the first metre, but these were regarded to be due to the obstacle effect and not the choking effect. The distance where the highest percentage increase at the bank started on the bed was noted. The highest percentage increase then extended all the way to the bank of the channel. The distance was measured from the edge of the boulder (x_e).

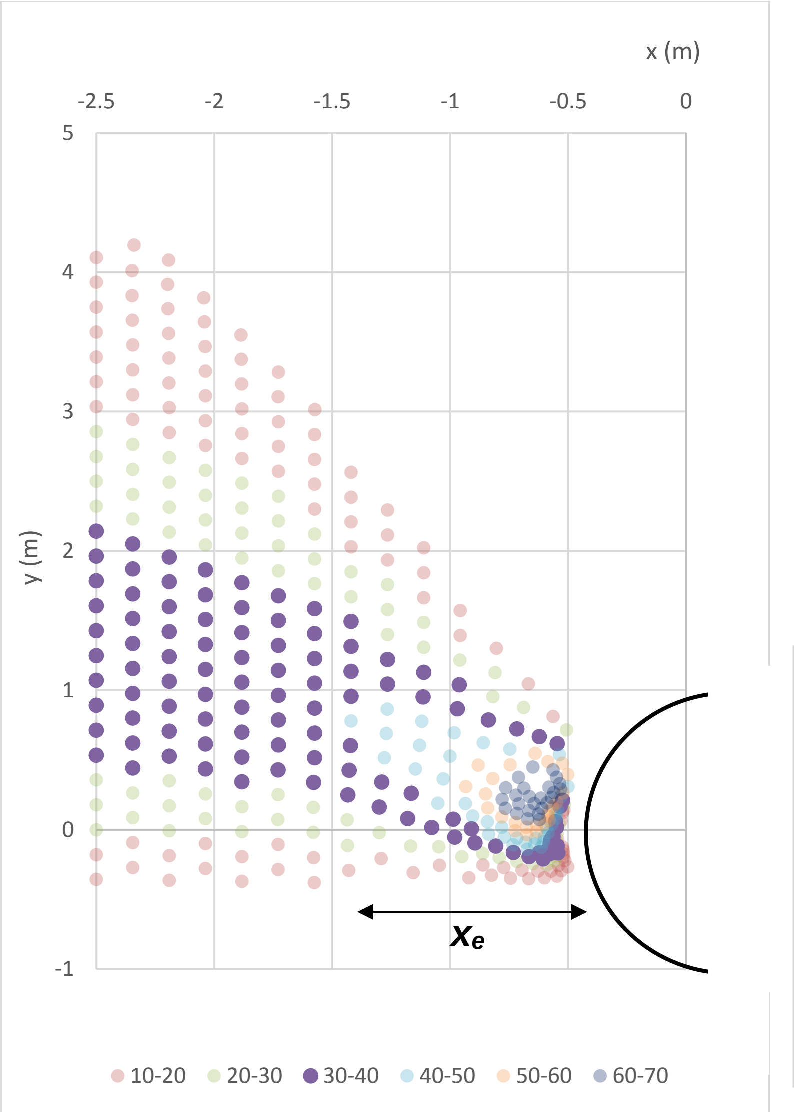

Figure 6-14: Extension of i_b on the bed

The highest percentage velocity increase experienced at the banks of the channel can be calculated. This percentage variation will also occur on the bed of the channel. The distance which the percentage increase in velocity starts occurring was measured from the edge of the boulder in terms of the boulder diameter (x_e/d). A linear relationship was found when comparing x_e/d to the blockage ratio, as seen in Figure 6-15. The percentage variation will extend from x_e/d to the bank of the channel. x_e/d can be calculated as follows:

$$\frac{x_e}{d} = -5.81\,\frac{d}{b} + 2.86 \qquad 6\text{-}15$$

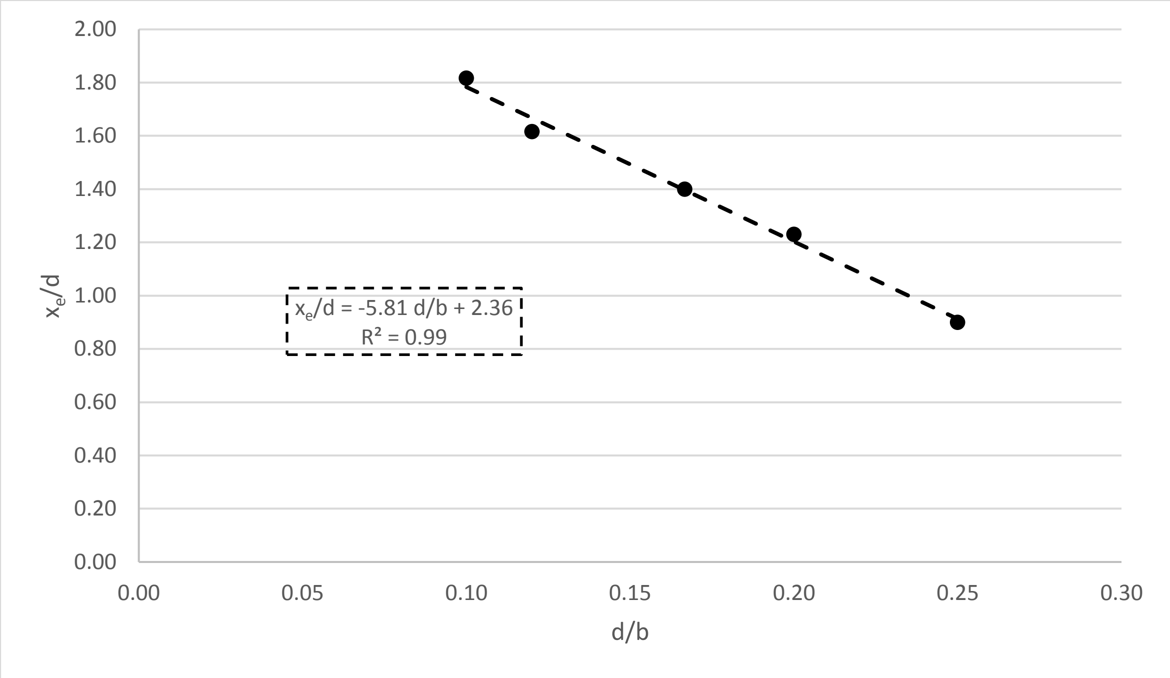

Figure 6-15: Extension of the velocity increase on the bed

6.4.3 Downstream

An analysis of the downstream velocity profile revealed that the blockage limit did not cause the profile to change as with the upstream and side directions. It was assumed that the downstream ZOI could be estimated using the relationship developed for 1 boulder not in choking conditions (Section 5, equation 5-19).

Figure 6-16 below compares the ZOI length predicted by the software was compared to the ZOI length predicted by the proposed relationship for the downstream direction. The comparison between the software and relationship shows that equation 5-19 adequately predicts the ZOI length. A detailed comparison between the software and relationship ZOI length can be found in Appendix D.

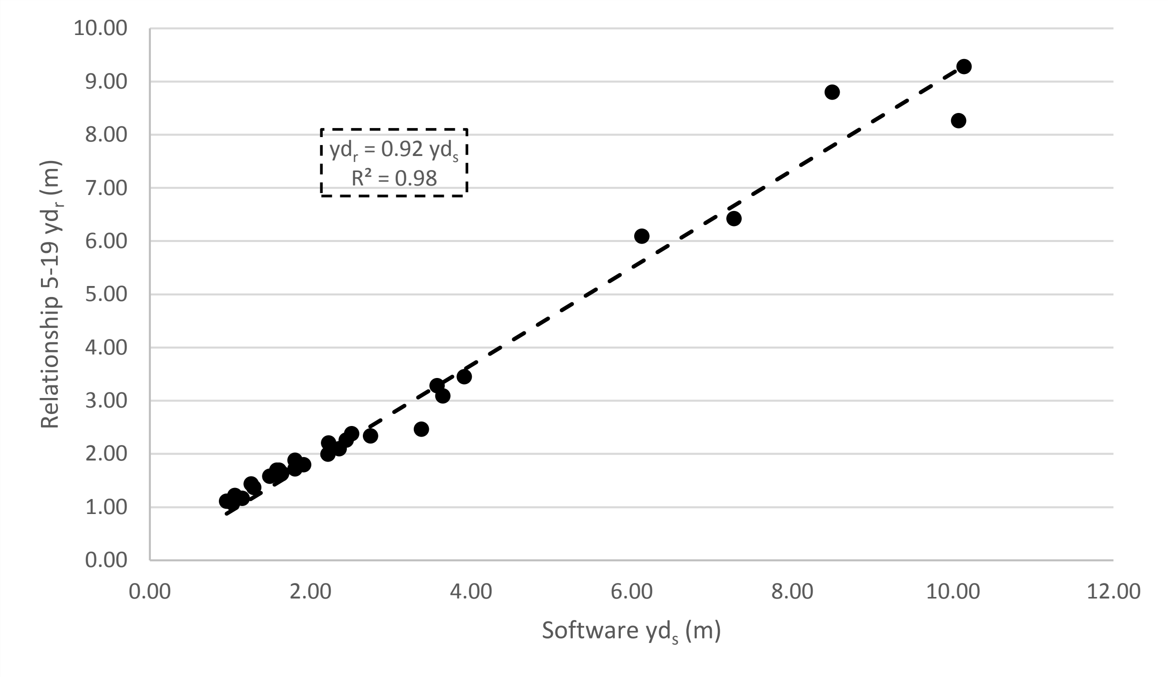

Figure 6-16: Downstream software vs relationship 5-19 for higher blockage ratios

6.5 Conclusion

The theoretical energy principles proved effective in predicting the blockage ratio above which choking occurs. The location of the boulder becomes a control if the following conditions are met:

$$d > b - \frac{Q}{\left(\left(\frac{2}{3}\,E\right)^{3} x\,g\right)^{0.5}} \qquad \text{6-7}$$

The fundamental utilisation of the disturbed flow differs above and below the blockage ratio limit. Below the blockage limit the downstream velocity distribution is the largest. Above the blockage limit the upstream velocity distribution increases to such an extent that the downstream flow changes become insignificant.

The control created by the boulder results in additional hydraulic changes upstream of the boulder. The flow upstream of the boulder slows down in order to gain energy to flow past the transition. The backed-up flow is no longer localised around the boulder but instead changes the flow conditions across the entire channel width and a distance upstream. The flow conditions return to uniform in the upstream direction by means of a M1 gradually varied flow profile. The flow depth and velocity upstream of the boulder due to the choking were effectively predicted by the same energy principles used to predict the blockage limit.

Gradually varied flow computations were used to evaluate the length of the upstream M1 profile. A relationship proposed by Samuels (1989) accurately predicted the length in a computationally effective manner by only requiring the new upstream flow depth (*H1*). The gradually varied computations showed that the flow would be altered hundreds of metres upstream. The large upstream ZOIs have the potential to be create large aquatic habitats.

$$L = \frac{0.7\,H1}{S} \qquad \text{6-12}$$

The large area of disturbed flow upstream of the boulder did however provide additional risks; namely flooding and erosion. The new upstream approach conditions caused by the gradually varied flow profile created increased flow depths across the entire width of the channel. It was found that the increase in flow depth was less than 10cm for blockage ratios up to 0.25. Flood risks are however site specific and should still be analysed. A convenient relationship was developed which can predict the maximum flow depth.

$$\frac{H\ maximum}{H\ uniform} = 1.53\,\frac{d}{b} + 0.87 \qquad \text{6-13}$$

The second risk associated with large blockage ratios was that of potential erosion of the channel banks and bed due to the increased velocities. The sides of the boulder showed increased ZOI dimensions when compared to models below the blockage limit. The increased velocity zones were higher and also extended to the channel bank. A relationship was developed which predicts the highest percentage increase of velocity at the bank of the channel using the blockage ratio.

$$i_b = 220.34\,\frac{d}{b} - 10.97 \qquad \text{6-14}$$

This percentage variation will also occur on the bed of the channel. The distance which the percentage increase in velocity starts occurring was measured from the edge of the boulder in terms of the boulder diameter. The percentage variation will extend from x_e/d to the bank of the channel. x_e/d can be calculated as follows:

$$\frac{x_e}{d} = -5.81\ \frac{d}{b} + 2.86 \qquad \text{6-15}$$

The increase in velocities proved to be a greater risk than flooding. It is proposed that the blockage ratio should not exceed 0.25 as velocity increases at the bank of the channel are expected to be greater than 50%.

An analysis of the downstream velocity profile revealed that the blockage limit did not cause the profile to change as with the upstream and side directions and that the ZOI relationship developed in Section 5 is still applicable.

7 INFLUENCE OF 2 TRANSVERSE BOULDERS

The following chapter analyses the velocity variations around two boulders. Boulders of the same diameter were placed along the transverse axis (*X*-axis) a specified spacing apart (Figure 7-1). The spacing between the boulders (*Sp*) was varied to see what effect this had on the ZOI that was formed. Boulders were placed at a considerable distance apart and then brought closer together. When far apart the boulders' effect could be estimated by the previous analysis of 1 boulder, when they were brought closer to each other their respective velocity disturbances started to interact. This interaction was analysed in order to recommend a favourable spacing with regards to the velocity variations.

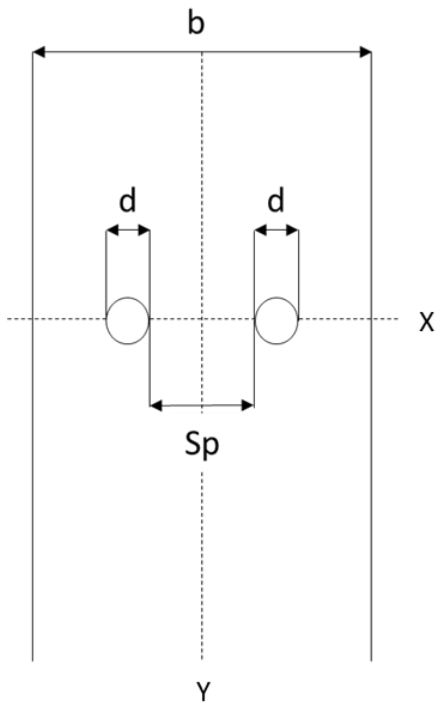

Figure 7-1: 2 Boulders geometrical setup

Hamuy-Blanco (2013) and Riddet (2012) discovered that the disturbance suddenly increased in the upstream direction when there was local control induced between two boulders. When a local control was present the ZOI approximately doubled in the longitudinal direction whilst staying close to constant in the transverse direction (Hamuy -Blanco, 2013). Hamuy-Blanco and James (2014) state that the boulder spacing needed to induce a local control depends on the discharge, channel characteristics and boulder size.

The chapter started with an investigation of the velocity distribution for a particular case. The effect of spacing was analysed by incrementally reducing the spacing between the boulders. The investigation of two boulders at different spacings was conducted to provide a recommendation on a favourable spacing. It was found that the point of local control was the most favourable spacing between the boulders and a spacing formula to determine a local control was created for different Froude number ranges.

The form of the dimensionless ZOI relationship developed for 1 boulder was used for 2 boulders, which defined the ZOI as a dimensionless function of the blockage ratio and Froude number. The ZOI length was defined at the favourable spacing and all models were below the overall blockage limit.

7.1 Velocity Distribution Investigation

The following discussion investigates the velocity distribution around 2 boulders for a particular case (Table 7-1). The velocity distribution was analysed in terms of the ZOI and an areal velocity change for a range of different spacings. This example provided a feel for the size of the disturbed flow area when spacing is varied. An equivalent change in velocity was then found for one boulder to assess what size single boulder would cause the same flow disturbance. The following discussion used Model 6; which had the following conditions.

Table 7-1: Model 6 Conditions

***Q* (m^3/s)**	***S***	***n***	***b* (m)**	***d* (m)**	***H* (m)**	***v* (m/s)**
1.25	0.00080	0.010	10.0	0.30	0.156	0.802

7.2 Change in Velocity with Spacing

The spacing was varied from 1.5m between the boulders and reduced incrementally to analyse the effect of the boulders on the flow variables. Figure 7-2 to Figure 7-5 show spacings of interest. The blue points represent all points which had an absolute percentage variation of 10% or more from uniform velocity. The red points show the points where the Froude number was greater than 1.0, which indicate that there was supercritical flow.

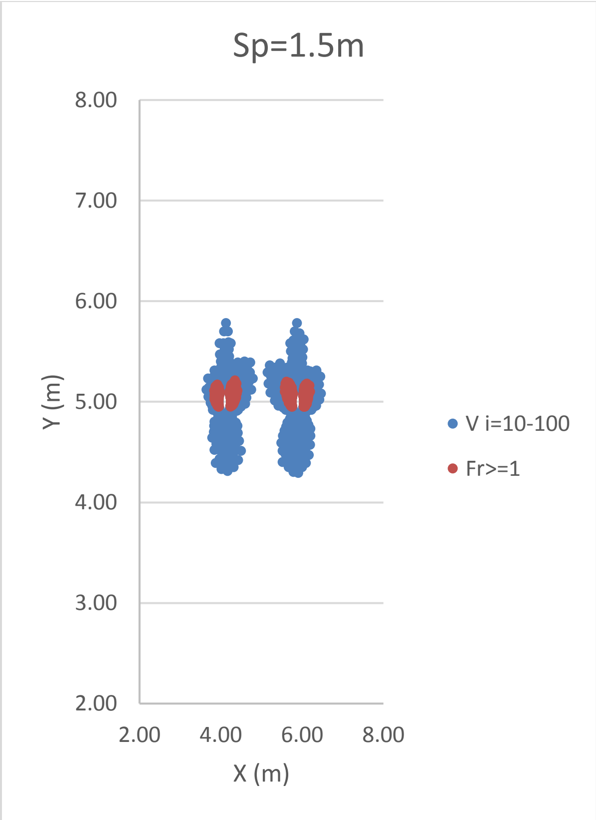

Figure 7-2: Model 6 *Sp*=1.5m

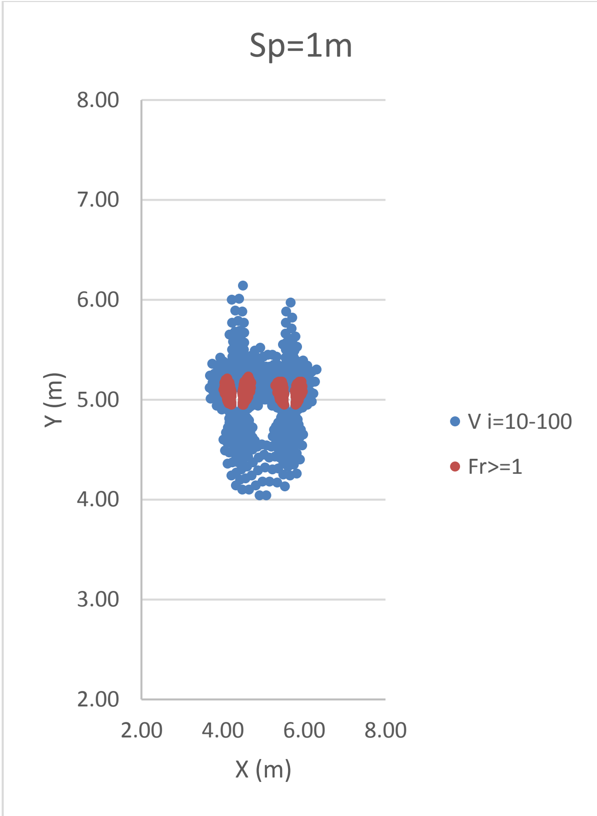

Figure 7-3: Model 6 *Sp*=1.0m

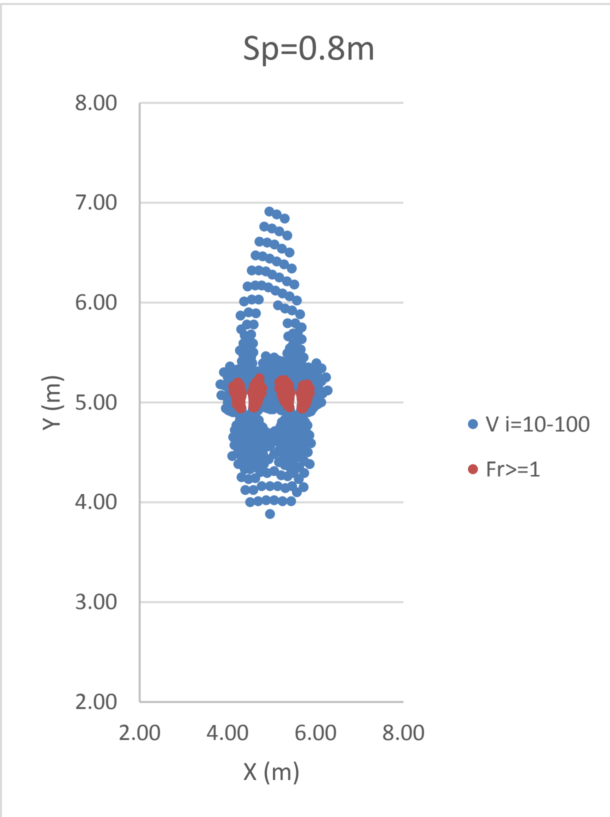

Figure 7-4: Model 6 *Sp*=0.8m

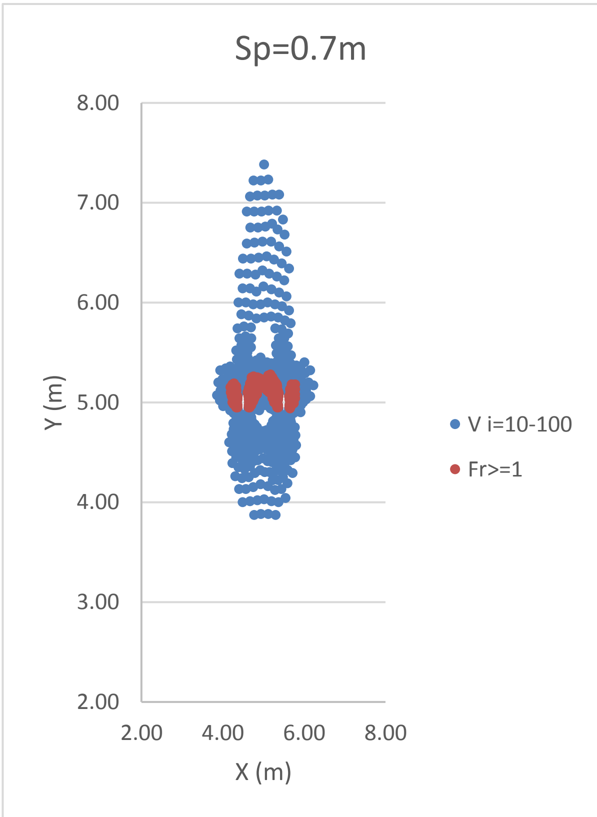

Figure 7-5: Model 6 *Sp*=0.7m

The two boulders acted independently when a considerable distance apart. Thereafter their velocity distributions started overlapping, first in the upstream and side directions. As the spacing between the boulders was reduced the areal change in velocity increased. Once a local control was formed the velocity distributions of the two boulders overlapped and started acting similar to the distribution of one boulder.

It was possible to identify a local control by looking at the points where the Froude number was greater than or equal to 1.0. As the spacing was reduced more supercritical points were found between the boulders. The spacing of 0.7m showed that the Froude number was greater than or equal to one across the entire spacing.

Figure 7-7 below shows the areal velocity change for a range of spacings. The size of the velocity distributions was found by considering the areal velocity coverage of all points which had an absolute percentage variation of 10% or more from uniform velocity.

The areal coverage shows that the disturbed velocity increased as the boulders are brought closer together. Interestingly when local control was initiated, the size of the areal coverage reached approximately 1.5 times the size at a 1.5m spacing. Once the local control spacing was decreased further it was found that the disturbed velocity size increased only slightly and then started to decrease.

The areal coverage showed that there is a linear increase as the spacing is reduced to the point of a local control (Figure 7-7). This was of interest as it showed that the local control did not have a sudden additional effect on the velocity distribution but rather there was a slow and constant build up to the point of local control.

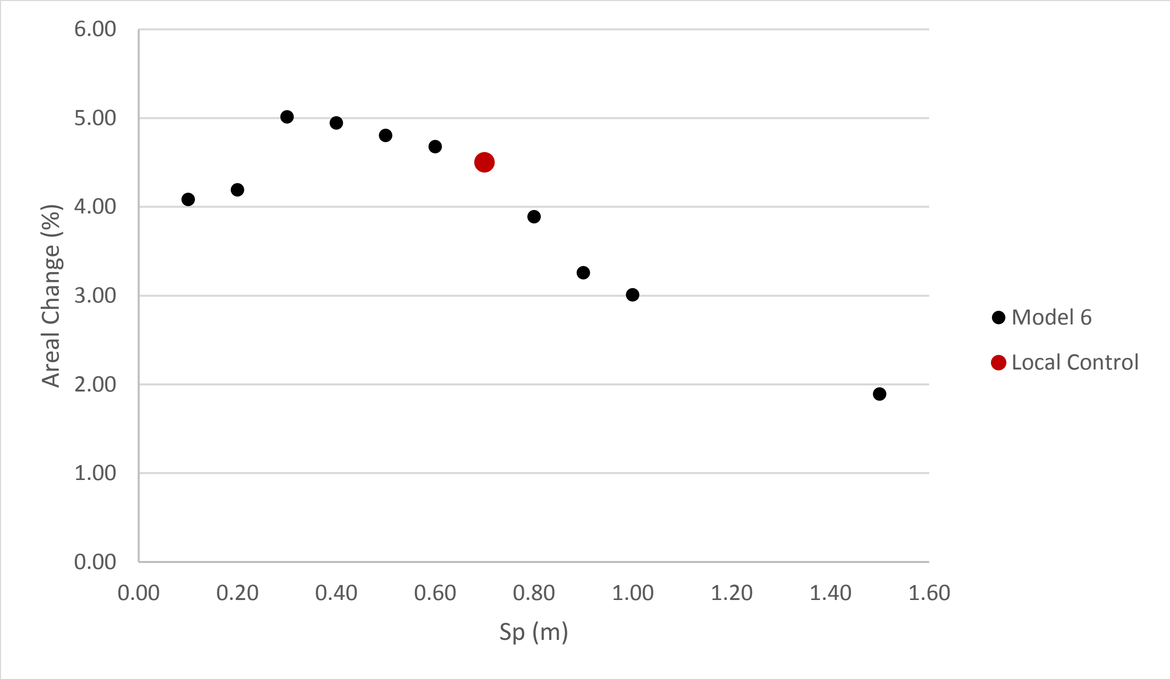

Figure 7-6: Areal velocity change with reduction in spacing (Model 6)

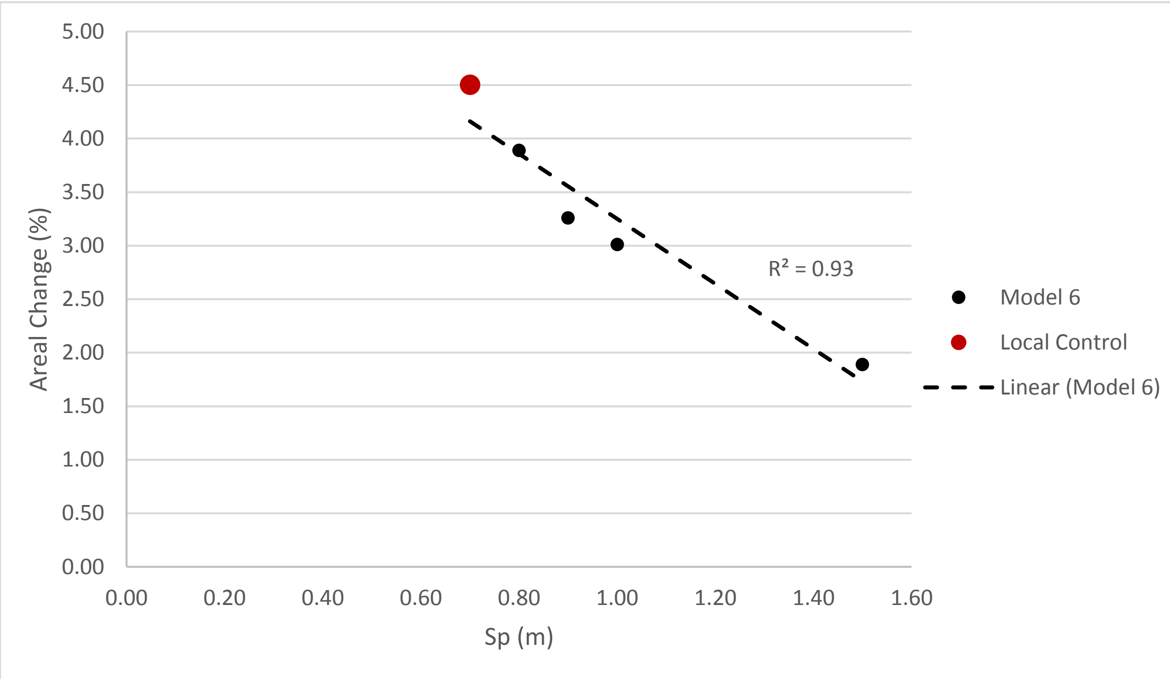

Figure 7-7: Linear areal velocity changes up to local control (Model 6)

Figure 7-8 shows a velocity areal histogram for the spacings discussed above. All data points with a 10% or more change in velocity were included in the areal analysis. The largest area of the 4 models was used as the reference area for each model. The reduction is spacing between boulders caused a larger flow reduction, with the most prominent being the 10-20% range. A reduction in spacing did not cause much change within the faster velocities' ranges.

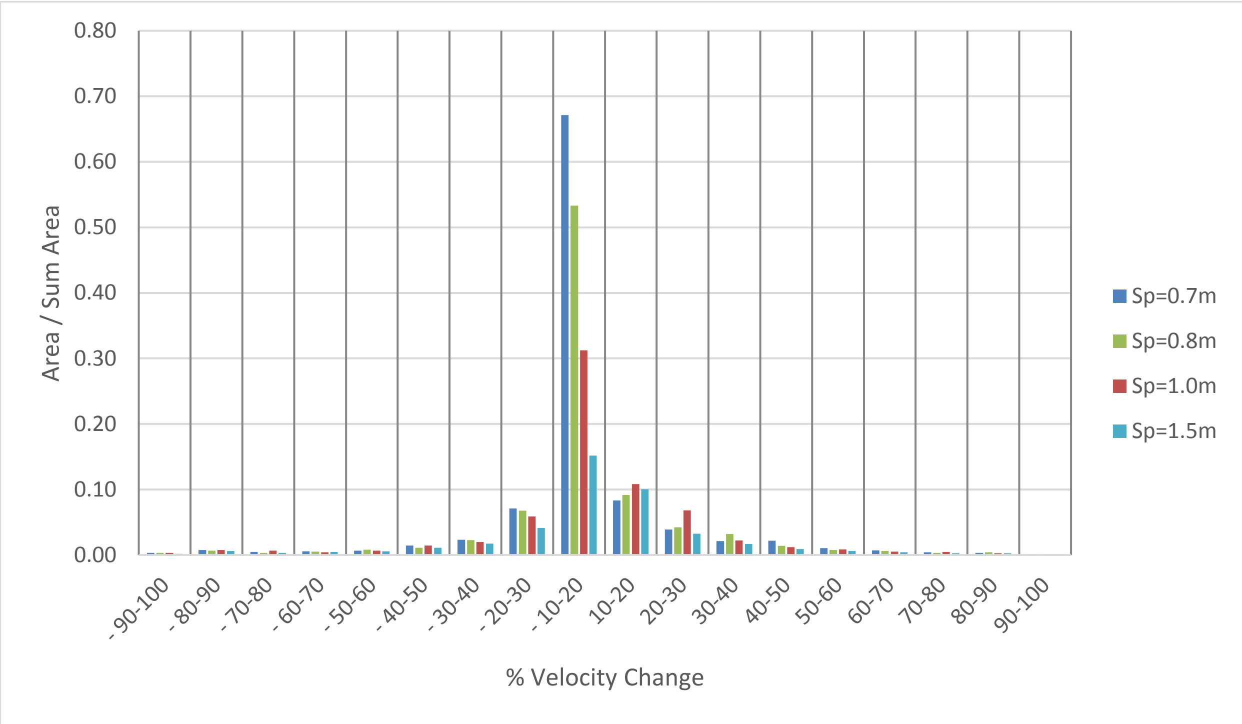

Figure 7-8: Areal histogram with reduction in spacing (Model 6)

7.3 Spacing Relationship

The effectiveness of the spacing between boulders at local control was investigated and it was found that this was a favourable spacing. The effect of the blockage ratio and Froude number were confirmed to be the key variables which were then used to create a relationship which determined the spacing needed for local control.

7.3.1 Effectiveness of Spacing at Local Control

Models 1-6 below were used to assess the efficiency of the local control spacing and guide the dimensional analysis.

Table 7-2: Model 1-6 conditions

Model	*b*	*d*	*2d/b*	*Fr*
1	5.0	0.20	0.080	0.67
2	5.0	0.10	0.040	0.67
3	10.0	0.20	0.040	0.65

Model	*b*	*d*	*2d/b*	*Fr*
4	10.0	0.10	0.020	0.65
5	10.0	0.40	0.080	0.65
6	10.0	0.30	0.060	0.65

The investigation of two boulders at different spacings was conducted to provide a recommendation on a favourable spacing. It was shown that the velocity disturbance increases as the spacing is reduced. Figure 7-6 showed that at the point of local control, the areal change is velocity was much larger when considering two boulders at a considerable distance effectively acting independently. When the spacing was reduced further the areal velocity change did increase further, in some circumstances, but at a reduced rate. The point of local control also holds practical value as it is a point which can be identified for different cases. The resultant velocity distribution at a local control spacing was analysed to ascertain how favourable the point of local control would be.

The resultant size of the velocity distribution with a 10% or greater change from uniform velocity was analysed for the first 6 Models at their respective spacings for local control (*Sp* for *LC*). The same flow conditions were then used to determine the areal velocity change caused by a single boulder with varying diameters. Using the areal velocity change as a common variable, it was possible to compare the equivalent single boulder size which would be needed to get the same areal velocity change as two boulders.

Figure 7-9 and Figure 7-10 show the spacings for local control for several Models, a single boulder diameter and the resultant velocity change of each. Model 1, for example, has a 1.80m^2 velocity change at local control spacing. As indicated on Figure 7-9, a 1.80m^2 velocity change from a single boulder would be caused by a single boulder with a diameter of 0.39m.

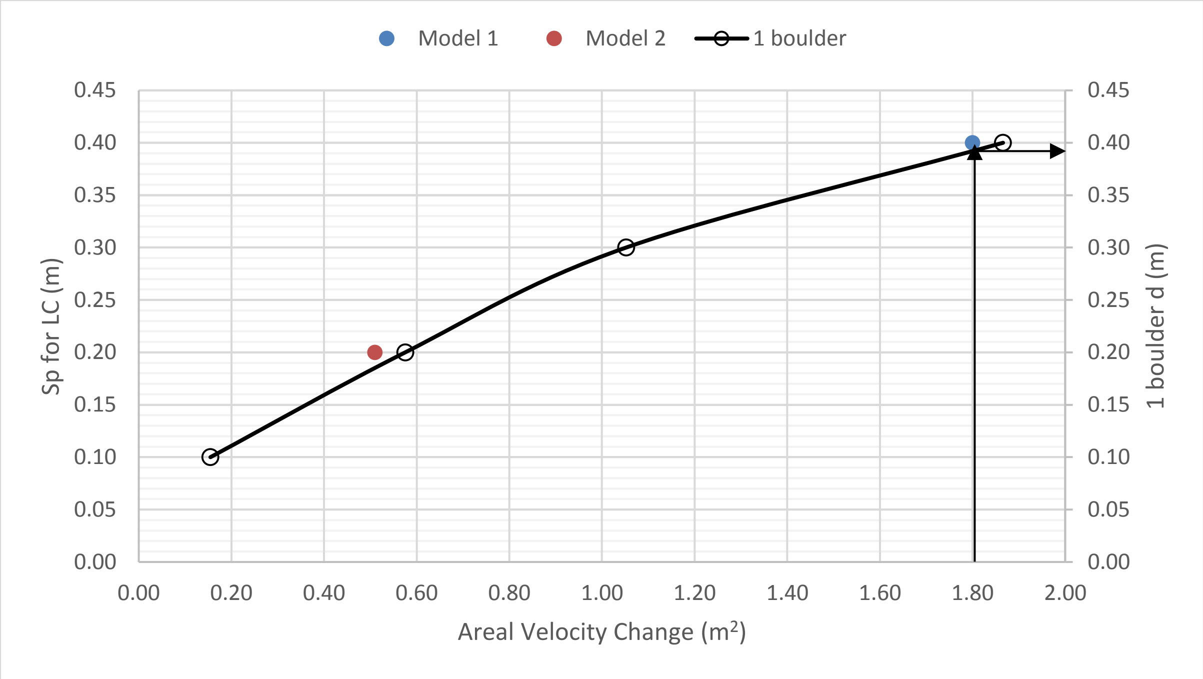

Figure 7-9: Areal velocity change for 1 boulder and 2 boulders (Model 1 and 2)

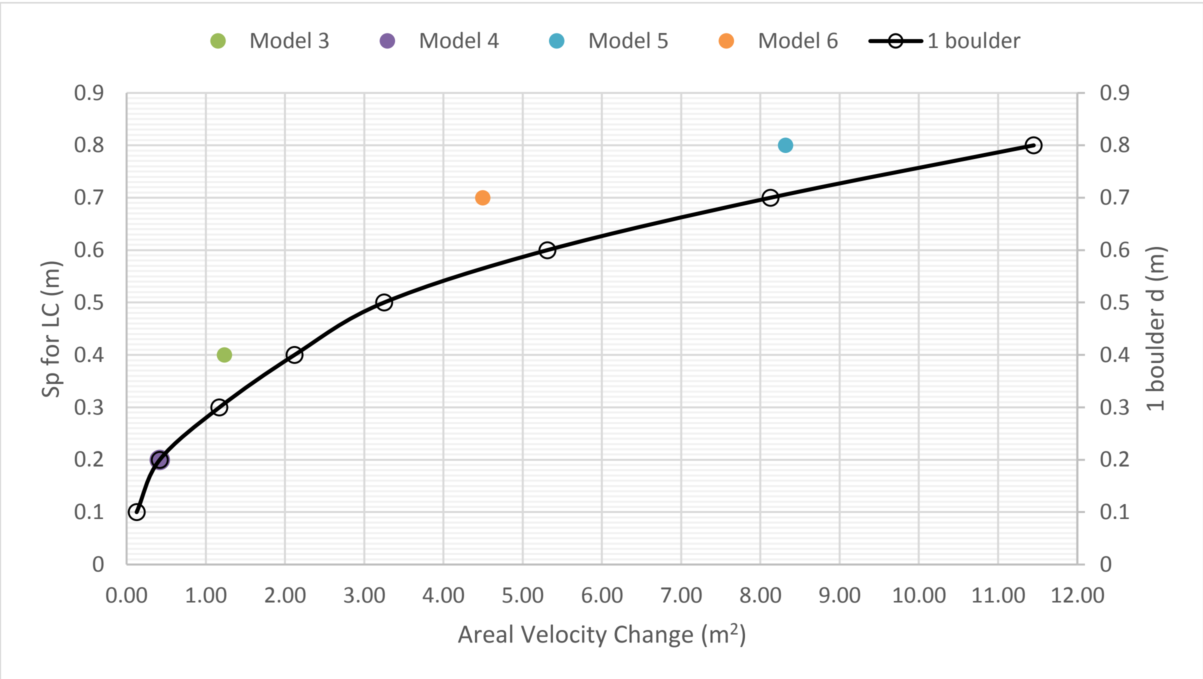

Figure 7-10: Areal velocity change for 1 boulder and 2 boulders (Model 3, 4, 5 and 6)

Table 7-3 below shows the equivalent boulder diameters for Models 1 to 6 at a local control spacing. It was found that equivalent single boulder diameter was between 1.8 and 2 times the diameter of a 2-boulder diameter. The effectiveness of a local control is clear when considering the area. The area for 2 boulders, each of a diameter d, equates to half the area of a single boulder with a diameter 2*d* (Equation 7-1).

$$A_{1\ boulder} = \frac{\pi(2d)^2}{4} = \pi d^2 \qquad A_{2\ boulders} = 2\frac{\pi(d)^2}{4} = \frac{\pi d^2}{2} \qquad 7\text{-}1$$

Table 7-3: Areal velocity change 2 boulders vs 1 boulder

Model	Areal Velocity Change at *LC* (m^2)	2-Boulder *d* (m)	Equivalent 1-Boulder *d* (m)	1-Boulder *d*/ 2-Boulder *d*
1	1.80	0.20	0.39	1.95
2	0.51	0.10	0.19	1.90
3	1.23	0.20	0.35	1.75
4	0.42	0.10	0.20	2.00
5	8.32	0.40	0.72	1.80
6	4.50	0.30	0.57	1.90

It has been shown that 2 boulders spaced at local control is indeed effective and provides the same areal velocity change as 1 boulder, but with half the area. The volume of rock needed for 2 boulders would also be half of 1 boulder which reduces the volumetric material cost while also allowing for easier transportation and deposition. Furthermore 2 boulders can provide the same effect as 1 boulder while taking up half of the flow area. The above analysis of the effectiveness of a local control spacing shows that placing 2 boulders at local control is valuable.

7.3.2 Blockage Ratio

The blockage ratio was varied between 0.020 and 0.10 to explore the effect on the resultant velocity distribution. The hydraulic conditions were kept constant (Model 6) and the size of the boulder was varied. Figure 7-11 shows the resultant areal velocity change at a local control spacing for a range of blockage ratios. As shown in the analysis for 1 boulder, a clear relationship exists between velocity disturbance and the blockage ratio.

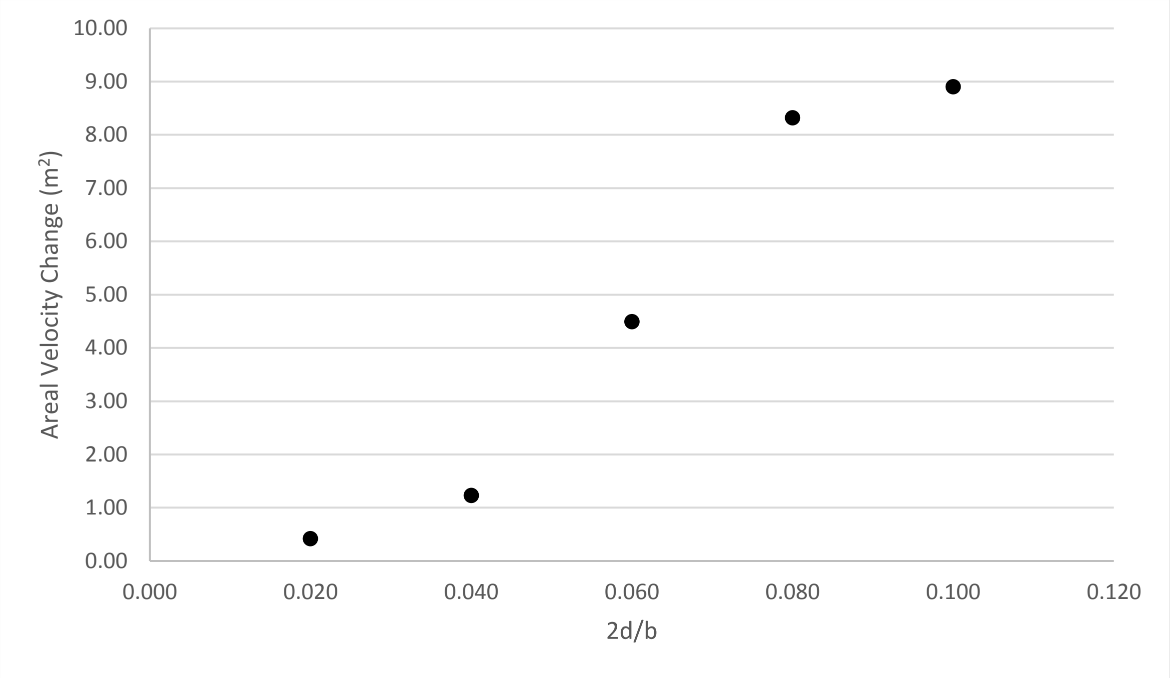

Figure 7-11: Blockage ratio vs areal velocity change

7.3.3 Froude Number

The Froude number was varied to determine the effect on the resultant local control spacing. The Froude number was varied while the blockage ratio was kept constant (*b*=10.0m, *d*=0.30m). Figure 7-12 below shows larger local control spacings were needed as the Froude number increased.

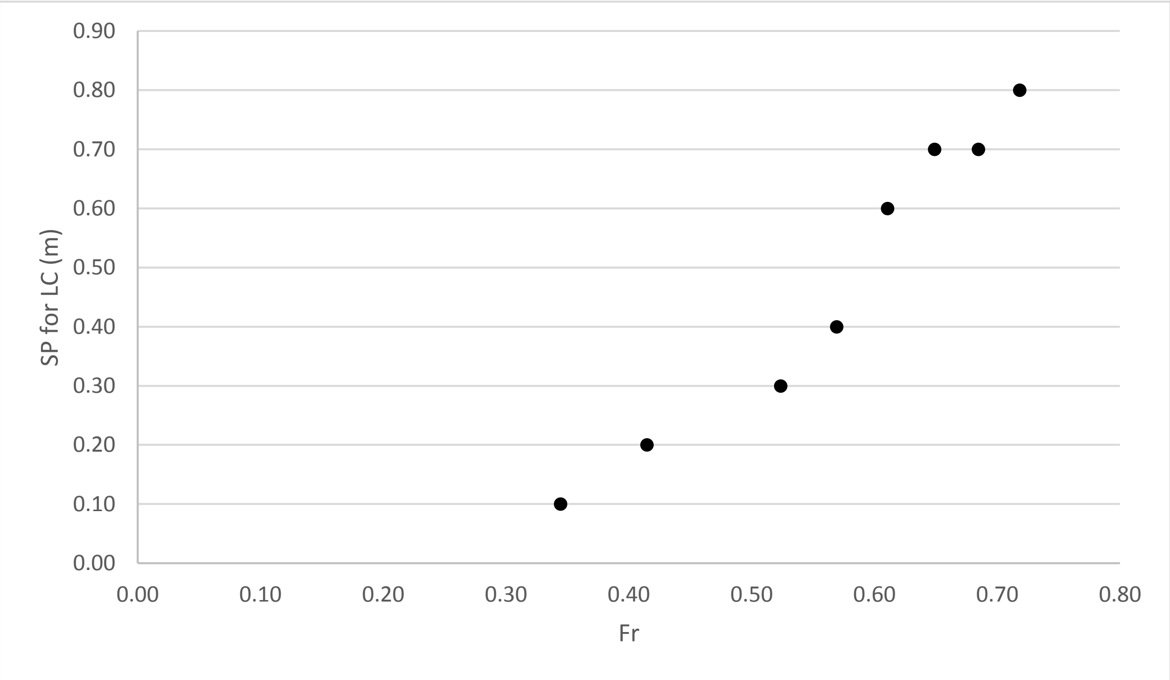

Figure 7-12: Froude number vs local control spacing

7.3.4 Dimensional Analysis

It has been shown that the optimum spacing between two boulders is dependent on the breadth of the channel, the size of boulders and the Froude number. A relationship was created which would allow one to calculate the spacing at which to place to boulders along the same transverse axis to create a local control.

As the relationship development was empirical it was necessary to arrange the variables in a way that allowed conditions to be calculated that were not used in the formulation. The blockage ratio having been effectively used for the analysis of one boulder and was found to be useful again as it eliminated the importance of exactly what *b* and *d* were used but rather focuses on the relationship between them. Equation 7-2 below shows the relationship hypothesised by a dimensional analysis.

$$\frac{Sp}{d/b} = f\left(\frac{2d}{b}, Fr\right) \qquad 7\text{-}2$$

7.3.5 Froude Number Ranges

A spacing formula to a determine local control was created for different Froude number ranges. The ranges allowed for a practical recommendation. This allowed a ZOI relationship to be created for the spacing ranges. Table 7-4 below shows the Froude ranges considered.

Table 7-4: Froude number ranges

Froude Number Range	Approach
>0.70	No analysis carried out as a global local control is imminent
0.60-0.70	Spacing relationship developed
0.50-0.60	Spacing relationship developed
0.40-0.50	Spacing relationship developed
<0.40	No analysis as the spacing for local control was found to be very small

A representative Froude number was chosen for each range in the analysis which follows. This assumes that the local control spacing will stay constant over a 0.10 change in Froude number. Table 7-5 shows the local control spacing for Froude numbers in the 0.60-0.70 range. The local control spacing was either the same or changed by 0.10m at most. It should be noted that the boulders were moved in 0.10m increments so the change in spacing could very well be less. Keeping in mind that the point of local control did not provide a rapid increase in the disturbed velocity area but rather the change was linear, it was decided that this variance was acceptable for practical purposes.

Table 7-5: Froude range 0.60-0.70 spacing variation

Model	***d* (m)**	***b* (m)**	***S***	***Fr***	***Sp* for *LC* (m)**
6	0.30	10.0	0.00080	0.65	0.70
8	0.30	10.0	0.00070	0.61	0.60
9	0.30	10.0	0.00090	0.68	0.70

7.3.6 Dimensionless Spacing

Figure 7-13 shows the spacings for the 0.60-0.70 Froude range, which increase linearly with larger blockage ratios. When the same blockage ratio was used but with different values of *b* and *d* it was found that the spacing required was not the same.

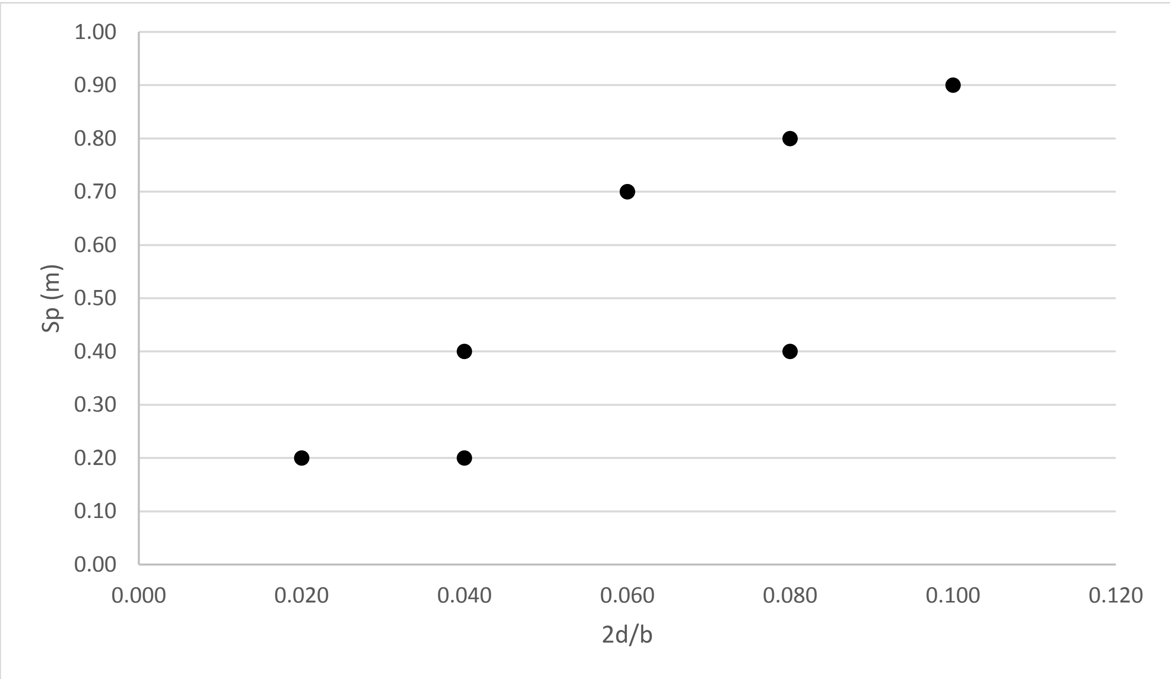

Figure 7-13: Spacing versus blockage ratio (Froude number 0.60-0.70)

Figure 7-14 shows when normalising the spacing by the channel width a clear relationship developed. Models which had different spacing requirements for the same blockage ratio are now also normalised and a strong linear trend is present. The proposed relationship for spacing is therefore as follows:

$$\frac{Sp}{b} = f\left(\frac{2d}{b}, Fr\right) \qquad \text{7-3}$$

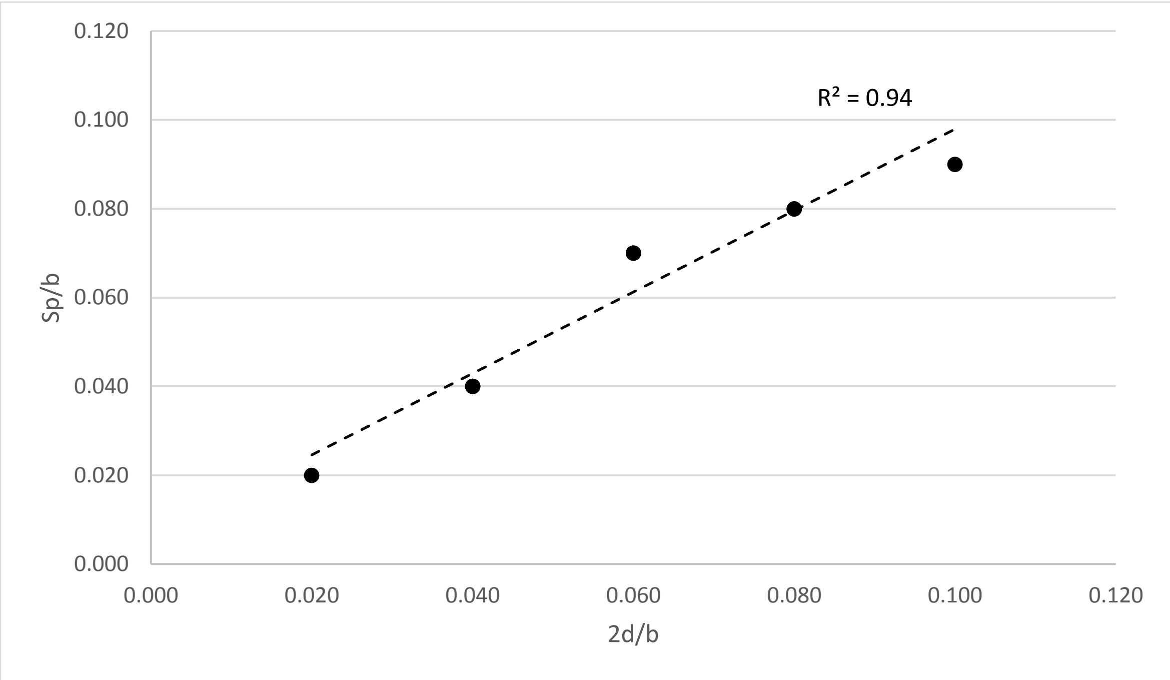

Figure 7-14: Dimensionless spacing versus blockage ratio (Froude number 0.60-0.70)

7.3.7 Model Conditions

The models used to develop the relationship varied the blockage ratio between 0.0 and 0.10 and fell within the three Froude number ranges (Figure 7-15). All model conditions can be found in Appendix E.

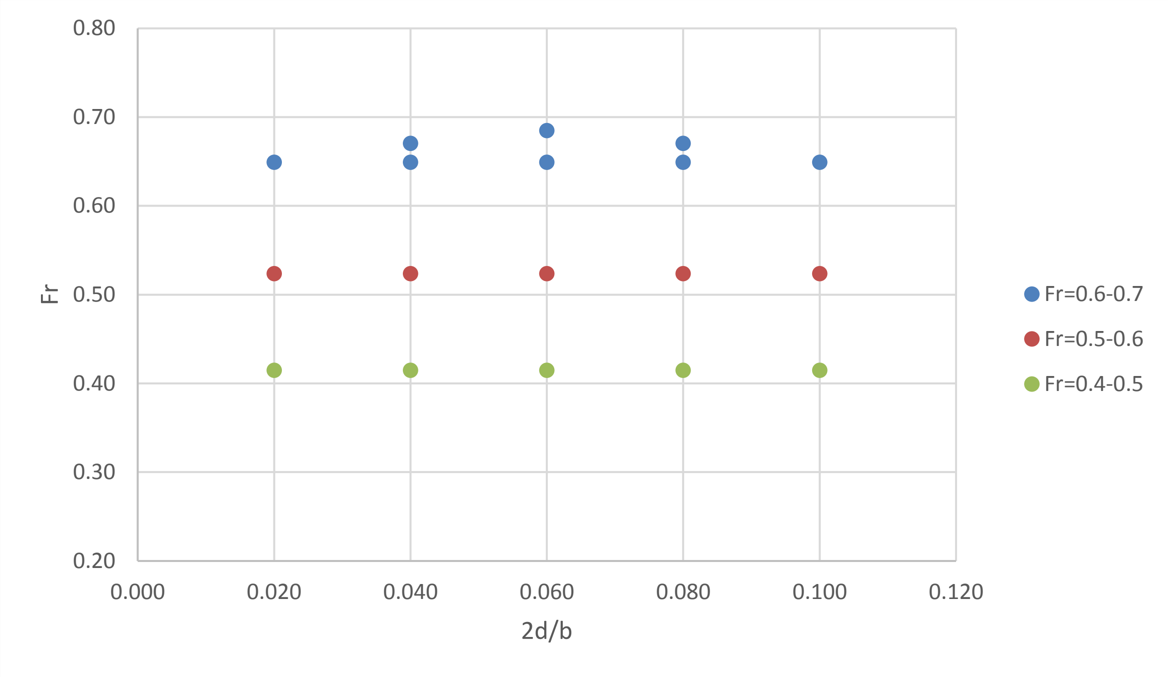

Figure 7-15: Model conditions for spacing relationship

7.3.8 Proving the Relationship

Figure 7-16 below shows the relationships for the three Froude ranges which were investigated. Each range has a strong linear trend which can be used to easily determine the local control spacing. The channel width was used on each side of the equation and can be cancelled out, resulting in a simple spacing relationship which is only dependant on the boulder diameter.

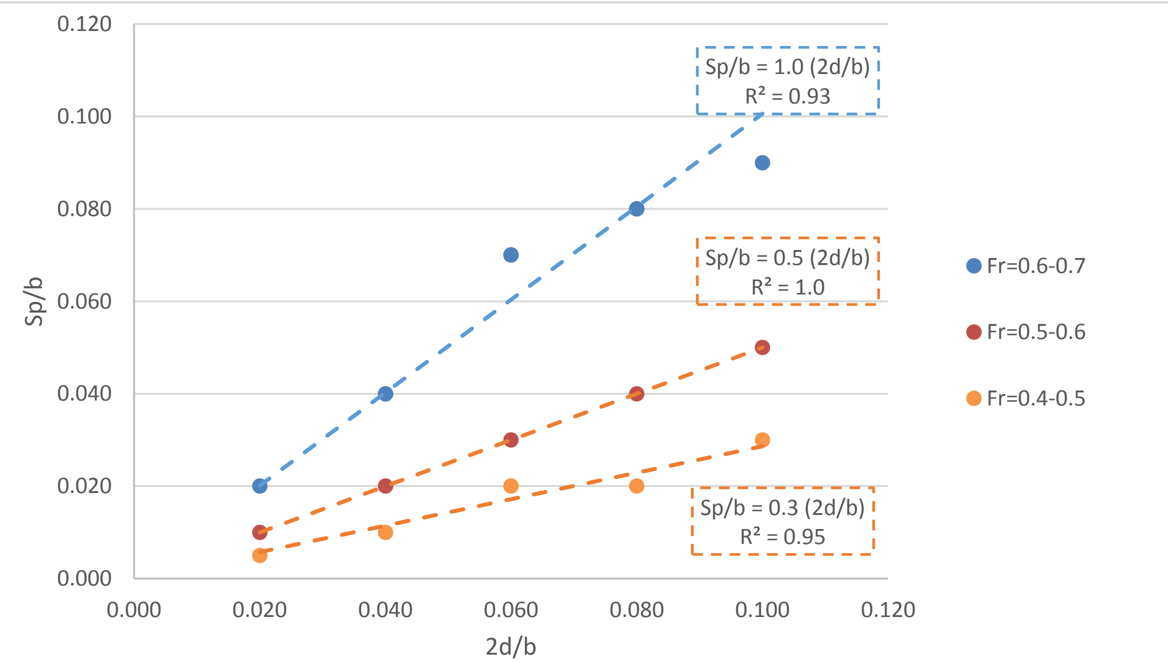

Figure 7-16: Spacing relationships for Froude ranges

Table 7-6 summarises the spacing relationships which were developed by the above analysis. The spacing recommendation proved to be simple and hold practical use in design.

Table 7-6: Froude number ranges spacing recommendations

Froude Number Range	Spacing for Local Control
>0.70	No analysis carried out as a global local control is imminent
0.60-0.70	$Sp = 2d$
0.50-0.60	$Sp = d$
0.40-0.50	$Sp = 0.6d$
<0.40	No analysis as the spacing for local control was found to be very small

7.4 ZOI Relationship at Local Control

A relationship was also needed to determine the ZOI at the spacings recommended. The same dimensionless relationship developed for 1 boulder was used for 2 boulders, which defines the ZOI as a dimensionless function of the blockage ratio and Froude number. The relationship for each direction had the same form but different constants. Similarly, for each direction the constants varied for different percentage variations. The base relationship was described as follows:

$$\frac{yu_i, yd_i, x_i}{b} = n_i \times \left(\frac{d}{b}\right)^{o_i} \times Fr^{\,p_i} \qquad 7\text{-}4$$

7.4.1 Setup

The resultant ZOI dimensions were determined at the recommended spacings and relationships developed to determine the ZOI dimensions in the upstream, downstream and side directions. The following should be noted:

- The downstream results were calibrated by using the correction factors determined from the experimental results. The experimental runs found that reduced velocities, up to 20%, extended beyond the boundary of the flume. Only velocities greater than 20% were used to create a relationship for the downstream direction.

Table 7-7: Downstream correction factors for 2 boulders

Velocity Correction Factor, *Cv*	**Distance Correction Factor, *Cyd***
0.90	3.40

- The relationships were developed for percentage variations ranging from 10% to 100%. All percentage variations included, had ZOI lengths which were in the order of 0.10m.
- The following model conditions were used in the development of a relationship. Detailed model conditions can be found in Appendix E. All models created only a localised local control, and the effect of an overall local control was not considered.

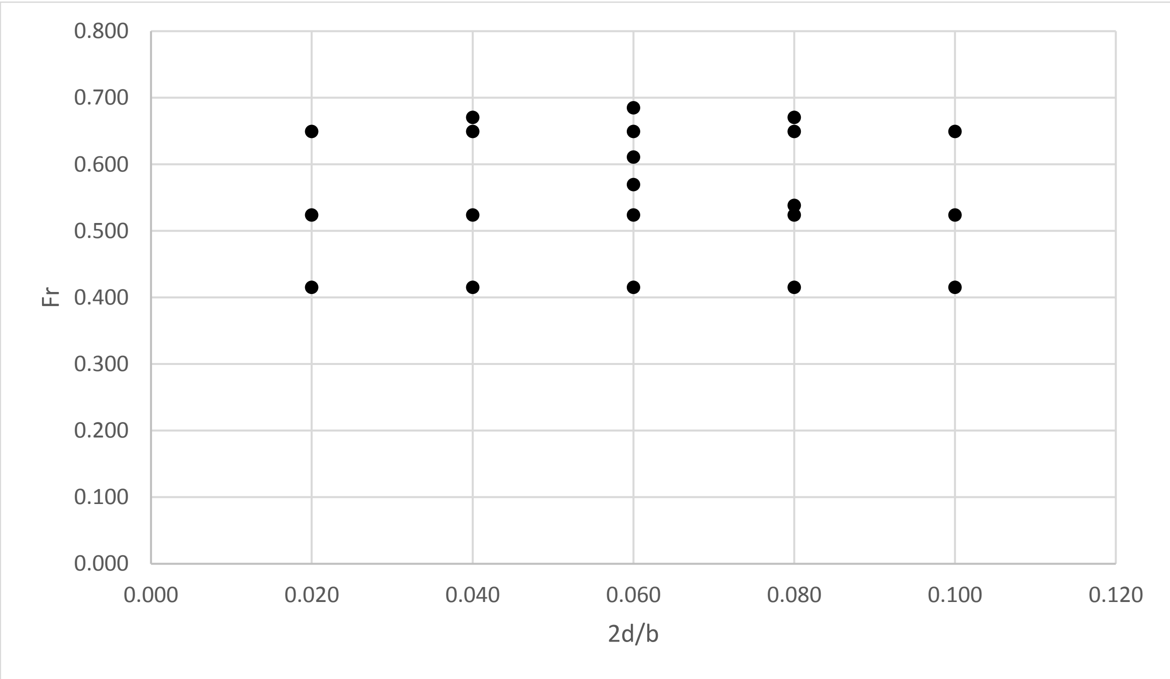

Figure 7-17: 2 boulder ZOI relationship model conditions

7.4.2 Results

The final relationship and associated coefficients for each direction was found to be as follows:

Upstream

$$\frac{yu_i}{b} = n_i \times \left(\frac{2d}{b}\right)^{o_i} \times Fr^{p_i} \qquad \text{7-5}$$

Table 7-8: Upstream ZOI coefficients

Constant	**Percentage variation, *i* %**								
	10	**20**	**30**	**40**	**50**	**60**	**70**	**80**	**90**
n_i	2.64	0.91	0.64	0.61	0.50	0.41	0.35	0.37	0.28
o_i	1.00	0.96	0.99	1.04	1.06	1.04	1.04	1.09	1.03
p_i	0.61	0.07	0.04	0.17	0.06	0.07	0.00	0.05	-0.01

Downstream

$$\frac{yd_i}{b} = n_i \times \left(\frac{2d}{b}\right)^{o_i} \times Fr^{\,p_i} \qquad 7\text{-}6$$

Table 7-9: Downstream ZOI coefficients

Constant	**Percentage variation, *i* %**							
	20	**30**	**40**	**50**	**60**	**70**	**80**	**90**
n_i	6.64	2.75	2.41	2.35	2.50	2.36	2.42	2.44
o_i	0.96	0.80	0.82	0.85	0.91	0.91	0.93	1.01
p_i	0.49	0.76	0.83	0.92	0.95	1.00	1.12	0.99

Sides

$$\frac{x_i}{b} = n_i \times \left(\frac{2d}{b}\right)^{o_i} \times Fr^{\,p_i} \qquad 7\text{-}7$$

Table 7-10: Side ZOI coefficients

Constant	**Percentage variation, *i* %**								
	10	**20**	**30**	**40**	**50**	**60**	**70**	**80**	**90**
n_i	1.92	1.61	1.49	1.53	1.48	1.45	1.39	1.34	1.34
o_i	0.91	0.92	0.93	0.96	0.98	0.97	0.98	0.98	0.99
p_i	0.75	0.75	0.72	0.74	0.71	0.76	0.73	0.74	0.73

7.4.3 Effectiveness

The effectiveness of the created relationship was reviewed by considering two statistical factors, namely the absolute percentage variation between the software and relationship ZOI length and the coefficient of determination *(R^2)*. Shown in Table 7-11 below is a summary of the average absolute percentage error of the predicted values from the relationship compared to the software output. The upstream and side directions had errors below 5% and R^2 values above 0.97. The downstream direction had slightly higher errors, but they were still mostly below 10%, showing that the relationship is still effective. The higher variability in the downstream direction could be due to the correction factors applied. A more detailed comparison of percentage errors can be found in Appendix F.

Table 7-11: % Error and R^2 values

***i* (%)**	**Upstream**		**Downstream**		**Sides**	
	% Error	**R^2**	**% Error**	**R^2**	**% Error**	**R^2**
10	4.28	0.98	-	-	6.54	0.97
20	4.48	0.98	11.37	0.93	4.51	0.99
30	3.58	0.99	9.47	0.93	3.42	0.99
40	1.95	1.00	7.77	0.96	3.80	0.99
50	3.22	0.99	6.13	0.97	2.99	0.99
60	2.42	1.00	4.96	0.98	3.63	0.99
70	3.70	0.99	7.61	0.97	3.24	0.99
80	1.85	1.00	6.20	0.98	3.57	0.99
90	2.27	1.00	8.49	0.96	3.47	0.99

The ZOI length predicted by the software was compared to the ZOI length predicted by the proposed relationship. Figure 7-18,

Figure 7-19 and Figure 7-20 show a comparison of lengths for all percentage variations in the upstream, downstream and side directions respectively. The high R^2 values for each direction furthermore indicated that there was minimal scatter.

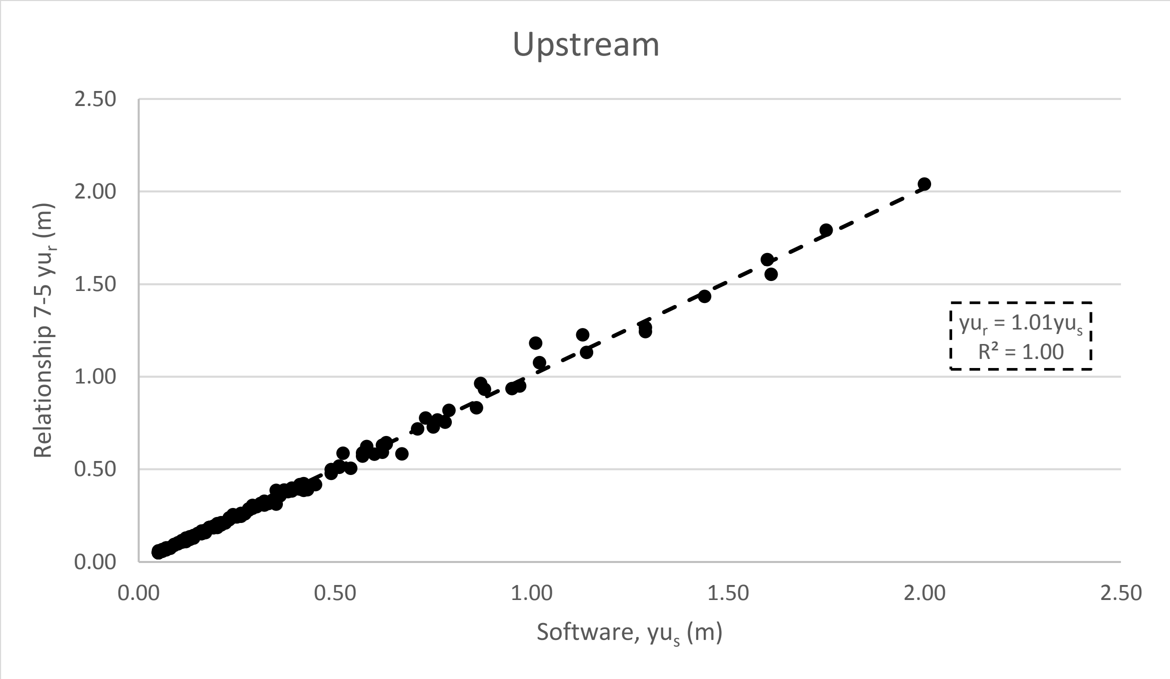

Figure 7-18: Upstream software vs relationship 7-5

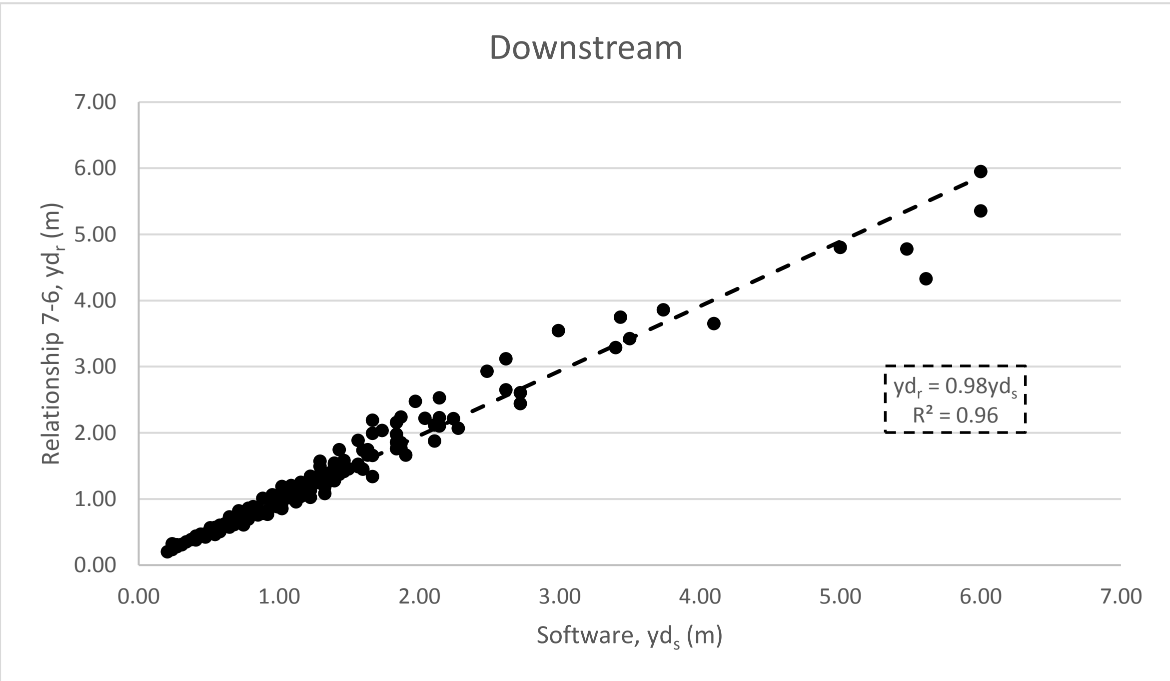

Figure 7-19: Downstream software vs relationship 7-6

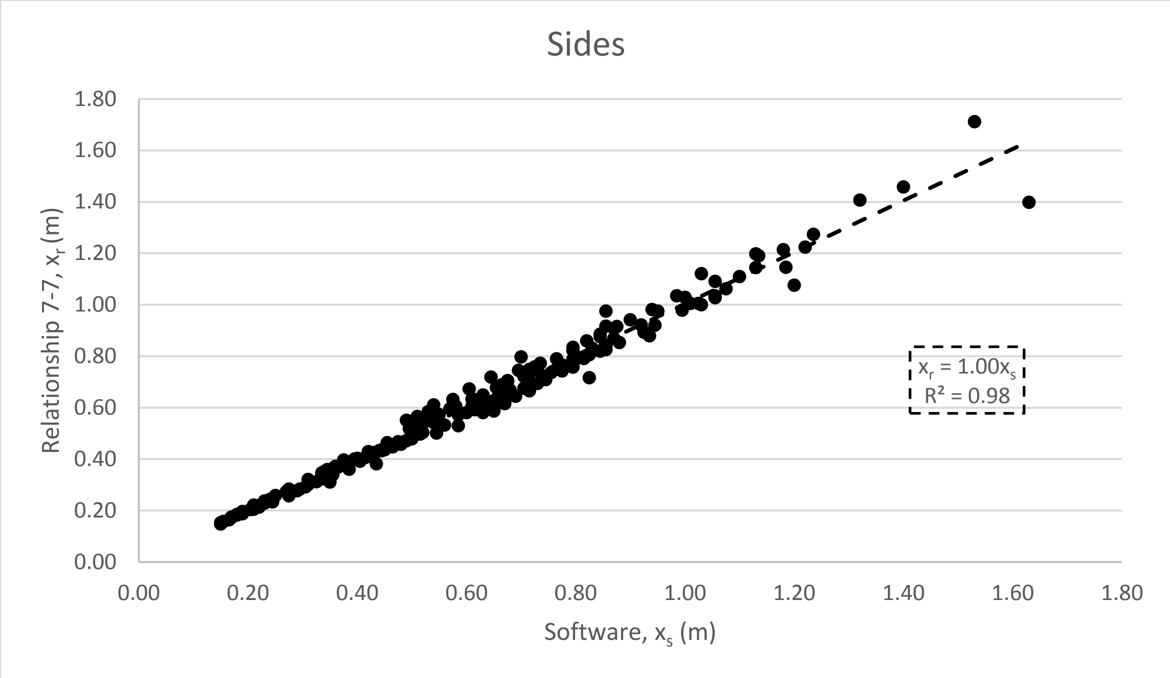

Figure 7-20: Sides software vs relationship 7-7

7.5 ZOI Practical Approximation at Local Control

As with the analysis for 1 boulder a practical approximation to determine the ZOI was developed. The primary variable influencing the ZOI was found to be the blockage ratio. A relationship was developed which eliminated the Froude number and predicted the ZOI using the blockage ratio only. Having a relationship to describe the ZOI without a Froude number yields a relationship which is independent of hydraulic variables. This held practical convenience as an approximate ZOI size could be calculated irrespective of the design discharge.

7.5.1 Results

A relationship was created to predict the dimensionless ZOI ratio using the blockage ratio. Regressions were undertaken to determine the *r* and *t* coefficients in the relationship below:

$$\frac{yu_i, yd_i, x_i}{b} = r_i \times \left(\frac{d}{b}\right)^{t_i} \qquad 7\text{-}8$$

The final relationship for each direction is as follows:

Upstream

$$\frac{yu_i}{b} = r_i \times \left(\frac{d}{b}\right)^{t_i} \qquad 7\text{-}9$$

Table 7-12: Upstream practical ZOI coefficient

Constant	Percentage variation, *i* %								
	10	**20**	**30**	**40**	**50**	**60**	**70**	**80**	**90**
r_i	1.75	0.88	0.62	0.55	0.49	0.40	0.35	0.36	0.28
t_i	0.99	0.96	0.99	1.04	1.07	1.04	1.04	1.09	1.03

Downstream

$$\frac{yd_i}{b} = r_i \times \left(\frac{d}{b}\right)^{t_i} \qquad 7\text{-}10$$

Table 7-13: Downstream practical ZOI coefficient

Constant	Percentage variation, i %							
	20	**30**	**40**	**50**	**60**	**70**	**80**	**90**
r_i	5.05	1.80	1.52	1.40	1.47	1.35	1.34	1.41
t_i	0.96	0.81	0.84	0.86	0.92	0.92	0.96	1.02

Sides

$$\frac{x_i}{b} = r_i \times \left(\frac{d}{b}\right)^{t_i} \qquad 7\text{-}11$$

Table 7-14: Sides practical ZOI coefficient

Constant	Percentage variation, *i*, %							
	20	**30**	**40**	**50**	**60**	**70**	**80**	**90**
r_i	1.26	1.06	1.00	1.01	0.99	0.95	0.93	0.90
t_i	0.92	0.93	0.94	0.97	0.99	0.98	0.99	1.00

7.5.2 Effectiveness

The effectiveness of the created relationship was once again quantified by comparing the ZOI predicted by the software to the ZOI ratio predicted by the proposed relationship. Shown in Table 7-15 below is a summary of the average absolute percentage error of the predicted values from the relationship compared to the software output. The errors for the downstream and sides were larger than 10% with an average error of 15.5% and 12.8% respectively. Although the errors were larger the relationship still holds value in the conceptual design stage.

Table 7-15: % Error and R^2 values practical approximation

***i* (%)**	**Upstream**		**Downstream**		**Sides**	
	% Error	***R*²**	**% Error**	***R2***	**% Error**	***R2***
10	9.67	0.95	-	-	12.91	0.90
20	4.53	0.98	13.63	0.90	12.87	0.91
30	3.67	0.99	13.29	0.84	12.33	0.92
40	3.36	0.99	13.78	0.85	12.74	0.92
50	3.55	0.99	15.14	0.85	12.25	0.93
60	2.62	1.00	14.99	0.86	13.48	0.92
70	3.69	0.99	16.08	0.84	12.61	0.93
80	1.85	1.00	18.55	0.84	12.81	0.93
90	2.28	1.00	18.44	0.86	13.12	0.93

Figure 7-21, Figure 7-22 and Figure 7-23 below show the correlation for all percentage variations for the upstream, downstream and side directions respectively. The correlation proves that the practical approximation is adequate for initial design.

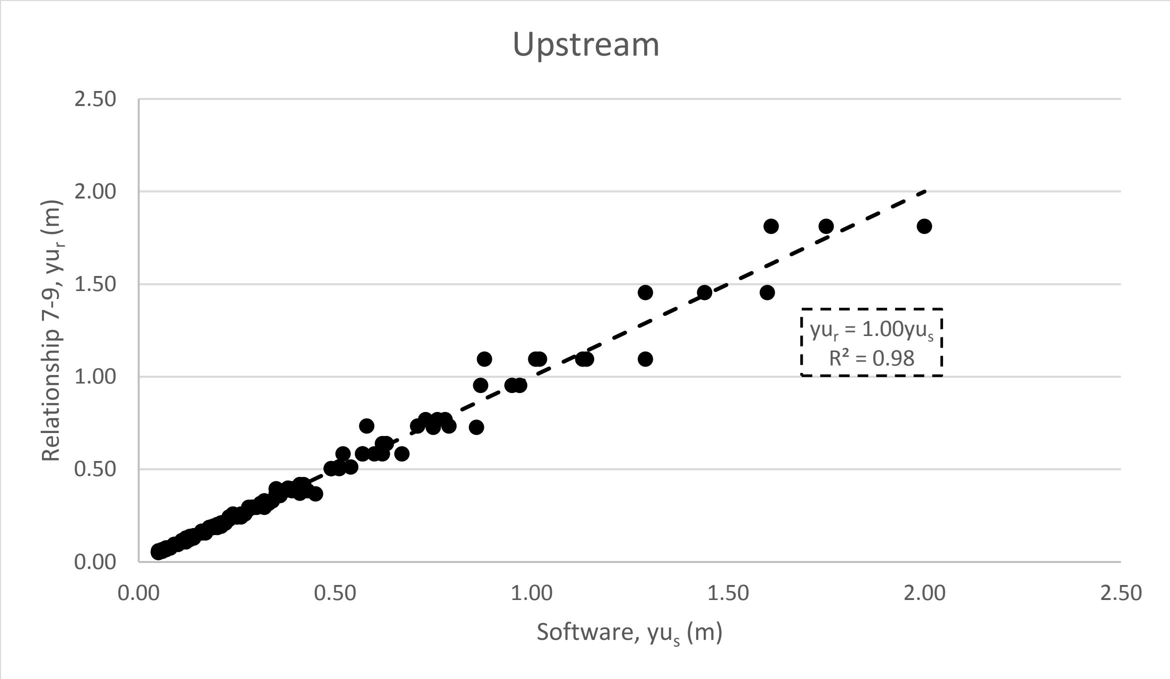

Figure 7-21: Upstream software vs relationship 7-9

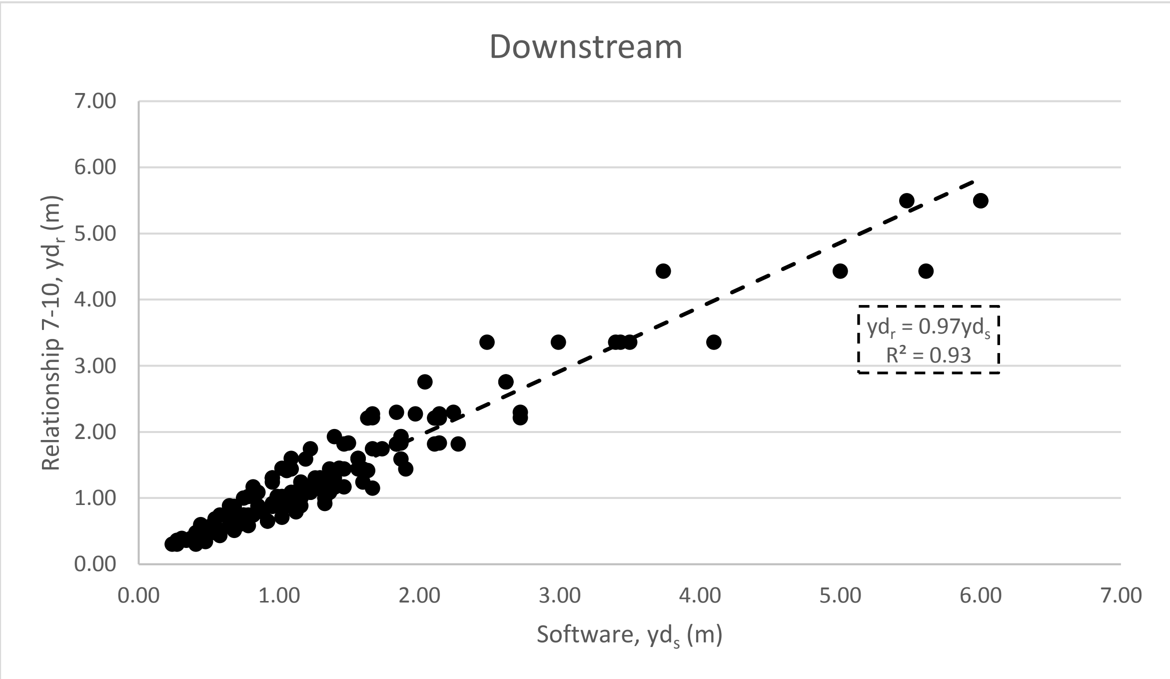

Figure 7-22: Downstream software vs relationship 7-10

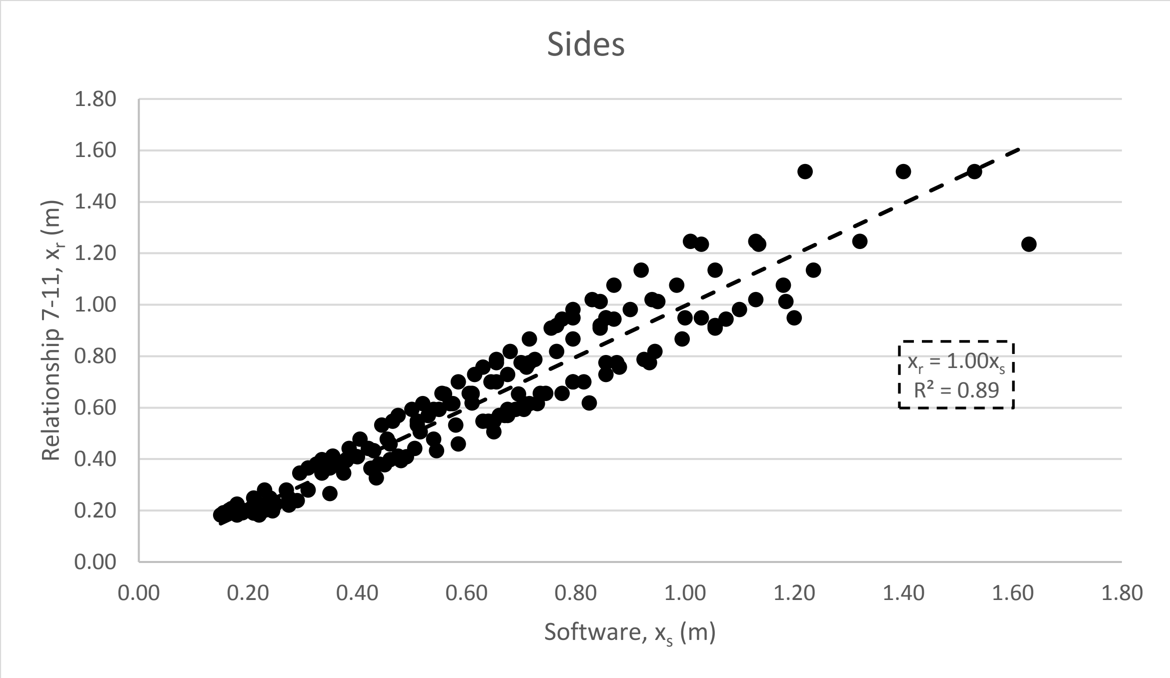

Figure 7-23: Sides software vs relationship 7-11

7.6 Conclusion

The section started with an investigation of the velocity distribution for a particular case. The effect of spacing was analysed by incrementally reducing the spacing between the boulders. The two boulders acted independently when a considerable distance apart. As the spacing between the boulder was reduced the areal change in velocity increased and the velocity distribution resembled that produced by one boulder. The reduction in spacing caused an almost linear change in areal velocity up to the point of local control and when the spacing was reduced further the areal velocity increased only slightly.

The resultant velocity distribution at a local control spacing was analysed to ascertain how favourable the point of local control would be. The point of local control also holds practical value as it is a point which can be identified for different cases. It was found that 2 boulders placed at local control created an areal velocity change equivalent to 1 boulder with double the area of the 2 boulders, which means that using two boulders would reduce material cost and flow constriction. It was found that the spacing needed to create a local control between two boulders was dependant on the blockage ratio and Froude number and that the width of the channel was the appropriate normalising variable for spacing.

A spacing formula to determine a local control was created for different Froude number ranges. The ranges allowed for a practical recommendation for spacing which was only dependant on the boulder diameter.

Table 7-6: Spacing for local control for different Froude number ranges

Froude Number Range	Spacing for Local Control
>0.70	No analysis carried out as a global local control is imminent
0.60-0.70	$Sp = 2d$
0.50-0.60	$Sp = d$
0.40-0.50	$Sp = 0.6d$
<0.4	No analysis as the spacing for local control was found to be very small

The ZOI relationship was determined for boulders at the local control spacing relationship. The second relationship predicts the ZOI by using the channel width and boulder diameter only. The negation of the Froude number results in a relationship which is independent of flow conditions within the channel, which holds practical value within conceptual design stages.

It was found that the ZOI for the upstream, transverse and downstream directions can be predicted by:

$$\frac{yu_i, yd_i, x_i}{b} = n_i \times \left(\frac{2d}{b}\right)^{o_i} \times Fr^{\,p_i} \qquad \text{7-4}$$

$$\frac{yu_i, yd_i, x_i}{b} = r_i \times \left(\frac{2d}{b}\right)^{t_i} \qquad \text{7-8}$$

8 DESIGN EXAMPLES

The following section summarised the findings from the research paper by means of design examples. Three design examples were presented to demonstrate the findings of each main section; namely 1 boulder below the blockage limit, 2 boulders and 1 boulder above the blockage limit.

8.1 1 Boulder Below the Blockage Limit

A rectangular channel with a width of 5.0m and a slope of 0.00080 has a flow rate of 1.20m^3/s. The bed is composed of alluvial material with a representative particle size of 10.0mm.

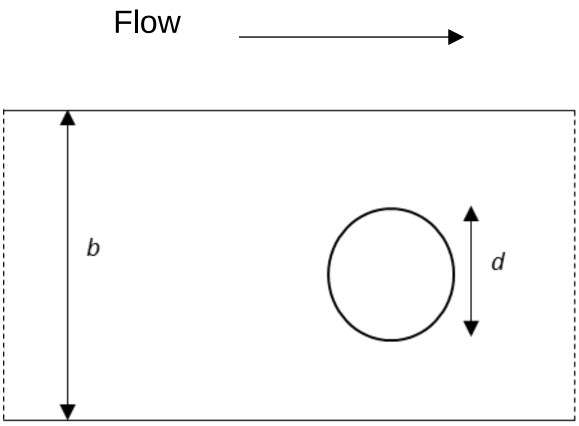

Figure 8-1: 1 boulder below blockage limit design example

Calculate uniform flow conditions

Calculate Manning's *n* using the Strickler formula, where *D* is the representative particle size in meters.

$$n = \frac{D^{\frac{1}{6}}}{6.7\ g^{0.5}} \qquad 8\text{-}1$$

$$n = \frac{0.010^{\frac{1}{6}}}{6.7\ 9.81^{0.5}} = 0.022$$

Calculate the uniform flow depth *H* from Manning's equation.

$$Q = \frac{A}{n} R^{\frac{2}{3}} S^{\frac{1}{2}}$$ 8-2

$$1.20 = \frac{5.0H}{0.022} (\frac{5.0H}{5.0 + 2.0H})^{\frac{2}{3}} 0.00080^{\frac{1}{2}}$$

$$H = 0.39m$$

Calculate uniform velocity *v* from continuity principles.

$$Q = vA$$ 8-3

$$v = \frac{Q}{A} = \frac{1.20}{5.0 \ x \ 0.39} = 0.62 \ m/s$$

Calculate the velocity which would cause scour on the bed

Included below is a simplistic check to determine if there would be scour of the bed. This check has been included in the design examples to highlight that a scour check would be important in the design process and necessary at this point. Boulder stability was not within the scope of work for this research project and additional work would be needed to determine an adequate scour checking method.

The shear stress (τ_o) is defined as follows. Where γ is the specific weight of water,

$$\tau_o = \gamma HS$$ 8-4

The slope (*S)* can be related to Manning's equation and the flow depth related to velocity by continuity.

$$S = \frac{v^2 \ n^2}{H^{\frac{4}{3}}}$$ 8-5

$$H = \frac{q}{v}$$ 8-6

The shear stress relationship can therefore be simplified as follows:

$$\tau_o = \gamma \ x \ \frac{q}{v} \ x \ \frac{v^2 \ n^2}{H^{\frac{4}{3}}}$$

$$\tau_o = \gamma \frac{v^{\frac{2}{3}} n^2}{q^{\frac{1}{3}}}$$

Erosion of the bed material will occur if the shear stress is equal to or greater than the critical shear stress (τ_{oc}). The Shields parameter (τ_{*c}) can be assumed to be 0.047 for large particles and the specific gravity of the sediment is assumed to be 2.65.

$$\tau_{oc} = \tau_{*c} \, \gamma D(S_s - 1) \qquad 8\text{-}7$$

$$\tau_{oc} = 0.047 \, \gamma D(S_s - 1)$$

The velocity at which erosion will just start to occur is when the shear stress is equal to the critical shear stress.

$$\tau_o = \tau_{oc} \qquad 8\text{-}8$$

$$\gamma \frac{v^{\frac{2}{3}} n^2}{q^{\frac{1}{3}}} = 0.047 \, \gamma D(2.65 - 1)$$

$$v = \left(\frac{0.047 \, D(S_s - 1) q^{\frac{1}{3}}}{n^2} \right)^{\frac{3}{2}} \qquad 8\text{-}9$$

$$v = \left(\frac{0.047 \, x \, 0.010(2.65 - 1) \left(\frac{1.20}{5.0} \right)^{\frac{1}{3}}}{0.022^2} \right)^{\frac{3}{2}} = 0.99 \, m/s$$

A velocity of 0.99 m/s or greater will cause erosion of the bed material This velocity equates to a 60% increase from the uniform velocity.

Choose boulder type

In this example, erosion of the bed material will occur with a 60% increase in velocity. If one boulder above the blockage ratio were chosen, then there is a strong chance of erosion. Furthermore if 2 boulders were chosen then the increase of the sides is expected to be up to 90%. It is therefore recommended that 1 boulder below the blockage ratio be chosen.

Calculate the minimum width for choking of the flow to occur

$$bmin = \frac{Q}{\left(\left(\frac{2}{3}\,E\right)^3 x\ g\right)^{0.5}} \qquad 8\text{-}10$$

where *E* is the specific energy of the uniform flow.

$$E = H + \frac{v^2}{2g} = 0.39 + \frac{0.62^2}{2\ x\ 9.81} = 0.41m \qquad 8\text{-}11$$

$$bmin = \frac{1.20}{\left(\left(\frac{2}{3}\,0.41\right)^3 x\ 9.81\right)^{0.5}} = 2.72m$$

$$bmin = b - d \qquad 8\text{-}12$$

$$d = b - bmin = 5.00 - 2.72 = 2.28m$$

A boulder with a diameter of 2.28m or greater will cause choking in the flow.

Select the boulder diameter

The maximum boulder diameter (2.28m) is very large and practically a much smaller boulder diameter will be chosen in order to save on material and placement costs. A boulder diameter of 0.50m will be analysed.

Calculate the ZOI dimensions using the relationships developed

The dimensions for the ZOI were calculated using the relationships and coefficients from Section 5. The ZOI dimensions for upstream, side and downstream directions were calculated using Equation 5-17 and the coefficients from Table 5-4 to 5-6.

$$\frac{yu_i, yd_i, x_i}{b} = n_i \times \left(\frac{d}{b}\right)^{o_i} \times\ Fr^{\,p_i} \qquad 5\text{-}17$$

Table 8-1: 1 boulder below blockage limit: ZOI dimensions

ZOI	Percentage variation, *i* %						
	10	**20**	**30**	**40**	**50**	**60**	**70**
yu_i (m)	1.24	0.78	0.61	0.51	0.45	0.21	0.35
yd_i (m)	-	4.50	1.80	1.26	1.06	0.89	0.82
x_i (m)	1.03	0.53	-	-	-	-	-

Analyse effect on habitat

Assuming that the flow depth is constant at 0.39 m and using
Figure 2-2 for fish and Figure 2-3 for invertabrates the following aquatic habitats are expected.

Table 8-2: 1 boulder below blockage limit: habitats created with relevant ZOI dimensions

Decreased velocity, i %	v (m/s)	yu_i (m)	yd_i (m)	Invertebrates
0	0.62	-	-	VFFS
10	0.56	1.24	-	VFFS
20	0.50	0.78	4.50	FFS
30	0.43	0.61	1.80	FFS
40	0.37	0.51	1.26	FFS
50	0.31	0.45	1.06	FFS
60	0.25	0.21	0.89	SFS
70	0.19	0.35	0.82	SFS

8.2 2 Boulders

A rectangular channel with a width of 10.0m and a slope of 0.0020 has a flow rate of 5.0m^3/s. The bed is composed of material with a representative particle size of 65.0mm.

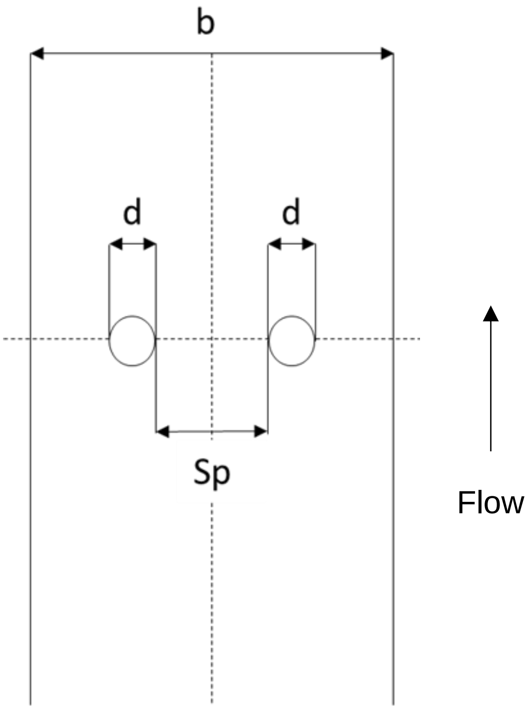

Figure 8-2: 2 boulders design example

Calculate uniform flow conditions

Calculate Manning's *n* using the Strickler formula, where *D* is the representative particle size in meters.

$$n = \frac{D^{\frac{1}{6}}}{6.7\ g^{0.5}} \qquad 8\text{-}13$$

$$n = \frac{0.0650^{\frac{1}{6}}}{6.7\ 9.81^{0.5}} = 0.030$$

Calculate the uniform flow depth *H* from Manning's equation.

$$Q = \frac{A}{n} R^{\frac{2}{3}} S^{\frac{1}{2}}$$ 8-14

$$5.0 = \frac{10.0H}{0.030} \left(\frac{10.0H}{10.0 + 2.0H}\right)^{\frac{2}{3}} 0.0020^{\frac{1}{2}}$$

$$H = 0.54m$$

Calculate uniform velocity *v* from continuity principles.

$$Q = vA$$ 8-15

$$v = \frac{Q}{A} = \frac{5.0}{10.0 \; x \; 0.54} = 0.92 \; m/s$$

Calculate the velocity which would cause scour on the bed

The Shields parameter (τ_{*c}) can be assumed to be 0.047 for large particles and the specific gravity of the sediment is assumed to be 2.65. Using the simplified equation from design example 1.

$$v = \left(\frac{0.047 \; D(S_s - 1)q^{\frac{1}{3}}}{n^2}\right)^{\frac{3}{2}}$$ 8-16

$$v = \left(\frac{0.047 \; x \; 0.0650(2.65 - 1)\left(\frac{5.0}{10.0}\right)^{\frac{1}{3}}}{0.030^2}\right)^{\frac{3}{2}} = 1.88 \; m/s$$

A velocity of 1.88 m/s or greater will cause erosion of the bed material This velocity equated to a 104% increase from the uniform velocity.

Choose boulder type

In this example, erosion of the bed material will only occur with a large increase in velocity. As a result, it would be possible to use either 1 or 2 boulders. It was shown that 2 boulders cause the same disturbed area as 1 boulder but use less material, they do however cause larger velocity increases. Given that 2 boulders cause velocity percentage increases up to 100% it would be safe to use 2 boulders.

Calculate the minimum width for choking of the flow to occur

$$bmin = \frac{Q}{\left(\left(\frac{2}{3}\,E\right)^3 x\, g\right)^{0.5}} \qquad 8\text{-}17$$

where *E* is the specific energy of the uniform flow.

$$E = H + \frac{v^2}{2g} = 0.54 + \frac{0.92^2}{2\,x\,9.81} = 0.58m \qquad 8\text{-}18$$

$$bmin = \frac{5.0}{\left(\left(\frac{2}{3}\,0.58\right)^3 x\,9.81\right)^{0.5}} = 6.56m$$

$$bmin = b - 2d \qquad 8\text{-}19$$

$$d = \frac{b - bmin}{2} = \frac{10.00 - 6.56}{2.00} = 1.72m$$

Two boulders, each with a diameter of 1.72m or greater will cause choking in the flow.

Select the boulder diameter

The maximum boulder diameter (1.72m) is very large and practically a much smaller boulder diameter will be chosen in order to save on material and placement costs. A boulder diameter of 0.50m will be analysed.

Calculate the optimal spacing between the boulders

Determine the Froude number range.

$$Fr = \frac{v}{\sqrt{gH}} \qquad 8\text{-}20$$

$$Fr = \frac{0.92}{\sqrt{9.81x0.54}} = 0.40$$

From Table 7-6, the boulders should be placed 0.60*d* away from each other at *Sp*=0.30m.

Table 7-6: Froude number ranges

Froude Number Range	**Spacing for Local Control**
>0.7	No analysis carried out as a global local control is imminent
0.6-0.7	$Sp = 2d$
0.5-0.6	$Sp = d$
0.4-0.5	$Sp = 0.6d$
<0.4	No analysis as the spacing for local control was found to be very small

Calculate the ZOI dimensions using the relationships developed

The dimensions for the ZOI were calculated using the relationships and coefficients from Section 7. The ZOI dimensions for upstream, side and downstream directions were calculated using Equation 7-4 and the coefficients from Table 7-8 to 7-10.

$$\frac{yu_i, yd_i, x_i}{b} = n_i \times \left(\frac{d}{b}\right)^{o_i} \times Fr^{\,p_i} \qquad 7\text{-}4$$

Table 8-3: 2 boulders: ZOI dimensions

ZOI	Percentage variation, *i* %						
	10	20	30	40	50	60	70
yu_i (m)	1.51	0.94	0.63	0.48	0.41	0.35	0.32
yd_i (m)	-	4.65	2.18	1.71	1.43	1.29	1.16
x_i (m)	1.19	0.98	0.91	0.85	0.81	0.78	0.75

Analyse effect on habitat

Assuming that the flow depth is contant for change in velocity and using Figure 2-2 for fish and Figure 2-3 for invertabrates the following aquatic habitats are expected.

Table 8-4: 1 boulder below blockage limit: habitats created with relevant ZOI dimensions

Decreased velocity, i %	v (m/s)	yu_i (m)	yd_i (m)	Invertebrates
0	0.92	-	-	VFCS
10	0.83	1.51		VFCS
20	0.74	0.94	4.65	VFCS
30	0.65	0.63	2.18	VFCS
40	0.55	0.48	1.71	FCS
50	0.46	0.41	1.43	FCS
60	0.37	0.35	1.29	FCS
70	0.28	0.32	1.16	SCS
80	0.18	0.29	1.02	SCS
90	0.09	0.26	0.97	VSCS

8.3 1 Boulder Above the Blockage Limit

A rectangular channel with a width of 4.0m and a slope of 0.00080 has a flow rate of 1.250m^3/s. The channel has a Manning's *n* of 0.010. The bed around the boulder has a representative soil size of 50.0mm. A large singular boulder is under consideration.

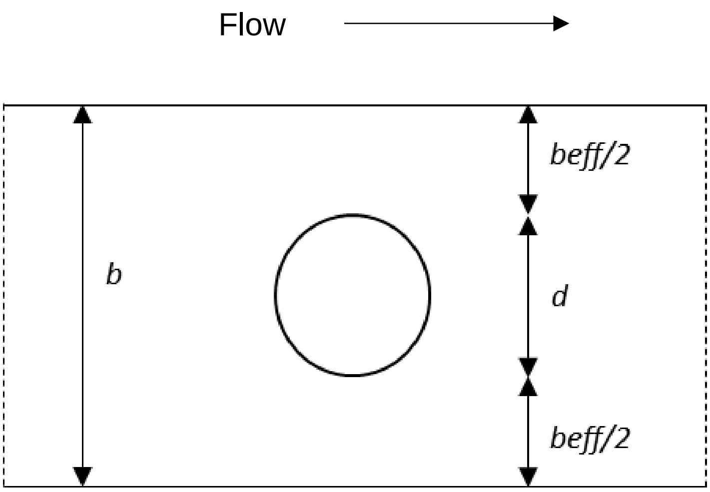

Figure 8-3: 1 boulder above blockage limit design example

Calculate uniform flow conditions

Calculate the uniform flow depth *H* from Manning's equation.

$$Q = \frac{A}{n} R^{\frac{2}{3}} S^{\frac{1}{2}} \quad 8\text{-}21$$

$$1.250 = \frac{4.0H}{0.010} \left(\frac{4.0H}{4.0 + 2.0H}\right)^{\frac{2}{3}} 0.00080^{\frac{1}{2}}$$

$$H = 0.28m$$

Calculate uniform velocity *v* from continuity principles

$$Q = vA \quad 8\text{-}22$$

$$v = \frac{Q}{A} = \frac{1.250}{4.0\ x\ 0.28} = 1.11\ m/s$$

Calculate the minimum width for choking of the flow to occur

$$bmin = \frac{Q}{\left(\left(\frac{2}{3}E\right)^3 x\, g\right)^{0.5}} \qquad 8\text{-}23$$

where *E* is the specific energy of the uniform flow.

$$E = H + \frac{v^2}{2g} = 0.28 + \frac{0.211^2}{2\,x\,9.81} = 0.34m \qquad 8\text{-}24$$

$$bmin = \frac{1.250}{\left(\left(\frac{2}{3}\,0.34\right)^3 x\,9.81\right)^{0.5}} = 3.63m$$

$$bmin = b - d \qquad 8\text{-}25$$

$$d = b - bmin = 4.00 - 3.63 = 0.37m$$

A boulder with a diameter of 0.37m or greater will cause choking in the flow.

Calculate the velocity which would cause scour on the bed

The Shields parameter (τ_{*c}) can be assumed to be 0.047 for large particles and the specific gravity of the sediment is assumed to be 2.65. Using the simplified equation from design example 1.

$$v = \left(\frac{0.047\,D(S_s - 1)q^{\frac{1}{3}}}{n^2}\right)^{\frac{3}{2}} \qquad 8\text{-}26$$

$$v = \left(\frac{0.047\,x\,0.050(2.65 - 1)\left(\frac{1.250}{4.0}\right)^{\frac{1}{3}}}{0.029^2}\right)^{\frac{3}{2}} = 1.63\,m/s$$

A velocity of 1.63 m/s or greater will cause erosion of the bed material This velocity equated to a 47% increase from the uniform velocity.

Select the boulder diameter

Start with a boulder diameter of *d*=1.20m. From the minimum width above, this boulder will cause choking.

Estimate the largest percentage velocity increase at the banks of the channel and the distance this velocity occurs.

$$i_b = 220.34\,\frac{d}{b} - 10.97 = 220.34\frac{1.2}{4} - 10.97 = 55\% \qquad \text{6-14}$$

$$\frac{x_e}{d} = -5.81\,\frac{d}{b} + 2.86 = -5.81\frac{1.2}{4} + 2.86 \qquad \text{6-15}$$

$x_e = 1.34$m

It is estimated that a velocity increase of 55% is expected. This velocity will occur 1.34m from the edge of the boulder to the channel banks. Given that the boulder is placed in the middle of the channel the 55% increase in velocity will occur over a 0.66m distance.

This velocity increase on the bed is larger than the velocity which will just cause incipient motion of the bed material (47% increase). It is advised that the boulder diameter be reduced to avoid erosion of the bed.

Select a smaller boulder diameter

Select the boulder diameter to be 0.80m. This diameter will still cause choking of the flow.

Estimate the largest percentage velocity increase at the banks of the channel and the distance this velocity occurs.

$$i_b = 220.34\,\frac{d}{b} - 10.97 = 220.34\frac{0.8}{4} - 10.97 = 33\% \qquad 6\text{-}14$$

$$\frac{x_e}{d} = -5.81\,\frac{d}{b} + 2.86 = -5.81\frac{0.8}{4} + 2.86 \qquad 6\text{-}15$$

$x_e = 1.36$m

The smaller boulder diameter produces a velocity increase of 33% which extends to the bank. This velocity is smaller than the critical velocity and large-scale erosion is not expected to be a concern.

Calculate the new approach conditions

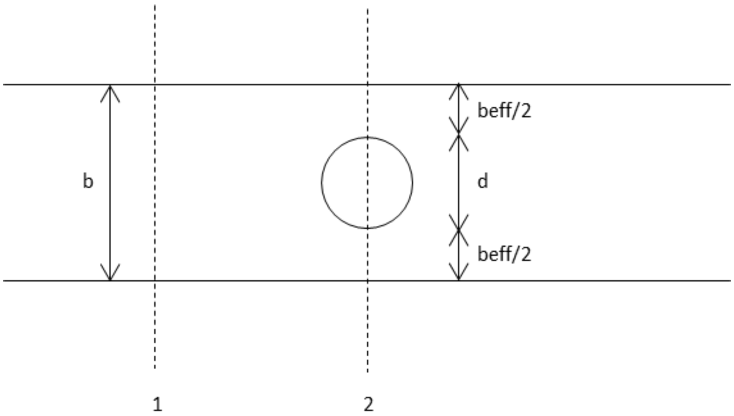

Figure 8-4: Upstream approach conditions

The flow conditions at 2 will be of the critical condition, determined by the discharge and effective width.

$$Hc = H2 = \sqrt[3]{\frac{\left(\frac{Q}{beff}\right)^2}{g}} \qquad 8\text{-}27$$

$$Hc = H2 = \sqrt[3]{\frac{\left(\frac{1.250}{4.0 - 0.80}\right)^2}{9.81}} = 0.25m$$

The specific energy at 2 will be equal to the specific energy at 1.

$$Ec = E2 = \frac{3}{2}\ Hc = \frac{3}{2}\ 0.25 = 0.37m = \ E1 \qquad \text{8-28}$$

The specific energy at 1 differs to that of 2 because of the different channel widths. Solve for the subcritical flow depth at 1 using the specific energy relationship and then solve for the velocity using continuity.

$$E1 = H1 + \frac{\left(\frac{Q}{b}\right)^2}{2g\ H1^2} \qquad \text{8-29}$$

$$0.37 = H1 + \frac{\left(\frac{1.25}{4.0}\right)^2}{2g\ H1^2}$$

$$H1 = 0.33m$$

The upstream flow depth has only increased by 0.05m. It is not expected that the boulder will cause localised flooding.

$$v1 = \frac{\frac{Q}{b}}{H1} \qquad \text{8-30}$$

$$v1 = \frac{\frac{1.25}{4}}{0.33} = 0.95\ m/s$$

The new approach velocity was found to be 0.95 m/s which is 14.38% less than the uniform flow velocity. This falls in the 10-20% velocity change range.

The new approach conditions tend to the uniform flow depth in the upstream condition by means of a M1 flow profile. The gradually varied flow profile will start with the calculated approach velocity and approach uniform flow some distance upstream (*L*). It is estimated that uniform velocity will occur 287m upstream.

$$L = \frac{0.7\ H1}{S} \qquad \text{6-12}$$

$$L = \frac{0.7\ x\ 0.33}{0.0008} = 287.20m$$

Calculate the upstream and downstream ZOI

The upstream ZOI dimensions can be calculated for all percentage variations higher than the new approach velocity. The ZOI dimensions for upstream and downstream directions were calculated using Equation 5-17 and the coefficients from Table 5-4 to 5-6. The $yu_{20\%}$ however comes from the calculation above.

Table 8-5: 1 boulder above blockage limit: upstream and downstream ZOI dimensions

ZOI	**Percentage variation, *i* %**						
	10	**20**	**30**	**40**	**50**	**60**	**70**
yu_i (m)	-	287.20	0.91	0.79	0.66	0.32	0.52
yd_i (m)	-	7.04	2.63	1.87	1.60	1.37	1.31

Analyse effect on habitat

Assuming that the flow depth is contant for change in velocity and using

Figure 2-2 for fish and Figure 2-3 for invertabrates the following aquatic habitats are expected.

Table 8-6: 1 boulder above blockage limit: habitats created with relevant ZOI dimensions

Decreased velocity, i %	**v (m/s)**	**yu_i (m)**	**yd_i (m)**	**Invertebrates**
0	1.11	-	VFCS	FI
10	1.00	-	VFCS	FI
20	0.89	287.20	VFCS	FD
30	0.78	0.91	VFCS	FI
40	0.67	0.79	VFCS	FI
50	0.56	0.66	FCS	FI
60	0.44	0.32	FCS	FI
70	0.33	0.52	FCS	FI

9 CONCLUSION AND RECOMMENDATIONS

The use of boulders to increase habitat heterogeneity for the purpose of aquatic biodiversity was found to be effective. Initial guidelines have been produced to determine the effect of boulders on flow conditions which are summarised below.

9.1 Software Correlation

The software and experimental velocity profiles were compared for the upstream, side and downstream directions. The comparison showed that the software adequately predicted velocities in the upstream and side directions.

The software was found to negate the turbulent wakes downstream of the boulder and showed a poor correlation to the experimental results. The velocities predicted by the software were firstly too high and secondly the predicted velocities were prematurely predicted. The software results were adjusted by the application of two correction factors; one for velocity and one for distance. The correction factors resulted in higher coefficients of regression and it was assumed that adequate downstream correlation was reached.

9.2 1 Boulder Below the Blockage Ratio Limit

The analysis of flow around a single boulder highlighted important aspects of the resultant disturbed velocity.

- The changes in flow depth were observed at small localised areas around the edges of the boulders. The velocity changes on the other hand were in the order of magnitude of several metres. The effect of boulders was therefore quantified using velocities. The investigation above the blockage ratio limit did however show more substantial flow depth changes and the flow depth was incorporated into the analysis.
- Low percentage variations from uniform velocity occupied the greatest area of disturbed flow.
- The downstream direction showed the largest region of disturbed flow followed by the upstream direction. Both the upstream and downstream

direction exhibited velocity decreases up to 100% from the uniform velocity and occurred several metres away from the boulder.

- The sides showed smaller high velocity zones. The increase in velocities ranged up to 50% from uniform velocity for one boulder and were generally less than a metre away from the boulder.

The area of flow which was disturbed by the placement of a boulder was quantified by using a ZOI. The ZOI measured the distance from the boulder where a certain percentage variation of velocity was experienced along the *X* and *Y* axes. The core relationship to predict the ZOI was defined by the hydraulic conditions (*Fr*) and geometric conditions (*d* and *b*) of a channel. This dimensionless relationship was effectively used for each direction; for 1 boulder and 2 boulders with only the empirical coefficients changing.

$$\frac{yu_i, yd_i, x_i}{b} = n_i \times \left(\frac{d}{b}\right)^{o_i} \times Fr^{p_i} \qquad 5\text{-}17$$

It was found that the channel geometry was the dominant variable when compared to the flow conditions. Another ZOI relationship was created which eliminated the Froude number from the above equation and predicted the ZOI using the blockage ratio only. Having a relationship to describe the ZOI without a Froude number yields a relationship which is independent of hydraulic variables. This held practical convenience as an initial ZOI size could be calculated irrespective of the design discharge.

9.3 1 Boulder Above the Blockage Ratio Limit

The disturbed area around a boulder was clearly different when the blockage ratios became larger. Following the identification of the blockage ratio limit it was found that the fundamental utilisation of the disturbed flow differs above and below the blockage ratio limit. Below the blockage limit the downstream velocity distribution is the largest. Above the blockage limit the upstream velocity distribution increases to hundreds of meters upstream.

The sides of the boulder showed increased ZOI dimensions when compared to models below the blockage limit. The increased velocity zones were higher and also extended to the channel bank. This highlighted a potential risk of erosion of the channel banks and bed due to the increased velocities.

It is important to note that with large blockage ratios it is possible to achieve a backwater effect without a full-width structure such as a weir or a riffle. This allows longitudinal connectivity of the river while still attaining a large hydraulic change.

9.4 2 Boulders

The velocity distribution of two boulders acted independently when a considerable distance apart. As the spacing between the boulder was reduced the areal change in velocity increased and the velocity distribution resembled that produced by one boulder. The reduction in spacing caused an almost linear change in areal velocity up to the point of local control between the boulders, and when the spacing was reduced further the areal velocity increased only slightly.

It has been shown that 2 boulders spaced at local control is indeed effective and provides the same areal velocity change as 1 boulder, but with half the area. A spacing formula to determine a local control was created for different Froude number ranges. The ranges allowed for a practical recommendation for spacing which was only dependent on the boulder diameter.

The same dimensionless ZOI relationships developed for 1 boulder was used for 2 boulders. The ZOI relationship was determined for boulders at the local control spacing.

9.5 Additional Considerations

This research report outlined a method for determining the size of the disturbed flow caused by boulders. The quantification of flow changes is key for aquatic habitat creation, but it must be highlighted that river rehabilitation projects are complex interdisciplinary projects. Apart from habitat quantification some other aspects which require consideration are summarised as follows:

- The geomorphology of the channel under consideration should be investigated, most notably the sediment loads and the dynamics of the bed.
- The water quality should be considered to ensure that it is adequate to support the target species.
- Stability of the boulders within the substrate material should be analysed and it should be determined whether additional stabilisation methods would be necessary.
- Type of construction/placement methods should consider possible secondary disturbances to the system. Construction methods should also be evaluated with regards to cost and possible local employment creation.
- Regulatory authorisations may be necessary. In the South African context, a water licence and environmental impact assessment could be necessary depending on the final volume of boulders.
- Lastly an adaptive monitoring programme should be created to measure the success of rehabilitation and to provide learnings for future projects.

9.6 Recommendations for Further Research

Several future research aspects stemming from the findings were noted.

- The experimental velocities downstream of boulders showed decreased velocities extending to the downstream extent of the flume. Investigation of the downstream velocity profile in a longer flume is needed to analyse the distance over which the velocity returns to uniform.
- Alternative software should be investigated, and a recommendation made on what software is capable of determining the resultant downstream velocities. In such an investigation, it would be recommended that the downstream velocity be compared to downstream experimental results separately, as comparing the overall velocity correlation could skew the results.
- The theoretical relationship presented to determine the blockage ratio should be confirmed experimentally.
- It would be beneficial to extend the ZOI equations in each section to predict areal velocity changes. This will allow the created habitats to be described by area and not just length.

- The optimum spacing for 2 boulders placed in a channel with Froude numbers below 0.4 and above 0.7 should be investigated.
- The research on 2 boulders should be extended to include the optimal spacing and resultant ZOI dimensions for more than 2 boulders. The research should also be extended to include boulders not only in the transverse direction but also for boulders placed at angles to each other. This placement would appeal to an aesthetic rehabilitation plan.
- The downstream placement of subsequent boulders should be investigated. An intuitive placement arrangement would be to place boulders so that their respective ZOIs do not interfere with one another and as a starting point this distance should be defined.
- The relationships developed within this research should be replicated for boulders with different shapes.
- The effect of submergence on the velocity distributions should be investigated.
- Investigation on the scour around boulders and the conditions of embedding should be investigated.
- Boulder stability was not within the scope of work for this research project and additional work would be needed to determine an adequate method for the determination of possible scour of the bed and what point this would threaten boulder stability.

REFERENCES

Argus Holdings., 1997. *Argus ONE, Argus Open Numerical Environments – A GIS Modelling System*. Argus Holdings, New York, USA.

Birkhead, A., 2010. The role of ecohydraulics in the South African Ecological Reserve, Chapter 9 in *Ecohydraulics for South African Rivers: A Review and Guide,* C.S. James and J.M. King (Eds). WRC Report No. TT 453/10. Water Research Commission, Pretoria, South Africa.

Birkhead, A., Hirshowitz, P., James, C., 2007. Hydraulic modelling for ecological studies for South African rivers. WRC Report No. TT 1508/1/07. Water Research Commission, Pretoria, South Africa.

Blackburn, J., Steffler, P., 2002. *Two-dimensional depth averaged model of river hydrodynamics and fish habitat*. River2D user's manual. University of Alberta, Canada.

Brown, E., Johnson, P., 1999. *Marylands Waterway Construction Guidelines*, 2nd ed. Maryland Department of the Environment, USA.

Crowder, D.W., Diplas, P., 2000. Using two-dimensional hydrodynamic models at scales of ecological importance. *Journal of Hydrology* 230,172-191.

Crowder, D.W., Diplas, P., 2005. Applying spatial hydraulic principles to quantify stream habitats. *River Research and Applications* 22, 79-89.

Cullis, J., King, J., Paxton, B., Ractliffe, G., 2010. Describing hydraulic habitat, Chapter 4 in *Ecohydraulics for South African Rivers: A Review and Guide,* C.S. James and J.M. King (Eds). WRC Report No. TT 453/10. Water Research Commission, Pretoria, South Africa.

Day, L., King, H., Rountree, M., 2016a. Literature Review, in *The development of a comprehensive manual for river rehabilitation in South Africa,* L. Day, M.

Rountree and H. King (Eds). WRC Report No. KSA K/2270. Water Research Commission, Pretoria, South Africa.

Day, L., King, H., Rountree, M., 2016b. Guidelines for river rehabilitation, Volume 1 in *The development of a comprehensive manual for river rehabilitation in South Africa*. L. Day, M. Rountree and H. King (Eds). WRC Report No. KSA K/2270. Water Research Commission, Pretoria, South Africa.

Day, L., King, H., Rountree, M., 2016c. Technical manual, Volume 2 in *The development of a comprehensive manual for river rehabilitation in South Africa*. L. Day, M. Rountree and H. King (Eds). WRC Report No. KSA K/2270. Water Research Commission, Pretoria, South Africa.

DEAT., 2007. *South Africa Environment Outlook: A report on the state of the environment. Executive and key findings*. Department of Environmental Affairs and Tourism, Pretoria, South Africa.

Department of Water Affairs and Forestry (DWAF). 1997. *White paper on a national water policy for South Africa*. Department of Water Affairs and Forestry, Pretoria, South Africa.

Diplas, P., Shen, Y., 2007. Application of two- and three-dimensional computational fluid dynamics models to complex ecological stream flows. *Journal of Hydrology* 348, 195-214.

FLO-2D Software., 2009. *RiverFLO-2D Two-Dimensional Finite-Element River Dynamics Model User's Manual*. FLO-2D Software. Florida, USA.

Fogg, J., Wells, G., 1998. *Stream corridor restoration: principles, processes, and practices*. United States Department of Agriculture, USA.

Geller, L., 2010. *Frequently asked questions in IFIM: An overview of Instream Flow Incremental Methodology*, 2nd ed. Department of Ecology, State of Washington, USA.

Hamuy-Blanco, A., 2013. Enhancement of Habitat Heterogeneity by Placement of Boulders in Streams (MSc Project Report). University of the Witwatersrand, School of Civil and Environmental Engineering.

Hamuy-Blanco, A., James, C., 2014. Enhancement of Habitat Heterogeneity by Placement of Boulders in Streams. Presented at the River Flow 2014, Taylor and Francis Group, London, pp. 2321–2329.

Harrison, S.S.C., Pretty, J.L., Shepherd, D.J., Smith, C., Hildrew, A.G., Hey, R.D., 2003. River rehabilitation and fish populations: assessing the benefit of instream structures. *Journal of Applied Ecology* 40, 251–265.

Hirschowitz, PM., Birkhead, A.L., James, C, S., 2007. *Hydraulic modelling for ecological studies for South African Rivers.* WRC Report No. 1508/1/07, Water Research Commission, Pretoria, South Africa.

Hydronia, LLC., 2015. RiverFlow2D *Two-Dimensional River Dynamics Model, Reference Manual*. Hydronia LLC, Florida, USA.

Jeong, S., Kil, J.T., Lee, J.H., 2010. Evaluation of physical fish habitat quality enhancement designs in urban streams using a 2D hydrodynamic model. *Ecological Engineering* 36, 1251–1259.

Jordanova, A.A., Birkhead, A.L., James, C.S., Kleynhans, C., 2004. *Hydraulics for determination of the Ecological Reserve for rivers*. WRC Report No. 1174/1/04, Water Research Commission, Pretoria, South Africa.

King, J., Paxton, B., Ractliffe, G., 2010. The river as a living system, Chapter 3 in *Ecohydraulics for South African Rivers: A Review and Guide,* C.S. James and J.M. King (Eds). WRC Report No. TT 453/10. Water Research Commission, Pretoria, South Africa.

King, J., Scheepers, A., Fisher, R., Reinecke, M., Smith, L., 2003. *River Rehabilitation: Literature Review, Case Studies and Emerging Principles*.

WRC Report No. 1161/1/03. Water Research Commission, Pretoria, South Africa.

Kleynhans, C J., 1999. The development of a fish index to assess the biological integrity of South African rivers. *Water S.A*. 25 (3), 265-278.

Lovett, S, Edgar, B, 2002. *Planning for River Restoration, Fact Sheet 9.* Land and Water Australia, Australia.

Malmqvist, B., Rundle, S., 2002. Threats to the running water ecosystems of the world. *Environmental Conservation* 29, 134-153.

Nortek AS., 2004. *Vectrino Velocimeter User Guide*. Nortek AS, Norway.

NWA., 1998. National Water Act No. 36 of 1998 of the Republic of South Africa. Government Gazette <https://www.dwa.gov.za/Documents/Legislature/nw_act/NWA.pdf> (accessed 4.28.15)

Palmer, M.A., Menninger, H.L., Bernhardt, E., 2010. River restoration, habitat heterogeneity and biodiversity: a failure of theory or practice? *Freshwater Biology* 55, 205–222.

Pasternack, G.B., Gilbert, A.T., Wheaton, J.M., Buckland, E.M., 2005. Error propagation for velocity and shear stress prediction using 2D models for environmental management. *Journal of Hydrology* 328, 227-241.

Pierce, C. H., Lee, L., Hartwell, O. W., *1941. Investigations of Methods and Equipment used in stream gaging, Part 1.* Performance of current meters in water of shallow depth. U.S. Geological Survey, *Water Supply Paper* 868, 1-35.

Riddet, M., 2012. The Influence of Large Roughness Elements on the Velocity Distribution in Streams (MSc Project Report). University of the Witwatersrand, School of Civil and Environmental Engineering.

Rutherfurd, I., Jerie, K., Marsh, N., 2000a. *A Rehabilitation Manual for Australian Streams, Volume 1*. Cooperative Research Centre for Catchment Hydrology, Land and Water Resources Research and Development Corporation, Australia.

Rutherfurd, I., Jerie, K., Marsh, N., 2000b. *A Rehabilitation Manual for Australian Streams, Volume 2.* Cooperative Research Centre for Catchment Hydrology, Land and Water Resources Research and Development Corporation, Australia.

Saldi-Caromile, K., Bates, K.K., Skidmore, P., Barenti, J., Pineo, D., 2004. *Stream Habitat Restoration Guidelines: Final Draft*. Washington Departments of Fish and Wildlife and Ecology and the U.S. Fish and Wildlife Service. Olympia, Washington, USA.

Samuels, P.G., 1989. Backwater Lengths in Rivers. Proceeding of the Institution of Civil Engineers, 87:4, 571-582.

Schueler, T.R., Brown, K., 2004. *Urban stream repair practices, Manual 4*. Centre for Watershed Protection, Washington, USA.

Shamloo, H., 1997. Hydraulics of Simple Habitat Structures on Open Channels. (Ph.D. Thesis). University of the Alberta, School of Civil and Environmental Engineering.

State of the Environment South Africa., 2007. Themes - Biodiversity & ecosystems - State of ecosystems - Rivers <http://soer.deat.gov.za/424/_2672.html> (accessed 4.28.15).

Swales, S., 1993. Rehabilitation, mitigation and restoration of fish habitat in regulated rivers, in: Sustainable Fisheries through Sustaining Fish Habitats. Presented at the Australian Society for Fish Biology Workshop.

United States Department of the Interior Bureau of Reclamation., 2001. *Water Measurement Manual*. Third ed. United States Department of the Interior Bureau of Reclamation, Washington DC, USA.

Waddle, T., 2010. Field evaluation of a two-dimensional hydrodynamic model near boulders for habitat calculation. *River Research and Applications* 26, 730-741.

APPENDIX A: SOFTWARE AND EXPERIMENTAL CORRELATION

The tables below compare the experimental and software velocities. It should be noted that the software results are after a multiple regression and with the software factor applied.

Table_A- 1: 1 Boulder Test 1 d=0.11m experimental and software results

Test	d (m)	Direction	Distance (m)	Experimental v (m/s)	Software v (m/s)	% Error
1	0.11	Down	5	0.310	0.466	50.61
1	0.11	Down	4.5	0.327	0.451	38.02
1	0.11	Down	4	0.324	0.434	33.91
1	0.11	Down	3.5	0.320	0.416	29.99
1	0.11	Down	3	0.323	0.396	22.85
1	0.11	Down	2.5	0.328	0.374	14.00
1	0.11	Down	2	0.307	0.348	13.46
1	0.11	Down	1.8	0.306	0.337	10.12
1	0.11	Down	1.6	0.310	0.324	4.50
1	0.11	Down	1.5	0.303	0.318	4.79
1	0.11	Down	1.4	0.295	0.311	5.37
1	0.11	Down	1.2	0.307	0.296	3.73
1	0.11	Down	1	0.290	0.279	3.56
1	0.11	Down	1	0.289	0.279	3.46
1	0.11	Down	0.9	0.284	0.270	4.82
1	0.11	Down	0.8	0.270	0.260	3.84
1	0.11	Down	0.7	0.262	0.249	4.87
1	0.11	Down	0.6	0.238	0.237	0.38
1	0.11	Down	0.5	-0.189	0.224	218.19
1	0.11	Down	0.4	0.121	0.208	72.07
1	0.11	Down	0.3	-0.032	0.190	695.87
1	0.11	Down	0.2	-0.028	0.167	694.54
1	0.11	Down	0.1	-0.037	0.134	464.40
1	0.11	Up	0.1	0.205	0.268	31.02
1	0.11	Up	0.2	0.308	0.287	6.89
1	0.11	Up	0.3	0.346	0.299	13.67
1	0.11	Up	0.4	0.333	0.308	7.67
1	0.11	Up	0.5	0.347	0.314	9.29
1	0.11	Up	0.5	0.336	0.314	6.51
1	0.11	Up	0.6	0.351	0.320	8.84
1	0.11	Up	0.7	0.351	0.325	7.45
1	0.11	Up	0.8	0.358	0.329	8.08
1	0.11	Up	0.9	0.359	0.333	7.25

Test	d (m)	Direction	Distance (m)	Experimental v (m/s)	Software v (m/s)	% Error
1	0.11	Up	1	0.357	0.337	5.75
1	0.11	Up	1.5	0.355	0.350	1.32
1	0.11	Up	2	0.360	0.360	0.15
1	0.11	Up	2.5	0.368	0.368	0.14
1	0.11	Up	3	0.363	0.375	3.32
1	0.11	Sides	0.1	0.431	0.461	6.82
1	0.11	Sides	0.2	0.402	0.433	7.91
1	0.11	Sides	0.3	0.389	0.418	7.52
1	0.11	Sides	0.4	0.385	0.407	5.96
1	0.11	Sides	0.5	0.378	0.399	5.81
1	0.11	Sides	0.6	0.385	0.393	2.14
1	0.11	Sides	0.7	0.368	0.388	5.47
1	0.11	Sides	0.8	0.376	0.383	2.02

Table_A- 2: 1 Boulder Test 1 d=0.175m experimental and software results

Test	d (m)	Direction	Distance (m)	Experimental v (m/s)	Software v (m/s)	% Error
1	0.175	Down	5	0.338	0.460	36.25
1	0.175	Down	4.5	0.325	0.444	36.39
1	0.175	Down	4	0.322	0.426	32.24
1	0.175	Down	3.5	0.310	0.408	31.42
1	0.175	Down	3	0.305	0.387	26.65
1	0.175	Down	2.5	0.305	0.363	19.03
1	0.175	Down	2	0.271	0.337	24.31
1	0.175	Down	1.8	0.274	0.325	18.69
1	0.175	Down	1.6	0.265	0.312	17.73
1	0.175	Down	1.4	0.253	0.298	17.88
1	0.175	Down	1.2	0.257	0.283	10.15
1	0.175	Down	1	0.216	0.266	22.98
1	0.175	Down	0.9	0.200	0.257	28.38
1	0.175	Down	0.8	0.168	0.247	47.29
1	0.175	Down	0.7	0.058	0.236	309.19
1	0.175	Down	0.6	0.061	0.224	266.01
1	0.175	Down	0.5	-0.127	0.210	265.51
1	0.175	Down	0.4	-0.142	0.195	237.37
1	0.175	Down	0.3	-0.168	0.177	205.20
1	0.175	Down	0.2	-0.002	0.154	8069.20
1	0.175	Up	0.2	0.239	0.299	24.90
1	0.175	Up	0.3	0.297	0.308	3.90
1	0.175	Up	0.4	0.328	0.315	3.88
1	0.175	Up	0.5	0.335	0.321	4.15

Test	d (m)	Direction	Distance (m)	Experimental v (m/s)	Software v (m/s)	% Error
1	0.175	Up	0.6	0.350	0.325	7.13
1	0.175	Up	0.7	0.347	0.329	5.10
1	0.175	Up	0.8	0.339	0.332	2.07
1	0.175	Up	0.9	0.325	0.335	3.28
1	0.175	Up	1	0.349	0.338	3.25
1	0.175	Up	1.5	0.336	0.348	3.73
1	0.175	Up	2	0.347	0.356	2.64
1	0.175	Up	2.5	0.361	0.362	0.24
1	0.175	Up	3	0.356	0.367	3.13
1	0.175	Sides	0.15	0.470	0.500	6.26
1	0.175	Sides	0.2	0.456	0.479	5.20
1	0.175	Sides	0.3	0.404	0.452	11.90
1	0.175	Sides	0.4	0.381	0.433	13.60
1	0.175	Sides	0.5	0.382	0.419	9.65
1	0.175	Sides	0.6	0.379	0.408	7.63
1	0.175	Sides	0.7	0.361	0.399	10.48
1	0.175	Sides	0.8	0.375	0.392	4.34

Table_A- 3: 1 Boulder Test 1 d=0.235m experimental and software results

Test	d (m)	Direction	Distance (m)	Experimental v (m/s)	Software v (m/s)	% Error
1	0.235	Down	5	0.269	0.614	128.23
1	0.235	Down	4.5	0.305	0.559	83.09
1	0.235	Down	4	0.297	0.503	69.46
1	0.235	Down	3.5	0.298	0.447	49.84
1	0.235	Down	3	0.281	0.389	38.58
1	0.235	Down	2.5	0.209	0.331	58.21
1	0.235	Down	2	0.202	0.271	34.70
1	0.235	Down	1.8	0.242	0.247	1.96
1	0.235	Down	1.6	0.232	0.223	3.91
1	0.235	Down	1.4	0.216	0.198	8.62
1	0.235	Down	1.2	0.226	0.172	23.78
1	0.235	Down	1	0.204	0.146	28.18
1	0.235	Down	0.9	0.188	0.133	29.15
1	0.235	Down	0.8	0.165	0.120	27.24
1	0.235	Down	0.7	0.137	0.107	22.19
1	0.235	Down	0.6	0.075	0.093	23.99
1	0.235	Down	0.5	0.030	0.079	159.88
1	0.235	Down	0.4	0.024	0.065	172.14
1	0.235	Down	0.3	0.024	0.050	108.89
1	0.235	Down	0.25	0.007	0.043	496.10

Test	d (m)	Direction	Distance (m)	Experimental v (m/s)	Software v (m/s)	% Error
1	0.235	Up	0.25	0.188	0.258	37.06
1	0.235	Up	0.3	0.200	0.264	32.07
1	0.235	Up	0.4	0.270	0.275	1.99
1	0.235	Up	0.5	0.306	0.284	7.17
1	0.235	Up	0.6	0.331	0.291	12.02
1	0.235	Up	0.7	0.321	0.297	7.55
1	0.235	Up	0.8	0.336	0.303	9.89
1	0.235	Up	0.9	0.331	0.307	7.24
1	0.235	Up	1	0.351	0.312	11.25
1	0.235	Up	1.5	0.332	0.330	0.76
1	0.235	Up	2	0.346	0.343	0.91
1	0.235	Up	2.5	0.346	0.354	2.23
1	0.235	Up	3	0.333	0.363	8.96
1	0.235	Sides	0.2	0.483	0.525	8.65
1	0.235	Sides	0.3	0.453	0.497	9.62
1	0.235	Sides	0.4	0.412	0.479	16.29
1	0.235	Sides	0.5	0.401	0.465	15.93
1	0.235	Sides	0.6	0.393	0.453	15.51
1	0.235	Sides	0.7	0.412	0.444	7.90
1	0.235	Sides	0.8	0.395	0.437	10.41

Table_A- 4: 1 Boulder Test 2 d=0.11m experimental and software results

Test	d (m)	Direction	Distance (m)	Experimental v (m/s)	Software v (m/s)	% Error
2	0.11	Down	5	0.298	0.406	36.47
2	0.11	Down	4.5	0.305	0.394	29.23
2	0.11	Down	4	0.287	0.381	32.71
2	0.11	Down	3.5	0.287	0.367	27.82
2	0.11	Down	3	0.283	0.351	24.23
2	0.11	Down	2.5	0.277	0.333	20.34
2	0.11	Down	2	0.272	0.313	15.08
2	0.11	Down	1.8	0.272	0.303	11.61
2	0.11	Down	1.6	0.260	0.293	12.83
2	0.11	Down	1.4	0.270	0.282	4.70
2	0.11	Down	1.2	0.256	0.270	5.50
2	0.11	Down	1	0.255	0.256	0.41
2	0.11	Down	0.9	0.254	0.249	2.15
2	0.11	Down	0.8	0.240	0.240	0.31
2	0.11	Down	0.7	0.252	0.231	8.06
2	0.11	Down	0.6	0.232	0.221	4.67
2	0.11	Down	0.5	0.206	0.210	1.89

Test	d (m)	Direction	Distance (m)	Experimental v (m/s)	Software v (m/s)	% Error
2	0.11	Down	0.4	0.181	0.197	8.92
2	0.11	Down	0.3	0.112	0.181	61.84
2	0.11	Down	0.2	-0.095	0.162	269.68
2	0.11	Down	0.15	-0.063	0.149	337.03
2	0.11	Up	0.15	0.268	0.250	6.72
2	0.11	Up	0.2	0.288	0.257	10.77
2	0.11	Up	0.3	0.298	0.266	10.63
2	0.11	Up	0.4	0.311	0.274	12.16
2	0.11	Up	0.5	0.324	0.279	13.91
2	0.11	Up	0.6	0.320	0.284	11.25
2	0.11	Up	0.7	0.310	0.288	7.11
2	0.11	Up	0.8	0.311	0.291	6.46
2	0.11	Up	0.9	0.316	0.294	6.80
2	0.11	Up	1	0.309	0.297	3.85
2	0.11	Up	1.5	0.310	0.308	0.38
2	0.11	Up	2	0.312	0.317	1.57
2	0.11	Up	2.5	0.326	0.323	0.81
2	0.11	Up	3	0.323	0.328	1.78
2	0.11	Sides	0.1	0.406	0.413	1.74
2	0.11	Sides	0.2	0.374	0.387	3.34
2	0.11	Sides	0.3	0.345	0.372	7.84
2	0.11	Sides	0.4	0.339	0.362	7.02
2	0.11	Sides	0.5	0.336	0.355	5.54
2	0.11	Sides	0.6	0.328	0.349	6.27
2	0.11	Sides	0.7	0.341	0.344	0.87
2	0.11	Sides	0.8	0.339	0.339	0.05

Table_A- 5: 1 Boulder Test 2 d=0.175m experimental and software results

Test	d (m)	Direction (m)	Distance	Experimental v (m/s)	Software v (m/s)	% Error
2	0.175	Down	5	0.303	0.399	31.64
2	0.175	Down	4.5	0.291	0.386	32.91
2	0.175	Down	4	0.289	0.373	29.16
2	0.175	Down	3.5	0.286	0.359	25.62
2	0.175	Down	3	0.280	0.343	22.57
2	0.175	Down	2.5	0.279	0.325	16.72
2	0.175	Down	2	0.260	0.304	16.99
2	0.175	Down	1.8	0.257	0.295	14.93
2	0.175	Down	1.6	0.252	0.285	13.00
2	0.175	Down	1.4	0.238	0.274	15.28
2	0.175	Down	1.2	0.244	0.262	7.35

Test	d (m)	Direction (m)	Distance	Experimental v (m/s)	Software v (m/s)	% Error
2	0.175	Down	1	0.236	0.248	5.40
2	0.175	Down	0.9	0.220	0.241	9.63
2	0.175	Down	0.8	0.202	0.233	15.24
2	0.175	Down	0.7	0.197	0.224	13.56
2	0.175	Down	0.6	0.167	0.214	28.34
2	0.175	Down	0.5	0.113	0.203	78.92
2	0.175	Down	0.4	0.058	0.190	229.56
2	0.175	Down	0.3	-0.113	0.174	254.82
2	0.175	Down	0.2	-0.010	0.155	1622.63
2	0.175	Up	0.2	0.246	0.271	10.20
2	0.175	Up	0.3	0.268	0.278	3.65
2	0.175	Up	0.4	0.300	0.283	5.53
2	0.175	Up	0.5	0.313	0.287	8.37
2	0.175	Up	0.6	0.317	0.291	8.33
2	0.175	Up	0.7	0.312	0.293	5.83
2	0.175	Up	0.8	0.311	0.296	4.73
2	0.175	Up	0.9	0.319	0.298	6.54
2	0.175	Up	1	0.322	0.300	6.80
2	0.175	Up	1.5	0.317	0.308	2.86
2	0.175	Up	2	0.320	0.314	1.89
2	0.175	Up	2.5	0.323	0.319	1.21
2	0.175	Up	3	0.315	0.322	2.29
2	0.175	Sides	0.15	0.424	0.433	2.06
2	0.175	Sides	0.2	0.401	0.416	3.83
2	0.175	Sides	0.3	0.369	0.394	6.83
2	0.175	Sides	0.4	0.354	0.379	7.06
2	0.175	Sides	0.5	0.347	0.368	5.91
2	0.175	Sides	0.6	0.335	0.359	6.95
2	0.175	Sides	0.7	0.349	0.351	0.78
2	0.175	Sides	0.8	0.342	0.345	0.99

Table_A- 6: 1 Boulder Test 2 d=0.235m experimental and software results

Test	d (m)	Direction	Distance (m)	Experimental v (m/s)	Software v (m/s)	% Error
2	0.235	Down	5	0.290	0.524	80.50
2	0.235	Down	4.5	0.289	0.482	66.99
2	0.235	Down	4	0.281	0.439	56.02
2	0.235	Down	3.5	0.274	0.394	43.95
2	0.235	Down	3	0.257	0.349	35.57
2	0.235	Down	2.5	0.272	0.302	11.08
2	0.235	Down	2	0.246	0.253	2.69

Test	d (m)	Direction	Distance (m)	Experimental v (m/s)	Software v (m/s)	% Error
2	0.235	Down	1.8	0.247	0.232	5.91
2	0.235	Down	1.6	0.244	0.212	13.29
2	0.235	Down	1.4	0.230	0.190	17.34
2	0.235	Down	1.2	0.215	0.168	21.80
2	0.235	Down	1	0.216	0.146	32.55
2	0.235	Down	0.9	0.217	0.134	38.24
2	0.235	Down	0.8	0.165	0.122	26.23
2	0.235	Down	0.7	0.148	0.110	25.83
2	0.235	Down	0.6	0.053	0.097	84.54
2	0.235	Down	0.5	-0.066	0.084	227.98
2	0.235	Down	0.4	-0.140	0.070	150.24
2	0.235	Down	0.3	-0.162	0.056	134.46
2	0.235	Down	0.25	-0.013	0.048	484.96
2	0.235	Up	0.25	0.239	0.234	2.25
2	0.235	Up	0.3	0.245	0.239	2.31
2	0.235	Up	0.4	0.278	0.248	10.67
2	0.235	Up	0.5	0.281	0.255	8.98
2	0.235	Up	0.6	0.289	0.261	9.41
2	0.235	Up	0.7	0.309	0.267	13.62
2	0.235	Up	0.8	0.301	0.271	9.93
2	0.235	Up	0.9	0.307	0.276	10.37
2	0.235	Up	1	0.314	0.279	11.13
2	0.235	Up	1.5	0.322	0.294	8.53
2	0.235	Up	2	0.319	0.305	4.30
2	0.235	Up	2.5	0.318	0.314	1.29
2	0.235	Up	3	0.330	0.322	2.54
2	0.235	Sides	0.2	0.415	0.446	7.29
2	0.235	Sides	0.3	0.402	0.426	6.01
2	0.235	Sides	0.4	0.368	0.413	12.21
2	0.235	Sides	0.5	0.344	0.403	17.04
2	0.235	Sides	0.6	0.334	0.395	18.19
2	0.235	Sides	0.7	0.338	0.388	14.64
2	0.235	Sides	0.8	0.347	0.382	10.26

Table_A- 7: 1 Boulder Test 3 d=0.11m experimental and software results

Test	d (m)	Direction	Distance (m)	Experimental v (m/s)	Software v (m/s)	% Error
3	0.11	Down	5	0.219	0.294	33.80
3	0.11	Down	4.5	0.213	0.286	34.51
3	0.11	Down	4	0.220	0.278	26.72
3	0.11	Down	3.5	0.210	0.270	28.18

Test	d (m)	Direction	Distance (m)	Experimental v (m/s)	Software v (m/s)	% Error
3	0.11	Down	3	0.209	0.260	24.59
3	0.11	Down	2.5	0.208	0.249	19.79
3	0.11	Down	2	0.203	0.236	15.97
3	0.11	Down	1.8	0.196	0.230	17.29
3	0.11	Down	1.6	0.197	0.224	13.44
3	0.11	Down	1.4	0.193	0.217	11.98
3	0.11	Down	1.2	0.202	0.209	3.54
3	0.11	Down	1	0.192	0.200	4.31
3	0.11	Down	0.9	0.194	0.195	0.53
3	0.11	Down	0.8	0.188	0.189	0.67
3	0.11	Down	0.7	0.186	0.183	1.37
3	0.11	Down	0.6	0.184	0.177	3.77
3	0.11	Down	0.5	0.172	0.169	1.40
3	0.11	Down	0.4	0.143	0.160	12.12
3	0.11	Down	0.3	0.075	0.150	100.87
3	0.11	Down	0.2	-0.052	0.136	362.57
3	0.11	Down	0.15	-0.068	0.127	286.66
3	0.11	Up	0.15	0.209	0.188	9.70
3	0.11	Up	0.2	0.217	0.193	10.97
3	0.11	Up	0.3	0.226	0.201	11.20
3	0.11	Up	0.4	0.233	0.206	11.57
3	0.11	Up	0.5	0.231	0.211	8.98
3	0.11	Up	0.6	0.232	0.214	7.62
3	0.11	Up	0.7	0.235	0.217	7.41
3	0.11	Up	0.8	0.257	0.220	14.35
3	0.11	Up	0.9	0.255	0.223	12.84
3	0.11	Up	1	0.251	0.225	10.44
3	0.11	Up	2	0.239	0.240	0.39
3	0.11	Up	3	0.242	0.249	3.07
3	0.11	Sides	0.1	0.328	0.305	6.90
3	0.11	Sides	0.2	0.284	0.288	1.16
3	0.11	Sides	0.3	0.255	0.278	8.81
3	0.11	Sides	0.4	0.252	0.271	7.67
3	0.11	Sides	0.5	0.252	0.266	5.67
3	0.11	Sides	0.6	0.247	0.262	6.23
3	0.11	Sides	0.7	0.250	0.259	3.50
3	0.11	Sides	0.8	0.262	0.256	2.59

Table_A- 8: 1 Boulder Test 3 d=0.175m experimental and software results

Test	d (m)	Direction	Distance (m)	Experimental v (m/s)	Software v (m/s)	% Error
3	0.175	Down	5	0.208	0.287	38.27
3	0.175	Down	4.5	0.192	0.280	46.11
3	0.175	Down	4	0.202	0.273	34.62
3	0.175	Down	3.5	0.197	0.264	33.86
3	0.175	Down	3	0.195	0.255	30.36
3	0.175	Down	2.5	0.189	0.244	29.01
3	0.175	Down	2	0.175	0.231	32.04
3	0.175	Down	1.8	0.189	0.226	19.58
3	0.175	Down	1.6	0.168	0.219	30.53
3	0.175	Down	1.4	0.173	0.213	22.85
3	0.175	Down	1.2	0.174	0.205	17.95
3	0.175	Down	1	0.172	0.196	14.19
3	0.175	Down	0.9	0.162	0.191	17.84
3	0.175	Down	0.8	0.163	0.186	14.49
3	0.175	Down	0.7	0.165	0.180	9.55
3	0.175	Down	0.6	0.159	0.174	9.48
3	0.175	Down	0.5	0.127	0.167	31.22
3	0.175	Down	0.4	0.095	0.158	66.93
3	0.175	Down	0.3	-0.044	0.148	437.41
3	0.175	Down	0.2	-0.048	0.134	382.23
3	0.175	Up	0.2	0.198	0.206	3.86
3	0.175	Up	0.3	0.219	0.211	3.58
3	0.175	Up	0.4	0.245	0.215	12.40
3	0.175	Up	0.5	0.256	0.218	14.73
3	0.175	Up	0.6	0.241	0.221	8.44
3	0.175	Up	0.7	0.249	0.223	10.34
3	0.175	Up	0.8	0.249	0.225	9.78
3	0.175	Up	0.9	0.245	0.227	7.36
3	0.175	Up	1	0.245	0.228	6.86
3	0.175	Sides	0.15	0.317	0.320	0.73
3	0.175	Sides	0.2	0.279	0.308	10.52
3	0.175	Sides	0.3	0.269	0.293	9.11
3	0.175	Sides	0.4	0.272	0.283	3.93
3	0.175	Sides	0.5	0.260	0.275	5.74
3	0.175	Sides	0.6	0.271	0.269	0.80
3	0.175	Sides	0.7	0.269	0.264	2.20
3	0.175	Sides	0.8	0.252	0.259	2.73

Table_A- 9: 2 Boulders Test 1 d=0.076m experimental and software results

Test	d (m)	Direction	Distance (m)	Experimental v (m/s)	Software v (m/s)	% Error
1	0.076	Down	6.5	0.337	0.338	0.26
1	0.076	Down	6	0.330	0.336	2.01
1	0.076	Down	5.5	0.319	0.335	4.78
1	0.076	Down	5	0.319	0.333	4.28
1	0.076	Down	4.5	0.315	0.330	5.00
1	0.076	Down	4	0.328	0.328	0.16
1	0.076	Down	3.5	0.316	0.325	2.87
1	0.076	Down	3	0.309	0.322	4.33
1	0.076	Down	2.5	0.300	0.319	6.23
1	0.076	Down	2	0.304	0.314	3.33
1	0.076	Down	1.5	0.314	0.309	1.82
1	0.076	Down	1.3	0.306	0.306	0.03
1	0.076	Down	1.1	0.305	0.303	0.61
1	0.076	Down	1	0.307	0.301	2.03
1	0.076	Down	0.9	0.329	0.299	9.10
1	0.076	Down	0.8	0.319	0.296	7.28
1	0.076	Down	0.7	0.331	0.305	7.88
1	0.076	Down	0.6	0.345	0.316	8.39
1	0.076	Down	0.5	0.355	0.330	7.04
1	0.076	Down	0.4	0.380	0.347	8.68
1	0.076	Down	0.3	0.401	0.371	7.59
1	0.076	Down	0.2	0.430	0.407	5.46
1	0.076	Down	0.15	0.464	0.435	6.20
1	0.076	Up	0.15	0.312	0.338	8.16
1	0.076	Up	0.2	0.322	0.341	5.88
1	0.076	Up	0.3	0.330	0.346	4.77
1	0.076	Up	0.4	0.331	0.349	5.57
1	0.076	Up	0.5	0.349	0.352	0.70
1	0.076	Up	0.6	0.337	0.354	5.17
1	0.076	Up	0.7	0.364	0.356	2.06
1	0.076	Up	0.8	0.369	0.358	3.07
1	0.076	Up	0.9	0.368	0.359	2.41
1	0.076	Up	1	0.372	0.360	3.00
1	0.076	Up	1.1	0.362	0.362	0.05
1	0.076	Up	1.3	0.367	0.364	0.93
1	0.076	Up	1.5	0.375	0.366	2.59
1	0.076	Up	1.7	0.357	0.367	2.97
1	0.076	Up	1.9	0.380	0.369	2.88
1	0.076	Side	0.2	0.295	0.444	50.52
1	0.076	Side	0.3	0.370	0.425	14.75
1	0.076	Side	0.4	0.378	0.412	9.17
1	0.076	Side	0.5	0.367	0.403	9.83
1	0.076	Side	0.6	0.381	0.395	3.85

Test	d (m)	Direction	Distance (m)	Experimental v (m/s)	Software v (m/s)	% Error
1	0.076	Side	0.7	0.380	0.389	2.42
1	0.076	Side	0.8	0.365	0.384	4.95

Table_A- 10: 2 Boulders Test 1 d=0.11m experimental and software results

Test	d (m)	Direction	Distance (m)	Experimental v (m/s)	Software v (m/s)	% Error
1	0.11	Down	6.5	0.336	0.334	0.47
1	0.11	Down	6	0.328	0.333	1.59
1	0.11	Down	5.5	0.317	0.332	4.53
1	0.11	Down	5	0.321	0.331	3.11
1	0.11	Down	4.5	0.312	0.329	5.66
1	0.11	Down	4	0.326	0.328	0.42
1	0.11	Down	3.5	0.314	0.326	3.96
1	0.11	Down	3	0.314	0.324	3.37
1	0.11	Down	2.5	0.325	0.322	0.93
1	0.11	Down	2	0.299	0.319	6.87
1	0.11	Down	1.5	0.312	0.316	1.13
1	0.11	Down	1.3	0.318	0.314	1.35
1	0.11	Down	1.1	0.339	0.312	7.94
1	0.11	Down	1	0.329	0.311	5.52
1	0.11	Down	0.9	0.331	0.316	4.39
1	0.11	Down	0.8	0.329	0.329	0.07
1	0.11	Down	0.7	0.338	0.345	2.10
1	0.11	Down	0.6	0.344	0.364	5.68
1	0.11	Down	0.5	0.371	0.387	4.44
1	0.11	Down	0.4	0.394	0.418	6.03
1	0.11	Down	0.3	0.431	0.462	7.02
1	0.11	Down	0.2	0.447	0.431	18.78
1	0.11	Down	0.1	0.534	0.554	26.34
1	0.11	Up	0.1	0.323	0.366	13.28
1	0.11	Up	0.2	0.311	0.365	17.48
1	0.11	Up	0.3	0.316	0.365	15.35
1	0.11	Up	0.4	0.321	0.364	13.27
1	0.11	Up	0.5	0.341	0.364	6.58
1	0.11	Up	0.6	0.343	0.364	5.83
1	0.11	Up	0.7	0.352	0.363	3.22
1	0.11	Up	0.8	0.361	0.363	0.50
1	0.11	Up	0.9	0.364	0.363	0.26
1	0.11	Up	1	0.352	0.363	2.99
1	0.11	Up	1.1	0.356	0.363	1.92
1	0.11	Up	1.3	0.358	0.362	1.09

Test	d (m)	Direction	Distance (m)	Experimental v (m/s)	Software v (m/s)	% Error
1	0.11	Up	1.5	0.365	0.362	0.66
1	0.11	Up	1.7	0.370	0.362	2.14
1	0.11	Up	1.9	0.368	0.362	1.61
1	0.11	Side	0.3	0.279	0.425	52.64
1	0.11	Side	0.4	0.385	0.412	6.84
1	0.11	Side	0.5	0.386	0.402	4.17
1	0.11	Side	0.6	0.389	0.393	1.06
1	0.11	Side	0.7	0.388	0.387	0.25
1	0.11	Side	0.8	0.378	0.381	0.84

Table_A- 11: 2 Boulders Test 2 d=0.076m experimental and software results

Test	d (m)	Direction	Distance (m)	Experimental v (m/s)	Software v (m/s)	% Error
2	0.076	Down	6.5	0.272	0.257	5.30
2	0.076	Down	6	0.264	0.256	3.08
2	0.076	Down	5.5	0.256	0.255	0.44
2	0.076	Down	5	0.255	0.254	0.51
2	0.076	Down	4.5	0.260	0.253	2.66
2	0.076	Down	4	0.262	0.251	4.07
2	0.076	Down	3.5	0.251	0.250	0.62
2	0.076	Down	3	0.253	0.248	2.25
2	0.076	Down	2.5	0.247	0.245	0.49
2	0.076	Down	2	0.246	0.243	1.29
2	0.076	Down	1.5	0.253	0.239	5.47
2	0.076	Down	1.3	0.252	0.238	5.85
2	0.076	Down	1.1	0.255	0.236	7.46
2	0.076	Down	1	0.247	0.235	5.03
2	0.076	Down	0.9	0.262	0.231	11.65
2	0.076	Down	0.8	0.252	0.235	6.77
2	0.076	Down	0.7	0.266	0.239	10.13
2	0.076	Down	0.6	0.263	0.244	7.23
2	0.076	Down	0.5	0.277	0.249	10.04
2	0.076	Down	0.4	0.294	0.256	12.74
2	0.076	Down	0.3	0.304	0.266	12.57
2	0.076	Down	0.2	0.347	0.280	19.38
2	0.076	Up	0.15	0.257	0.256	0.52
2	0.076	Up	0.2	0.264	0.259	1.87
2	0.076	Up	0.3	0.273	0.263	3.64
2	0.076	Up	0.4	0.282	0.266	5.80
2	0.076	Up	0.5	0.290	0.268	7.40

Test	d (m)	Direction	Distance (m)	Experimental v (m/s)	Software v (m/s)	% Error
2	0.076	Up	0.6	0.261	0.270	3.56
2	0.076	Up	0.7	0.295	0.272	7.91
2	0.076	Up	0.8	0.281	0.273	2.67
2	0.076	Up	0.9	0.293	0.275	6.28
2	0.076	Up	1	0.297	0.276	7.06
2	0.076	Up	1.1	0.300	0.277	7.90
2	0.076	Up	1.3	0.301	0.278	7.61
2	0.076	Up	1.5	0.303	0.280	7.60
2	0.076	Up	1.7	0.297	0.281	5.35
2	0.076	Up	1.9	0.296	0.283	4.56
2	0.076	Side	0.2	0.318	0.336	5.68
2	0.076	Side	0.3	0.300	0.322	7.44
2	0.076	Side	0.4	0.289	0.312	7.99
2	0.076	Side	0.5	0.283	0.305	7.67
2	0.076	Side	0.6	0.293	0.299	2.04
2	0.076	Side	0.7	0.299	0.294	1.76
2	0.076	Side	0.8	0.299	0.290	2.89

Table_A- 12: 2 Boulders Test 2 d=0.11m experimental and software results

Test	d (m)	Direction	Distance (m)	Experimental v (m/s)	Software v (m/s)	% Error
2	0.11	Down	6.5	0.267	0.254	5.13
2	0.11	Down	6	0.264	0.253	4.09
2	0.11	Down	5.5	0.260	0.253	2.72
2	0.11	Down	5	0.262	0.252	3.93
2	0.11	Down	4.5	0.256	0.251	1.77
2	0.11	Down	4	0.256	0.251	2.20
2	0.11	Down	3.5	0.241	0.250	3.51
2	0.11	Down	3	0.258	0.249	3.60
2	0.11	Down	2.5	0.247	0.248	0.34
2	0.11	Down	2	0.255	0.247	3.51
2	0.11	Down	1.5	0.260	0.245	5.81
2	0.11	Down	1.3	0.265	0.244	7.81
2	0.11	Down	1.1	0.274	0.244	11.00
2	0.11	Down	1	0.271	0.243	10.35
2	0.11	Down	0.9	0.263	0.249	5.37
2	0.11	Down	0.8	0.277	0.256	7.68
2	0.11	Down	0.7	0.293	0.263	10.17
2	0.11	Down	0.6	0.284	0.272	4.02
2	0.11	Down	0.5	0.298	0.284	4.65
2	0.11	Down	0.4	0.306	0.298	2.58
2	0.11	Down	0.3	0.319	0.318	0.24

Test	d (m)	Direction	Distance (m)	Experimental v (m/s)	Software v (m/s)	% Error
2	0.11	Down	0.2	0.349	0.348	0.23
2	0.11	Down	0.1	0.379	0.406	7.14
2	0.11	Up	0.1	0.281	0.280	0.37
2	0.11	Up	0.2	0.253	0.280	10.53
2	0.11	Up	0.3	0.267	0.280	4.63
2	0.11	Up	0.4	0.273	0.280	2.62
2	0.11	Up	0.5	0.282	0.280	0.78
2	0.11	Up	0.6	0.284	0.280	1.43
2	0.11	Up	0.7	0.294	0.280	4.95
2	0.11	Up	0.8	0.291	0.280	3.81
2	0.11	Up	0.9	0.297	0.280	5.76
2	0.11	Up	1	0.297	0.280	5.88
2	0.11	Up	1.1	0.289	0.280	3.15
2	0.11	Up	1.3	0.283	0.280	1.17
2	0.11	Up	1.5	0.289	0.280	2.95
2	0.11	Up	1.7	0.286	0.280	2.17
2	0.11	Up	1.9	0.281	0.280	0.17
2	0.11	Side	0.3	0.328	0.313	4.45
2	0.11	Side	0.4	0.294	0.306	4.35
2	0.11	Side	0.5	0.294	0.301	2.45
2	0.11	Side	0.6	0.301	0.297	1.50
2	0.11	Side	0.7	0.301	0.293	2.67
2	0.11	Side	0.8	0.307	0.290	5.32

Table_A- 13: 2 Boulders Test 2 d=0.275m experimental and software results

Test	d (m)	Direction	Distance (m)	Experimental v (m/s)	Software v (m/s)	% Error
2	0.275	Down	6.5	0.319	0.252	21.07
2	0.275	Down	6	0.313	0.252	19.47
2	0.275	Down	5.5	0.315	0.252	20.13
2	0.275	Down	5	0.305	0.252	17.27
2	0.275	Down	4.5	0.313	0.252	19.34
2	0.275	Down	4	0.321	0.253	21.32
2	0.275	Down	3.5	0.309	0.253	18.20
2	0.275	Down	3	0.308	0.253	17.70
2	0.275	Down	2.5	0.325	0.254	22.01
2	0.275	Down	2	0.319	0.254	20.32
2	0.275	Down	1.5	0.305	0.269	11.89
2	0.275	Down	1.3	0.324	0.274	15.64
2	0.275	Down	1.1	0.325	0.280	13.95
2	0.275	Down	1	0.327	0.283	13.28

Test	d (m)	Direction	Distance (m)	Experimental v (m/s)	Software v (m/s)	% Error
2	0.275	Down	0.9	0.335	0.287	14.21
2	0.275	Down	0.8	0.337	0.292	13.39
2	0.275	Down	0.7	0.345	0.297	13.90
2	0.275	Down	0.6	0.365	0.303	17.09
2	0.275	Down	0.5	0.364	0.310	14.85
2	0.275	Down	0.4	0.384	0.319	16.80
2	0.275	Down	0.3	0.391	0.331	15.36
2	0.275	Down	0.2	0.397	0.349	11.97
2	0.275	Up	0.1	0.360	0.316	12.21
2	0.275	Up	0.2	0.321	0.305	5.15
2	0.275	Up	0.3	0.299	0.298	0.28
2	0.275	Up	0.4	0.276	0.294	6.46
2	0.275	Up	0.5	0.268	0.290	8.04
2	0.275	Up	0.6	0.275	0.287	4.53
2	0.275	Up	0.7	0.283	0.285	0.69
2	0.275	Up	0.8	0.282	0.283	0.33
2	0.275	Up	0.9	0.284	0.281	1.14
2	0.275	Up	1	0.288	0.279	3.11
2	0.275	Up	1.1	0.278	0.278	0.06
2	0.275	Up	1.3	0.269	0.275	2.29
2	0.275	Up	1.5	0.288	0.273	4.99
2	0.275	Up	1.7	0.290	0.271	6.41
2	0.275	Up	1.9	0.290	0.270	7.05
2	0.275	Side	0.6	0.427	0.469	9.88
2	0.275	Side	0.65	0.395	0.444	12.56
2	0.275	Side	0.7	0.382	0.423	10.72
2	0.275	Side	0.75	0.375	0.404	7.65
2	0.275	Side	0.8	0.369	0.387	4.65

Table_A- 14: 2 Boulders Test 2 d=0.076m experimental and software results

Test	d (m)	Direction	Distance (m)	Experimental v (m/s)	Software v (m/s)	% Error
3	0.076	Down	6.5	0.192	0.196	1.82
3	0.076	Down	5.5	0.188	0.194	3.12
3	0.076	Down	5	0.188	0.193	2.64
3	0.076	Down	4.5	0.187	0.192	2.99
3	0.076	Down	4	0.191	0.191	0.04
3	0.076	Down	3.5	0.191	0.190	0.69
3	0.076	Down	3	0.185	0.188	1.63
3	0.076	Down	2.5	0.188	0.186	0.85
3	0.076	Down	2	0.180	0.184	2.48

Test	d (m)	Direction	Distance (m)	Experimental v (m/s)	Software v (m/s)	% Error
3	0.076	Down	1.5	0.185	0.181	1.88
3	0.076	Down	1.3	0.187	0.180	3.55
3	0.076	Down	1.1	0.190	0.178	6.25
3	0.076	Down	1	0.187	0.177	5.20
3	0.076	Down	0.9	0.188	0.176	6.21
3	0.076	Down	0.8	0.193	0.175	9.08
3	0.076	Down	0.7	0.196	0.174	11.16
3	0.076	Down	0.6	0.193	0.173	10.65
3	0.076	Down	0.5	0.195	0.178	8.80
3	0.076	Down	0.4	0.211	0.188	10.99
3	0.076	Down	0.3	0.214	0.201	5.97
3	0.076	Down	0.2	0.230	0.221	3.55
3	0.076	Down	0.15	0.241	0.237	1.65
3	0.076	Up	0.15	0.185	0.195	5.62
3	0.076	Up	0.2	0.190	0.197	3.76
3	0.076	Up	0.3	0.196	0.201	2.29
3	0.076	Up	0.4	0.204	0.203	0.41
3	0.076	Up	0.5	0.196	0.205	4.75
3	0.076	Up	0.6	0.208	0.206	0.78
3	0.076	Up	0.7	0.208	0.208	0.05
3	0.076	Up	0.8	0.216	0.209	3.56
3	0.076	Up	0.9	0.220	0.210	4.66
3	0.076	Up	1	0.217	0.211	2.96
3	0.076	Up	1.1	0.211	0.211	0.10
3	0.076	Up	1.3	0.211	0.213	0.78
3	0.076	Up	1.5	0.206	0.214	3.99
3	0.076	Up	1.7	0.214	0.215	0.60
3	0.076	Up	1.9	0.219	0.216	1.44
3	0.076	Side	0.2	0.237	0.253	6.77
3	0.076	Side	0.3	0.208	0.243	16.87
3	0.076	Side	0.4	0.201	0.236	17.52
3	0.076	Side	0.5	0.206	0.230	11.82
3	0.076	Side	0.6	0.207	0.226	9.38
3	0.076	Side	0.7	0.213	0.223	4.49
3	0.076	Side	0.8	0.214	0.220	2.48

Table_A- 15: 2 Boulders Test 3 d=0.11m experimental and software results

Test	d (m)	Direction	Distance (m)	Experimental v (m/s)	Software v (m/s)	% Error
3	0.11	Down	6.5	0.195	0.195	0.15
3	0.11	Down	6	0.193	0.194	0.58

Test	d (m)	Direction	Distance (m)	Experimental v (m/s)	Software v (m/s)	% Error
3	0.11	Down	5.5	0.189	0.193	2.17
3	0.11	Down	5	0.189	0.192	1.73
3	0.11	Down	4.5	0.185	0.192	3.40
3	0.11	Down	4	0.189	0.191	0.70
3	0.11	Down	3.5	0.186	0.189	2.10
3	0.11	Down	3	0.184	0.188	2.30
3	0.11	Down	2.5	0.186	0.187	0.29
3	0.11	Down	2	0.192	0.185	3.75
3	0.11	Down	1.5	0.189	0.182	3.59
3	0.11	Down	1.3	0.197	0.181	7.89
3	0.11	Down	1.1	0.184	0.180	2.35
3	0.11	Down	1	0.202	0.182	10.00
3	0.11	Down	0.9	0.209	0.186	11.12
3	0.11	Down	0.8	0.199	0.191	4.24
3	0.11	Down	0.7	0.211	0.197	6.67
3	0.11	Down	0.6	0.212	0.203	4.15
3	0.11	Down	0.5	0.212	0.212	0.05
3	0.11	Down	0.4	0.217	0.222	2.60
3	0.11	Down	0.3	0.226	0.237	4.90
3	0.11	Down	0.2	0.236	0.259	9.68
3	0.11	Down	0.1	0.265	0.301	13.53
3	0.11	Up	0.1	0.204	0.212	4.13
3	0.11	Up	0.2	0.194	0.213	9.58
3	0.11	Up	0.3	0.201	0.213	6.07
3	0.11	Up	0.4	0.190	0.213	12.07
3	0.11	Up	0.5	0.208	0.214	2.66
3	0.11	Up	0.6	0.208	0.214	2.66
3	0.11	Up	0.7	0.211	0.214	1.38
3	0.11	Up	0.8	0.212	0.214	0.88
3	0.11	Up	0.9	0.215	0.214	0.45
3	0.11	Up	1	0.216	0.214	0.81
3	0.11	Up	1.1	0.217	0.214	1.15
3	0.11	Up	1.3	0.213	0.214	0.51
3	0.11	Up	1.5	0.215	0.214	0.30
3	0.11	Up	1.7	0.214	0.214	0.06
3	0.11	Up	1.9	0.224	0.214	4.39
3	0.11	Side	0.3	0.237	0.237	0.01
3	0.11	Side	0.4	0.217	0.232	6.76
3	0.11	Side	0.5	0.212	0.228	7.43
3	0.11	Side	0.6	0.210	0.225	7.29
3	0.11	Side	0.7	0.220	0.223	1.26
3	0.11	Side	0.8	0.216	0.220	1.97

Table_A- 16: 2 Boulders Test 3 d=0.275m experimental and software results

Test	d (m)	Direction	Distance (m)	Experimental v (m/s)	Software v (m/s)	% Error
3	0.275	Down	6.5	0.207	0.192	7.43
3	0.275	Down	6	0.209	0.192	8.08
3	0.275	Down	5.5	0.198	0.192	2.85
3	0.275	Down	5	0.220	0.192	12.71
3	0.275	Down	4.5	0.217	0.192	11.48
3	0.275	Down	4	0.219	0.192	12.59
3	0.275	Down	3.5	0.217	0.192	11.65
3	0.275	Down	3	0.213	0.192	9.94
3	0.275	Down	2.5	0.209	0.192	8.19
3	0.275	Down	2	0.223	0.201	10.07
3	0.275	Down	1.5	0.229	0.207	9.59
3	0.275	Down	1.3	0.231	0.210	9.39
3	0.275	Down	1.1	0.229	0.213	6.68
3	0.275	Down	1	0.222	0.216	2.92
3	0.275	Down	0.9	0.239	0.218	9.00
3	0.275	Down	0.8	0.229	0.221	3.54
3	0.275	Down	0.7	0.239	0.224	6.23
3	0.275	Down	0.6	0.247	0.227	7.79
3	0.275	Down	0.5	0.246	0.232	5.73
3	0.275	Down	0.4	0.253	0.237	6.43
3	0.275	Down	0.3	0.262	0.244	6.67
3	0.275	Down	0.2	0.276	0.255	7.81
3	0.275	Down	0.1	0.284	0.274	3.38
3	0.275	Up	0.1	0.260	0.241	7.27
3	0.275	Up	0.2	0.231	0.233	0.92
3	0.275	Up	0.3	0.216	0.228	5.50
3	0.275	Up	0.4	0.212	0.225	6.22
3	0.275	Up	0.5	0.205	0.222	8.56
3	0.275	Up	0.6	0.198	0.220	11.35
3	0.275	Up	0.7	0.202	0.219	8.19
3	0.275	Up	0.8	0.212	0.217	2.66
3	0.275	Up	0.9	0.211	0.216	2.24
3	0.275	Up	1	0.204	0.215	5.24
3	0.275	Up	1.1	0.205	0.214	4.59
3	0.275	Up	1.3	0.212	0.212	0.33
3	0.275	Up	1.5	0.202	0.211	4.29
3	0.275	Up	1.7	0.209	0.209	0.22
3	0.275	Up	1.9	0.222	0.208	5.98
3	0.275	Side	0.6	0.304	0.338	11.21

Test	d (m)	Direction	Distance (m)	Experimental v (m/s)	Software v (m/s)	% Error
3	0.275	Side	0.65	0.276	0.322	16.77
3	0.275	Side	0.7	0.270	0.308	14.34
3	0.275	Side	0.75	0.263	0.296	12.68
3	0.275	Side	0.8	0.258	0.285	10.29
3	0.275	Down	6.5	0.207	0.192	7.43

Table_A- 17: 2 Boulders Test 2 d=0.11m experimental and software results

Test	d (m)	Direction	Distance (m)	Experimental v (m/s)	Software v (m/s)	% Error
2	0.11	Down	6.5	0.267	0.254	5.13
2	0.11	Down	6	0.264	0.253	4.09
2	0.11	Down	5.5	0.260	0.253	2.72
2	0.11	Down	5	0.262	0.252	3.93
2	0.11	Down	4.5	0.256	0.251	1.77
2	0.11	Down	4	0.256	0.251	2.20
2	0.11	Down	3.5	0.241	0.250	3.51
2	0.11	Down	3	0.258	0.249	3.60
2	0.11	Down	2.5	0.247	0.248	0.34
2	0.11	Down	2	0.255	0.247	3.51
2	0.11	Down	1.5	0.260	0.245	5.81
2	0.11	Down	1.3	0.265	0.244	7.81
2	0.11	Down	1.1	0.274	0.244	11.00
2	0.11	Down	1	0.271	0.243	10.35
2	0.11	Down	0.9	0.263	0.249	5.37
2	0.11	Down	0.8	0.277	0.256	7.68
2	0.11	Down	0.7	0.293	0.263	10.17
2	0.11	Down	0.6	0.284	0.272	4.02
2	0.11	Down	0.5	0.298	0.284	4.65
2	0.11	Down	0.4	0.306	0.298	2.58
2	0.11	Down	0.3	0.319	0.318	0.24
2	0.11	Down	0.2	0.349	0.348	0.23
2	0.11	Down	0.1	0.379	0.406	7.14
2	0.11	Up	0.1	0.281	0.280	0.37
2	0.11	Up	0.2	0.253	0.280	10.53
2	0.11	Up	0.3	0.267	0.280	4.63
2	0.11	Up	0.4	0.273	0.280	2.62
2	0.11	Up	0.5	0.282	0.280	0.78
2	0.11	Up	0.6	0.284	0.280	1.43
2	0.11	Up	0.7	0.294	0.280	4.95
2	0.11	Up	0.8	0.291	0.280	3.81
2	0.11	Up	0.9	0.297	0.280	5.76

Test	d (m)	Direction	Distance (m)	Experimental v (m/s)	Software v (m/s)	% Error
2	0.11	Up	1	0.297	0.280	5.88
2	0.11	Up	1.1	0.289	0.280	3.15
2	0.11	Up	1.3	0.283	0.280	1.17
2	0.11	Up	1.5	0.289	0.280	2.95
2	0.11	Up	1.7	0.286	0.280	2.17
2	0.11	Up	1.9	0.281	0.280	0.17
2	0.11	Side	0.3	0.328	0.313	4.45
2	0.11	Side	0.4	0.294	0.306	4.35
2	0.11	Side	0.5	0.294	0.301	2.45
2	0.11	Side	0.6	0.301	0.297	1.50
2	0.11	Side	0.7	0.301	0.293	2.67
2	0.11	Side	0.8	0.307	0.290	5.32

APPENDIX B: 1 BOULDER BELOW THE BLOCKAGE LIMIT MODEL CONDITIONS

Shown below are the model conditions used for the analysis of 1 boulder below the blockage ratio limit used in Section 5.

Table_B- 1: 1 Boulder below blockage limit model conditions

Model	**b (m)**	**d (m)**	**Q (m^3/s)**	**S**	**Fr**	**d/b**
1	5.00	0.20	1.25	0.000800	0.670	0.040
2	5.00	0.20	0.80	0.000800	0.649	0.040
3	5.00	0.20	2.00	0.000300	0.433	0.040
4	5.00	0.20	0.20	0.000010	0.077	0.040
5	5.00	0.20	0.60	0.000005	0.057	0.040
6	5.00	0.20	0.10	0.001000	0.602	0.040
7	5.00	0.20	0.08	0.000150	0.249	0.040
8	7.00	0.20	1.25	0.000800	0.663	0.029
9	8.00	0.20	1.25	0.000800	0.658	0.025
10	7.00	0.16	1.25	0.000800	0.663	0.023
11	5.00	0.20	0.20	0.000050	0.162	0.040
12	5.00	0.20	1.00	0.000200	0.345	0.040
13	5.00	0.20	2.50	0.000400	0.502	0.040
14	5.00	0.20	0.13	0.000800	0.555	0.040
15	5.00	0.20	12.50	0.000800	0.720	0.040
16	5.00	0.10	1.25	0.000800	0.670	0.020
17	4.00	0.24	1.25	0.000800	0.670	0.060
18	4.00	0.20	1.00	0.000800	0.661	0.050
19	6.00	0.20	1.50	0.000800	0.676	0.033
20	6.00	0.10	1.50	0.000800	0.676	0.017
21	7.00	0.10	1.50	0.000800	0.673	0.014
22	8.00	0.10	1.50	0.000800	0.669	0.013
23	8.00	0.16	1.50	0.000800	0.669	0.020
24	4.00	0.10	1.50	0.000800	0.676	0.025
26	5.00	0.40	1.25	0.000800	0.670	0.080
28	6.00	0.40	1.50	0.000800	0.676	0.067
29	6.00	0.50	1.50	0.000800	0.676	0.083
30	5.00	0.20	1.25	0.000300	0.423	0.040
31	5.00	0.20	1.25	0.001000	0.744	0.040
32	5.00	0.10	0.30	0.000800	0.600	0.020
33	5.00	0.10	0.13	0.000800	0.555	0.020
34	5.00	0.10	1.25	0.000005	0.057	0.020
35	5.00	0.10	1.25	0.000300	0.423	0.020

Model	b (m)	d (m)	Q (m^3/s)	S	Fr	d/b
36	5.00	0.10	1.25	0.001000	0.744	0.020
37	5.00	0.10	1.25	0.000150	0.305	0.020
38	5.00	0.10	1.25	0.000050	0.179	0.020
39	8.00	0.16	1.25	0.000300	0.420	0.020
40	8.00	0.16	1.25	0.000800	0.658	0.020
41	5.00	0.24	1.25	0.000800	0.670	0.048
42	5.00	0.16	1.25	0.000800	0.670	0.032
43	5.00	0.08	1.25	0.000800	0.670	0.016
44	8.00	0.32	1.25	0.000800	0.658	0.040
45	8.00	0.26	1.25	0.000800	0.658	0.033
46	8.00	0.14	1.25	0.000800	0.658	0.018
47	8.00	0.16	1.25	0.000050	0.183	0.020
48	8.00	0.16	1.25	0.000005	0.061	0.020
51	6.00	0.60	1.50	0.000050	0.183	0.100
52	6.00	0.60	1.50	0.000005	0.059	0.100
53	6.00	0.60	1.50	0.000300	0.428	0.100
56	4.00	0.40	1.25	0.000150	0.300	0.100
57	4.00	0.40	1.25	0.000600	0.584	0.100

APPENDIX C: 1 BOULDER BELOW THE BLOCKAGE LIMIT ZOI SOFTWARE AND RELATIONSHIP CORRELATION

The tables below compare the ZOI lengths as determined by the software and the relationships for 1 boulder below the blockage limit.

Table_C- 1: Software and relationship ZOI lengths for 1 boulder upstream (10%-30% from uniform velocity)

Model	Upstream								
	i = 10%			*i = 20%*			*i = 30%*		
	yu (m)	yu eqn 5-18 (m)	% Error	yu (m)	yu eqn 5-18 (m)	% Error	yu (m)	yu eqn 5-18 (m)	% Error
1	0.65	0.61	5.98	0.39	0.37	4.08	0.28	0.28	0.00
2	0.58	0.61	5.14	0.39	0.37	4.22	0.28	0.28	0.09
3	0.50	0.59	18.67	0.32	0.37	14.54	0.27	0.28	2.39
4	0.56	0.53	5.75	0.32	0.34	5.63	0.27	0.26	2.65
5	0.57	0.52	9.23	0.37	0.33	9.89	0.27	0.26	3.48
6	0.57	0.61	6.44	0.37	0.37	0.60	0.27	0.28	3.38
7	0.50	0.57	14.31	0.32	0.36	11.61	0.23	0.27	18.28
8	0.59	0.64	9.30	0.39	0.40	1.36	0.29	0.29	0.88
9	0.58	0.66	13.56	0.39	0.40	3.58	0.29	0.30	2.64
10	0.53	0.53	0.92	0.30	0.33	9.37	0.25	0.24	3.60
11	0.50	0.56	11.05	0.32	0.35	9.40	0.27	0.27	0.50
12	0.50	0.58	16.86	0.32	0.36	13.33	0.23	0.27	19.41
13	0.56	0.60	7.01	0.34	0.37	8.55	0.27	0.28	2.83
14	0.57	0.60	5.86	0.37	0.37	0.22	0.27	0.28	3.14
15	0.65	0.61	5.52	0.40	0.38	6.16	0.28	0.28	0.21
16	0.40	0.34	14.54	0.22	0.21	4.66	0.16	0.15	4.17
17	0.73	0.69	5.93	0.47	0.42	10.68	0.33	0.32	3.46
18	0.64	0.59	7.98	0.39	0.36	7.61	0.29	0.27	6.27
19	0.60	0.63	4.97	0.40	0.39	3.57	0.29	0.29	1.08
20	0.40	0.35	11.92	0.23	0.22	5.98	0.17	0.16	7.60
21	0.41	0.36	11.93	0.24	0.22	7.59	0.17	0.16	5.73
22	0.40	0.37	7.80	0.23	0.23	1.45	0.16	0.16	1.92
23	0.52	0.55	5.17	0.33	0.34	1.68	0.23	0.25	6.66
24	0.37	0.33	10.84	0.23	0.20	12.07	0.15	0.15	0.71
26	1.15	1.09	5.00	0.70	0.67	4.68	0.54	0.51	5.31
28	1.16	1.13	2.93	0.72	0.69	4.45	0.56	0.52	6.45
29	1.65	1.36	17.73	0.80	0.83	3.60	0.65	0.64	2.16
30	0.50	0.59	18.48	0.32	0.37	14.42	0.27	0.28	2.32
31	0.65	0.62	5.31	0.41	0.38	8.31	0.32	0.28	12.23

Model	Upstream								
	i = 10%			*i = 20%*			*i = 30%*		
	yu (m)	yu eqn 5-18 (m)	% Error	yu (m)	yu eqn 5-18 (m)	% Error	yu (m)	yu eqn 5-18 (m)	% Error
32	0.35	0.34	3.06	0.22	0.21	5.15	0.15	0.15	1.89
33	0.35	0.34	3.57	0.22	0.21	5.50	0.15	0.15	1.66
34	0.35	0.29	17.37	0.22	0.19	15.08	0.17	0.14	16.08
35	0.33	0.33	0.42	0.18	0.21	14.04	0.15	0.15	0.86
36	0.43	0.34	19.94	0.24	0.21	12.18	0.18	0.15	14.56
37	0.29	0.32	11.76	0.18	0.20	12.30	0.14	0.15	7.03
38	0.33	0.31	5.24	0.19	0.20	3.79	0.14	0.15	5.39
39	0.42	0.53	26.17	0.29	0.33	13.22	0.21	0.24	15.24
40	0.49	0.55	11.49	0.32	0.34	4.79	0.24	0.25	2.17
41	0.72	0.71	1.11	0.44	0.44	1.00	0.33	0.33	0.59
42	0.49	0.51	3.45	0.32	0.31	2.96	0.25	0.23	7.74
43	0.29	0.28	2.23	0.19	0.17	8.37	0.13	0.13	2.84
44	0.92	0.98	6.16	0.57	0.60	4.92	0.43	0.45	4.13
45	0.80	0.82	2.58	0.48	0.50	4.77	0.35	0.37	6.82
46	0.48	0.49	1.76	0.28	0.30	7.12	0.22	0.22	0.75
47	0.42	0.50	19.28	0.29	0.32	8.90	0.21	0.24	12.48
48	0.49	0.47	5.06	0.32	0.30	6.24	0.24	0.23	4.67
51	1.31	1.45	10.52	0.88	0.91	3.16	0.68	0.72	5.47
52	1.47	1.34	8.79	0.96	0.86	10.33	0.73	0.69	4.95
53	1.43	1.53	7.24	0.88	0.94	7.34	0.68	0.74	8.12
56	0.88	1.00	13.40	0.58	0.62	6.78	0.47	0.49	3.21
57	1.40	1.04	25.43	0.71	0.64	10.01	0.54	0.49	8.41
Average	-	-	9.26	-	-	7.08	-	-	5.19

Table_C- 2: Software and relationship ZOI lengths for 1 boulder upstream (40%-60% from uniform velocity)

Model	Upstream								
	i = 40%			*i = 50%*			*i = 60%*		
	yu (m)	yu eqn 5-18 (m)	% Error	yu (m)	yu eqn 5-18 (m)	% Error	yu (m)	yu eqn 5-18 (m)	% Error
1	0.23	0.22	2.92	0.20	0.19	3.82	0.17	0.17	2.01
2	0.23	0.22	3.00	0.20	0.19	3.79	0.17	0.17	1.66
3	0.20	0.22	10.37	0.18	0.19	7.23	0.16	0.18	9.43
4	0.23	0.21	8.27	0.20	0.20	2.21	0.17	0.21	25.46
5	0.23	0.21	8.97	0.20	0.20	1.99	0.17	0.22	29.73
6	0.23	0.22	3.20	0.20	0.19	3.74	0.17	0.17	0.80
7	0.20	0.22	8.79	0.18	0.19	7.68	0.16	0.19	16.55

8	0.22	0.23	3.99	0.19	0.20	4.63	0.16	0.18	13.68
9	0.22	0.23	5.00	0.19	0.20	6.01	0.16	0.19	17.76
10	0.19	0.19	2.08	0.16	0.16	1.58	0.14	0.15	10.10
11	0.20	0.22	7.58	0.18	0.19	8.03	0.16	0.20	22.37
12	0.20	0.22	9.72	0.18	0.19	7.41	0.16	0.18	12.30
13	0.22	0.22	0.72	0.18	0.19	7.11	0.16	0.17	7.61
14	0.23	0.22	3.40	0.20	0.19	3.68	0.16	0.17	6.38
15	0.23	0.22	2.74	0.20	0.19	3.87	0.17	0.17	2.81
16	0.13	0.12	9.65	0.11	0.10	6.45	0.09	0.10	10.65
17	0.28	0.26	7.11	0.23	0.22	3.52	0.19	0.18	5.22
18	0.24	0.22	8.51	0.21	0.19	10.36	0.17	0.16	7.35
19	0.21	0.23	7.78	0.19	0.20	3.05	0.16	0.17	9.01
20	0.08	0.12	48.83	0.12	0.10	12.71	0.09	0.10	15.86
21	0.13	0.12	7.39	0.10	0.11	6.34	-	-	-
22	0.13	0.12	6.49	0.10	0.11	7.73	-	-	-
23	0.19	0.19	1.10	0.17	0.16	3.14	0.15	0.16	6.26
24	0.13	0.12	11.10	0.10	0.10	0.69	0.09	0.09	4.37
26	0.45	0.42	5.68	0.37	0.36	2.81	0.32	0.28	12.93
28	0.45	0.43	4.39	0.37	0.37	1.08	0.33	0.29	11.59
29	0.54	0.53	2.02	0.48	0.45	6.74	0.40	0.34	13.93
30	0.20	0.22	10.30	0.18	0.19	7.25	0.16	0.18	9.72
31	0.23	0.22	2.66	0.20	0.19	3.89	0.17	0.16	3.17
32	0.12	0.12	2.41	0.10	0.10	2.99	0.09	0.10	12.06
33	0.12	0.12	2.60	0.10	0.10	3.06	0.09	0.10	13.06
34	0.15	0.11	26.60	0.12	0.10	12.61	0.08	0.13	65.01
35	0.12	0.12	3.29	0.10	0.10	3.27	0.09	0.10	16.61
36	0.14	0.12	15.88	0.12	0.10	14.31	0.09	0.10	9.35
37	0.08	0.12	43.82	0.11	0.10	5.88	0.09	0.11	21.06
38	0.08	0.11	41.85	0.11	0.10	5.50	-	-	-
39	0.18	0.19	3.13	0.16	0.17	3.28	0.14	0.17	20.05
40	0.19	0.19	1.14	0.16	0.16	2.92	0.14	0.16	14.04
41	0.28	0.26	5.58	0.23	0.23	1.40	0.21	0.19	9.18
42	0.19	0.18	4.44	0.16	0.16	1.70	0.14	0.14	0.82
43	0.11	0.10	13.17	0.08	0.08	5.17	-	-	-
44	0.37	0.36	3.49	0.30	0.31	2.61	0.26	0.27	2.72
45	0.30	0.29	1.81	0.26	0.26	1.84	0.22	0.23	4.06
46	0.17	0.17	2.37	0.13	0.15	12.29	0.11	0.14	31.45
47	0.18	0.18	0.92	0.16	0.17	3.93	0.14	0.18	31.98
48	0.18	0.18	1.92	0.17	0.17	1.36	0.14	0.21	49.51
51	0.56	0.61	8.12	0.50	0.53	6.61	0.45	0.46	1.66
52	0.60	0.59	2.04	0.53	0.54	1.45	0.45	0.52	15.72
53	0.56	0.62	10.55	0.50	0.53	5.92	0.45	0.42	7.72
56	0.39	0.41	4.84	0.34	0.35	4.12	0.30	0.29	3.89
57	0.42	0.42	0.94	0.37	0.35	4.80	0.31	0.27	13.80

Average	-	-	8.13	-	-	5.01	-	-	13.46

Table_C- 3: Software and relationship ZOI lengths for 1 boulder upstream (70% from uniform velocity)

Model	**Upstream**		
	i = 70%		
	yu (m)	**yu eqn 5-18 (m)**	**% Error**
1	0.15	0.15	2.67
2	0.15	0.15	2.61
3	0.15	0.15	1.87
4	0.15	0.15	1.35
5	0.15	0.15	1.91
6	0.15	0.15	2.47
7	0.15	0.15	0.85
8	0.14	0.15	6.67
9	0.14	0.15	7.64
10	0.12	0.12	1.06
11	0.15	0.15	0.06
12	0.15	0.15	1.45
13	0.15	0.15	2.14
14	0.15	0.15	2.32
15	0.15	0.15	2.80
16	0.07	0.08	9.22
17	0.17	0.17	0.31
18	0.15	0.14	4.08
19	0.15	0.15	1.49
20	0.07	0.08	10.54
21	-	-	-
22	0.08	0.08	1.38
23	0.12	0.12	1.95
24	0.08	0.08	5.86
26	0.28	0.28	0.43
28	0.28	0.28	0.77
29	0.34	0.35	2.20
30	0.15	0.15	1.83
31	0.15	0.15	2.86
32	0.08	0.08	4.23
33	0.08	0.08	4.09
34	0.09	0.08	11.04
35	0.08	0.08	3.61
36	0.08	0.08	4.62

Model	Upstream		
	i = 70%		
	yu (m)	**yu eqn 5-18 (m)**	**% Error**
37	0.07	0.08	10.84
38	0.09	0.08	12.93
39	0.12	0.12	2.84
40	0.12	0.12	1.97
41	0.17	0.17	1.81
42	0.12	0.12	1.21
43	0.06	0.06	3.47
44	0.23	0.23	1.60
45	0.19	0.19	1.32
46	0.11	0.11	1.79
47	0.12	0.13	4.44
48	0.12	0.13	6.60
51	0.41	0.42	2.95
52	0.41	0.43	5.16
53	0.41	0.42	1.33
56	0.28	0.28	0.42
57	0.28	0.28	1.65
Average	-	-	3.41

Table_C- 4: Software and relationship ZOI lengths for 1 boulder downstream (20%-40% from uniform velocity)

Model	Downstream								
	i = 20%			***i= 30%***			***i = 40%***		
	yd (m)	**yd eqn 5-19 (m)**	**% Error**	**yd (m)**	**yd eqn 5-19 (m)**	**% Error**	**yd (m)**	**yd eqn 5-19 (m)**	**% Error**
1	2.77	2.77	0.01	1.00	1.03	2.55	0.78	0.73	6.41
2	2.62	2.75	4.97	1.00	1.02	2.11	0.78	0.73	6.84
3	2.32	2.51	8.01	1.00	0.97	3.32	0.69	0.69	0.71
4	1.60	1.68	5.20	0.78	0.77	1.88	0.52	0.53	2.45
5	1.60	1.57	1.66	0.78	0.74	5.70	0.52	0.51	1.83
6	2.47	2.70	9.40	1.00	1.01	1.06	0.78	0.72	7.87
7	1.87	2.21	17.99	0.89	0.90	0.80	0.60	0.63	5.36
8	3.78	3.04	19.65	1.17	1.12	4.02	0.78	0.80	2.44
9	3.50	3.15	10.05	0.98	1.16	18.75	0.71	0.83	16.60
10	2.21	2.59	17.06	0.85	0.96	12.36	0.58	0.68	17.14
11	1.87	2.00	6.95	0.78	0.85	8.57	0.60	0.59	0.98
12	2.17	2.38	9.60	0.90	0.94	4.18	0.67	0.66	1.07

Model	Downstream								
	i = 20%			***i= 30%***			***i = 40%***		
	yd (m)	**yd eqn 5-19 (m)**	**% Error**	**yd (m)**	**yd eqn 5-19 (m)**	**% Error**	**yd (m)**	**yd eqn 5-19 (m)**	**% Error**
13	2.47	2.59	4.93	1.00	0.99	1.39	0.69	0.70	1.43
14	2.47	2.65	7.39	1.00	1.00	0.03	0.78	0.71	8.95
15	2.77	2.82	1.67	1.05	1.04	1.39	0.78	0.74	5.43
16	1.74	1.68	3.29	0.73	0.62	15.06	0.44	0.44	0.25
17	2.47	2.97	20.07	1.11	1.10	0.82	0.74	0.78	5.94
18	2.62	2.59	1.00	0.96	0.96	0.30	0.71	0.69	3.46
19	3.52	2.92	16.99	1.16	1.08	6.95	0.90	0.77	14.64
20	1.99	1.77	10.81	0.69	0.65	5.41	0.49	0.46	5.26
21	2.05	1.85	9.70	0.82	0.68	17.03	0.56	0.48	13.60
22	2.07	1.92	7.30	0.76	0.71	7.22	0.51	0.50	1.70
23	2.88	2.69	6.57	0.85	0.99	16.68	0.61	0.71	15.65
24	1.45	1.58	9.21	0.63	0.58	7.32	0.45	0.42	7.67
26	4.53	4.56	0.68	1.61	1.70	5.34	1.17	1.21	3.25
28	5.10	4.81	5.68	1.58	1.79	12.98	1.12	1.27	13.52
29	6.14	5.65	8.02	2.22	2.10	5.45	1.42	1.50	5.30
30	2.32	2.49	7.43	1.00	0.96	3.63	0.69	0.68	1.05
31	2.77	2.84	2.43	1.05	1.04	0.96	0.78	0.74	4.99
32	1.59	1.64	3.17	0.71	0.61	13.97	0.50	0.43	13.19
33	1.59	1.61	1.34	0.71	0.60	14.87	0.50	0.43	14.17
34	1.13	0.95	15.64	0.50	0.44	11.18	0.34	0.31	9.42
35	1.59	1.51	4.78	0.59	0.58	1.23	0.50	0.41	17.48
36	1.59	1.72	8.39	0.71	0.63	11.43	0.50	0.45	10.44
37	1.34	1.40	4.76	0.54	0.56	3.23	0.36	0.39	9.26
38	1.23	1.24	1.06	0.52	0.52	0.19	0.36	0.36	1.18
39	2.19	2.42	10.40	0.76	0.93	22.55	0.58	0.66	13.68
40	2.46	2.68	9.00	0.83	0.99	19.24	0.64	0.70	9.99
41	3.08	3.16	2.55	1.00	1.17	17.06	0.79	0.83	5.49
42	1.84	2.36	28.23	0.84	0.87	3.83	0.57	0.62	8.89
43	1.23	1.43	16.52	0.57	0.53	7.48	0.38	0.38	1.30
44	6.66	4.41	33.72	1.72	1.64	4.84	1.16	1.16	0.42
45	4.55	3.80	16.44	1.33	1.41	5.85	0.89	1.00	12.56
46	2.36	2.44	3.21	0.82	0.90	9.55	0.58	0.64	10.14
47	1.94	2.00	2.96	0.70	0.83	18.93	0.49	0.58	19.26
48	1.69	1.55	8.09	0.64	0.72	12.22	0.45	0.50	10.77
51	4.78	4.77	0.23	2.09	2.01	3.90	1.43	1.41	1.26
52	3.73	3.67	1.53	1.84	1.72	6.36	1.34	1.20	10.66
53	6.32	5.80	8.27	2.52	2.25	10.61	1.51	1.60	5.79
56	3.00	3.56	18.69	1.36	1.43	5.23	1.02	1.01	0.86
57	5.13	4.15	19.10	1.68	1.57	6.79	1.17	1.11	4.78
Average	-	-	8.86	-	-	7.52	-	-	7.31

Table_C- 5: Software and relationship ZOI lengths for 1 boulder downstream (50%-70% from uniform velocity)

Model	Downstream								
	i = 50%			***i= 60%***			***i = 70%***		
	yd (m)	**yd eqn 5-19 (m)**	**% Error**	**yd (m)**	**yd eqn 5-19 (m)**	**% Error**	**yd (m)**	**yd eqn 5-19 (m)**	**% Error**
1	0.60	0.60	0.55	0.52	0.51	2.21	0.51	0.43	15.50
2	0.60	0.59	1.06	0.52	0.51	2.72	0.46	0.43	6.79
3	0.60	0.56	7.31	0.51	0.47	7.27	0.40	0.40	0.41
4	0.43	0.42	2.14	0.37	0.35	4.12	0.32	0.30	5.06
5	0.43	0.40	6.66	0.37	0.34	8.68	0.32	0.29	9.45
6	0.60	0.59	2.27	0.52	0.50	3.95	0.46	0.42	7.93
7	0.51	0.51	0.25	0.43	0.43	0.33	0.37	0.37	0.72
8	0.67	0.65	3.11	0.58	0.55	5.05	0.50	0.46	8.91
9	0.60	0.67	11.81	0.51	0.57	11.40	0.45	0.47	3.41
10	0.50	0.55	9.95	0.40	0.47	16.26	0.33	0.38	14.67
11	0.46	0.47	3.23	0.40	0.40	0.46	0.34	0.34	0.85
12	0.52	0.54	3.11	0.46	0.46	0.99	0.40	0.39	3.20
13	0.60	0.57	5.08	0.51	0.48	4.97	0.46	0.41	10.59
14	0.60	0.58	3.53	0.51	0.49	3.37	0.46	0.42	9.12
15	0.67	0.60	9.90	0.60	0.51	14.23	0.51	0.44	14.52
16	0.36	0.36	1.07	0.30	0.30	0.24	0.25	0.24	3.06
17	0.65	0.65	0.70	0.56	0.55	1.24	0.49	0.48	1.49
18	0.62	0.56	9.29	0.53	0.48	9.31	0.46	0.41	9.99
19	0.66	0.63	5.14	0.59	0.53	9.78	0.51	0.45	12.72
20	0.41	0.37	8.86	0.33	0.31	4.61	0.28	0.25	10.60
21	0.42	0.39	7.54	0.33	0.33	1.07	0.23	0.26	11.62
22	0.40	0.40	0.35	0.32	0.34	5.26	0.18	0.26	45.74
23	0.50	0.57	13.92	0.42	0.48	14.51	0.37	0.39	4.75
24	0.38	0.34	11.36	0.30	0.29	4.90	0.25	0.23	6.54
26	1.04	1.00	3.87	0.84	0.86	2.36	0.74	0.77	3.56
28	0.97	1.05	8.14	0.77	0.90	16.89	0.69	0.79	14.72
29	1.12	1.24	10.59	1.00	1.07	6.59	0.88	0.95	8.27
30	0.60	0.55	7.65	0.51	0.47	7.62	0.40	0.40	0.03
31	0.67	0.61	9.44	0.60	0.52	13.77	0.51	0.44	14.07
32	0.41	0.35	14.68	0.34	0.30	13.16	0.27	0.24	11.84
33	0.41	0.35	15.74	0.34	0.29	14.28	0.27	0.24	12.94
34	0.27	0.24	11.43	0.22	0.20	9.34	0.17	0.16	4.33
35	0.34	0.33	2.73	0.26	0.28	7.16	0.27	0.23	16.66

36	0.41	0.36	11.67	0.34	0.31	10.01	0.21	0.25	17.35
37	0.30	0.31	4.55	0.28	0.26	5.78	0.22	0.21	3.00
38	0.30	0.29	3.99	0.24	0.24	0.68	0.18	0.20	8.86
39	0.45	0.53	17.43	0.38	0.45	17.15	0.32	0.36	12.36
40	0.54	0.57	5.22	0.45	0.48	6.61	0.38	0.39	1.74
41	0.71	0.68	3.74	0.61	0.58	4.29	0.54	0.50	7.15
42	0.48	0.51	5.28	0.40	0.43	7.35	0.30	0.36	19.35
43	0.31	0.30	2.70	0.25	0.25	1.58	0.20	0.20	0.67
44	0.91	0.95	4.61	0.81	0.81	0.15	0.71	0.69	3.16
45	0.75	0.82	8.75	0.63	0.69	10.02	0.54	0.58	7.16
46	0.37	0.51	39.03	0.41	0.43	5.75	0.34	0.35	1.78
47	0.38	0.46	21.64	0.32	0.39	21.19	0.29	0.31	8.43
48	0.34	0.39	13.98	0.29	0.32	11.50	0.25	0.26	5.43
51	1.13	1.15	1.72	0.88	0.99	11.95	0.81	0.90	10.86
52	1.03	0.96	7.07	0.87	0.82	6.24	0.75	0.75	0.32
53	1.19	1.32	10.76	1.03	1.13	10.13	0.87	1.03	18.36
56	0.78	0.83	6.36	0.68	0.71	4.82	0.60	0.65	8.02
57	0.89	0.92	3.78	0.78	0.80	2.08	0.64	0.72	12.77
Average	-	-	7.54	-	-	7.16	-	-	8.84

Table_C- 6: Software and relationship ZOI lengths for 1 boulder sides (10%-20% from uniform velocity)

Model	**Sides**					
	i = 10%			***i= 20%***		
	x (m)	**X eqn 5-20 (m)**	**% Error**	**x (m)**	**X eqn 5-20 (m)**	**% Error**
1	0.44	0.42	5.61	0.30	0.27	8.49
2	0.44	0.42	5.55	0.29	0.27	7.21
3	0.40	0.42	4.76	0.26	0.26	0.63
4	0.36	0.43	22.25	0.25	0.22	13.16
5	0.36	0.44	22.98	0.25	0.21	13.97
6	0.44	0.42	5.40	0.29	0.27	7.92
7	0.38	0.42	11.51	0.26	0.24	6.01
8	0.42	0.42	0.34	0.30	0.29	4.36
9	0.40	0.42	4.97	0.28	0.29	4.95
10	0.35	0.34	2.45	0.24	0.24	0.35
11	0.38	0.43	13.98	0.25	0.23	4.45
12	0.38	0.42	10.78	0.26	0.25	2.87
13	0.40	0.42	4.44	0.26	0.26	0.85
14	0.40	0.42	4.23	0.28	0.26	5.40
15	0.44	0.41	5.74	0.30	0.27	7.82
16	0.24	0.21	10.24	0.16	0.15	4.14

17	0.44	0.49	13.54	0.32	0.30	6.06
18	0.42	0.41	0.39	0.32	0.26	17.86
19	0.46	0.42	8.36	0.30	0.28	5.27
20	0.26	0.21	18.56	0.15	0.16	5.84
21	0.27	0.21	19.81	0.18	0.16	9.31
22	0.26	0.21	16.40	0.17	0.17	1.33
23	0.34	0.34	0.75	0.24	0.25	2.22
24	0.25	0.21	14.35	0.17	0.15	13.35
26	0.79	0.82	4.18	0.53	0.48	9.49
28	0.66	0.82	24.40	0.47	0.49	4.65
29	0.89	1.02	14.74	0.58	0.59	2.62
30	0.40	0.42	4.81	0.26	0.26	0.86
31	0.44	0.41	5.80	0.30	0.27	7.53
32	0.25	0.21	13.71	0.15	0.15	4.60
33	0.25	0.21	13.58	0.15	0.15	3.78
34	0.21	0.22	5.60	-	-	-
35	0.24	0.21	9.40	0.15	0.15	2.37
36	0.27	0.21	22.04	0.17	0.15	8.83
37	0.19	0.21	12.80	0.14	0.14	1.20
38	0.18	0.22	23.79	-	-	-
39	0.31	0.34	9.90	0.20	0.23	17.06
40	0.32	0.34	5.50	0.22	0.24	11.34
41	0.49	0.50	2.34	0.36	0.31	11.76
42	0.32	0.33	4.36	0.22	0.23	2.29
43	0.19	0.17	10.74	0.11	0.13	21.76
44	0.64	0.66	4.69	0.44	0.43	2.01
45	0.47	0.54	16.70	0.35	0.36	5.50
46	0.27	0.30	9.74	0.20	0.22	12.65
47	0.28	0.35	25.99	0.18	0.22	19.64
48	0.28	0.35	28.82	0.18	0.19	7.17
51	2.93	1.25	57.16	0.54	0.60	11.19
52	2.93	1.28	56.16	0.54	0.54	0.82
53	0.88	1.23	40.77	0.62	0.65	5.48
56	0.70	0.83	18.16	0.35	0.42	20.17
57	0.60	0.82	36.00	0.32	0.45	42.79
Average	-	-	13.91	-	-	7.99

APPENDIX D: 1 BOULDER ABOVE THE BLOCKAGE LIMIT ZOI SOFTWARE AND RELATIONSHIP CORRELATION

The tables below compare the ZOI lengths as determined by the software and the relationships for 1 boulder above the blockage limit.

Table_D- 1: Software and relationship ZOI lengths for 1 boulder upstream (10%-30% from uniform velocity)

Model	**Upstream**								
	i = 10%			***i = 20%***			***i = 30%***		
	yu (m)	**yu eqn 5-18 (m)**	**% Error**	**yu (m)**	**yu eqn 5-18 (m)**	**% Error**	**yu (m)**	**yu eqn 5-18 (m)**	**% Error**
25	1.70	1.52	10.38	1.02	0.94	7.40	0.78	0.73	6.88
27	-	-	-	1.78	1.44	18.92	1.20	1.13	5.60
49	-	-	-	1.85	1.49	19.49	1.29	1.16	10.06
50	1.76	1.57	10.82	1.11	0.97	12.19	0.78	0.74	4.62
54	-	-	-	1.64	1.39	15.27	1.34	1.10	17.89
Average	-	-	10.60	-	-	14.65	-	-	9.01

Table_D- 2: Software and relationship ZOI lengths for 1 boulder upstream (40%-60% from uniform velocity)

Model	**Upstream**								
	i = 40%			***i = 50%***			***i = 60%***		
	yu (m)	**yu eqn 5-18 (m)**	**% Error**	**yu (m)**	**yu eqn 5-18 (m)**	**% Error**	**yu (m)**	**yu eqn 5-18 (m)**	**% Error**
25	0.63	0.61	2.85	0.55	0.52	5.22	0.46	0.46	0.05
27	1.01	0.98	2.55	0.88	0.83	6.19	0.77	0.74	4.37
49	1.03	1.00	3.19	0.87	0.84	3.37	0.76	0.75	1.68
50	0.64	0.62	3.11	0.53	0.53	0.15	0.48	0.47	2.70
54	1.04	0.97	6.83	0.89	0.81	9.29	0.79	0.72	8.44
Average	-	-	3.71	-	-	4.85	-	-	3.45

Table_D- 3: Software and relationship ZOI lengths for 1 boulder upstream (70% from uniform velocity)

Model	Upstream		
	i = 70%		
	yu (m)	yu eqn 5-18 (m)	% Error
25	0.42	0.41	3.11
27	0.68	0.65	3.77
49	0.69	0.66	3.96
50	0.41	0.41	0.51
54	0.69	0.64	6.63
Average	-	-	3.60

Table_D- 4: Software and relationship ZOI lengths for 1 boulder downstream (20%-40% from uniform velocity)

Model	Downstream								
	i = 20%			*i = 30%*			*i = 40%*		
	yd (m)	yd eqn 5-19 (m)	% Error	yd (m)	yd eqn 5-19 (m)	% Error	yd (m)	yd eqn 5-19 (m)	% Error
25	6.13	6.09	0.57	2.44	2.26	7.49	1.56	1.61	3.17
27	8.50	8.80	3.58	3.58	3.28	8.22	2.75	2.34	14.80
49	10.14	9.28	8.45	3.91	3.45	11.76	3.38	2.46	27.19
50	7.28	6.43	11.66	2.51	2.38	5.38	1.61	1.70	5.36
54	10.07	8.27	17.93	3.65	3.09	15.29	2.23	2.20	0.99
Average	-	-	8.44	-	-	9.63	-	-	10.30

Table_D- 5: Software and relationship ZOI lengths for 1 boulder downstream (50%-70% from uniform velocity)

Model	Downstream								
	i = 50%			*i = 60%*			*i = 70%*		
	yd (m)	yd eqn 5-19 (m)	% Error	yd (m)	yd eqn 5-19 (m)	% Error	yd (m)	yd eqn 5-19 (m)	% Error
25	1.29	1.37	5.81	1.15	1.17	1.27	1.03	1.07	4.25
27	2.22	2.00	9.97	1.81	1.72	5.02	1.64	1.64	0.02
49	2.36	2.10	11.06	1.92	1.80	6.12	1.58	1.69	7.08
50	1.26	1.44	13.97	1.06	1.22	15.06	0.96	1.11	15.95

Model	Downstream								
	i = 50%			***i = 60%***			***i = 70%***		
	yd (m)	**yd eqn 5-19 (m)**	**% Error**	**yd (m)**	**yd eqn 5-19 (m)**	**% Error**	**yd (m)**	**yd eqn 5-19 (m)**	**% Error**
54	1.81	1.88	4.12	1.64	1.63	0.69	1.49	1.58	5.73
Average	-	-	8.98	-	-	5.63	-	-	6.61

APPENDIX E: 2 BOULDERS MODEL CONDITIONS

Shown below are the model conditions used for the analysis of 2 boulders used in Section 7.

Table_E- 1: 2 Boulders model conditions

Model	b (m)	d (m)	Q (m^3/s)	S	Fr	d/b
1	5.0	0.10	1.250	0.00080	0.670	0.040
2	5.0	0.20	1.250	0.00080	0.670	0.080
3	10.0	0.20	1.250	0.00080	0.649	0.040
4	10.0	0.10	1.250	0.00080	0.649	0.020
5	10.0	0.40	1.250	0.00080	0.649	0.080
6	10.0	0.30	1.250	0.00080	0.649	0.060
7	10.0	0.50	1.250	0.00080	0.649	0.100
8	10.0	0.30	1.250	0.00070	0.611	0.060
9	10.0	0.30	1.250	0.00090	0.685	0.060
10	10.0	0.30	1.250	0.00100	0.718	0.060
11	10.0	0.30	1.250	0.00060	0.569	0.060
12	10.0	0.30	1.250	0.00050	0.524	0.060
13	5.0	0.20	1.250	0.00050	0.538	0.080
14	5.0	0.20	1.250	0.00100	0.744	0.080
15	10.0	0.30	1.250	0.000080	0.226	0.060
16	10.0	0.30	1.250	0.00030	0.415	0.060
17	10.0	0.30	1.250	0.00020	0.345	0.060
18	10.0	0.10	1.250	0.00050	0.524	0.020
19	10.0	0.20	1.250	0.00050	0.524	0.040
20	10.0	0.40	1.250	0.00050	0.524	0.080
21	10.0	0.50	1.250	0.00050	0.524	0.100
22	10.0	0.10	1.250	0.00030	0.415	0.020
23	10.0	0.20	1.250	0.00030	0.415	0.040
24	10.0	0.40	1.250	0.00030	0.415	0.080
25	10.0	0.50	1.250	0.00030	0.415	0.100

APPENDIX F: 2 BOULDERS ZOI SOFTWARE AND RELATIONSHIP CORRELATION

The tables below compare the ZOI lengths as determined by the software and the relationships for 2 boulders.

Table_F- 1: Software and relationship ZOI lengths for 2 boulders upstream (10%-30% from uniform velocity)

Model	Upstream								
	i = 10%			*i = 20%*			*i = 30%*		
	yu (m)	yu eqn 7-5 (m)	% Error	yu (m)	yu eqn 7-5 (m)	% Error	yu (m)	yu eqn 7-5 (m)	% Error
1	0.86	0.83	3.14	0.43	0.39	9.40	0.26	0.26	0.56
2	0.45	0.42	7.28	0.20	0.20	0.00	0.13	0.13	0.18
3	0.79	0.82	3.57	0.39	0.40	2.34	0.27	0.26	3.67
4	0.41	0.41	0.04	0.21	0.20	2.43	0.13	0.13	0.78
5	1.60	1.63	2.09	0.73	0.78	6.51	0.51	0.52	1.24
6	1.13	1.23	8.50	0.57	0.59	3.43	0.37	0.39	4.99
7	2.00	2.04	2.03	0.87	0.96	10.77	0.63	0.64	2.20
8	1.01	1.18	16.97	0.52	0.59	12.92	0.37	0.39	4.70
9	1.29	1.27	1.80	0.62	0.59	4.57	0.42	0.39	7.29
11	1.14	1.13	0.71	0.67	0.58	12.76	0.42	0.39	8.05
12	1.02	1.08	5.49	0.60	0.58	3.12	0.37	0.38	3.99
13	0.75	0.73	2.85	0.39	0.38	1.54	0.26	0.26	1.53
16	0.88	0.93	6.07	0.57	0.57	0.42	0.37	0.38	2.92
18	0.36	0.36	0.09	0.20	0.20	1.01	0.12	0.13	8.15
19	0.71	0.72	1.14	0.41	0.39	4.01	0.26	0.26	0.91
20	1.44	1.43	0.44	0.76	0.77	0.87	0.51	0.51	0.28
21	1.75	1.79	2.34	0.97	0.95	2.04	0.63	0.64	1.24
22	0.35	0.31	10.85	0.20	0.20	0.53	0.14	0.13	8.26
23	0.58	0.62	7.40	0.35	0.39	10.72	0.24	0.25	6.24
24	1.29	1.24	3.59	0.78	0.75	3.22	0.54	0.51	6.26
25	1.61	1.55	3.50	0.95	0.94	1.51	0.62	0.63	1.81
Average	-	-	4.28	-	-	4.48	-	-	3.58

Table_F- 2: Software and relationship ZOI lengths for 1 boulder upstream (40%-60% from uniform velocity)

Model	Upstream								
	i = 40%			***i = 50%***			***i = 60%***		
	yu (m)	**yu eqn 7-5 (m)**	**% Error**	**yu (m)**	**yu eqn 7-5 (m)**	**% Error**	**yu (m)**	**yu eqn 7-5 (m)**	**% Error**
1	0.21	0.21	1.65	0.16	0.17	4.32	0.14	0.14	2.79
2	0.10	0.10	0.58	0.08	0.08	0.25	0.07	0.07	0.13
3	0.21	0.20	4.74	0.17	0.16	6.30	0.14	0.14	0.34
4	0.10	0.10	2.58	0.07	0.08	8.79	0.07	0.07	3.17
5	0.41	0.41	0.19	0.34	0.33	2.01	0.28	0.29	2.58
6	0.29	0.30	5.08	0.25	0.25	1.89	0.21	0.21	1.36
7	0.51	0.52	1.53	0.42	0.42	0.59	0.36	0.36	0.66
8	0.29	0.30	3.97	0.25	0.24	2.26	0.22	0.21	3.64
9	0.32	0.31	3.88	0.26	0.25	5.36	0.22	0.21	2.91
11	0.30	0.30	0.72	0.25	0.24	2.67	0.22	0.21	4.08
12	0.29	0.29	1.22	0.24	0.24	0.87	0.21	0.21	0.06
13	0.20	0.20	0.61	0.16	0.16	2.93	0.14	0.14	1.32
16	0.28	0.28	0.65	0.23	0.24	3.76	0.21	0.21	1.58
18	0.09	0.09	4.27	0.07	0.08	7.38	0.06	0.07	11.39
19	0.19	0.19	1.42	0.16	0.16	1.74	0.14	0.14	1.73
20	0.40	0.40	1.08	0.32	0.33	2.76	0.28	0.28	1.14
21	0.49	0.50	1.80	0.41	0.42	1.71	0.36	0.36	0.75
22	0.09	0.09	0.11	0.08	0.07	7.37	0.07	0.07	5.97
23	0.19	0.19	2.62	0.16	0.15	3.13	0.13	0.14	4.22
24	0.38	0.38	0.02	0.32	0.32	1.31	0.28	0.28	0.39
25	0.49	0.48	2.26	0.41	0.41	0.27	0.35	0.35	0.53
Average	-	-	1.95	-	-	3.22	-	-	2.42

Table_F- 3: Software and relationship ZOI lengths for 1 boulder upstream (70%-90% from uniform velocity)

Model	Upstream								
	i = 70%			***i = 80%***			***i = 90%***		
	yu (m)	**yu eqn 7-5 (m)**	**% Error**	**yu (m)**	**yu eqn 7-5 (m)**	**% Error**	**yu (m)**	**yu eqn 7-5 (m)**	**% Error**
1	0.12	0.13	4.42	0.12	0.12	2.75	0.10	0.10	3.44
2	0.05	0.06	21.74	-	-	-	0.05	0.05	1.14
3	0.13	0.12	6.35	0.12	0.11	8.49	0.10	0.10	1.16
4	0.06	0.06	1.43	0.05	0.05	3.48	0.05	0.05	1.09
5	0.25	0.25	0.25	0.23	0.23	1.32	0.20	0.21	3.47
6	0.18	0.19	3.18	0.17	0.17	0.31	0.15	0.15	2.51

7	0.33	0.32	4.18	0.29	0.30	2.39	0.27	0.26	3.50
8	0.19	0.19	2.23	0.17	0.17	0.03	0.15	0.15	2.55
9	0.20	0.19	7.15	0.17	0.17	0.56	0.16	0.15	3.94
11	0.19	0.19	2.21	0.17	0.17	0.30	0.16	0.15	3.80
12	0.18	0.19	3.24	0.17	0.17	0.68	0.16	0.15	3.74
13	0.13	0.13	3.56	0.11	0.12	5.01	0.10	0.10	3.62
16	0.18	0.19	3.31	0.17	0.17	1.75	0.15	0.15	2.87
18	0.06	0.06	1.37	0.05	0.05	2.45	0.05	0.05	0.93
19	0.13	0.12	6.29	0.11	0.11	1.16	0.10	0.10	1.33
20	0.25	0.25	0.30	0.23	0.23	0.32	0.21	0.21	1.29
21	0.32	0.32	1.13	0.29	0.29	1.37	0.27	0.26	3.33
22	0.06	0.06	1.31	0.05	0.05	1.35	0.05	0.05	0.75
23	0.12	0.12	1.58	0.11	0.11	2.23	0.10	0.10	1.52
24	0.25	0.25	0.37	0.23	0.23	0.76	0.21	0.21	1.11
25	0.31	0.32	2.12	0.29	0.29	0.28	0.26	0.26	0.57
Average	-	-	3.70	-	-	1.85	-	-	2.27

Table_F- 4: Software and relationship ZOI lengths for 1 boulder downstream (20%-40% from uniform velocity)

Model	**Downstream**								
	i = 20%			***i = 30%***			***i = 40%***		
	yd (m)	**yd eqn 7-6 (m)**	**% Error**	**yd (m)**	**yd eqn 7-6 (m)**	**% Error**	**yd (m)**	**yd eqn 7-6 (m)**	**% Error**
1	2.72	2.44	10.28	1.67	1.34	19.80	1.33	1.08	18.50
2	1.30	1.26	3.23	0.92	0.77	16.59	0.68	0.61	10.22
3	1.97	2.48	25.59	1.29	1.49	15.66	1.02	1.19	16.55
4	1.39	1.28	8.42	0.78	0.86	9.52	0.65	0.67	3.96
5	5.00	4.80	3.91	2.72	2.61	4.14	2.14	2.10	1.76
6	4.10	3.65	11.00	2.28	2.07	9.15	1.90	1.66	12.80
7	6.00	5.95	0.89	2.62	3.12	19.14	2.14	2.53	18.07
8	2.99	3.54	18.38	1.84	1.98	7.63	1.46	1.58	7.99
9	3.43	3.75	9.09	1.84	2.16	17.41	1.60	1.74	8.62
11	3.50	3.42	2.22	2.11	1.87	11.14	1.56	1.49	4.76
12	3.40	3.29	3.36	1.84	1.76	4.22	1.36	1.39	2.24
13	1.67	2.19	31.54	1.22	1.13	7.64	0.95	0.90	5.37
16	2.48	2.93	18.09	1.46	1.47	0.72	1.09	1.15	5.34
18	1.19	1.15	3.40	0.65	0.73	12.65	0.51	0.56	10.28
19	2.14	2.23	4.11	1.26	1.27	0.93	0.99	1.00	0.97
20	5.61	4.33	22.89	2.24	2.22	1.27	1.87	1.76	5.76
21	6.00	5.35	10.76	2.62	2.65	1.23	2.11	2.12	0.47
22	1.22	1.03	16.22	0.75	0.61	18.53	0.54	0.46	14.78
23	1.67	1.99	19.40	0.95	1.06	11.69	0.78	0.82	4.94

24	3.74	3.86	3.18	1.84	1.86	1.05	1.50	1.45	2.90
25	5.47	4.78	12.74	2.04	2.22	8.80	1.63	1.75	6.98
Average	-	-	11.37	-	-	9.47	-	-	7.77

Table_F- 5: Software and relationship ZOI lengths for 1 boulder downstream (50%-70% from uniform velocity)

Model	**Downstream**								
	i = 50%			***i = 60%***			***i = 70%***		
	yd (m)	**yd eqn 7-6 (m)**	**% Error**	**yd (m)**	**yd eqn 7-6 (m)**	**% Error**	**yd (m)**	**yd eqn 7-6 (m)**	**% Error**
1	1.12	0.95	15.05	1.02	0.86	16.11	0.92	0.79	13.44
2	0.58	0.53	8.42	0.44	0.46	2.97	0.48	0.42	11.11
3	0.95	1.03	7.95	0.82	0.88	8.18	0.71	0.82	14.75
4	0.54	0.57	4.91	0.48	0.47	1.37	0.41	0.44	6.92
5	1.87	1.85	1.04	1.63	1.66	1.70	1.39	1.54	10.38
6	1.60	1.45	9.28	1.36	1.28	6.10	1.33	1.18	10.67
7	1.87	2.24	19.59	1.73	2.03	17.29	1.56	1.88	20.52
8	1.29	1.37	6.12	1.22	1.21	1.52	1.09	1.11	2.44
9	1.39	1.52	9.25	1.22	1.34	9.79	1.16	1.25	8.13
11	1.33	1.29	3.06	1.12	1.13	0.50	1.16	1.04	10.14
12	1.16	1.19	3.02	1.09	1.04	4.24	1.02	0.96	6.30
13	0.88	0.78	11.88	0.78	0.69	11.19	0.68	0.64	6.23
16	0.95	0.96	0.98	0.85	0.83	1.79	0.75	0.76	1.14
18	0.44	0.47	6.07	0.37	0.38	2.41	0.34	0.35	3.52
19	0.85	0.84	0.68	0.75	0.72	3.72	0.71	0.66	7.42
20	1.56	1.52	2.80	1.39	1.35	2.86	1.29	1.24	3.91
21	1.87	1.84	1.76	1.67	1.66	0.40	1.56	1.52	2.76
22	0.41	0.38	7.24	0.31	0.31	0.28	0.27	0.28	2.43
23	0.68	0.68	0.22	0.58	0.58	0.18	0.54	0.52	3.81
24	1.19	1.23	3.12	1.05	1.08	2.93	0.95	0.98	3.23
25	1.39	1.48	6.38	1.22	1.33	8.61	1.09	1.20	10.65
Average	-	-	6.13	-	-	4.96	-	-	7.61

Table_F- 6: Software and relationship ZOI lengths for 1 boulder downstream (80%-90% from uniform velocity)

Model	**Downstream**					
	i = 80%			***i = 90%***		
	yd (m)	**yd eqn 7-6 (m)**	**% Error**	**yd (m)**	**yd eqn 7-6 (m)**	**% Error**
1	0.78	0.73	6.23	0.71	0.65	9.48

2	-	-	-	0.24	0.32	35.09
3	0.71	0.74	3.77	0.61	0.62	1.77
4	0.41	0.39	4.88	0.31	0.31	1.26
5	1.46	1.41	3.25	1.26	1.25	0.48
6	1.16	1.08	6.44	0.99	0.94	4.97
7	1.43	1.74	21.98	1.29	1.57	21.33
8	0.95	1.01	6.14	0.99	0.88	10.52
9	1.05	1.15	8.96	0.99	0.99	0.21
11	1.02	0.93	8.42	0.92	0.82	10.34
12	0.85	0.85	0.14	0.85	0.76	10.81
13	0.65	0.57	11.22	0.58	0.52	10.03
16	0.65	0.66	1.50	0.58	0.60	4.12
18	0.27	0.31	12.28	0.24	0.25	5.32
19	0.65	0.58	9.74	0.58	0.50	12.82
20	1.16	1.11	3.70	1.09	1.01	6.90
21	1.43	1.37	4.00	1.29	1.27	1.84
22	0.24	0.24	1.15	0.20	0.20	2.45
23	0.44	0.45	1.62	0.41	0.40	1.95
24	0.82	0.86	5.09	0.71	0.80	12.62
25	1.02	1.06	3.53	0.88	1.01	13.89
Average	-	-	6.20	-	-	8.49

Table_F- 7: Software and relationship ZOI lengths for 1 boulder sides (10%-30% from uniform velocity)

Model	**Sides**								
	i = 10%			***i = 20%***			***i = 30%***		
	x (m)	**x eqn 7-7 (m)**	**% Error**	**x (m)**	**x eqn 7-7 (m)**	**% Error**	**x (m)**	**x eqn 7-7 (m)**	**% Error**
1	0.83	0.62	25.10	0.65	0.51	22.08	0.59	0.46	21.48
2	0.44	0.33	24.90	0.35	0.27	24.03	0.29	0.24	17.66
3	0.70	0.65	5.99	0.58	0.53	8.31	0.54	0.48	11.56
4	0.38	0.35	7.88	0.31	0.28	9.94	0.28	0.25	9.71
5	1.63	1.24	24.18	1.19	1.01	14.52	1.06	0.92	12.92
6	1.20	0.95	20.95	0.94	0.78	17.08	0.82	0.70	14.08
7	1.53	1.52	0.83	1.32	1.25	5.57	1.24	1.13	8.18
8	1.00	0.95	5.14	0.86	0.78	9.33	0.80	0.70	11.92
9	1.03	0.95	7.90	0.88	0.78	11.40	0.80	0.70	11.92
11	0.86	0.95	10.95	0.70	0.78	10.75	0.65	0.70	8.57
12	0.86	0.95	10.95	0.72	0.78	8.43	0.66	0.70	6.91
13	0.61	0.62	1.30	0.52	0.51	1.65	0.46	0.46	0.14
16	0.80	0.95	19.32	0.66	0.78	18.36	0.59	0.70	19.70
18	0.34	0.35	3.11	0.27	0.28	3.40	0.24	0.25	3.46

19	0.61	0.65	7.11	0.51	0.53	4.27	0.46	0.48	4.97
20	1.14	1.24	8.89	0.95	1.01	6.63	0.85	0.92	8.72
21	1.40	1.52	8.38	1.13	1.25	10.31	1.06	1.13	7.49
22	0.30	0.35	17.10	0.23	0.28	21.39	0.21	0.25	18.24
23	0.56	0.65	16.67	0.45	0.53	19.50	0.41	0.48	17.93
24	1.03	1.24	19.99	0.85	1.01	19.88	0.77	0.92	20.09
25	1.22	1.52	24.37	1.01	1.25	23.41	0.92	1.13	23.26
Average	-	-	12.91	-	-	12.87	-	-	12.33

Table_F- 8: Software and relationship ZOI lengths for 1 boulder sides (40%-60% from uniform velocity)

Model	**Sides**								
	i = 40%			***i = 50%***			***i = 60%***		
	x (m)	**x eqn 7-7 (m)**	**% Error**	**x (m)**	**x eqn 7-7 (m)**	**% Error**	**x (m)**	**x eqn 7-7 (m)**	**% Error**
1	0.55	0.43	20.51	0.49	0.41	16.53	0.48	0.39	17.96
2	0.28	0.22	19.75	0.24	0.21	14.13	0.25	0.20	18.79
3	0.51	0.44	12.60	0.48	0.41	13.23	0.46	0.40	13.49
4	0.25	0.22	10.06	0.23	0.21	9.71	0.23	0.20	12.58
5	1.00	0.87	12.92	0.95	0.82	13.44	0.93	0.79	14.85
6	0.78	0.65	15.50	0.73	0.62	15.69	0.71	0.59	15.85
7	1.18	1.08	8.77	1.13	1.02	9.73	1.10	0.98	10.80
8	0.75	0.65	12.10	0.72	0.62	13.92	0.69	0.59	14.02
9	0.74	0.65	10.90	0.71	0.62	12.70	0.68	0.59	12.11
11	0.61	0.65	8.24	0.58	0.62	7.04	0.54	0.59	9.87
12	0.61	0.65	7.35	0.57	0.62	7.98	0.55	0.59	7.87
13	0.43	0.43	0.74	0.40	0.41	2.25	0.38	0.39	3.63
16	0.56	0.65	17.99	0.52	0.62	18.36	0.50	0.59	18.65
18	0.22	0.22	2.20	0.21	0.21	1.30	0.19	0.20	5.83
19	0.42	0.44	5.09	0.40	0.41	4.34	0.38	0.40	4.72
20	0.80	0.87	8.98	0.77	0.82	6.93	0.73	0.79	8.63
21	0.99	1.08	9.29	0.94	1.02	8.51	0.90	0.98	9.02
22	0.18	0.22	24.91	0.17	0.21	22.15	0.17	0.20	21.86
23	0.39	0.44	14.64	0.36	0.41	16.10	0.34	0.40	18.79
24	0.72	0.87	21.17	0.68	0.82	20.30	0.66	0.79	20.24
25	0.87	1.08	23.74	0.83	1.02	22.90	0.80	0.98	23.42
Average	-	-	12.74	-	-	12.25	-	-	13.48

Table_F- 9: Software and relationship ZOI lengths for 1 boulder sides (70%-90% from uniform velocity)

Model	**Sides**								
	i = 70%			***i = 80%***			***i = 90%***		
	x (m)	**x eqn 7-7 (m)**	**% Error**	**x (m)**	**x eqn 7-7 (m)**	**% Error**	**x (m)**	**x eqn 7-7 (m)**	**% Error**
1	0.45	0.38	15.90	0.43	0.36	14.32	0.43	0.36	15.92
2	0.21	0.19	9.37	-	-	-	0.21	0.18	14.88
3	0.44	0.38	13.49	0.43	0.37	15.09	0.42	0.36	13.85
4	0.22	0.19	13.00	0.22	0.18	16.79	0.21	0.18	12.76
5	0.88	0.76	13.99	0.86	0.73	14.82	0.83	0.71	13.37
6	0.68	0.57	15.70	0.64	0.55	14.56	0.64	0.54	15.57
7	1.08	0.94	12.15	1.06	0.91	13.78	1.03	0.89	12.85
8	0.67	0.57	15.07	0.65	0.55	15.87	0.63	0.54	14.90
9	0.66	0.57	13.78	0.63	0.55	13.20	0.62	0.54	13.53
11	0.53	0.57	7.37	0.51	0.55	7.22	0.49	0.54	9.41
12	0.53	0.57	7.37	0.51	0.55	7.22	0.50	0.54	8.31
13	0.36	0.38	5.13	0.35	0.36	5.55	0.34	0.36	5.10
16	0.48	0.57	19.80	0.47	0.55	17.60	0.45	0.54	20.48
18	0.19	0.19	0.74	0.18	0.18	1.70	0.17	0.18	5.20
19	0.37	0.38	4.28	0.35	0.37	4.32	0.34	0.36	6.72
20	0.71	0.76	6.61	0.68	0.73	7.90	0.67	0.71	7.48
21	0.87	0.94	8.55	0.85	0.91	7.64	0.82	0.89	8.93
22	0.16	0.19	23.49	0.15	0.18	22.03	0.15	0.18	19.22
23	0.33	0.38	17.12	0.31	0.37	17.78	0.31	0.36	17.22
24	0.63	0.76	20.15	0.62	0.73	18.42	0.60	0.71	19.12
25	0.78	0.94	21.86	0.76	0.91	20.47	0.74	0.89	20.71
Average	-	-	12.61	-	-	12.81	-	-	13.12